データ集

付 録A　衝撃力センサの検定時の出力波形

第I部にて説明した3種の衝撃力センサの、検定時の出力波形である。検定に関する詳細は第4章にて説明している。

それぞれの波形は、計測された過渡電圧そのものである。最大電圧 $E_{\max}$ は、第4章で説明している手順で雑音除去した後の値を示しているので、グラフの最大値とは微妙に異なる。

鋼球の質量	落下高さ	センサA	センサB	センサC
0.130g	30mm	Fig. A.1	Fig. A.5	Fig. A.7
	80mm	—	—	Fig. A.8
0.440g	30mm	Fig. A.2	Fig. A.6	Fig. A.9
	80mm	Fig. A.3	—	Fig. A.10
	150mm	Fig. A.4	—	—
2.030g	30mm	—	—	Fig. A.11
	80mm	—	—	Fig. A.12

$E_{\max} = 4.2352\,\mathrm{V}$
$\Delta t = 6.20\,\mu\mathrm{sec.}$
$F = 29.0683\,\mathrm{N}$

$E_{\max} = 4.1710\,\mathrm{V}$
$\Delta t = 6.05\,\mu\mathrm{sec.}$
$F = 29.7890\,\mathrm{N}$

$E_{\max} = 4.0059\,\mathrm{V}$
$\Delta t = 5.95\,\mu\mathrm{sec.}$
$F = 30.2897\,\mathrm{N}$

$E_{\max} = 4.3113\,\mathrm{V}$
$\Delta t = 6.10\,\mu\mathrm{sec.}$
$F = 29.5449\,\mathrm{N}$

$E_{\max} = 4.1401\,\mathrm{V}$
$\Delta t = 6.50\,\mu\mathrm{sec.}$
$F = 27.7267\,\mathrm{N}$

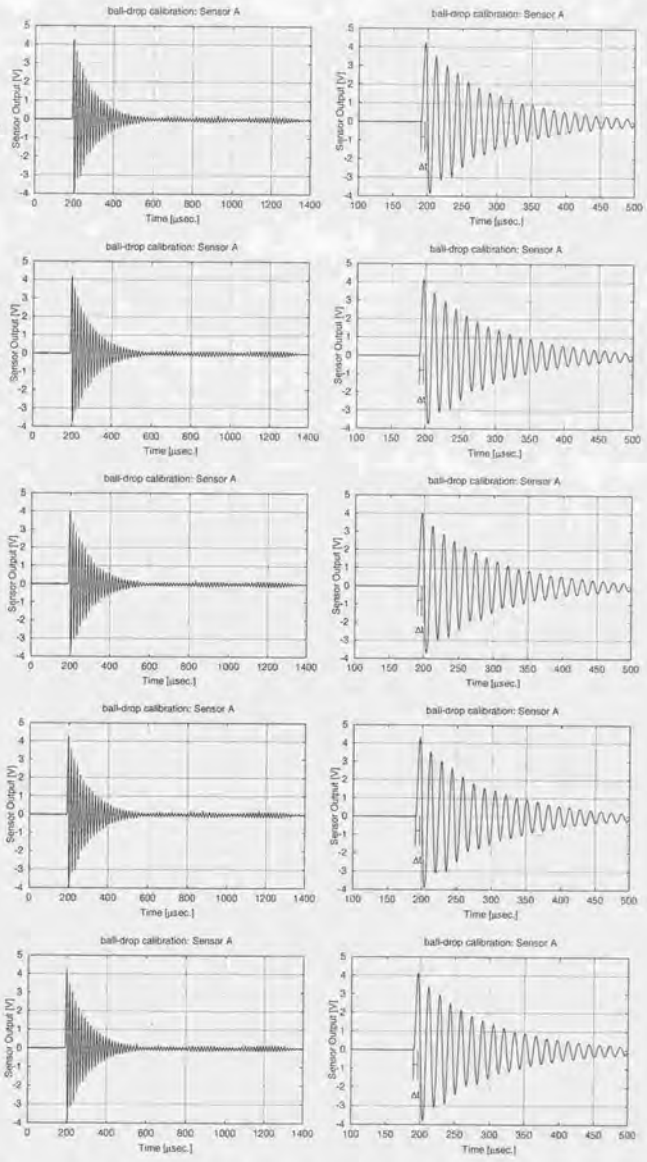

Fig. A.1: Output of Sensor A at ball-drop calibration. $m = 0.130\,\mathrm{g}$, $h = 30\,\mathrm{mm}$

$E_{\max} = 4.2776\,\mathrm{V}$
$\Delta t = 6.05\,\mu\mathrm{sec.}$
$F = 29.7890\,\mathrm{N}$

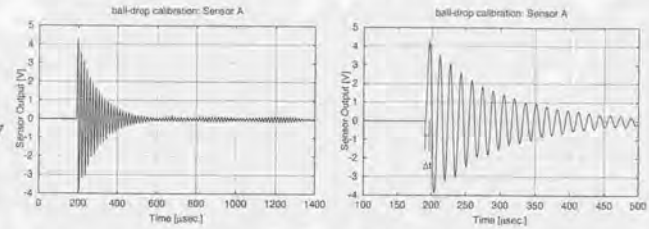

$E_{\max} = 4.1587\,\mathrm{V}$
$\Delta t = 6.35\,\mu\mathrm{sec.}$
$F = 28.3817\,\mathrm{N}$

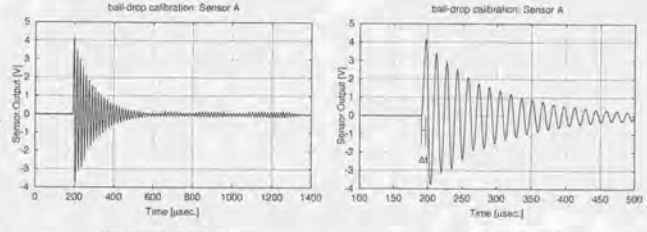

$E_{\max} = 4.2730\,\mathrm{V}$
$\Delta t = 6.05\,\mu\mathrm{sec.}$
$F = 29.7890\,\mathrm{N}$

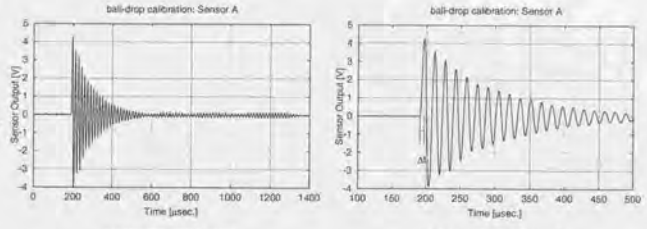

$E_{\max} = 4.1483\,\mathrm{V}$
$\Delta t = 6.05\,\mu\mathrm{sec.}$
$F = 29.7890\,\mathrm{N}$

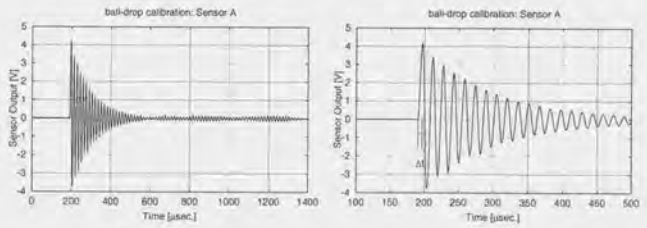

$E_{\max} = 4.2433\,\mathrm{V}$
$\Delta t = 5.95\,\mu\mathrm{sec.}$
$F = 30.2897\,\mathrm{N}$

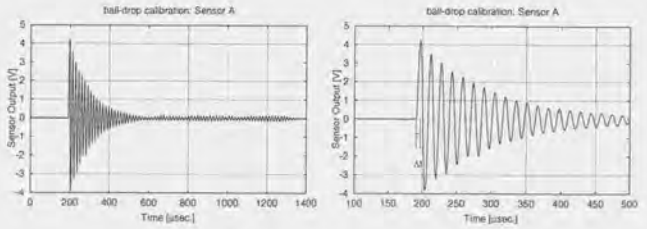

Fig. A.1: (continued)

$E_{\max} = 4.0167\,\mathrm{V}$
$\Delta t = 6.00\,\mu\mathrm{sec.}$
$F = 30.0373\,\mathrm{N}$

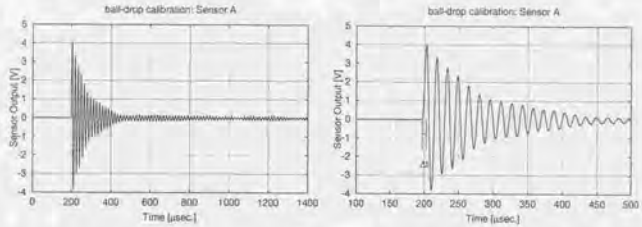

$E_{\max} = 3.9813\,\mathrm{V}$
$\Delta t = 6.20\,\mu\mathrm{sec.}$
$F = 29.0683\,\mathrm{N}$

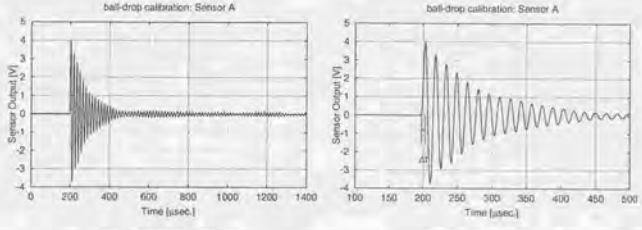

$E_{\max} = 4.0334\,\mathrm{V}$
$\Delta t = 6.35\,\mu\mathrm{sec.}$
$F = 28.3817\,\mathrm{N}$

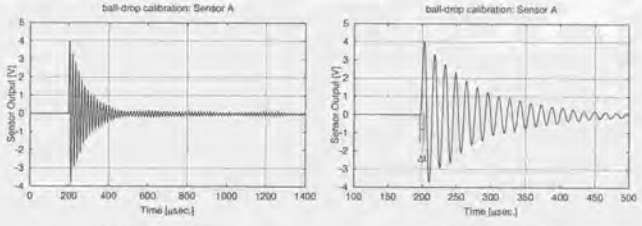

$E_{\max} = 4.1089\,\mathrm{V}$
$\Delta t = 5.85\,\mu\mathrm{sec.}$
$F = 30.8075\,\mathrm{N}$

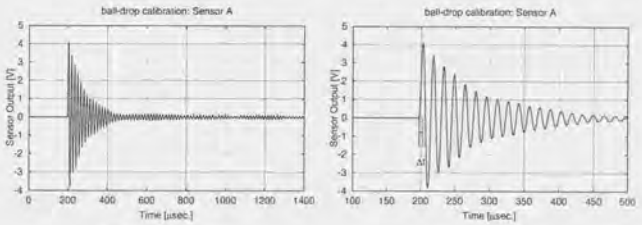

$E_{\max} = 3.8148\,\mathrm{V}$
$\Delta t = 6.30\,\mu\mathrm{sec.}$
$F = 28.6069\,\mathrm{N}$

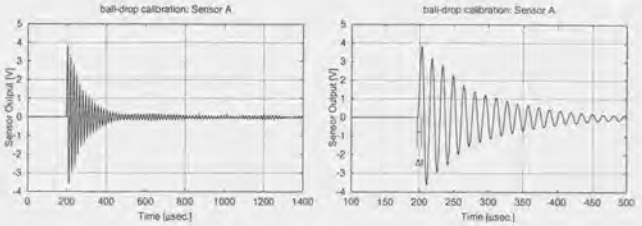

Fig. A.1: (continued)

$E_{\max} = 4.0592\,\mathrm{V}$
$\Delta t = 6.15\,\mu\mathrm{sec.}$
$F = 29.3046\,\mathrm{N}$

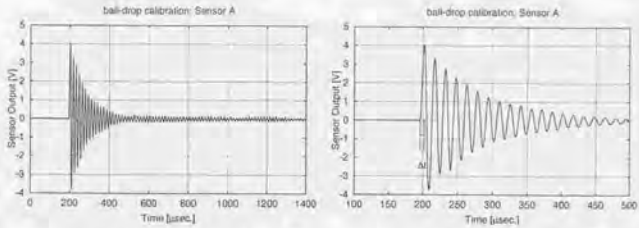

$E_{\max} = 3.9790\,\mathrm{V}$
$\Delta t = 5.80\,\mu\mathrm{sec.}$
$F = 31.0730\,\mathrm{N}$

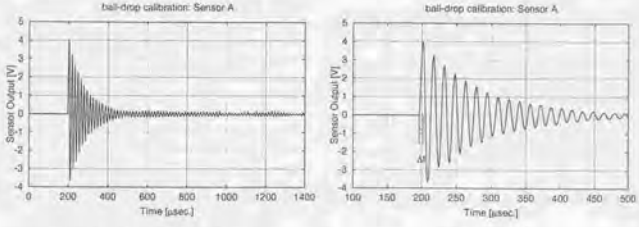

$E_{\max} = 4.2536\,\mathrm{V}$
$\Delta t = 5.80\,\mu\mathrm{sec.}$
$F = 31.0730\,\mathrm{N}$

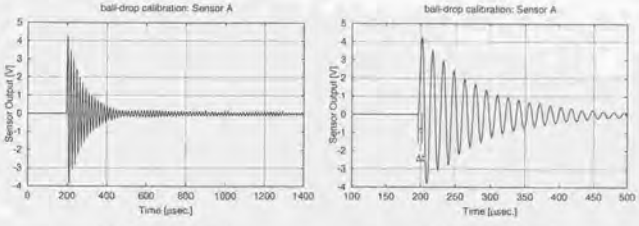

$E_{\max} = 4.0610\,\mathrm{V}$
$\Delta t = 5.80\,\mu\mathrm{sec.}$
$F = 31.0730\,\mathrm{N}$

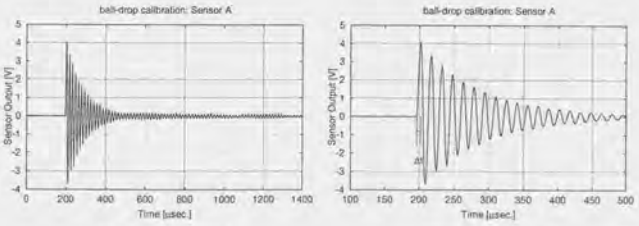

$E_{\max} = 3.8368\,\mathrm{V}$
$\Delta t = 6.00\,\mu\mathrm{sec.}$
$F = 30.0373\,\mathrm{N}$

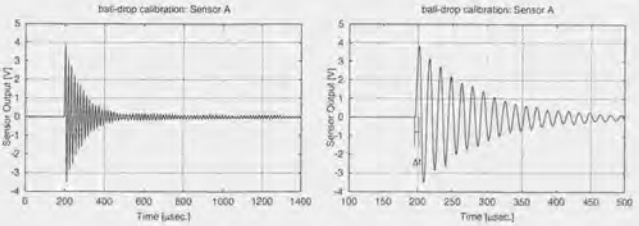

Fig. A.1: (continued)

$E_{\max} = 8.4529\,\mathrm{V}$
$\Delta t = 7.70\,\mu\mathrm{sec.}$
$F = 77.5971\,\mathrm{N}$

$E_{\max} = 8.0635\,\mathrm{V}$
$\Delta t = 7.75\,\mu\mathrm{sec.}$
$F = 77.0964\,\mathrm{N}$

$E_{\max} = 8.5576\,\mathrm{V}$
$\Delta t = 7.80\,\mu\mathrm{sec.}$
$F = 76.6022\,\mathrm{N}$

$E_{\max} = 8.3319\,\mathrm{V}$
$\Delta t = 7.50\,\mu\mathrm{sec.}$
$F = 79.6663\,\mathrm{N}$

$E_{\max} = 8.0655\,\mathrm{V}$
$\Delta t = 7.80\,\mu\mathrm{sec.}$
$F = 76.6022\,\mathrm{N}$

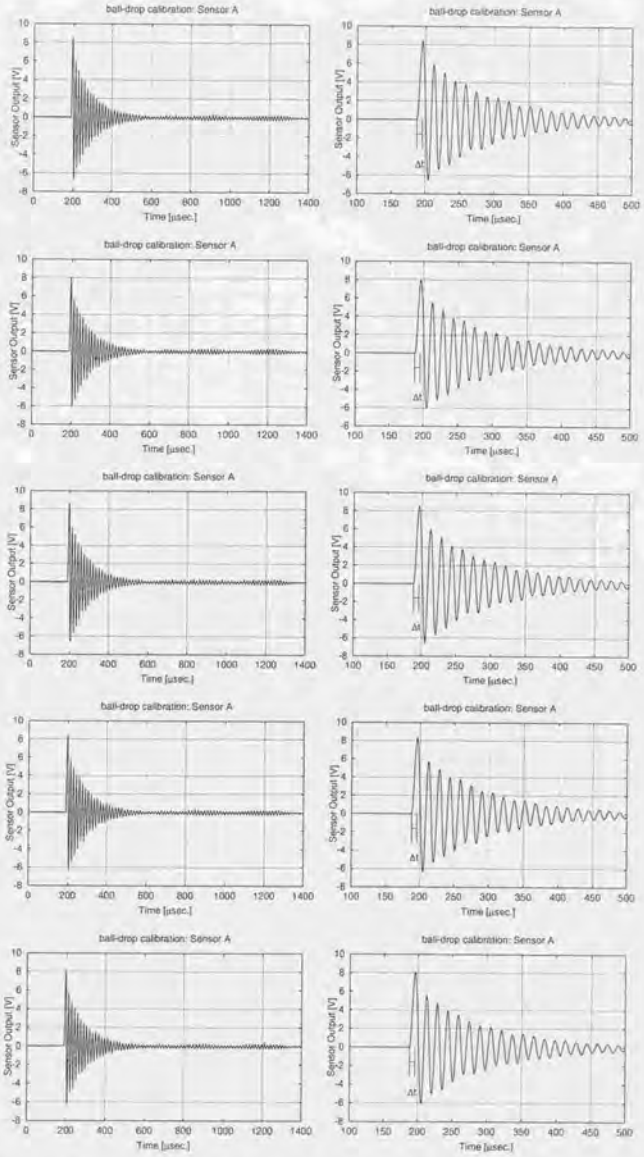

Fig. A.2: Output of Sensor A at ball-drop calibration. $m = 0.440\,\mathrm{g}$, $h = 30\,\mathrm{mm}$

$E_{\max} = 8.1199\,\mathrm{V}$
$\Delta t = 7.80\,\mu\mathrm{sec.}$
$F = 76.6022\,\mathrm{N}$

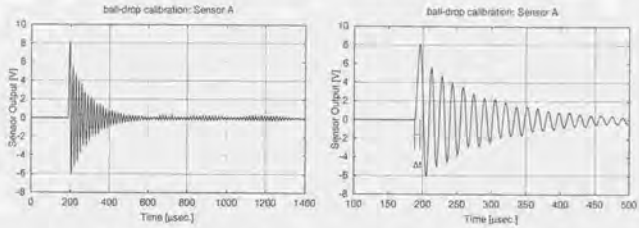

$E_{\max} = 8.1637\,\mathrm{V}$
$\Delta t = 7.50\,\mu\mathrm{sec.}$
$F = 79.6663\,\mathrm{N}$

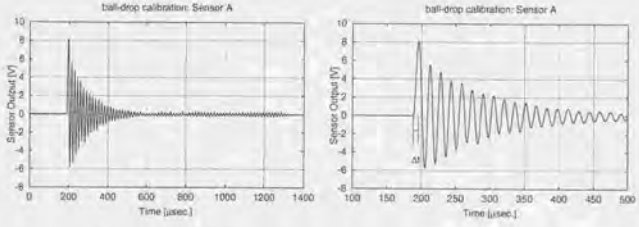

$E_{\max} = 8.1738\,\mathrm{V}$
$\Delta t = 7.90\,\mu\mathrm{sec.}$
$F = 75.6326\,\mathrm{N}$

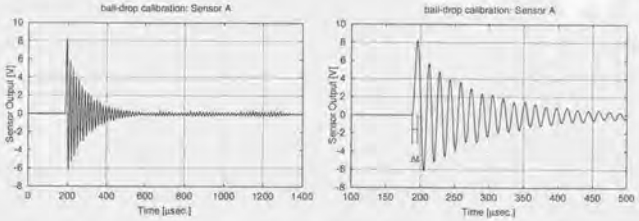

$E_{\max} = 8.0938\,\mathrm{V}$
$\Delta t = 9.00\,\mu\mathrm{sec.}$
$F = 66.3886\,\mathrm{N}$

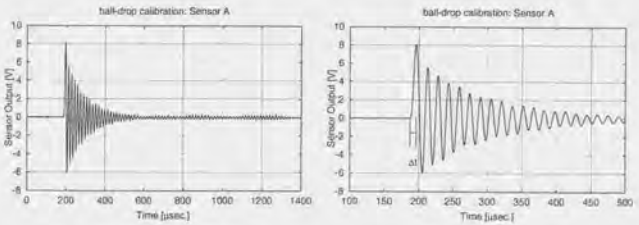

$E_{\max} = 8.2280\,\mathrm{V}$
$\Delta t = 7.75\,\mu\mathrm{sec.}$
$F = 77.0964\,\mathrm{N}$

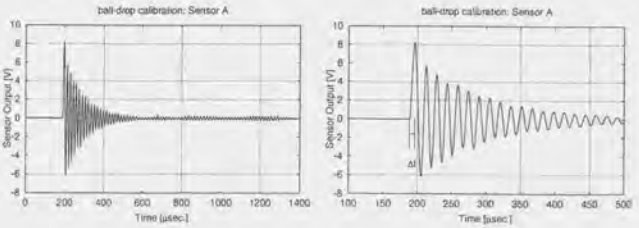

Fig. A.2: (continued)

$E_{\max} = 8.2258\,\mathrm{V}$
$\Delta t = 9.00\,\mu\mathrm{sec.}$
$F = 66.3886\,\mathrm{N}$

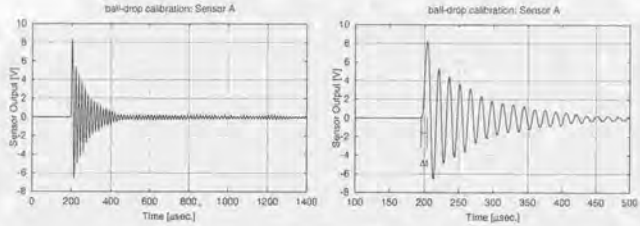

$E_{\max} = 7.8642\,\mathrm{V}$
$\Delta t = 8.25\,\mu\mathrm{sec.}$
$F = 72.4239\,\mathrm{N}$

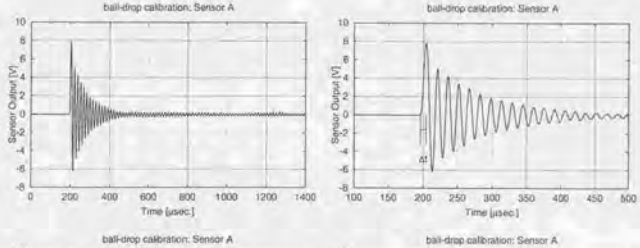

$E_{\max} = 8.8401\,\mathrm{V}$
$\Delta t = 7.60\,\mu\mathrm{sec.}$
$F = 78.6181\,\mathrm{N}$

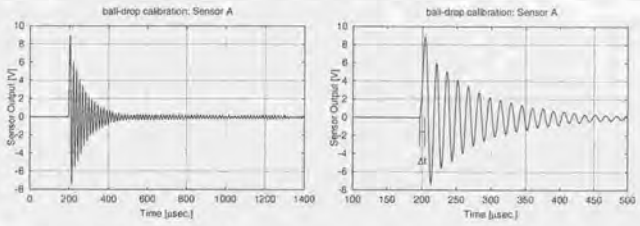

$E_{\max} = 8.6729\,\mathrm{V}$
$\Delta t = 7.75\,\mu\mathrm{sec.}$
$F = 77.0964\,\mathrm{N}$

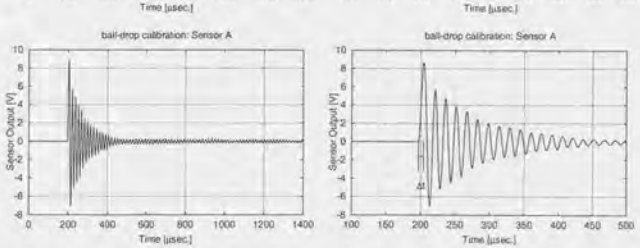

$E_{\max} = 8.0574\,\mathrm{V}$
$\Delta t = 8.40\,\mu\mathrm{sec.}$
$F = 71.1307\,\mathrm{N}$

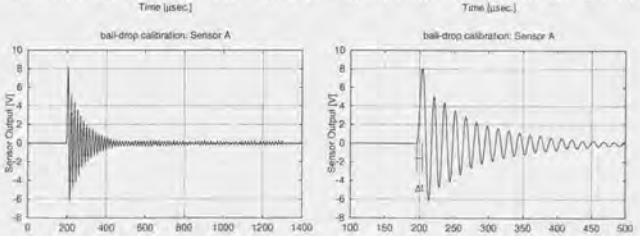

Fig. A.2: (continued)

$E_{\max} = 8.5781\,\mathrm{V}$
$\Delta t = 7.50\,\mu\mathrm{sec.}$
$F = 79.6663\,\mathrm{N}$

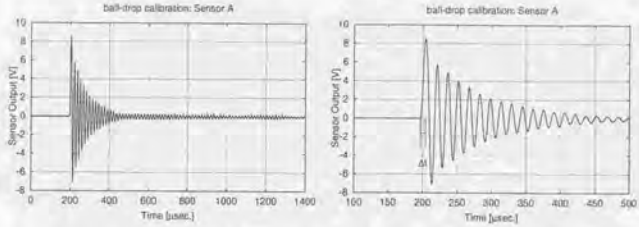

$E_{\max} = 8.2497\,\mathrm{V}$
$\Delta t = 9.30\,\mu\mathrm{sec.}$
$F = 64.2470\,\mathrm{N}$

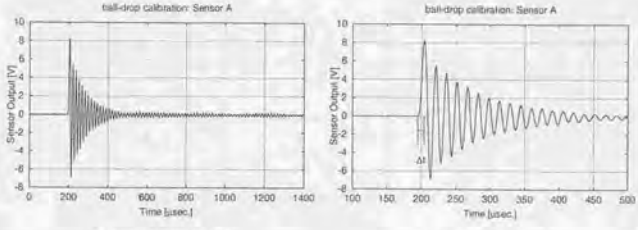

$E_{\max} = 8.4777\,\mathrm{V}$
$\Delta t = 7.55\,\mu\mathrm{sec.}$
$F = 79.1387\,\mathrm{N}$

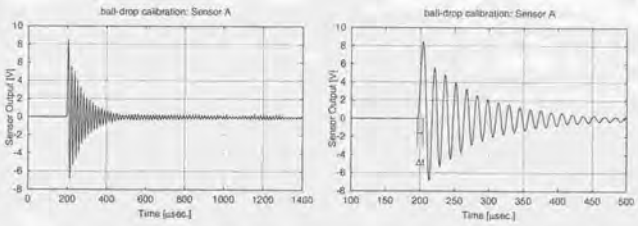

$E_{\max} = 8.6210\,\mathrm{V}$
$\Delta t = 7.60\,\mu\mathrm{sec.}$
$F = 78.6181\,\mathrm{N}$

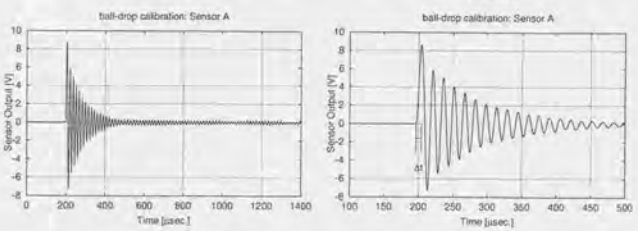

$E_{\max} = 8.6879\,\mathrm{V}$
$\Delta t = 7.60\,\mu\mathrm{sec.}$
$F = 78.6181\,\mathrm{N}$

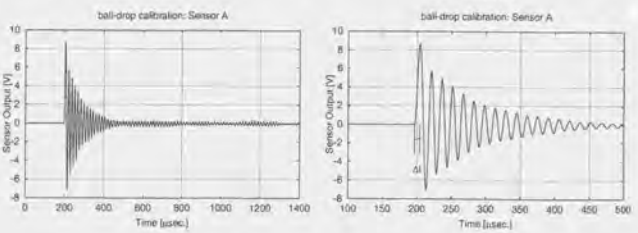

Fig. A.2: (continued)

$E_{\max} = 14.2563\,\mathrm{V}$
$\Delta t = 7.30\,\mu\mathrm{sec.}$
$F = 129.5834\,\mathrm{N}$

$E_{\max} = 14.6965\,\mathrm{V}$
$\Delta t = 6.95\,\mu\mathrm{sec.}$
$F = 138.9385\,\mathrm{N}$

$E_{\max} = 14.8411\,\mathrm{V}$
$\Delta t = 7.00\,\mu\mathrm{sec.}$
$F = 136.6562\,\mathrm{N}$

$E_{\max} = 14.5498\,\mathrm{V}$
$\Delta t = 7.25\,\mu\mathrm{sec.}$
$F = 131.9324\,\mathrm{N}$

$E_{\max} = 14.5708\,\mathrm{V}$
$\Delta t = 7.40\,\mu\mathrm{sec.}$
$F = 130.3599\,\mathrm{N}$

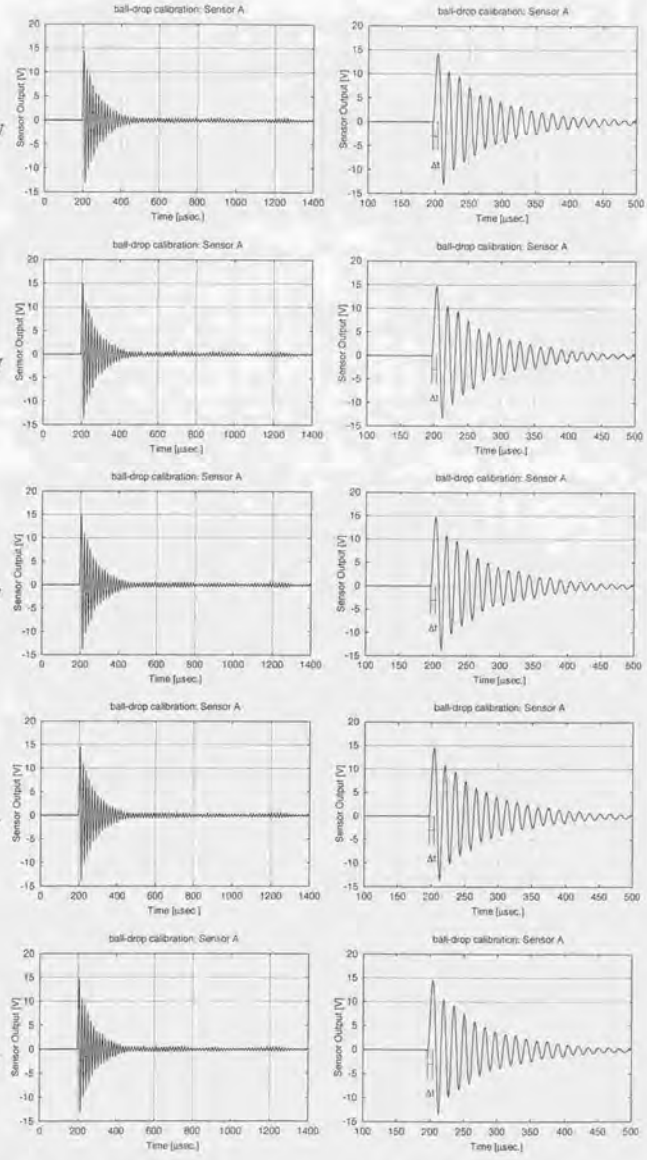

Fig. A.3: Output of Sensor A at ball-drop calibration. $m = 0.440\,\mathrm{g}$, $h = 80\,\mathrm{mm}$

$E_{\max} = 15.5820\,\mathrm{V}$
$\Delta t = 7.10\,\mu\mathrm{sec.}$
$F = 136.8674\,\mathrm{N}$

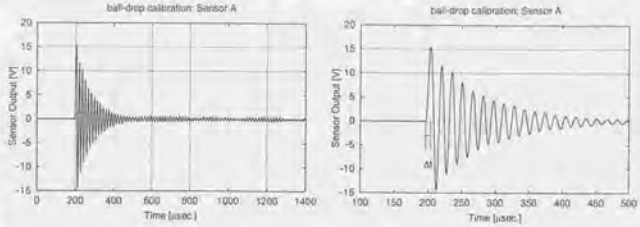

$E_{\max} = 12.5147\,\mathrm{V}$
$\Delta t = 7.35\,\mu\mathrm{sec.}$
$F = 128.5061\,\mathrm{N}$

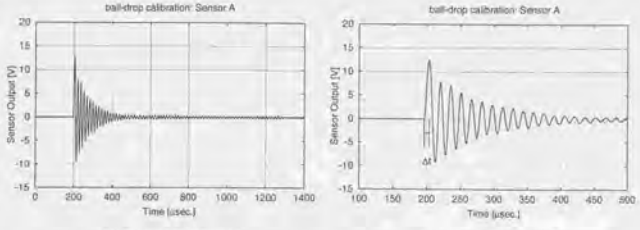

$E_{\max} = 13.1290\,\mathrm{V}$
$\Delta t = 7.45\,\mu\mathrm{sec.}$
$F = 126.7169\,\mathrm{N}$

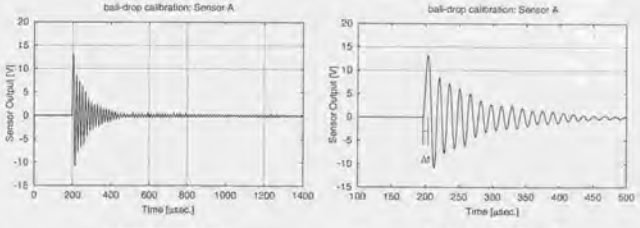

$E_{\max} = 14.1639\,\mathrm{V}$
$\Delta t = 7.40\,\mu\mathrm{sec.}$
$F = 129.1933\,\mathrm{N}$

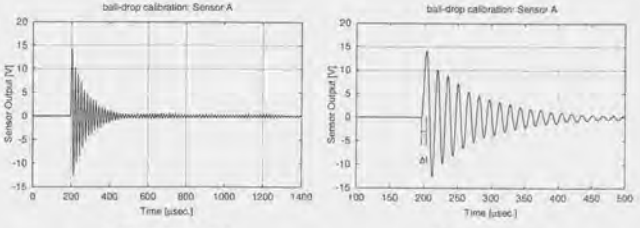

$E_{\max} = 14.6306\,\mathrm{V}$
$\Delta t = 7.40\,\mu\mathrm{sec.}$
$F = 129.2581\,\mathrm{N}$

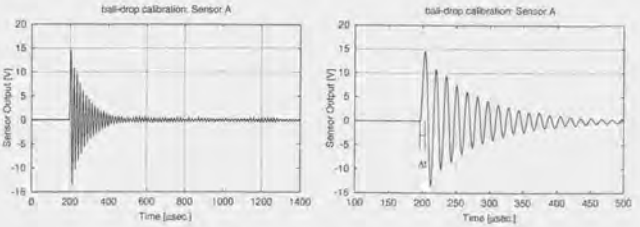

Fig. A.3: (continued)

$E_{\max} = 20.3467\,\mathrm{V}$
$\Delta t = 7.05\,\mu\mathrm{sec.}$
$F = 180.4704\,\mathrm{N}$

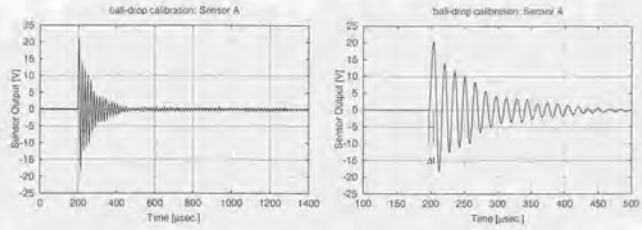

$E_{\max} = 22.1590\,\mathrm{V}$
$\Delta t = 6.80\,\mu\mathrm{sec.}$
$F = 187.3169\,\mathrm{N}$

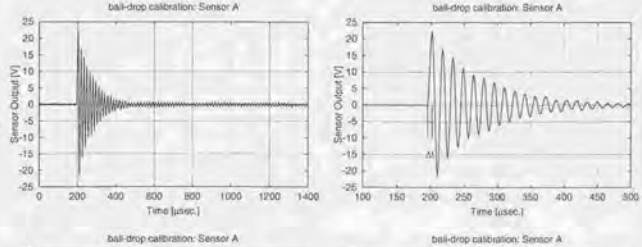

$E_{\max} = 22.6149\,\mathrm{V}$
$\Delta t = 6.90\,\mu\mathrm{sec.}$
$F = 185.5753\,\mathrm{N}$

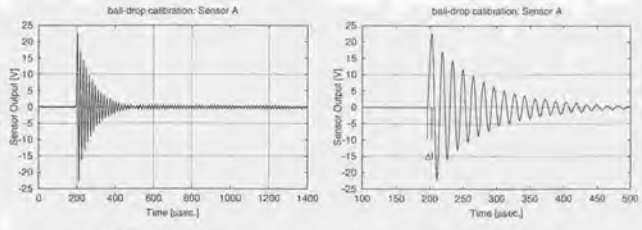

$E_{\max} = 23.0262\,\mathrm{V}$
$\Delta t = 6.90\,\mu\mathrm{sec.}$
$F = 186.4093\,\mathrm{N}$

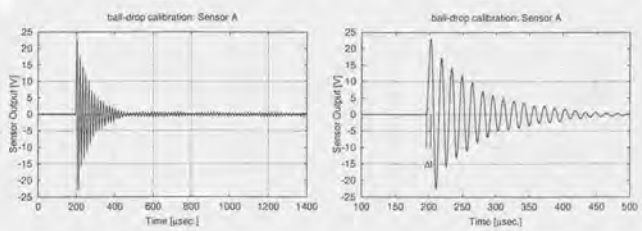

$E_{\max} = 23.8841\,\mathrm{V}$
$\Delta t = 7.05\,\mu\mathrm{sec.}$
$F = 183.3956\,\mathrm{N}$

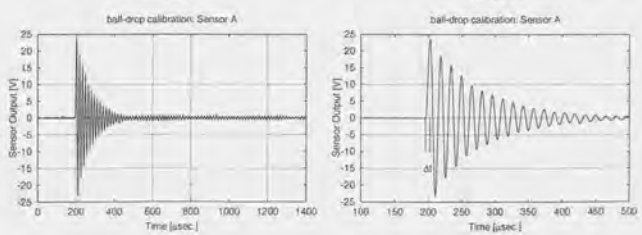

Fig. A.4: Output of Sensor A at ball-drop calibration. $m = 0.440\,\mathrm{g}$, $h = 150\,\mathrm{mm}$

$E_{\max} = 22.8021\,\mathrm{V}$
$\Delta t = 6.90\,\mu\mathrm{sec.}$
$F = 187.2434\,\mathrm{N}$

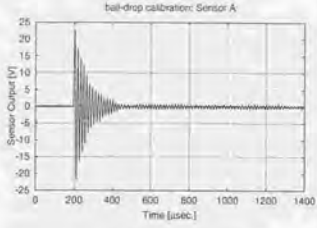

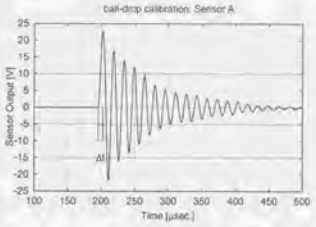

$E_{\max} = 24.3600\,\mathrm{V}$
$\Delta t = 6.70\,\mu\mathrm{sec.}$
$F = 193.3339\,\mathrm{N}$

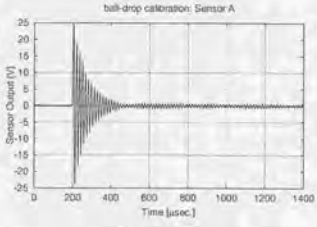

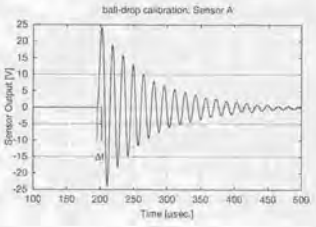

$E_{\max} = 21.8515\,\mathrm{V}$
$\Delta t = 6.95\,\mu\mathrm{sec.}$
$F = 183.4811\,\mathrm{N}$

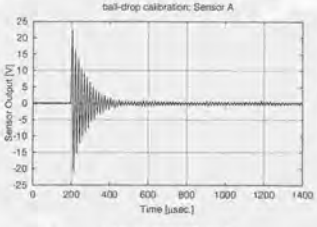

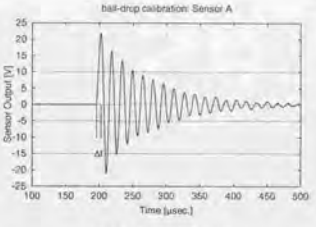

$E_{\max} = 21.9451\,\mathrm{V}$
$\Delta t = 7.20\,\mu\mathrm{sec.}$
$F = 177.9762\,\mathrm{N}$

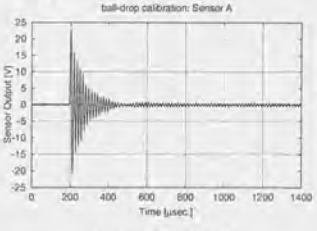

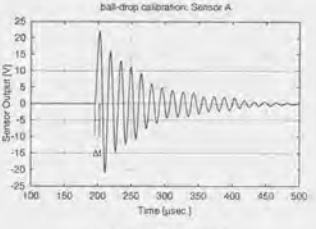

$E_{\max} = 22.4618\,\mathrm{V}$
$\Delta t = 7.05\,\mu\mathrm{sec.}$
$F = 181.6949\,\mathrm{N}$

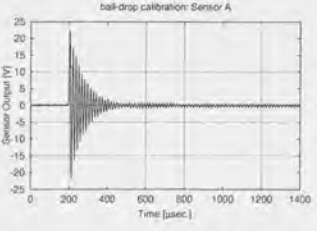

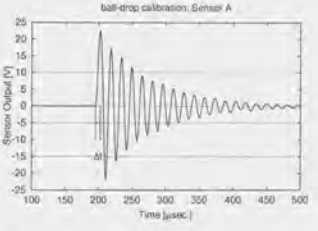

Fig. A.4: (continued)

$E_{\max} = 3.9956\,\mathrm{V}$
$\Delta t = 7.05\,\mu\mathrm{sec.}$
$F = 24.0923\,\mathrm{N}$

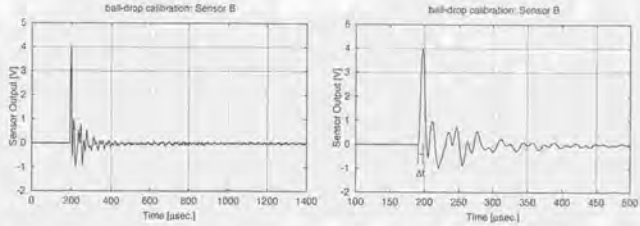

$E_{\max} = 4.2998\,\mathrm{V}$
$\Delta t = 6.80\,\mu\mathrm{sec.}$
$F = 24.9781\,\mathrm{N}$

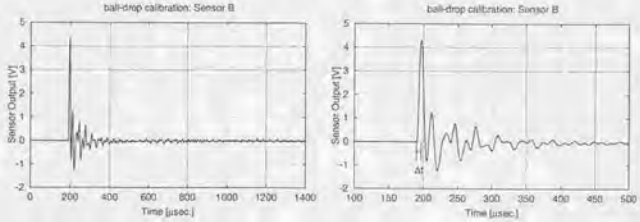

$E_{\max} = 4.3272\,\mathrm{V}$
$\Delta t = 7.15\,\mu\mathrm{sec.}$
$F = 23.7554\,\mathrm{N}$

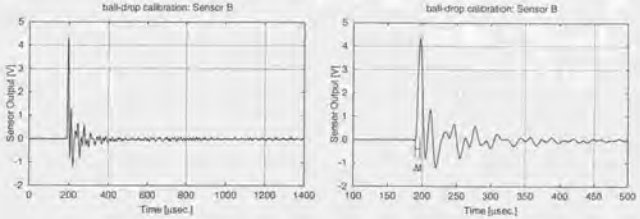

$E_{\max} = 4.1665\,\mathrm{V}$
$\Delta t = 8.00\,\mu\mathrm{sec.}$
$F = 21.2314\,\mathrm{N}$

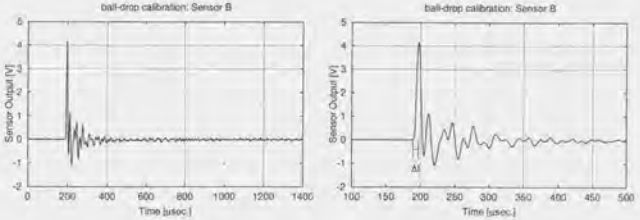

$E_{\max} = 4.3034\,\mathrm{V}$
$\Delta t = 7.50\,\mu\mathrm{sec.}$
$F = 22.6468\,\mathrm{N}$

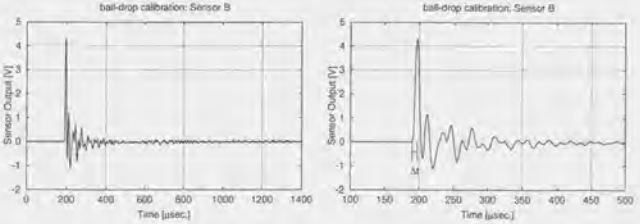

Fig. A.5: Output of Sensor B at ball-drop calibration. $m = 0.130\,\mathrm{g}$, $h = 30\,\mathrm{mm}$

$E_{\max} = 3.9732\,\mathrm{V}$
$\Delta t = 7.65\,\mu\mathrm{sec.}$
$F = 22.2027\,\mathrm{N}$

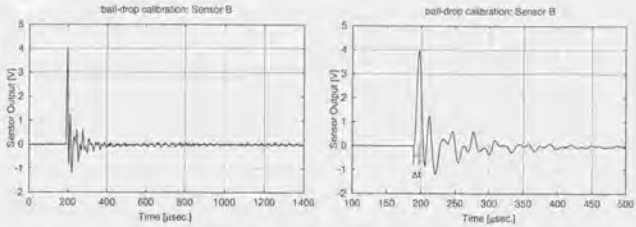

$E_{\max} = 3.8110\,\mathrm{V}$
$\Delta t = 7.35\,\mu\mathrm{sec.}$
$F = 23.1090\,\mathrm{N}$

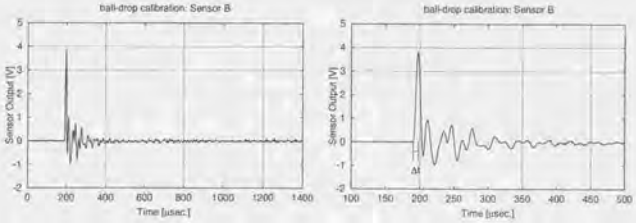

$E_{\max} = 4.2565\,\mathrm{V}$
$\Delta t = 6.70\,\mu\mathrm{sec.}$
$F = 25.3509\,\mathrm{N}$

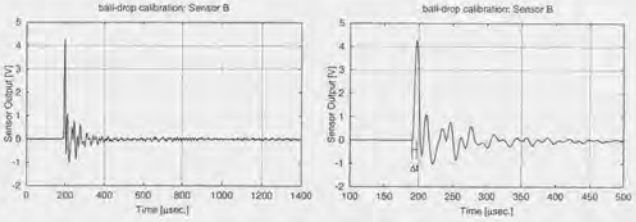

$E_{\max} = 3.9055\,\mathrm{V}$
$\Delta t = 7.50\,\mu\mathrm{sec.}$
$F = 22.6468\,\mathrm{N}$

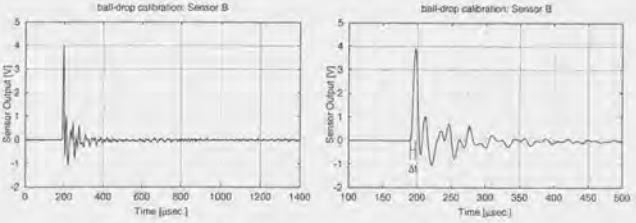

$E_{\max} = 4.5302\,\mathrm{V}$
$\Delta t = 6.85\,\mu\mathrm{sec.}$
$F = 24.7958\,\mathrm{N}$

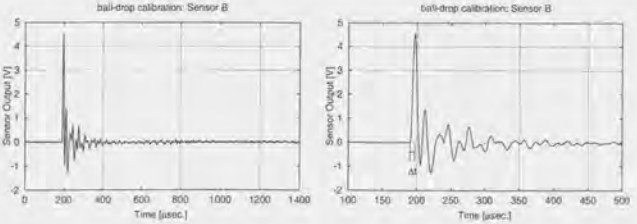

Fig. A.5: (continued)

$E_{\max} = 3.9786\,\mathrm{V}$
$\Delta t = 6.40\,\mu\mathrm{sec.}$
$F = 26.5392\,\mathrm{N}$

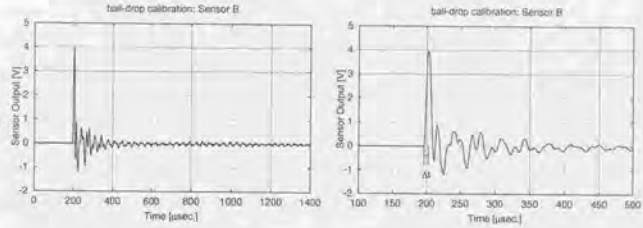

$E_{\max} = 3.9223\,\mathrm{V}$
$\Delta t = 5.05\,\mu\mathrm{sec.}$
$F = 33.6339\,\mathrm{N}$

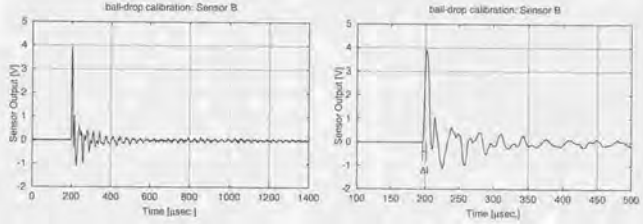

$E_{\max} = 3.8564\,\mathrm{V}$
$\Delta t = 6.60\,\mu\mathrm{sec.}$
$F = 25.7350\,\mathrm{N}$

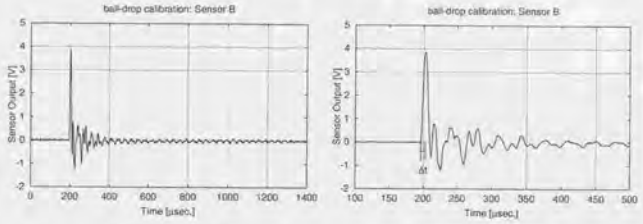

$E_{\max} = 3.5057\,\mathrm{V}$
$\Delta t = 7.10\,\mu\mathrm{sec.}$
$F = 23.9227\,\mathrm{N}$

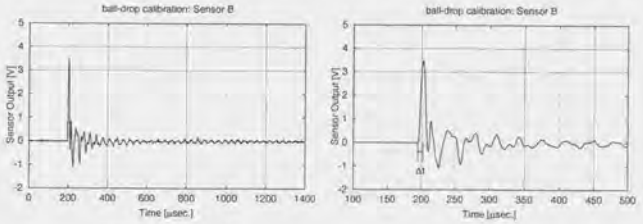

$E_{\max} = 3.7409\,\mathrm{V}$
$\Delta t = 7.05\,\mu\mathrm{sec.}$
$F = 24.0923\,\mathrm{N}$

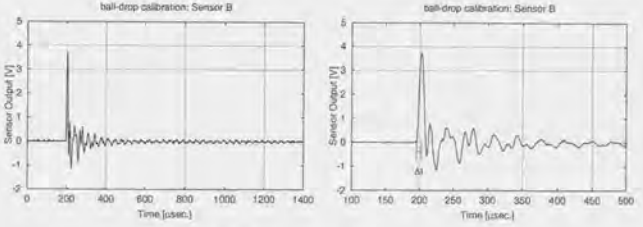

Fig. A.5: (continued)

$E_{\max} = 3.6446\,\mathrm{V}$
$\Delta t = 7.15\,\mu\mathrm{sec.}$
$F = 23.7554\,\mathrm{N}$

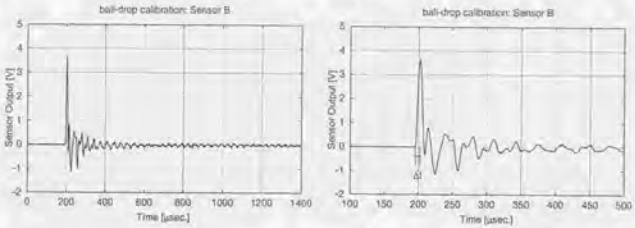

$E_{\max} = 3.9487\,\mathrm{V}$
$\Delta t = 5.75\,\mu\mathrm{sec.}$
$F = 29.5393\,\mathrm{N}$

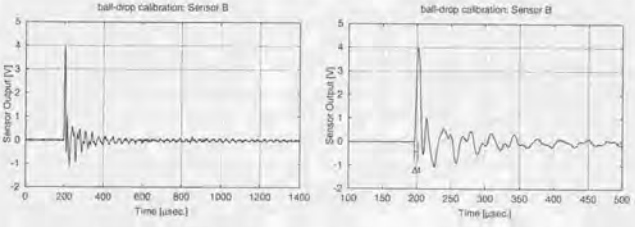

$E_{\max} = 4.5324\,\mathrm{V}$
$\Delta t = 5.20\,\mu\mathrm{sec.}$
$F = 32.6637\,\mathrm{N}$

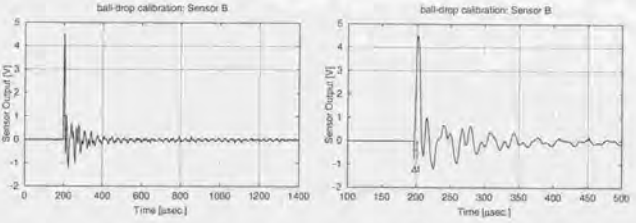

$E_{\max} = 3.9371\,\mathrm{V}$
$\Delta t = 6.85\,\mu\mathrm{sec.}$
$F = 24.7958\,\mathrm{N}$

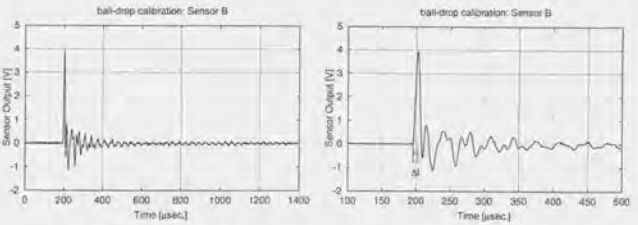

$E_{\max} = 4.7527\,\mathrm{V}$
$\Delta t = 4.95\,\mu\mathrm{sec.}$
$F = 34.3133\,\mathrm{N}$

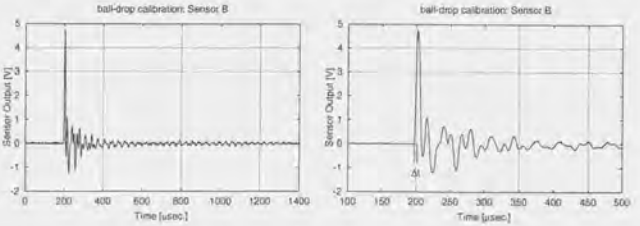

Fig. A.5: (continued)

$E_{\max} = 8.8055\,\mathrm{V}$
$\Delta t = 9.55\,\mu\mathrm{sec.}$
$F = 60.2322\,\mathrm{N}$

$E_{\max} = 7.6213\,\mathrm{V}$
$\Delta t = 10.60\,\mu\mathrm{sec.}$
$F = 54.2658\,\mathrm{N}$

$E_{\max} = 7.9057\,\mathrm{V}$
$\Delta t = 9.00\,\mu\mathrm{sec.}$
$F = 63.9131\,\mathrm{N}$

$E_{\max} = 7.7057\,\mathrm{V}$
$\Delta t = 11.70\,\mu\mathrm{sec.}$
$F = 49.1639\,\mathrm{N}$

$E_{\max} = 7.3368\,\mathrm{V}$
$\Delta t = 12.00\,\mu\mathrm{sec.}$
$F = 47.9348\,\mathrm{N}$

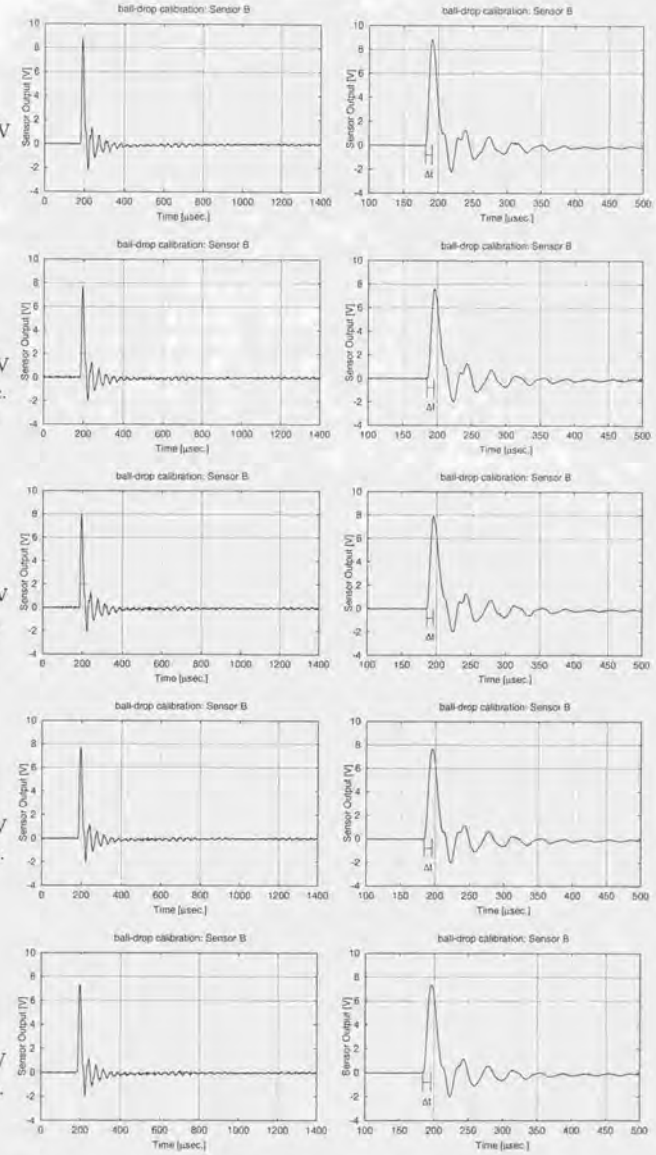

Fig. A.6: Output of Sensor B at ball-drop calibration. $m = 0.440\,g$, $h = 30\,\mathrm{mm}$

$E_{\max} = 9.7160\,\mathrm{V}$
$\Delta t = 11.65\,\mu\mathrm{sec.}$
$F = 49.3749\,\mathrm{N}$

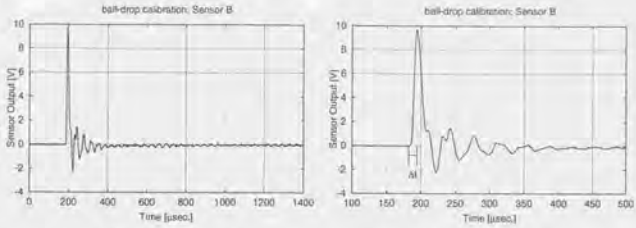

$E_{\max} = 7.4816\,\mathrm{V}$
$\Delta t = 10.60\,\mu\mathrm{sec.}$
$F = 54.2658\,\mathrm{N}$

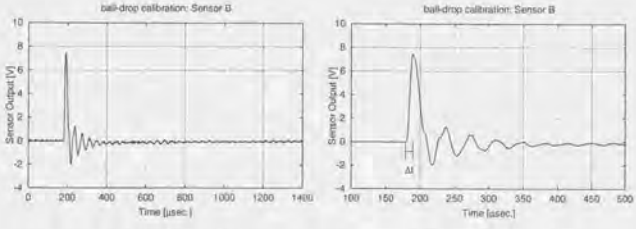

$E_{\max} = 8.1175\,\mathrm{V}$
$\Delta t = 9.10\,\mu\mathrm{sec.}$
$F = 63.2108\,\mathrm{N}$

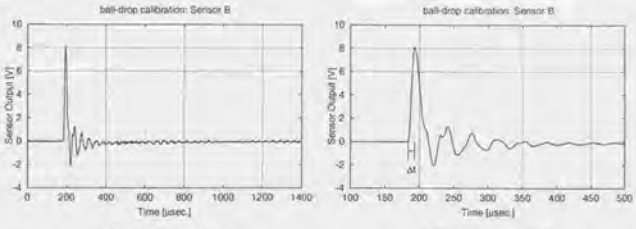

$E_{\max} = 7.3075\,\mathrm{V}$
$\Delta t = 10.55\,\mu\mathrm{sec.}$
$F = 54.5230\,\mathrm{N}$

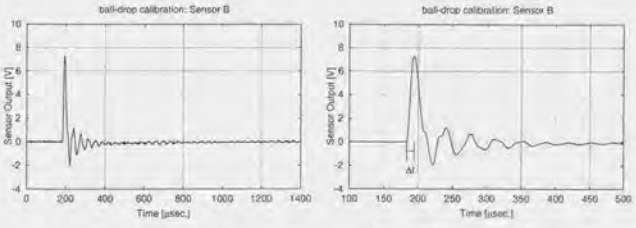

$E_{\max} = 7.9279\,\mathrm{V}$
$\Delta t = 9.75\,\mu\mathrm{sec.}$
$F = 58.9967\,\mathrm{N}$

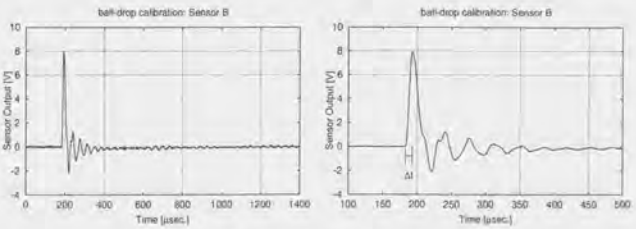

Fig. A.6: (continued)

$E_{\max} = 8.6622\,\mathrm{V}$
$\Delta t = 8.45\,\mu\mathrm{sec.}$
$F = 68.0731\,\mathrm{N}$

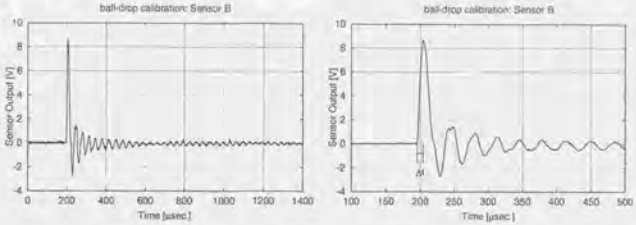

$E_{\max} = 8.0267\,\mathrm{V}$
$\Delta t = 9.05\,\mu\mathrm{sec.}$
$F = 63.5600\,\mathrm{N}$

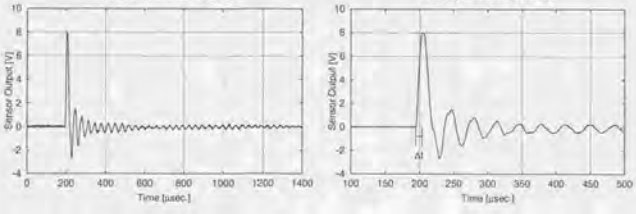

$E_{\max} = 7.5768\,\mathrm{V}$
$\Delta t = 10.55\,\mu\mathrm{sec.}$
$F = 54.5230\,\mathrm{N}$

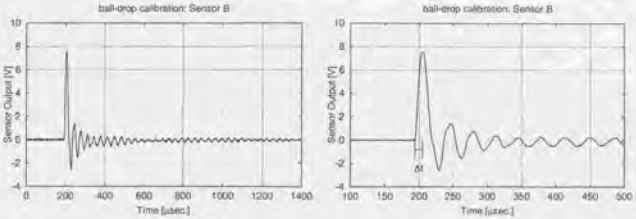

$E_{\max} = 8.9120\,\mathrm{V}$
$\Delta t = 8.65\,\mu\mathrm{sec.}$
$F = 66.4992\,\mathrm{N}$

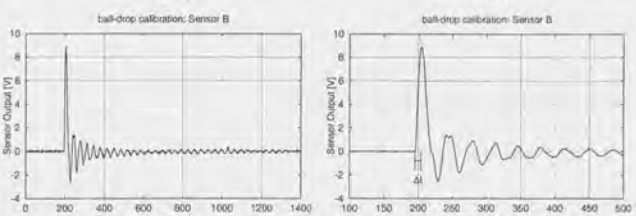

$E_{\max} = 6.5977\,\mathrm{V}$
$\Delta t = 13.15\,\mu\mathrm{sec.}$
$F = 43.7428\,\mathrm{N}$

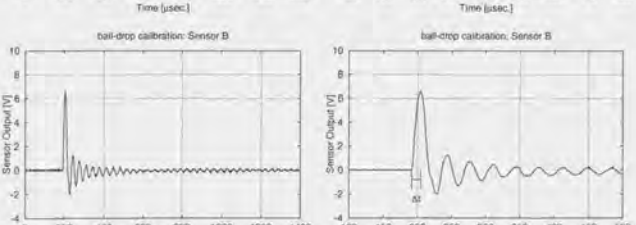

Fig. A.6: (continued)

$E_{\max} = 8.8935\,\mathrm{V}$
$\Delta t = 8.70\,\mu\mathrm{sec.}$
$F = 66.1170\,\mathrm{N}$

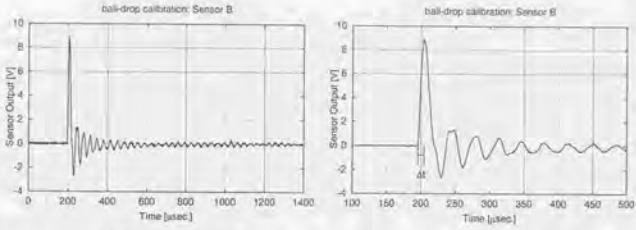

$E_{\max} = 7.9296\,\mathrm{V}$
$\Delta t = 11.10\,\mu\mathrm{sec.}$
$F = 51.8214\,\mathrm{N}$

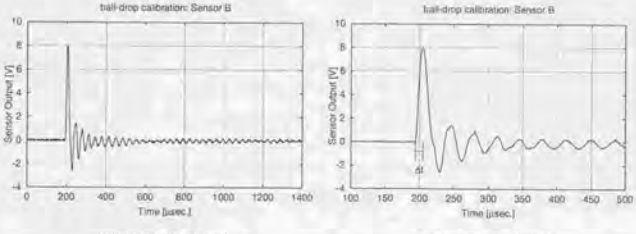

$E_{\max} = 8.3363\,\mathrm{V}$
$\Delta t = 9.20\,\mu\mathrm{sec.}$
$F = 62.5237\,\mathrm{N}$

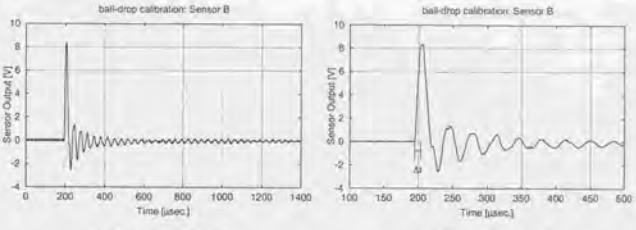

$E_{\max} = 8.0449\,\mathrm{V}$
$\Delta t = 10.10\,\mu\mathrm{sec.}$
$F = 56.9523\,\mathrm{N}$

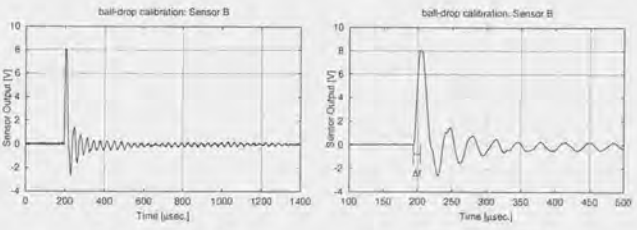

$E_{\max} = 7.6240\,\mathrm{V}$
$\Delta t = 9.60\,\mu\mathrm{sec.}$
$F = 59.9185\,\mathrm{N}$

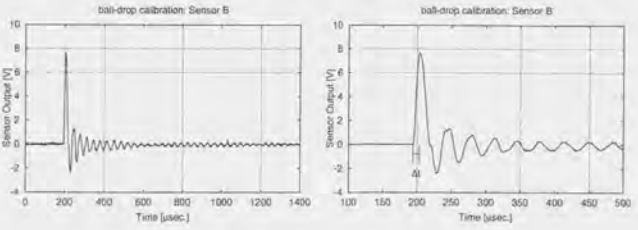

Fig. A.6: (continued)

$E_{\max} = 0.3152\,\mathrm{V}$
$\Delta t = 27.75\,\mu\mathrm{sec.}$
$F = 5.3921\,\mathrm{N}$

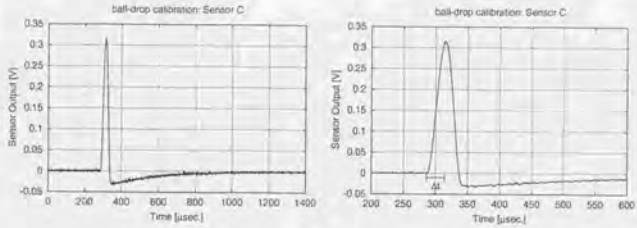

$E_{\max} = 0.3239\,\mathrm{V}$
$\Delta t = 26.30\,\mu\mathrm{sec.}$
$F = 5.6624\,\mathrm{N}$

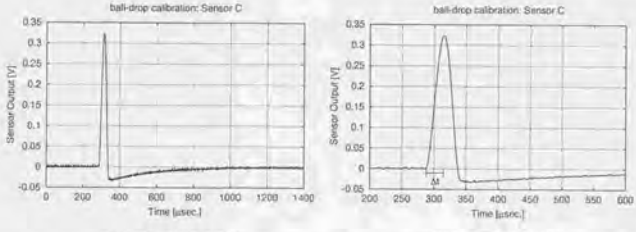

$E_{\max} = 0.3223\,\mathrm{V}$
$\Delta t = 26.40\,\mu\mathrm{sec.}$
$F = 5.6941\,\mathrm{N}$

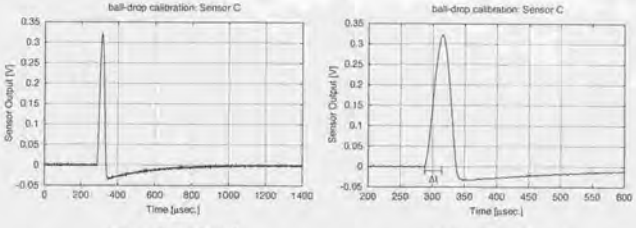

$E_{\max} = 0.3074\,\mathrm{V}$
$\Delta t = 38.50\,\mu\mathrm{sec.}$
$F = 3.8751\,\mathrm{N}$

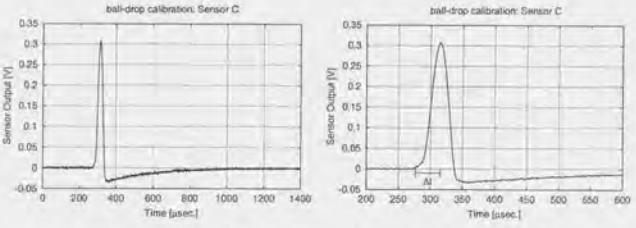

$E_{\max} = 0.2970\,\mathrm{V}$
$\Delta t = 33.30\,\mu\mathrm{sec.}$
$F = 4.4929\,\mathrm{N}$

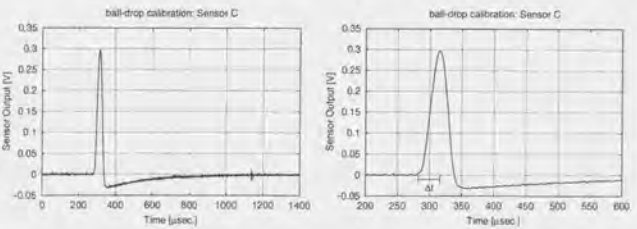

Fig. A.7: Output of Sensor C at ball-drop calibration. $m = 0.130\,\mathrm{g}$, $h = 30\,\mathrm{mm}$

$E_{\max} = 0.3284\,\mathrm{V}$
$\Delta t = 27.15\,\mu\mathrm{sec.}$
$F = 5.5162\,\mathrm{N}$

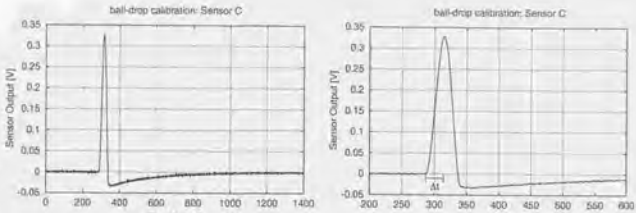

$E_{\max} = 0.3292\,\mathrm{V}$
$\Delta t = 26.80\,\mu\mathrm{sec.}$
$F = 5.6041\,\mathrm{N}$

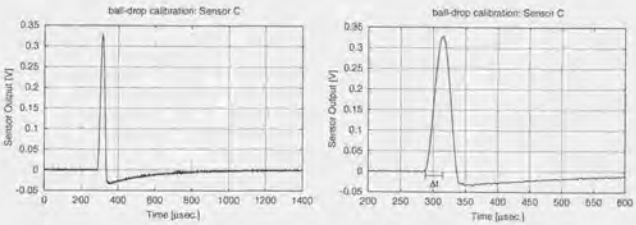

$E_{\max} = 0.3171\,\mathrm{V}$
$\Delta t = 28.10\,\mu\mathrm{sec.}$
$F = 5.3445\,\mathrm{N}$

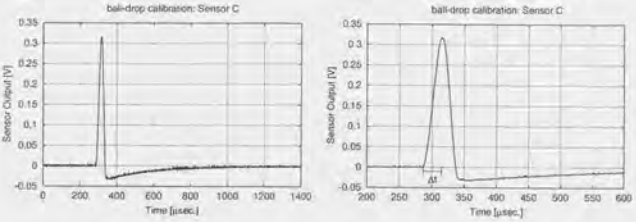

$E_{\max} = 0.3274\,\mathrm{V}$
$\Delta t = 26.65\,\mu\mathrm{sec.}$
$F = 5.6353\,\mathrm{N}$

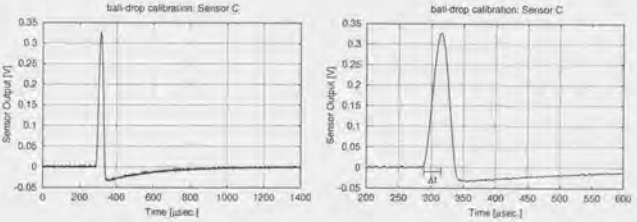

$E_{\max} = 0.3406\,\mathrm{V}$
$\Delta t = 26.40\,\mu\mathrm{sec.}$
$F = 5.7209\,\mathrm{N}$

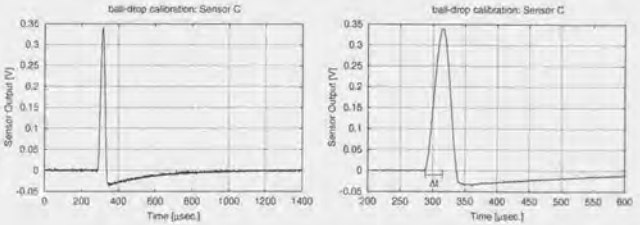

Fig. A.7: (continued)

$E_{\max} = 0.6268\,\mathrm{V}$
$\Delta t = 24.30\,\mu\mathrm{sec.}$
$F = 10.2595\,\mathrm{N}$

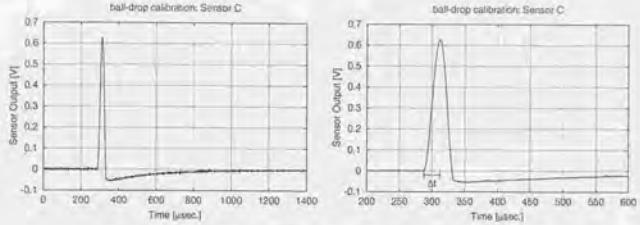

$E_{\max} = 0.3761\,\mathrm{V}$
$\Delta t = 23.20\,\mu\mathrm{sec.}$
$F = 10.7520\,\mathrm{N}$

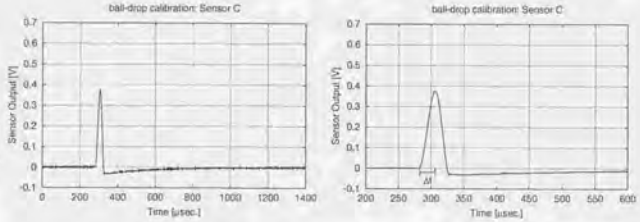

$E_{\max} = 0.6407\,\mathrm{V}$
$\Delta t = 23.45\,\mu\mathrm{sec.}$
$F = 10.6858\,\mathrm{N}$

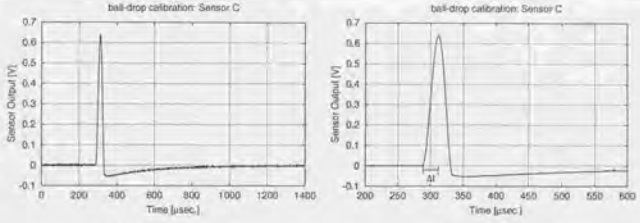

$E_{\max} = 0.6135\,\mathrm{V}$
$\Delta t = 23.05\,\mu\mathrm{sec.}$
$F = 10.8589\,\mathrm{N}$

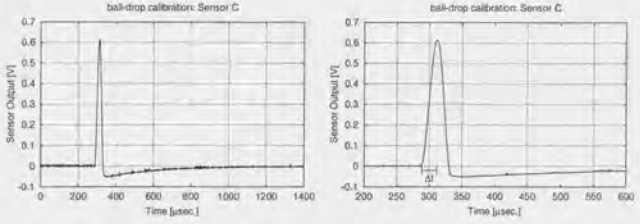

$E_{\max} = 0.6477\,\mathrm{V}$
$\Delta t = 24.60\,\mu\mathrm{sec.}$
$F = 10.1401\,\mathrm{N}$

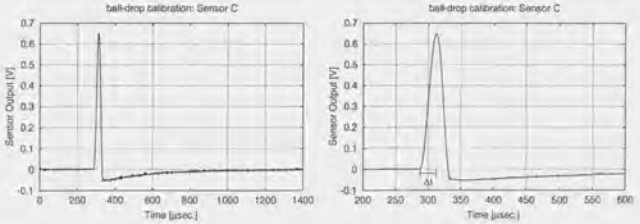

Fig. A.8: Output of Sensor C at ball-drop calibration. $m = 0.130\,\mathrm{g}$, $h = 80\,\mathrm{mm}$

$E_{\max} = 0.4801\,\mathrm{V}$
$\Delta t = 40.70\,\mu\mathrm{sec.}$
$F = 5.9931\,\mathrm{N}$

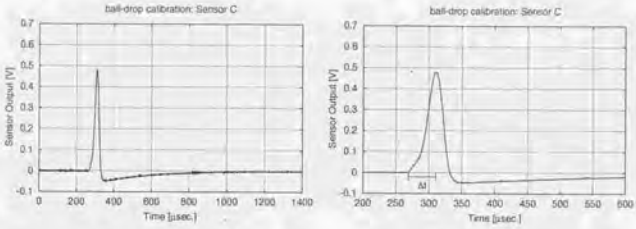

$E_{\max} = 0.6466\,\mathrm{V}$
$\Delta t = 25.90\,\mu\mathrm{sec.}$
$F = 9.6202\,\mathrm{N}$

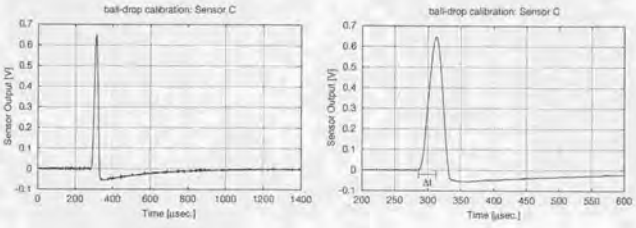

$E_{\max} = 0.4458\,\mathrm{V}$
$\Delta t = 27.90\,\mu\mathrm{sec.}$
$F = 8.8595\,\mathrm{N}$

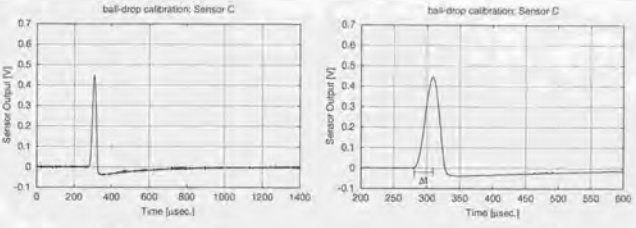

$E_{\max} = 0.4888\,\mathrm{V}$
$\Delta t = 23.85\,\mu\mathrm{sec.}$
$F = 10.5006\,\mathrm{N}$

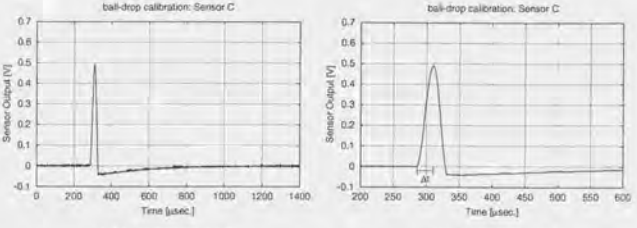

$E_{\max} = 0.6371\,\mathrm{V}$
$\Delta t = 24.10\,\mu\mathrm{sec.}$
$F = 10.3564\,\mathrm{N}$

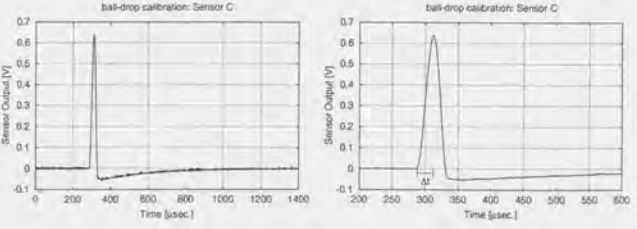

Fig. A.8: (continued)

$E_{\max} = 0.8532\,\mathrm{V}$
$\Delta t = 36.05\,\mu\mathrm{sec.}$
$F = 14.8051\,\mathrm{N}$

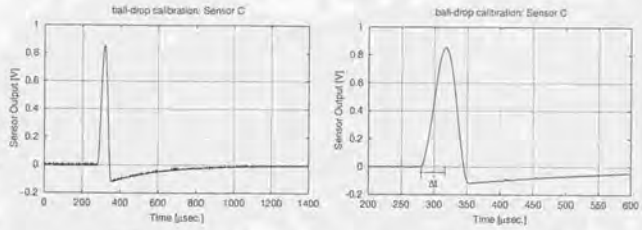

$E_{\max} = 0.8919\,\mathrm{V}$
$\Delta t = 34.65\,\mu\mathrm{sec.}$
$F = 15.3633\,\mathrm{N}$

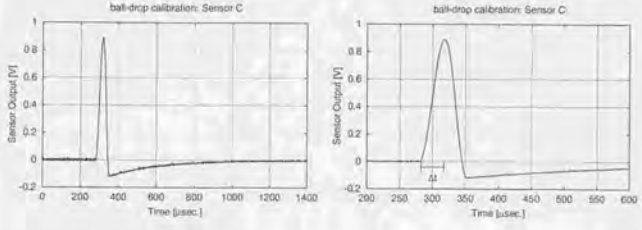

$E_{\max} = 0.8834\,\mathrm{V}$
$\Delta t = 34.40\,\mu\mathrm{sec.}$
$F = 15.4610\,\mathrm{N}$

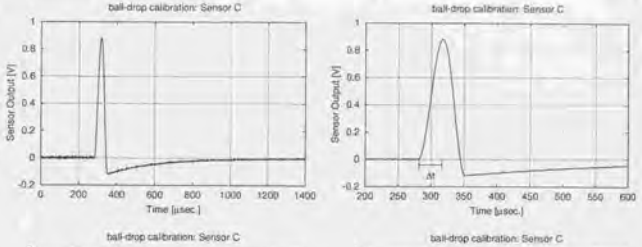

$E_{\max} = 0.8629\,\mathrm{V}$
$\Delta t = 37.40\,\mu\mathrm{sec.}$
$F = 14.3220\,\mathrm{N}$

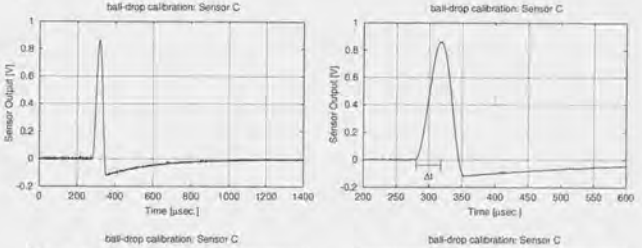

$E_{\max} = 0.8718\,\mathrm{V}$
$\Delta t = 35.10\,\mu\mathrm{sec.}$
$F = 15.2742\,\mathrm{N}$

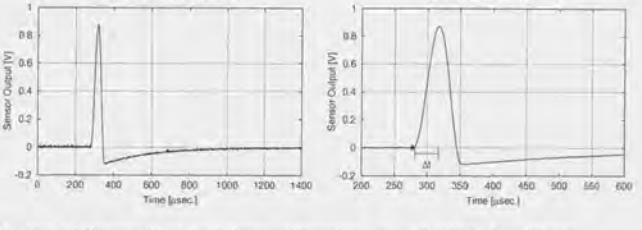

Fig. A.9: Output of Sensor C at ball-drop calibration. $m = 0.440\,\mathrm{g}$, $h = 30\,\mathrm{mm}$

$E_{\max} = 0.8362\,\mathrm{V}$
$\Delta t = 38.15\,\mu\mathrm{sec.}$
$F = 13.8533\,\mathrm{N}$

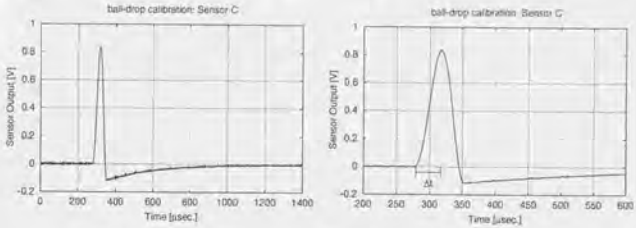

$E_{\max} = 0.8717\,\mathrm{V}$
$\Delta t = 36.85\,\mu\mathrm{sec.}$
$F = 14.6509\,\mathrm{N}$

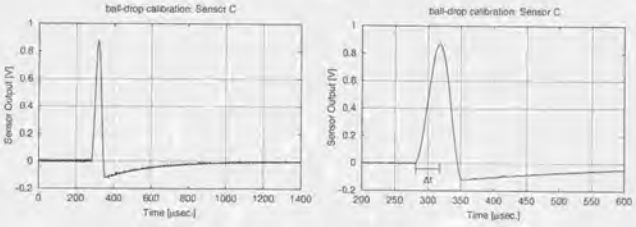

$E_{\max} = 0.8598\,\mathrm{V}$
$\Delta t = 35.95\,\mu\mathrm{sec.}$
$F = 14.8463\,\mathrm{N}$

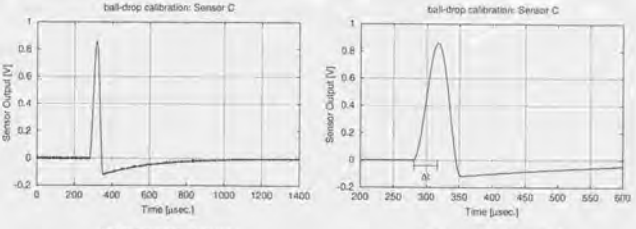

$E_{\max} = 0.8592\,\mathrm{V}$
$\Delta t = 36.60\,\mu\mathrm{sec.}$
$F = 14.5827\,\mathrm{N}$

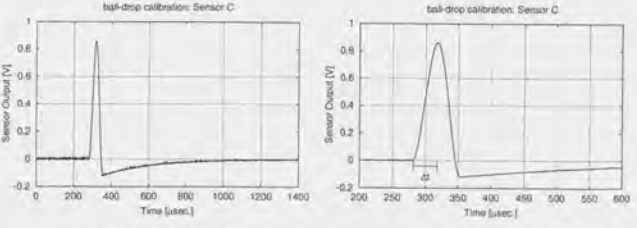

$E_{\max} = 0.8639\,\mathrm{V}$
$\Delta t = 36.35\,\mu\mathrm{sec.}$
$F = 14.7093\,\mathrm{N}$

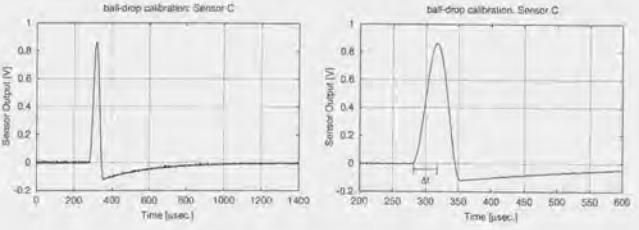

Fig. A.9: (continued)

$E_{\max} = 1.7310\,\mathrm{V}$
$\Delta t = 30.15\,\mu\mathrm{sec.}$
$F = 30.1502\,\mathrm{N}$

$E_{\max} = 1.4920\,\mathrm{V}$
$\Delta t = 39.05\,\mu\mathrm{sec.}$
$F = 23.0084\,\mathrm{N}$

$E_{\max} = 1.5547\,\mathrm{V}$
$\Delta t = 31.10\,\mu\mathrm{sec.}$
$F = 29.1830\,\mathrm{N}$

$E_{\max} = 1.6906\,\mathrm{V}$
$\Delta t = 30.25\,\mu\mathrm{sec.}$
$F = 30.0347\,\mathrm{N}$

$E_{\max} = 1.7071\,\mathrm{V}$
$\Delta t = 30.70\,\mu\mathrm{sec.}$
$F = 29.6570\,\mathrm{N}$

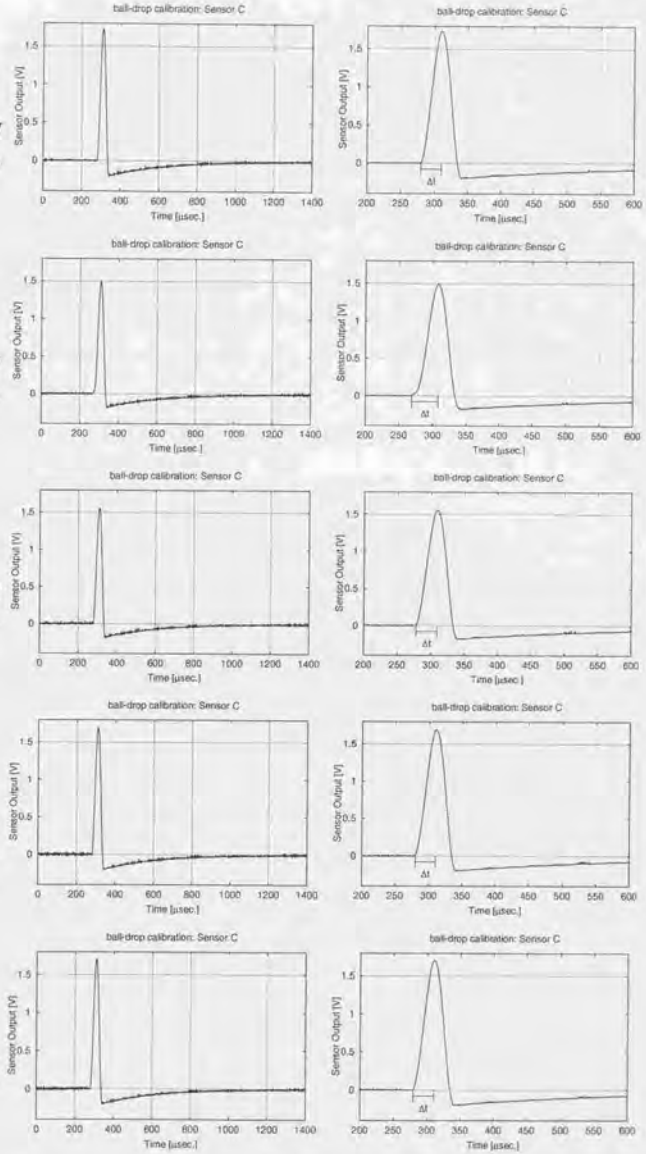

Fig. A.10: Output of Sensor C at ball-drop calibration. $m = 0.440\,\mathrm{g}$, $h = 80\,\mathrm{mm}$

$E_{\max} = 1.7174\,\mathrm{V}$
$\Delta t = 31.70\,\mu\mathrm{sec.}$
$F = 28.6911\,\mathrm{N}$

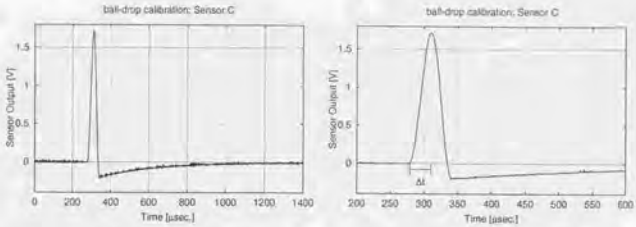

$E_{\max} = 1.6048\,\mathrm{V}$
$\Delta t = 30.50\,\mu\mathrm{sec.}$
$F = 30.2131\,\mathrm{N}$

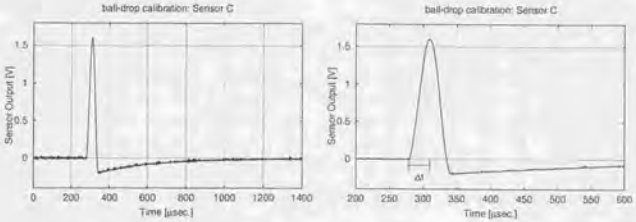

$E_{\max} = 1.7719\,\mathrm{V}$
$\Delta t = 30.00\,\mu\mathrm{sec.}$
$F = 30.3649\,\mathrm{N}$

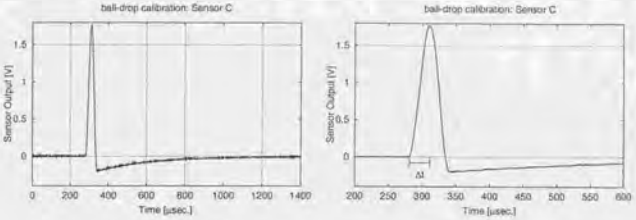

$E_{\max} = 1.4823\,\mathrm{V}$
$\Delta t = 30.95\,\mu\mathrm{sec.}$
$F = 29.3864\,\mathrm{N}$

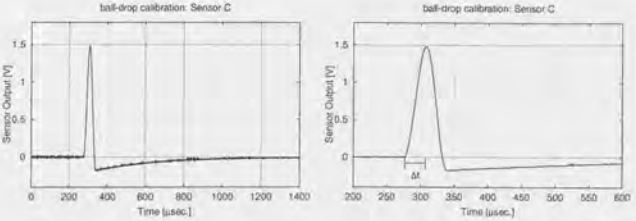

$E_{\max} = 1.6488\,\mathrm{V}$
$\Delta t = 30.95\,\mu\mathrm{sec.}$
$F = 29.2779\,\mathrm{N}$

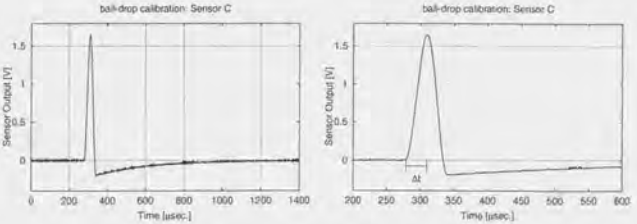

Fig. A.10: (continued)

$E_{\max} = 2.4455\,\mathrm{V}$
$\Delta t = 52.75\,\mu\mathrm{sec.}$
$F = 49.6662\,\mathrm{N}$

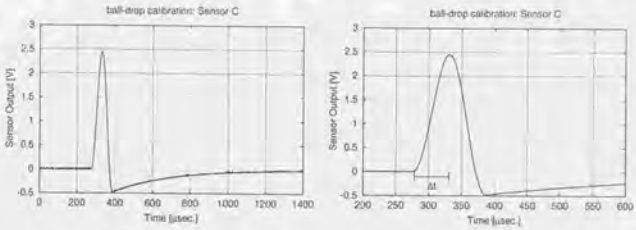

$E_{\max} = 2.5984\,\mathrm{V}$
$\Delta t = 52.55\,\mu\mathrm{sec.}$
$F = 50.1849\,\mathrm{N}$

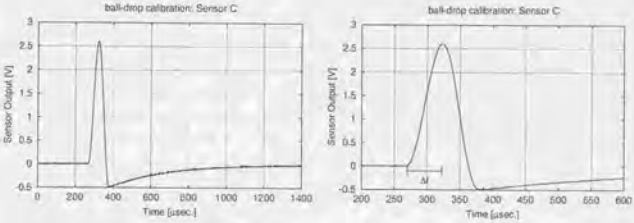

$E_{\max} = 2.7001\,\mathrm{V}$
$\Delta t = 51.90\,\mu\mathrm{sec.}$
$F = 51.3251\,\mathrm{N}$

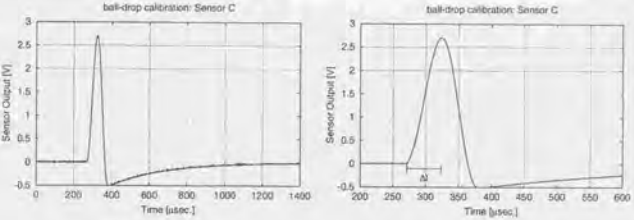

$E_{\max} = 2.1160\,\mathrm{V}$
$\Delta t = 53.15\,\mu\mathrm{sec.}$
$F = 49.1651\,\mathrm{N}$

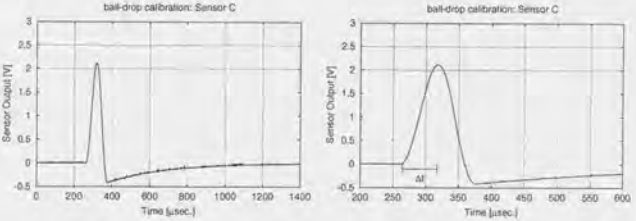

$E_{\max} = 2.5234\,\mathrm{V}$
$\Delta t = 55.30\,\mu\mathrm{sec.}$
$F = 46.4961\,\mathrm{N}$

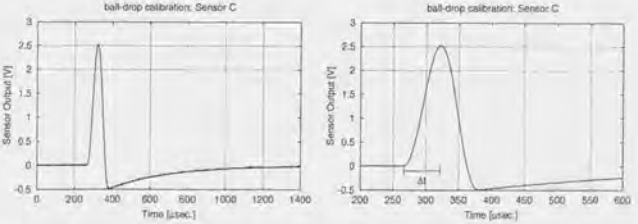

Fig. A.11: Output of Sensor C at ball-drop calibration. $m = 2.030\,\mathrm{g}$, $h = 30\,\mathrm{mm}$

$E_{\max} = 2.6043\,\mathrm{V}$
$\Delta t = 52.80\,\mu\mathrm{sec.}$
$F = 50.5759\,\mathrm{N}$

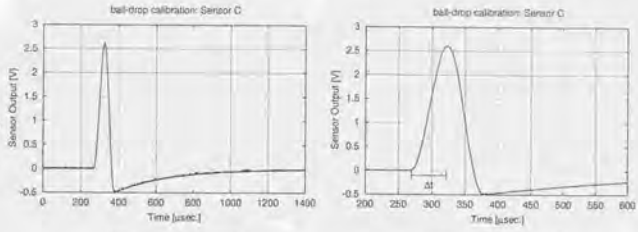

$E_{\max} = 2.8031\,\mathrm{V}$
$\Delta t = 52.10\,\mu\mathrm{sec.}$
$F = 51.3829\,\mathrm{N}$

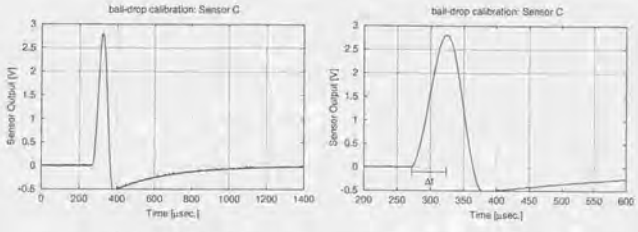

$E_{\max} = 2.5325\,\mathrm{V}$
$\Delta t = 54.55\,\mu\mathrm{sec.}$
$F = 49.6430\,\mathrm{N}$

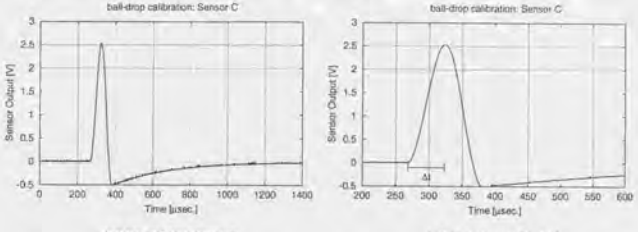

$E_{\max} = 2.7520\,\mathrm{V}$
$\Delta t = 55.65\,\mu\mathrm{sec.}$
$F = 47.5484\,\mathrm{N}$

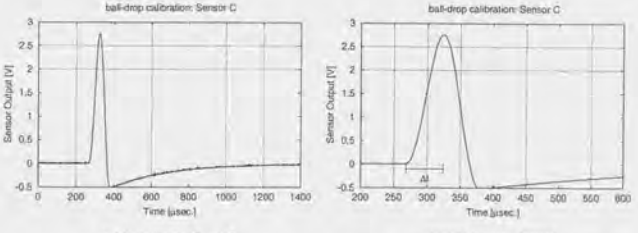

$E_{\max} = 2.7082\,\mathrm{V}$
$\Delta t = 56.80\,\mu\mathrm{sec.}$
$F = 46.8974\,\mathrm{N}$

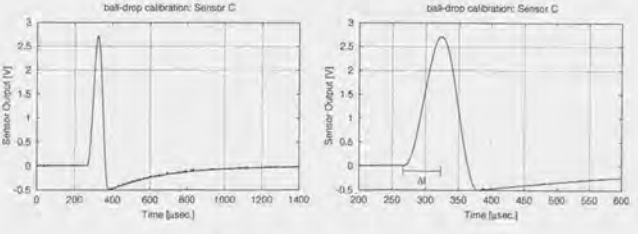

Fig. A.11: (continued)

$E_{\max} = 5.1152\,\mathrm{V}$
$\Delta t = 44.30\,\mu\mathrm{sec.}$
$F = 101.8637\,\mathrm{N}$

$E_{\max} = 4.9360\,\mathrm{V}$
$\Delta t = 44.45\,\mu\mathrm{sec.}$
$F = 101.5199\,\mathrm{N}$

$E_{\max} = 5.4179\,\mathrm{V}$
$\Delta t = 50.45\,\mu\mathrm{sec.}$
$F = 89.1831\,\mathrm{N}$

$E_{\max} = 5.4656\,\mathrm{V}$
$\Delta t = 43.55\,\mu\mathrm{sec.}$
$F = 103.8212\,\mathrm{N}$

$E_{\max} = 5.3578\,\mathrm{V}$
$\Delta t = 46.70\,\mu\mathrm{sec.}$
$F = 96.8183\,\mathrm{N}$

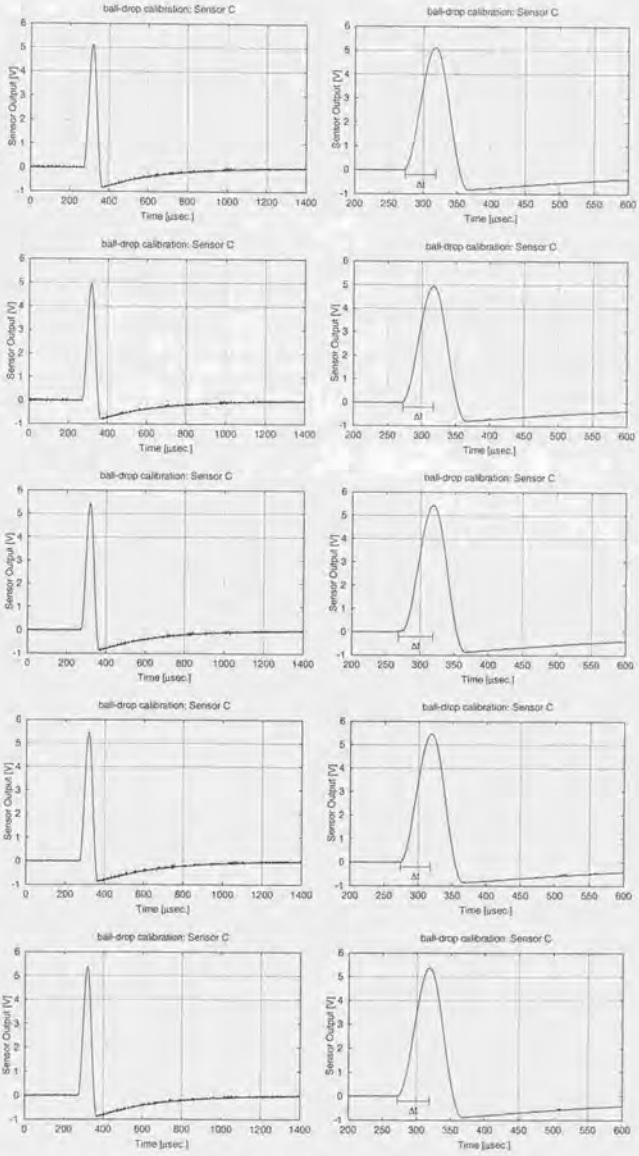

Fig. A.12: Output of Sensor C at ball-drop calibration. $m = 2.030\,\mathrm{g}$, $h = 80\,\mathrm{mm}$

$E_{\max} = 5.3871\,\mathrm{V}$
$\Delta t = 45.75\,\mu\mathrm{sec.}$
$F = 98.7320\,\mathrm{N}$

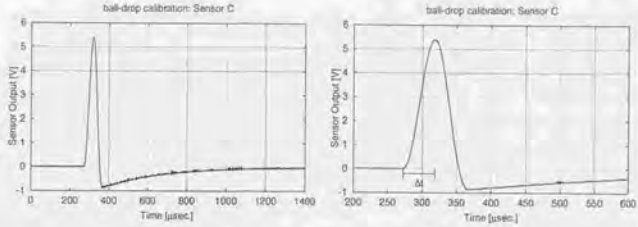

$E_{\max} = 5.2290\,\mathrm{V}$
$\Delta t = 45.90\,\mu\mathrm{sec.}$
$F = 98.0236\,\mathrm{N}$

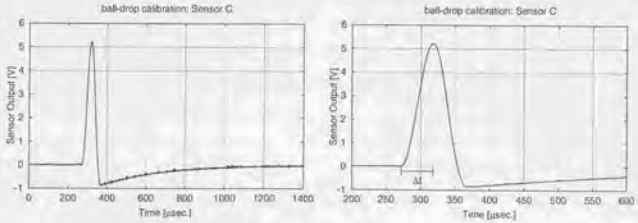

$E_{\max} = 5.3286\,\mathrm{V}$
$\Delta t = 44.20\,\mu\mathrm{sec.}$
$F = 102.2944\,\mathrm{N}$

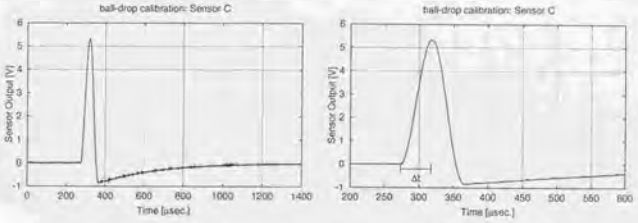

$E_{\max} = 5.3266\,\mathrm{V}$
$\Delta t = 46.05\,\mu\mathrm{sec.}$
$F = 98.0888\,\mathrm{N}$

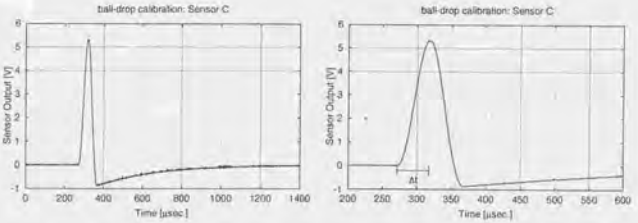

$E_{\max} = 5.2458\,\mathrm{V}$
$\Delta t = 46.00\,\mu\mathrm{sec.}$
$F = 97.8106\,\mathrm{N}$

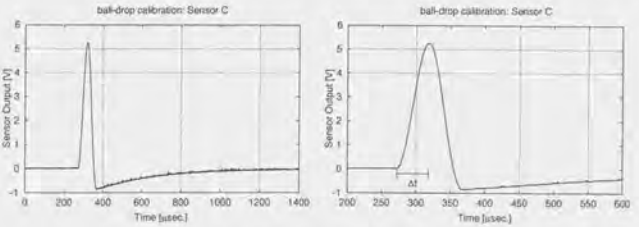

Fig. A.12: (continued)

付 録B　衝撃力センサの実験時の出力波形

第1部にて説明した3種の衝撃力センサの、キャビテーション衝撃力計測時の出力波形を示す。

この実験に関する詳細は第5章～第6章にて説明しているので、ここでは実験条件のみを示す。実験は、迎角8°、流速8m/sec.、キャビテーション数$\sigma_B = 1.25$の条件下で行った。この条件では周期的なクラウドキャビテーションが発生する。

なおそれぞれの波形は、計測された過渡電圧そのものである。各センサごとに、電圧の低い順に並べた。グラフの値域(y軸の幅)は各波形を詳しく見るために波形の最大、最小値に合わせて調整してあるので、グラフによってバラバラである。

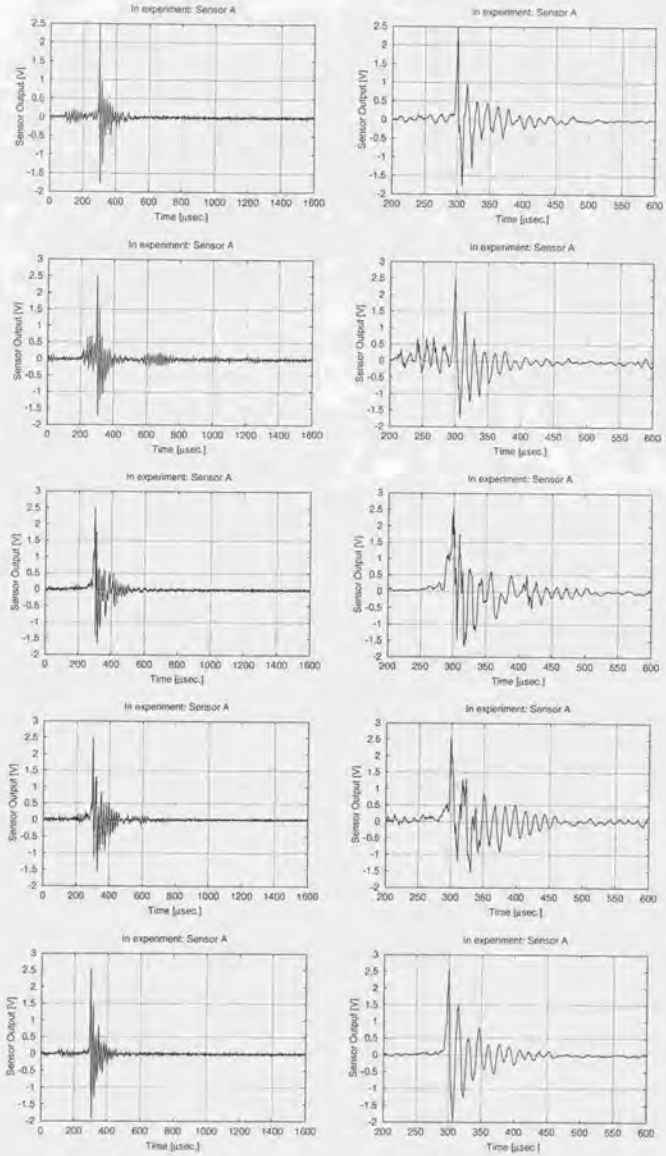

Fig. B.1: Produced signal of sensor A in experiment

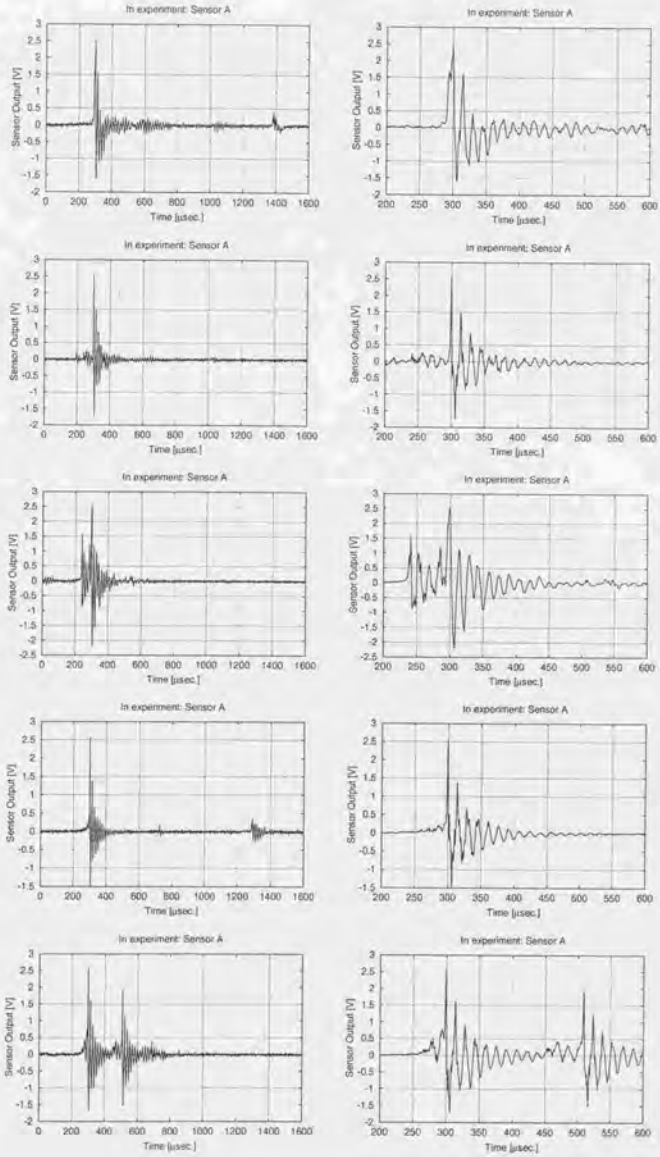

Fig. B.1: (continued)

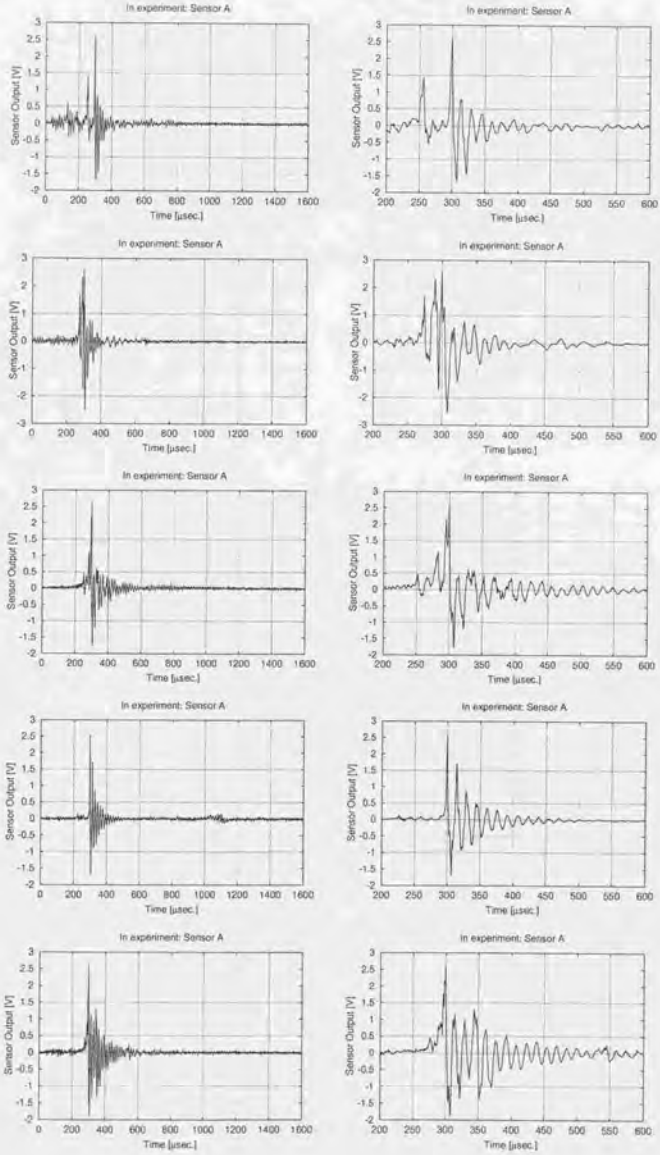

Fig. B.1: (continued)

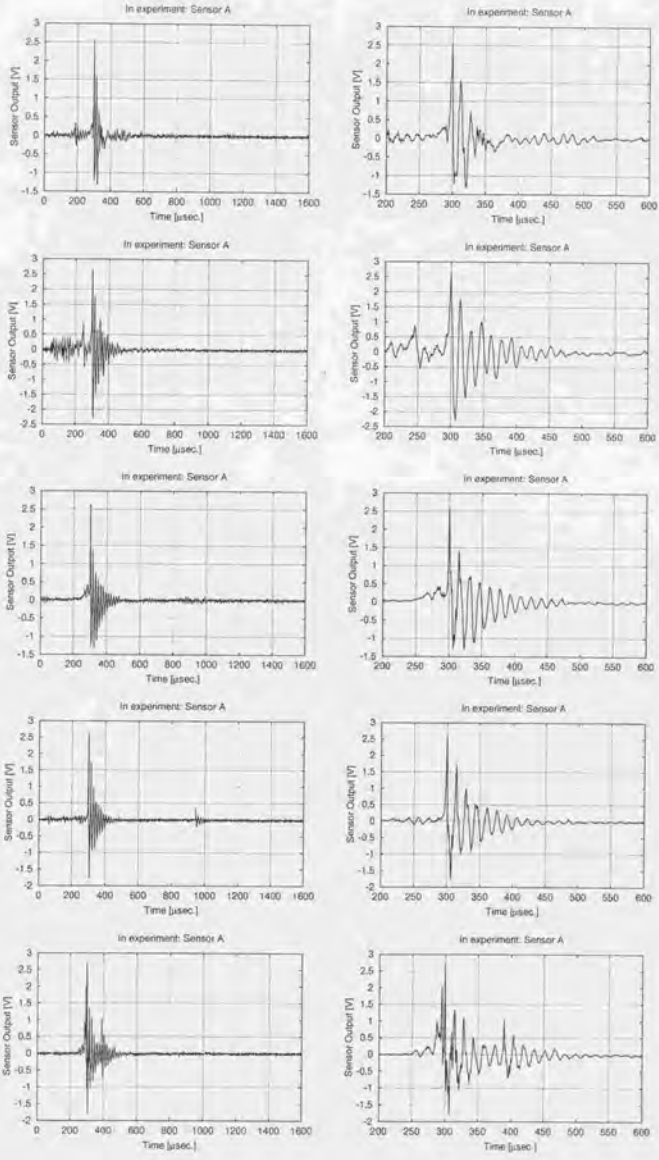

Fig. B.1: (continued)

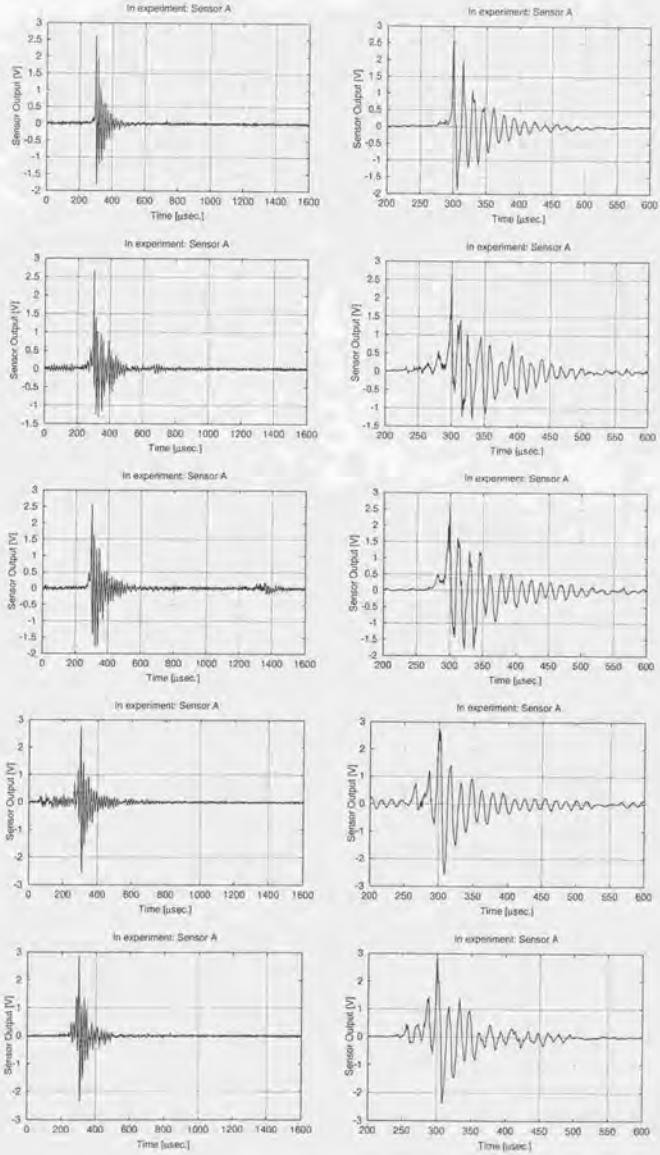

Fig. B.1: (continued)

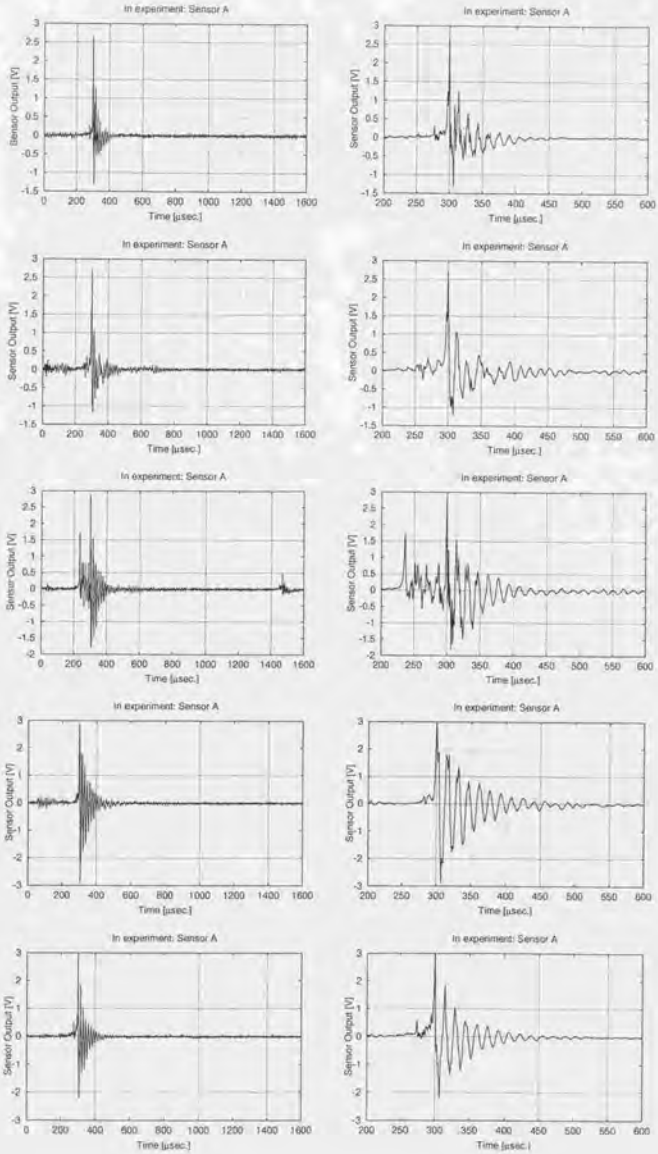

Fig. B.1: (continued)

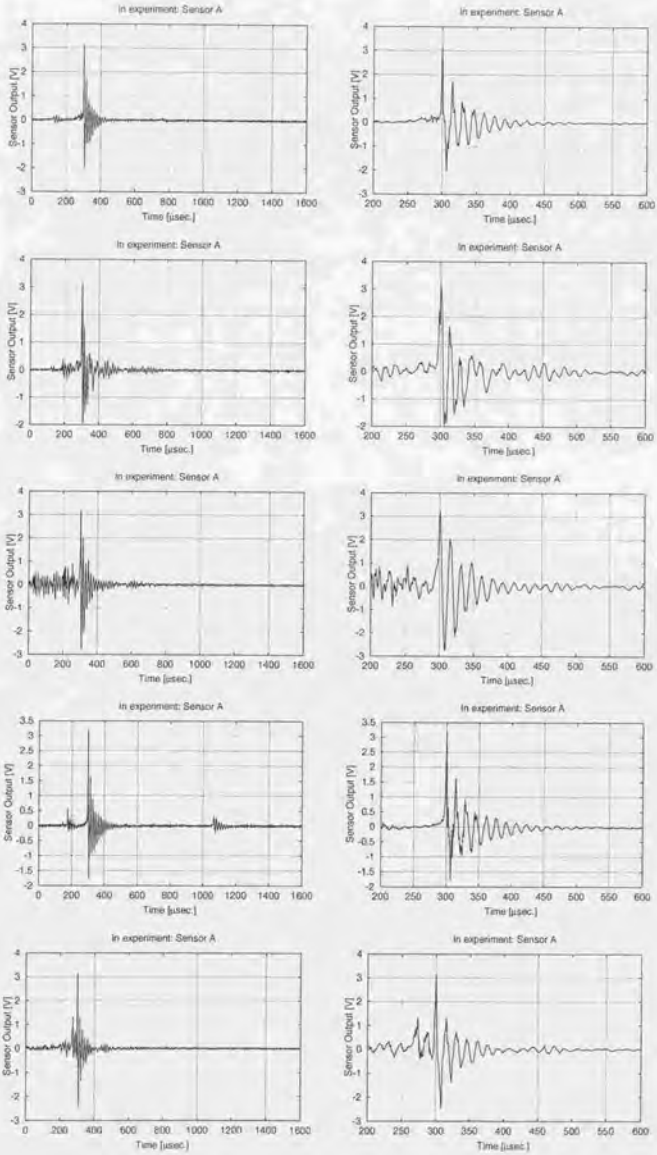

Fig. B.1: (continued)

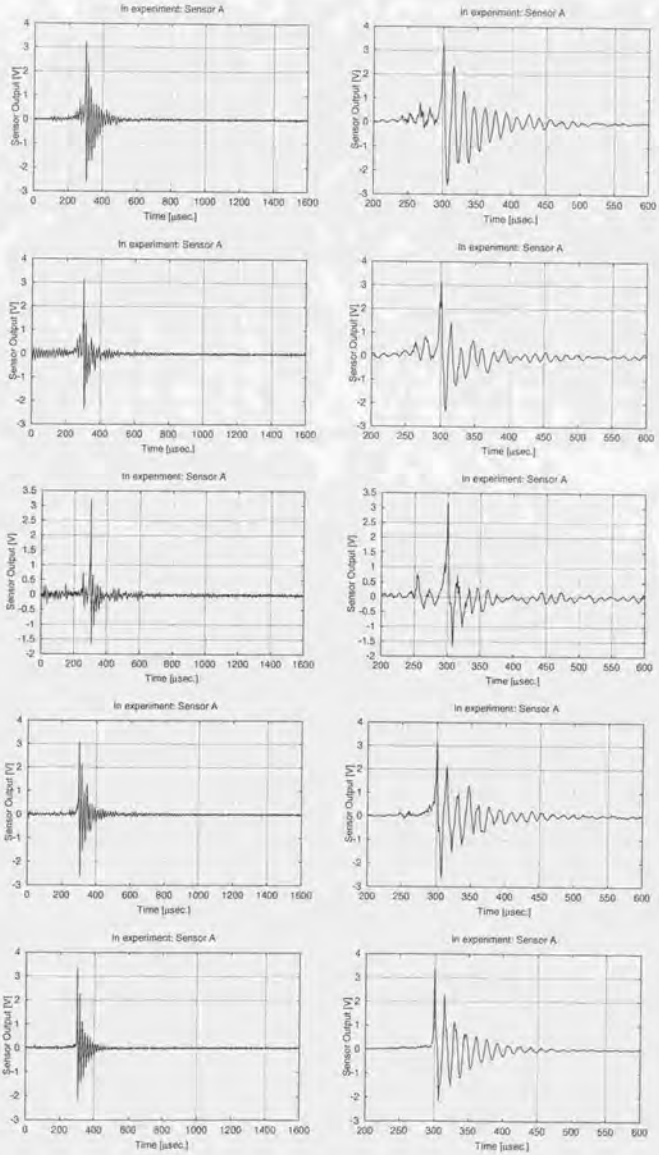

Fig. B.1: (continued)

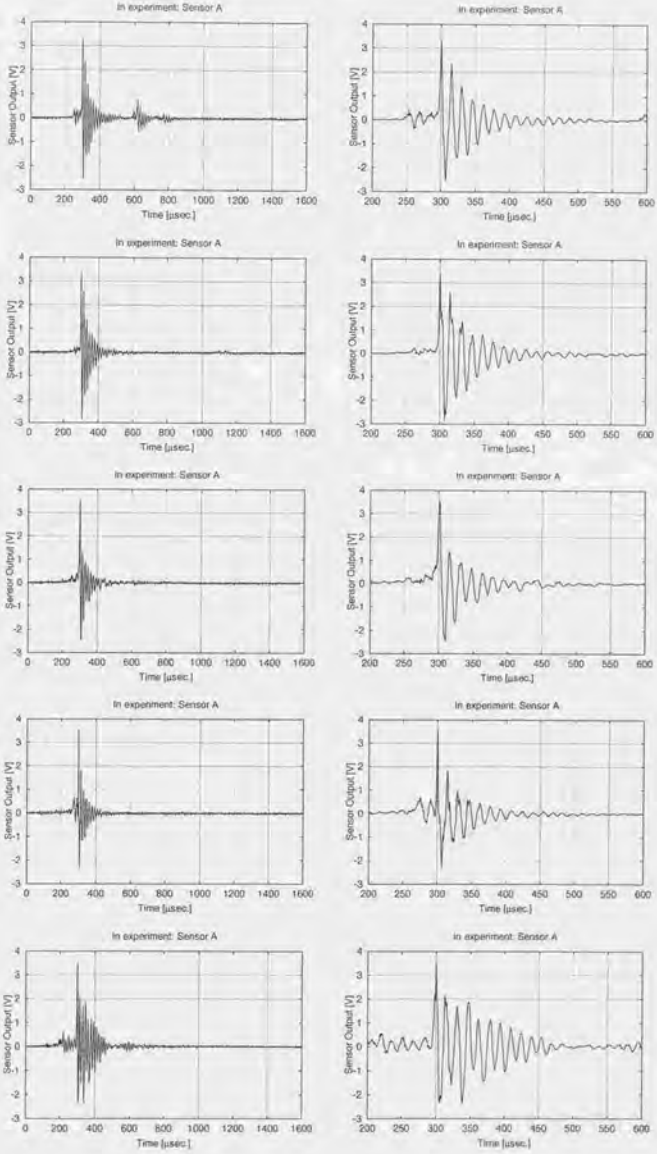

Fig. B.1: (continued)

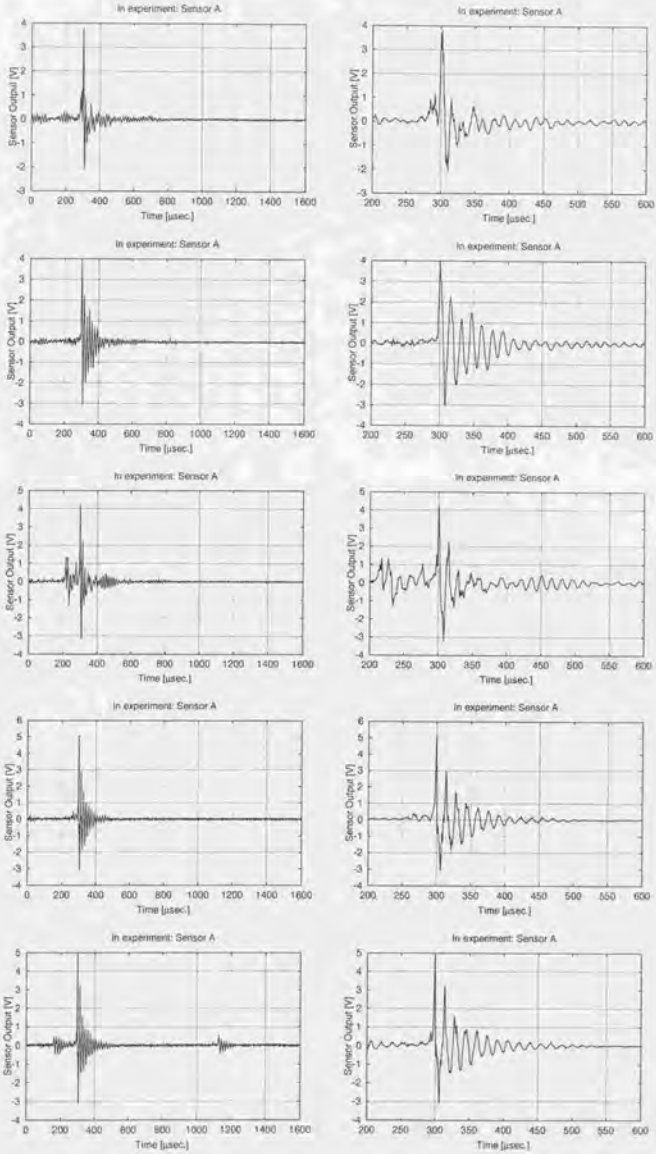

Fig. B.1: (continued)

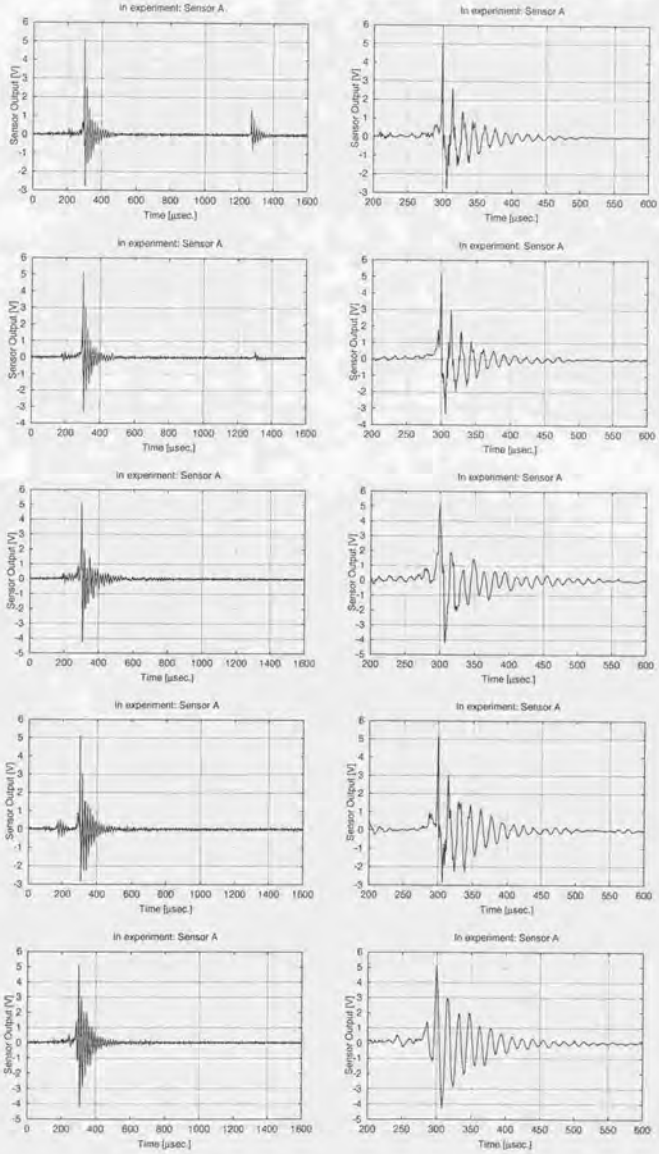

Fig. B.1: (continued)

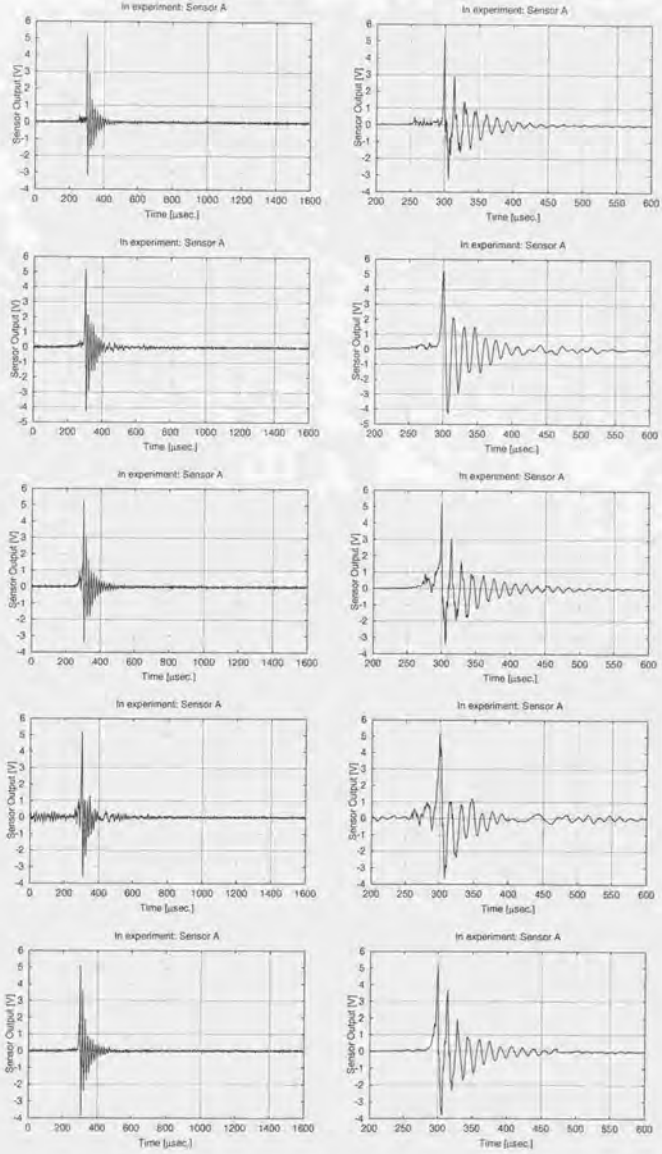

Fig. B.1: (continued)

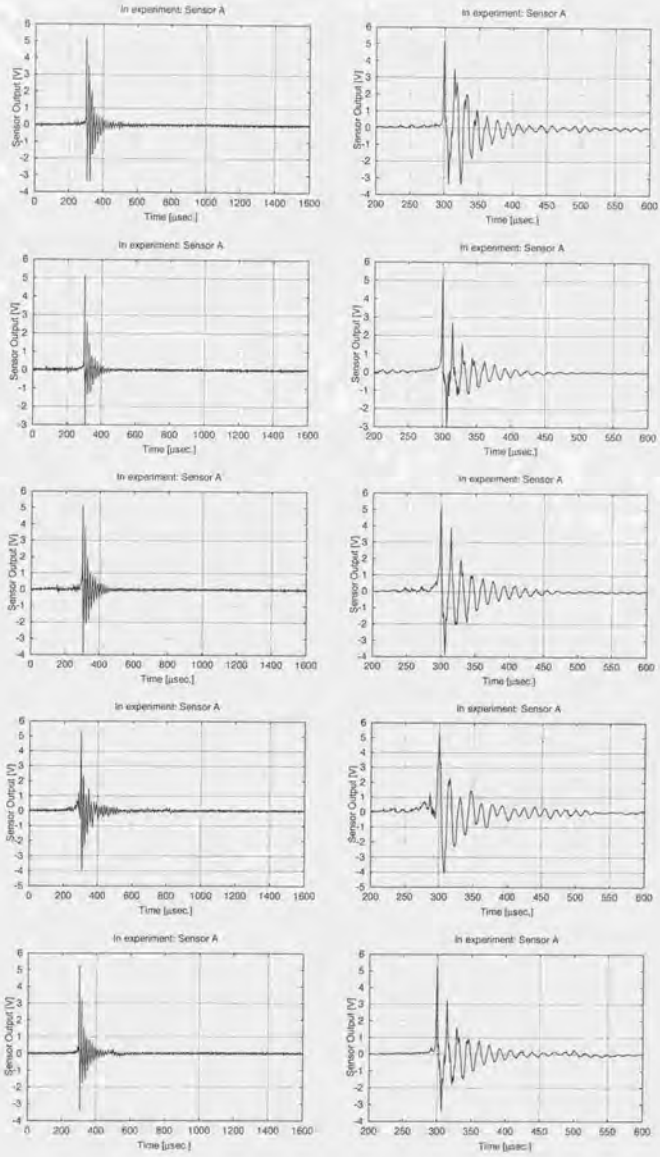

Fig. B.1: (continued)

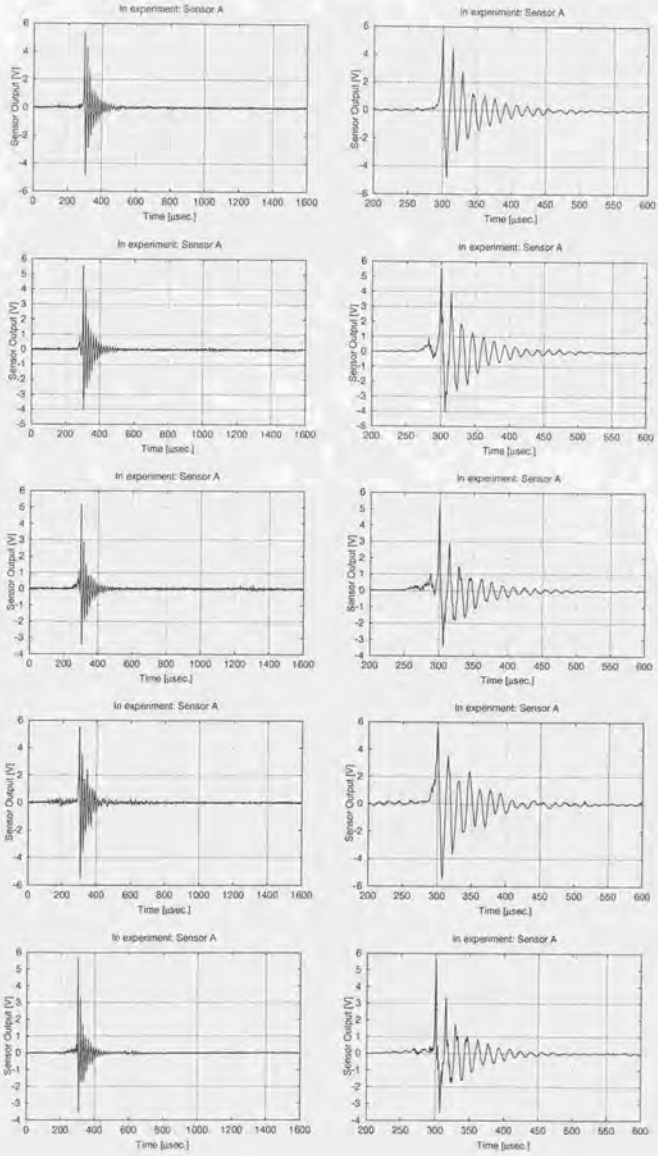

Fig. B.1: (continued)

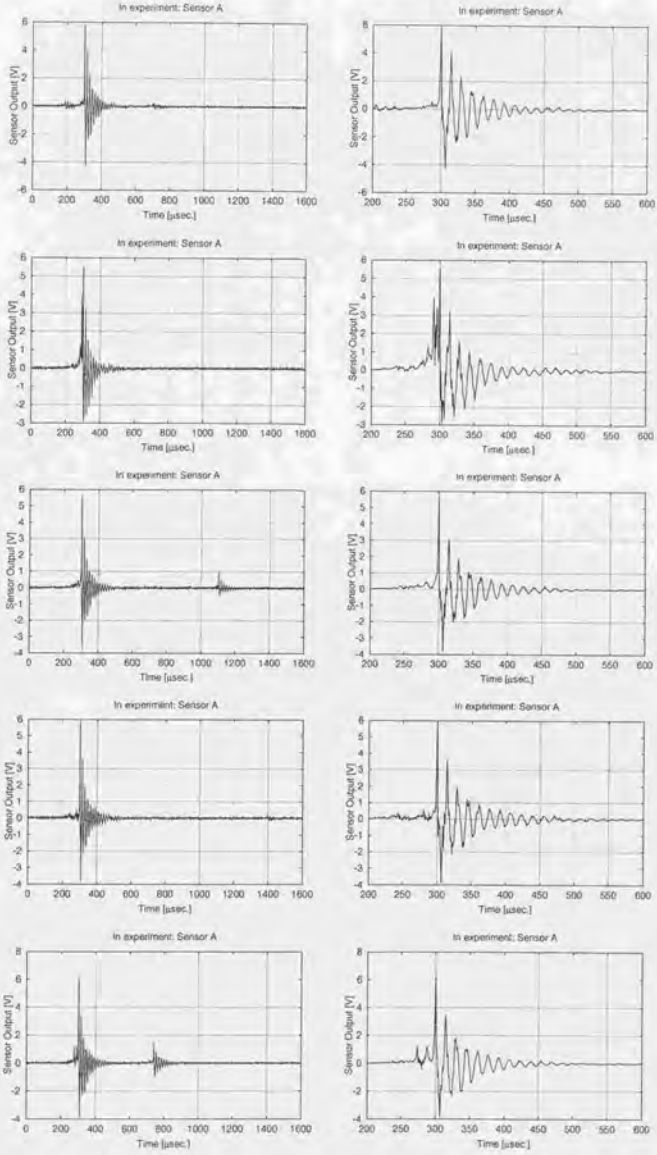

Fig. B.1: (continued)

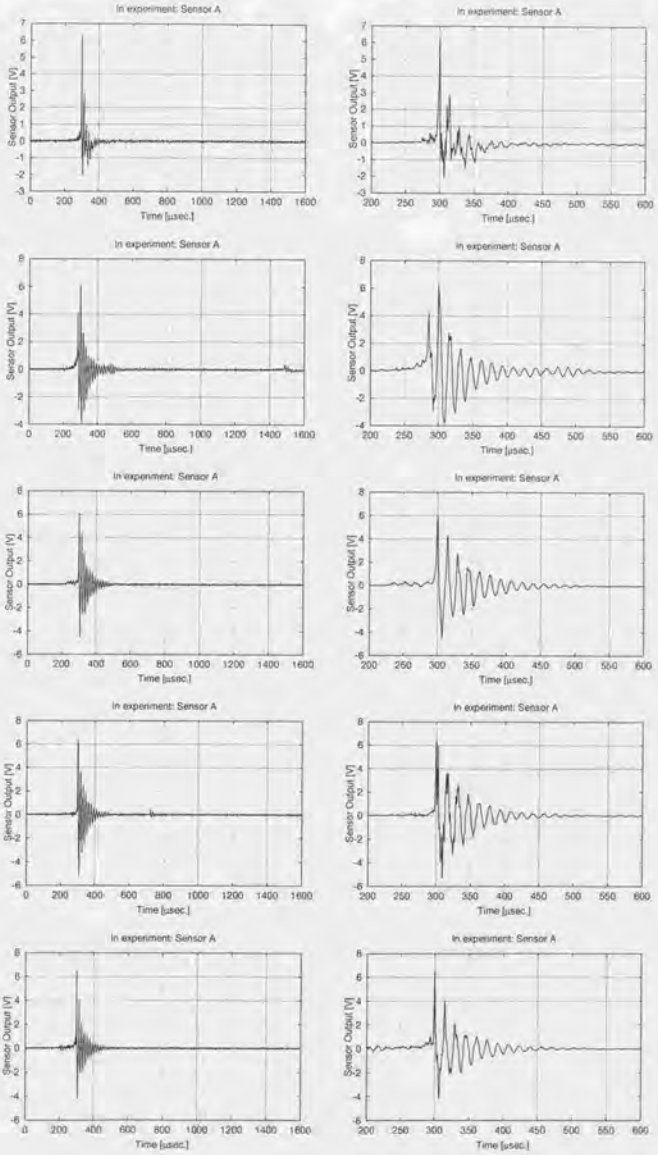

Fig. B.1: (continued)

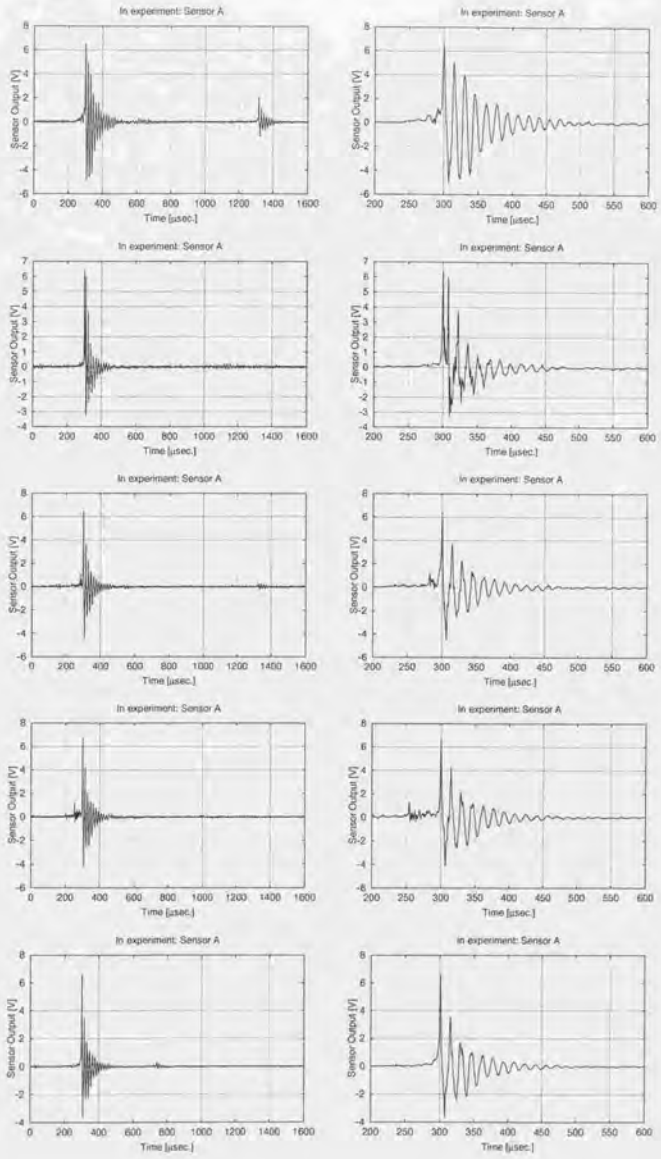

Fig. B.1: (continued)

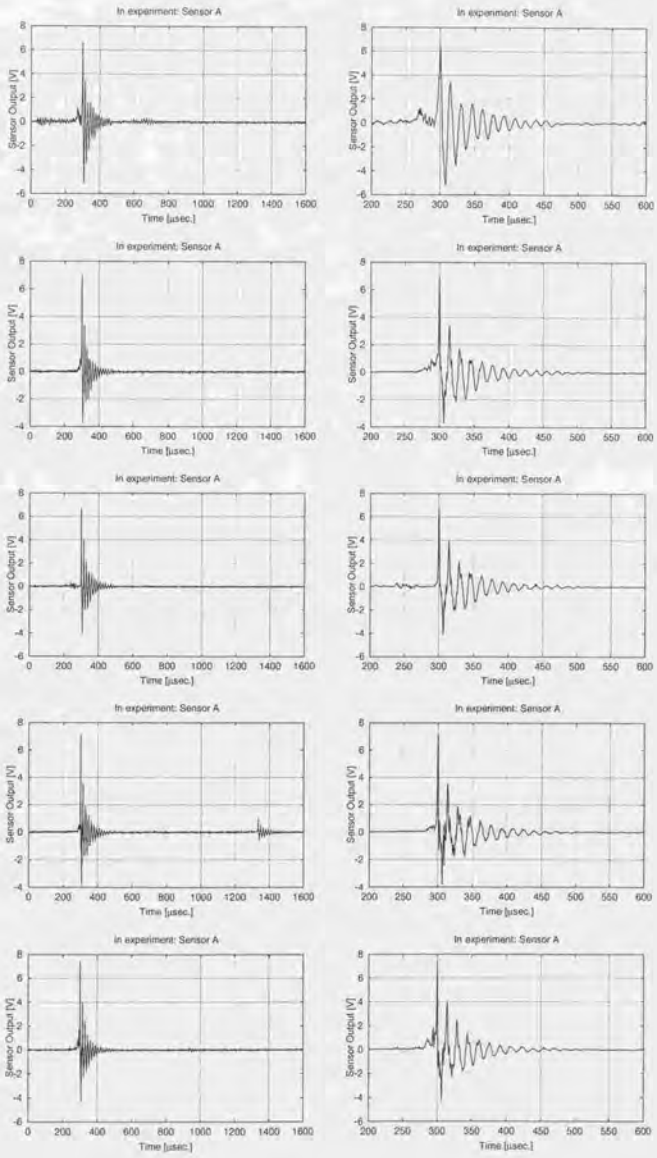

Fig. B.1: (continued)

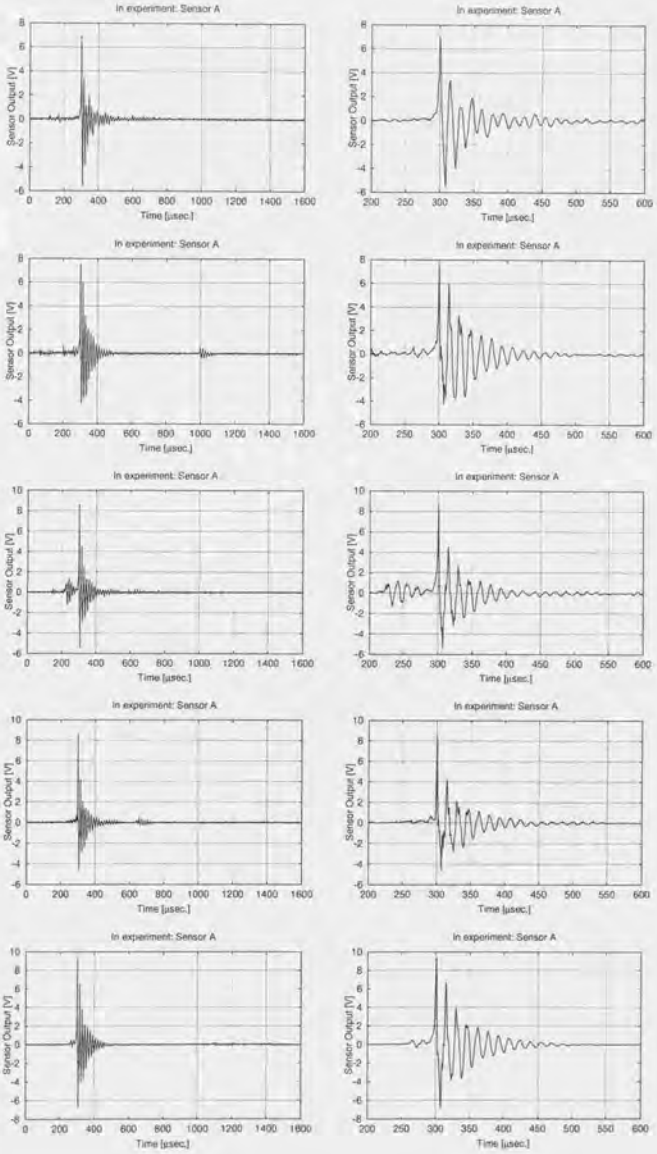

Fig. B.1: (continued)

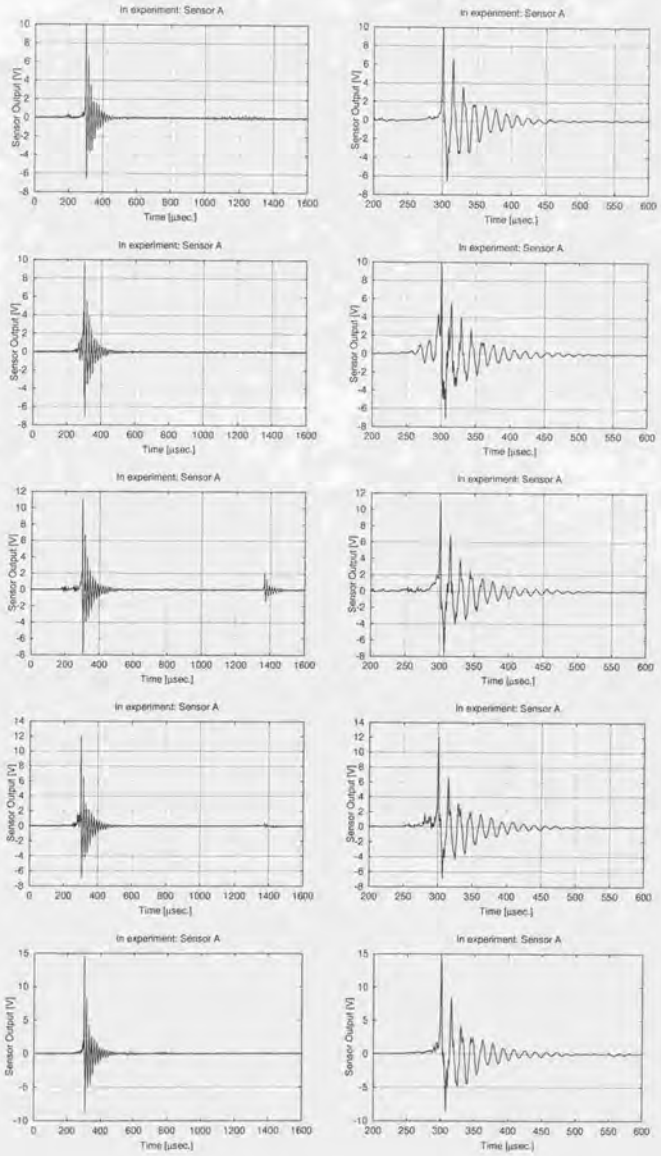

Fig. B.1: (continued)

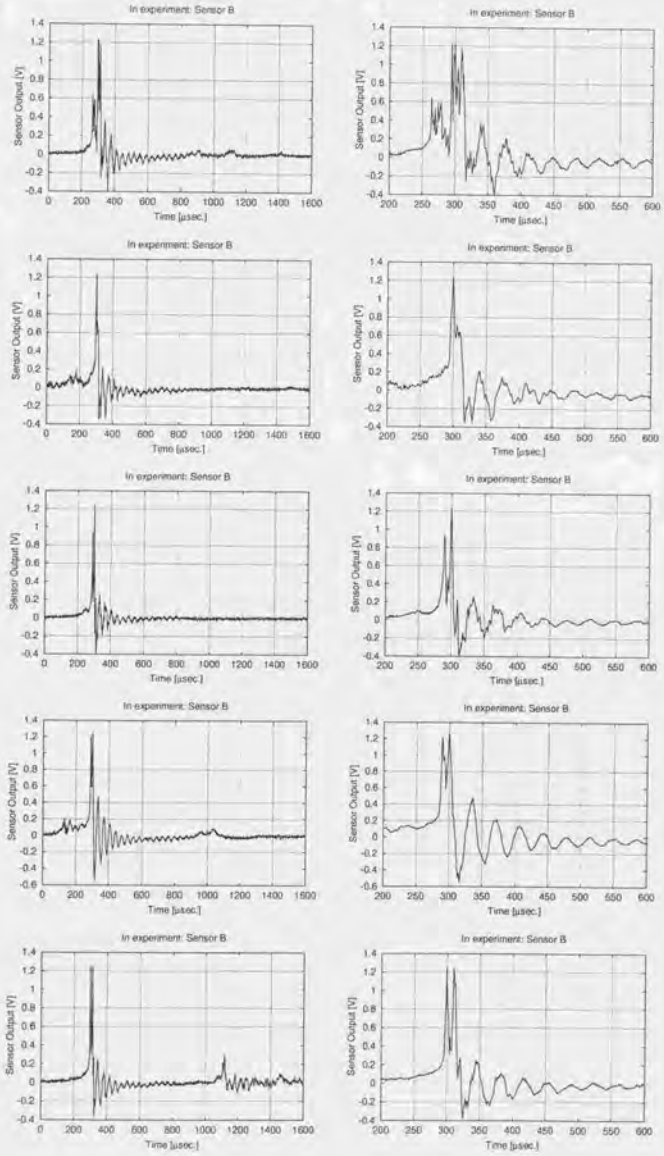

Fig. B.2: Produced signal of sensor B in experiment

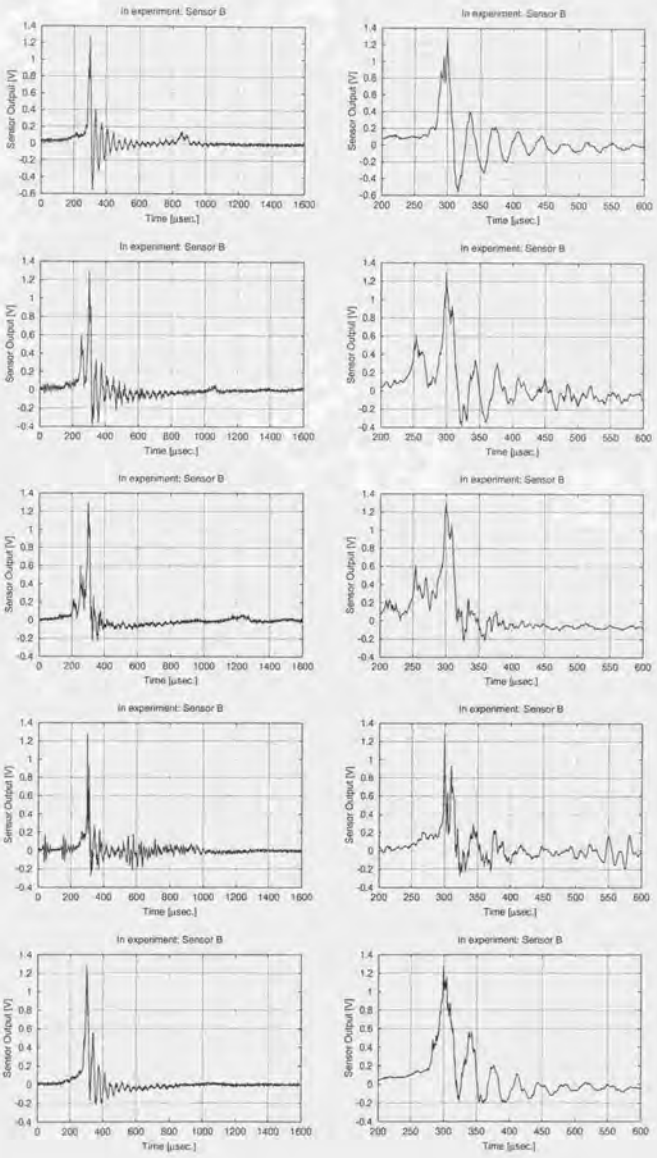

Fig. B.2: (continued)

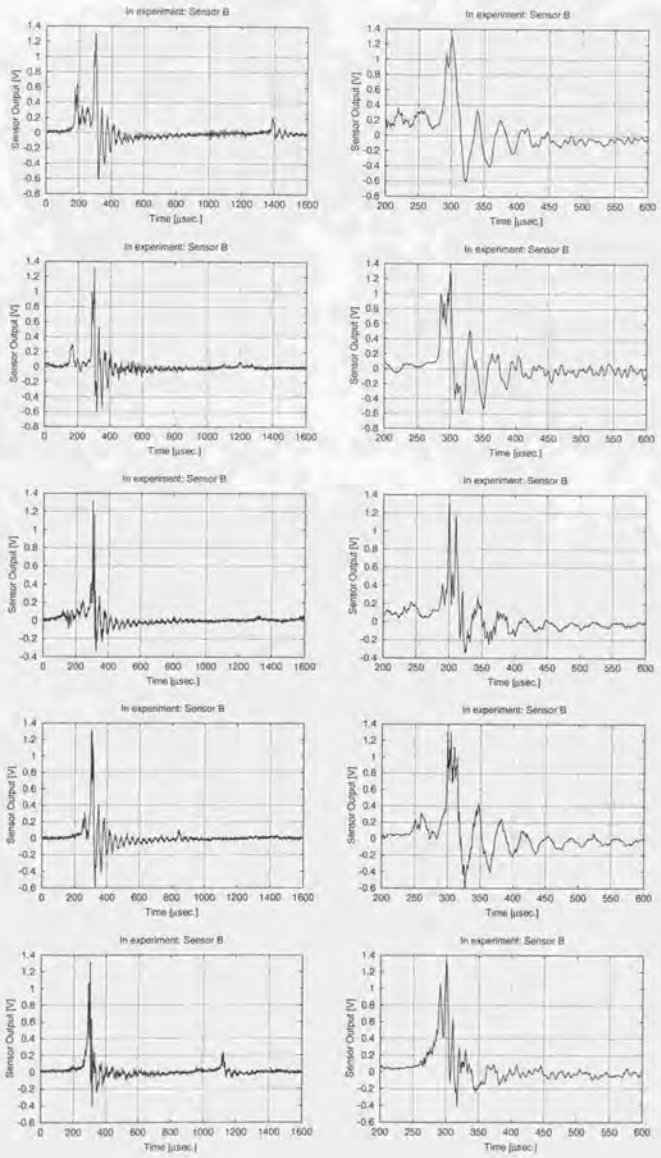

Fig. B.2: (continued)

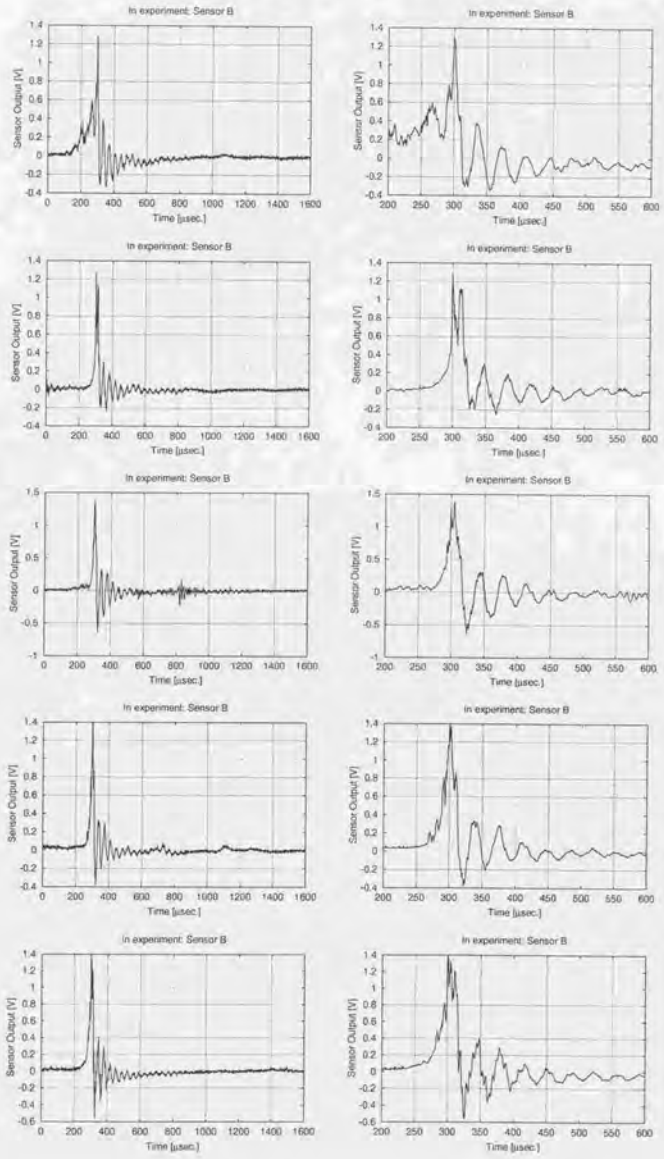

Fig. B.2: (continued)

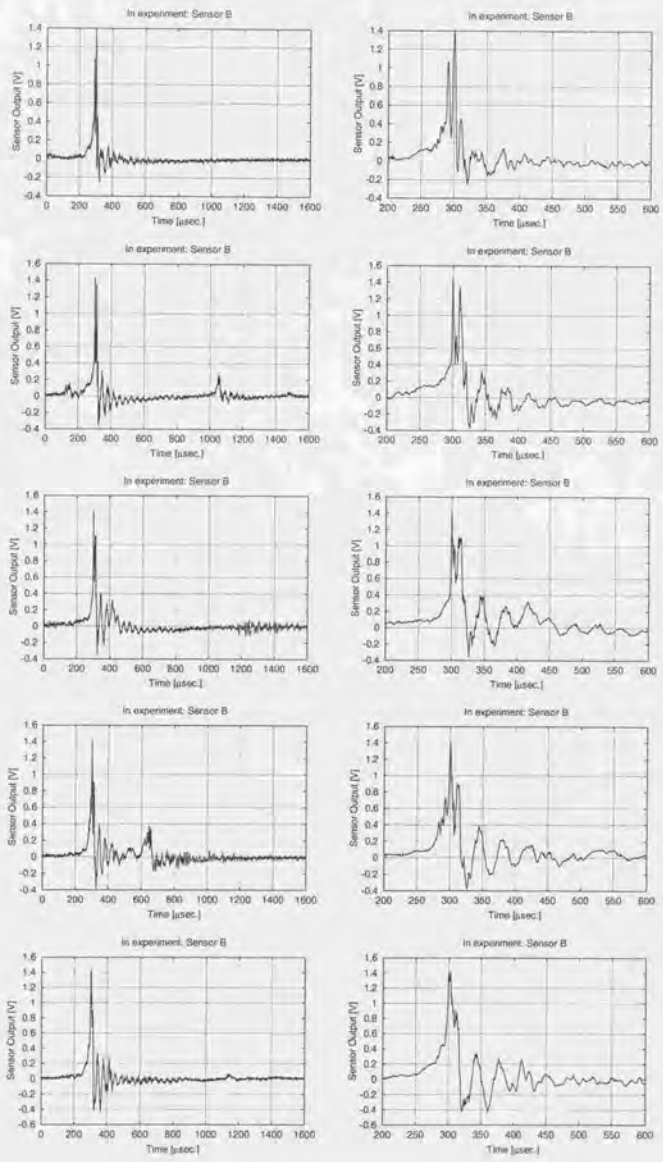

Fig. B.2: (continued)

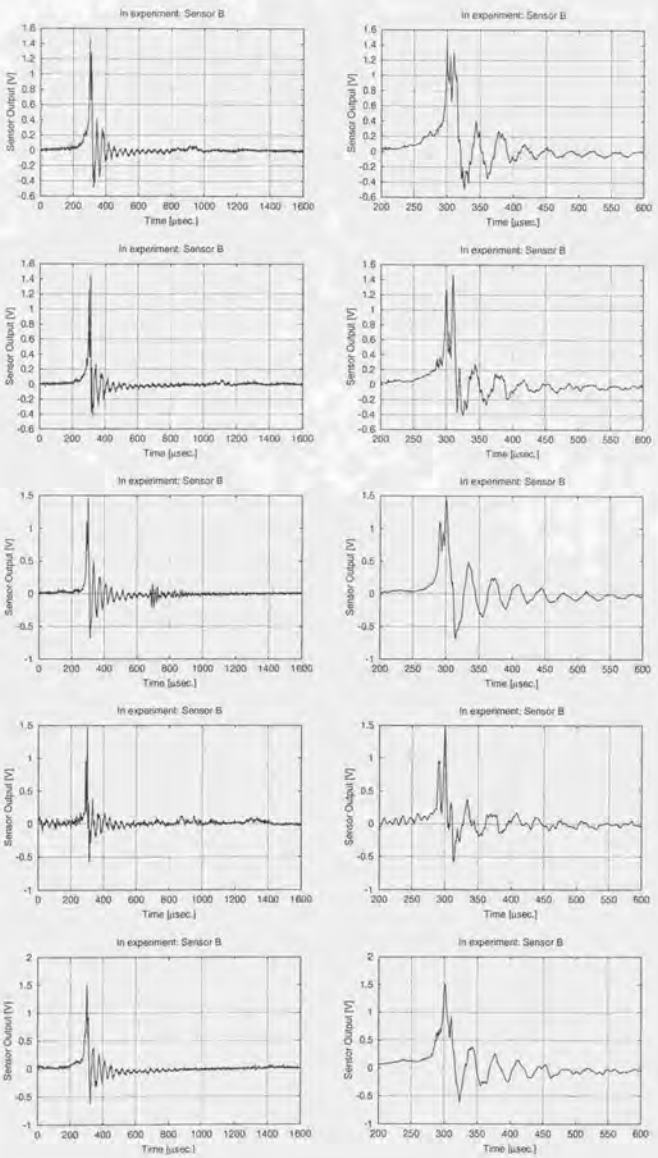

Fig. B.2: (continued)

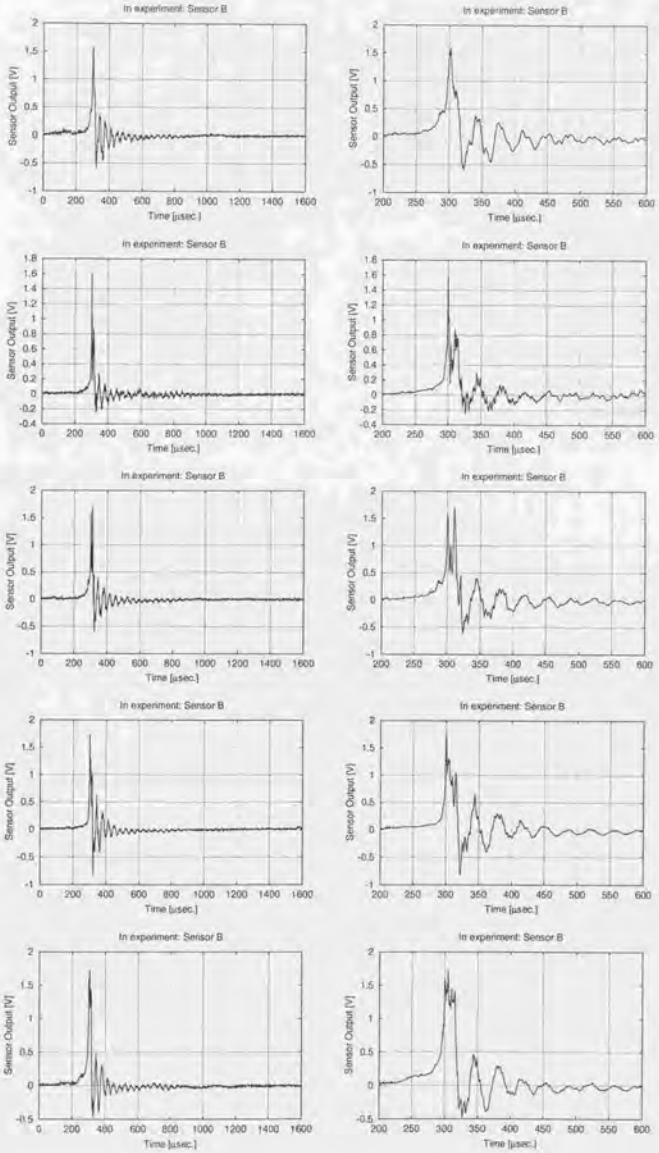

Fig. B.2: (continued)

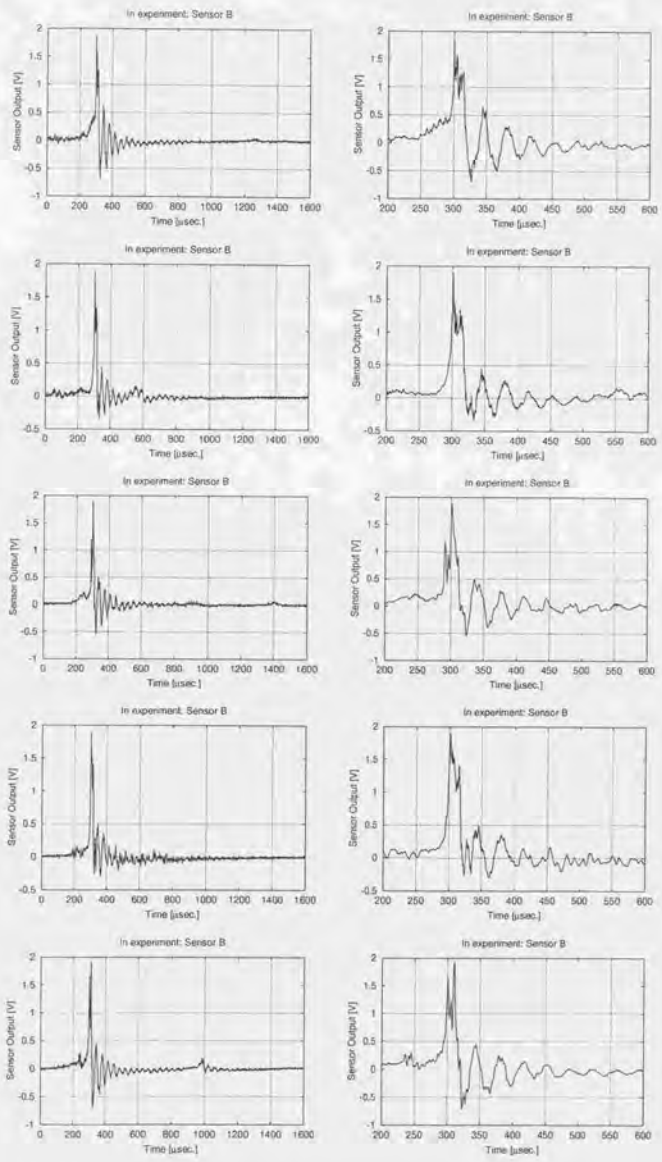

Fig. B.2: (continued)

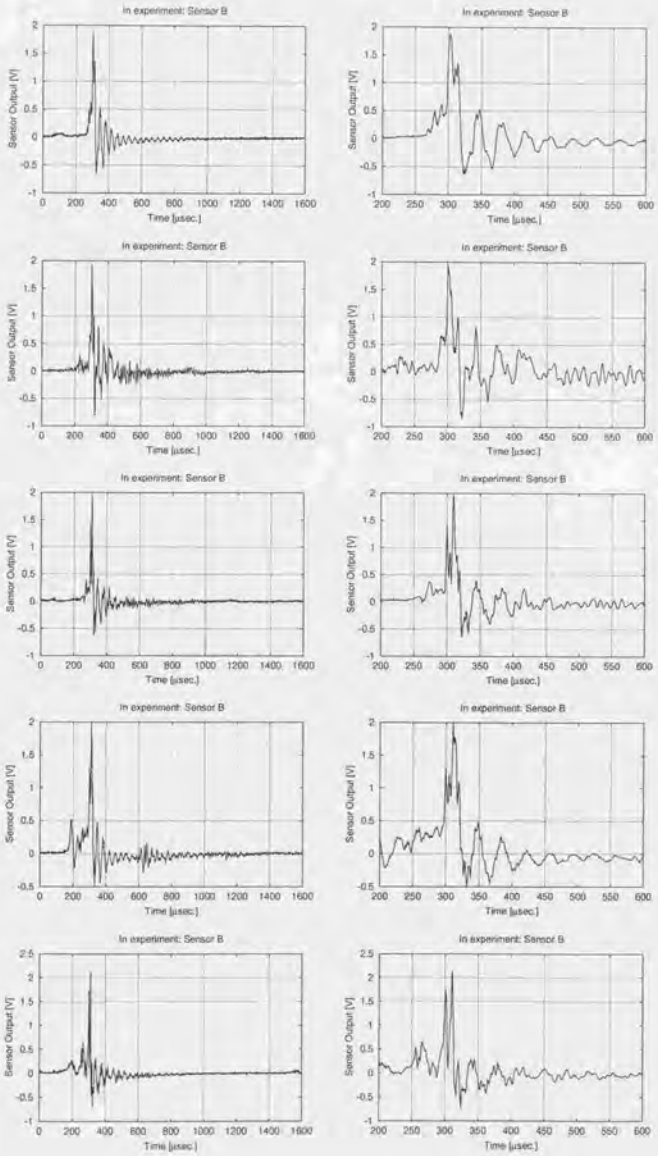

Fig. B.2: (continued)

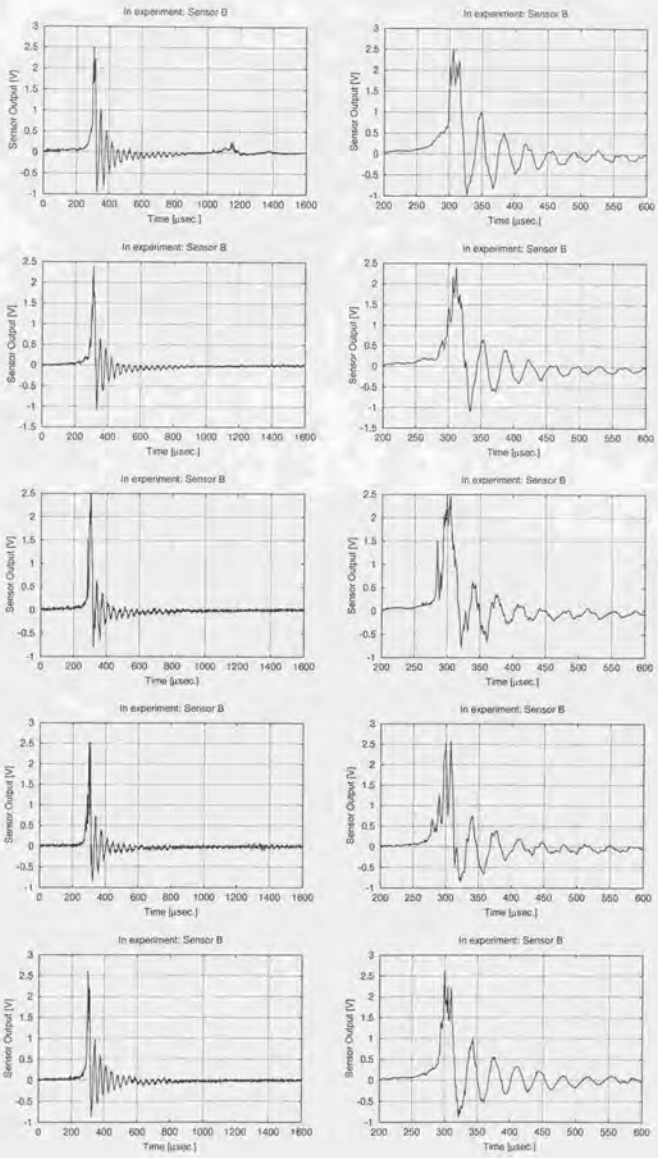

Fig. B.2: (continued)

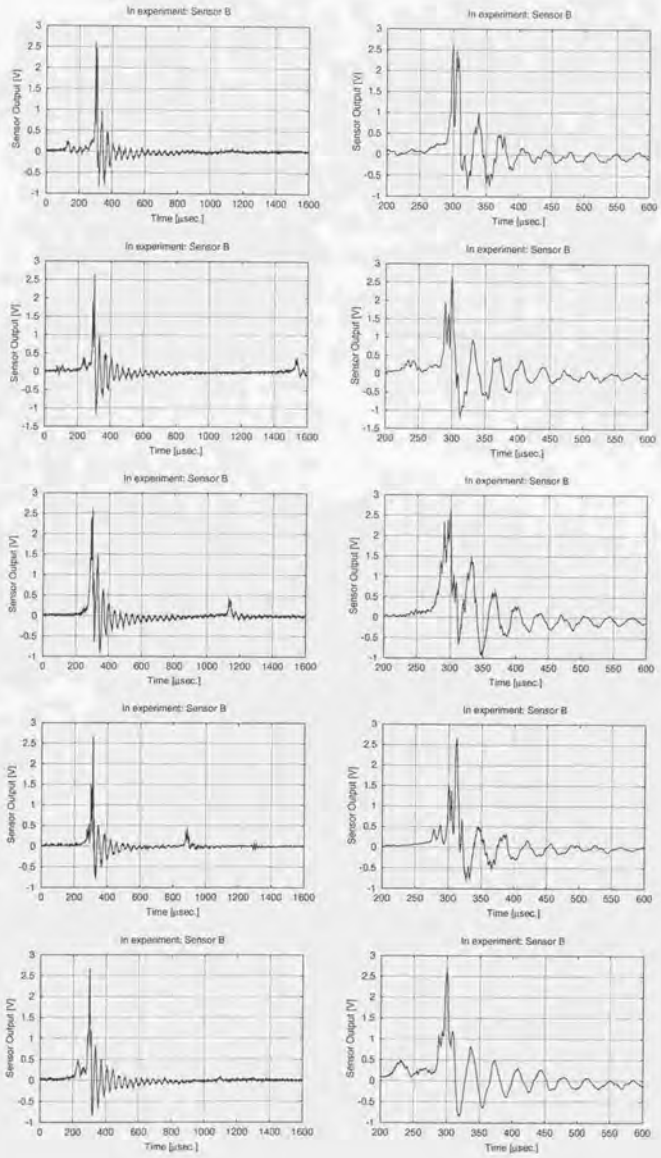

Fig. B.2: (continued)

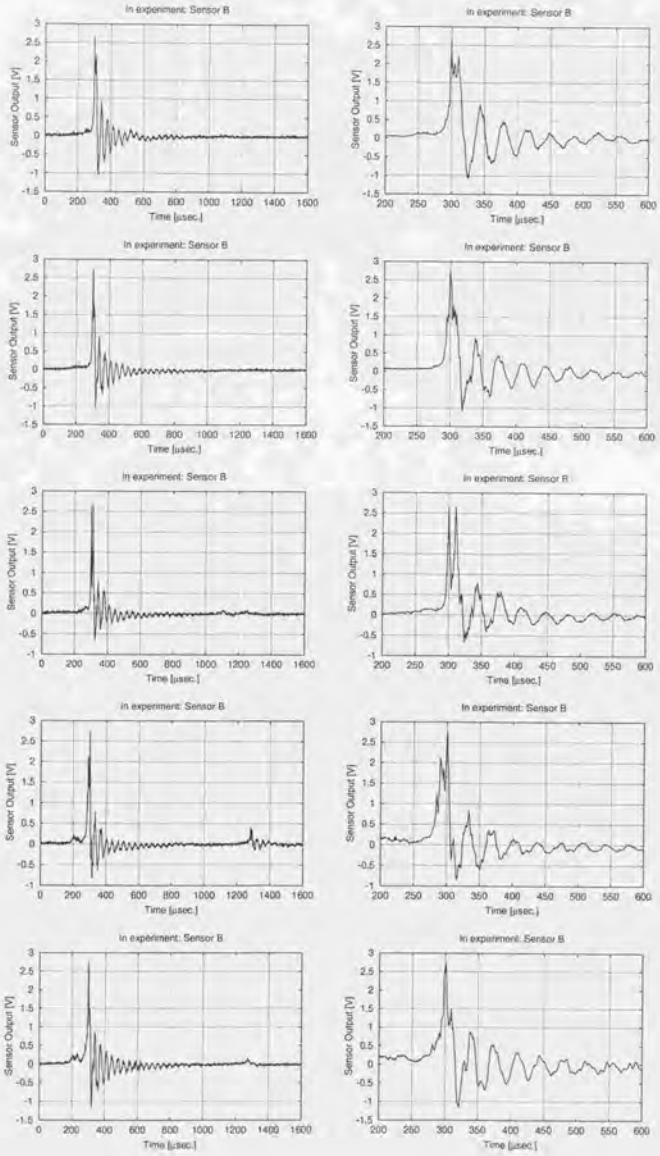

Fig. B.2: (continued)

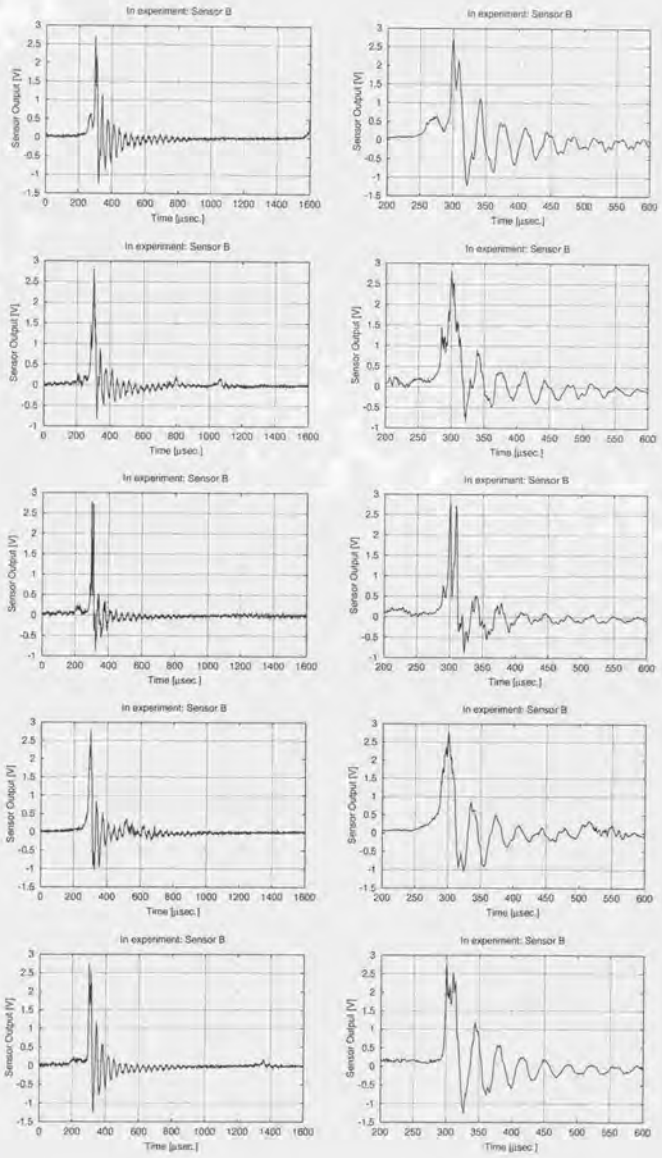

Fig. B.2: (continued)

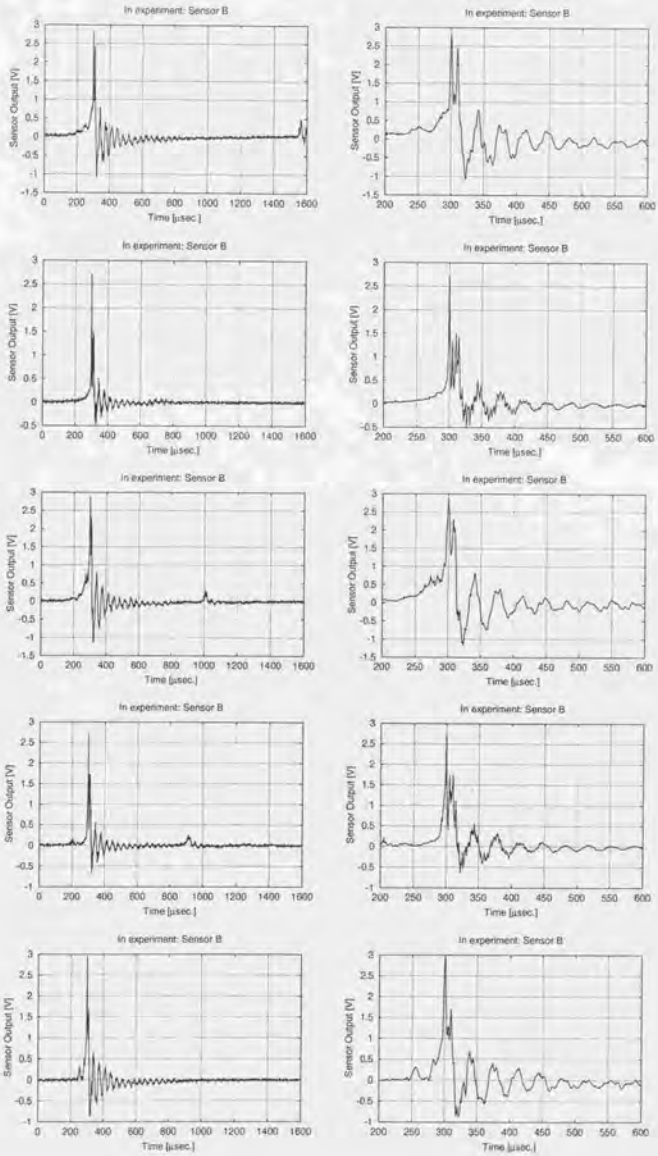

Fig. B.2: (continued)

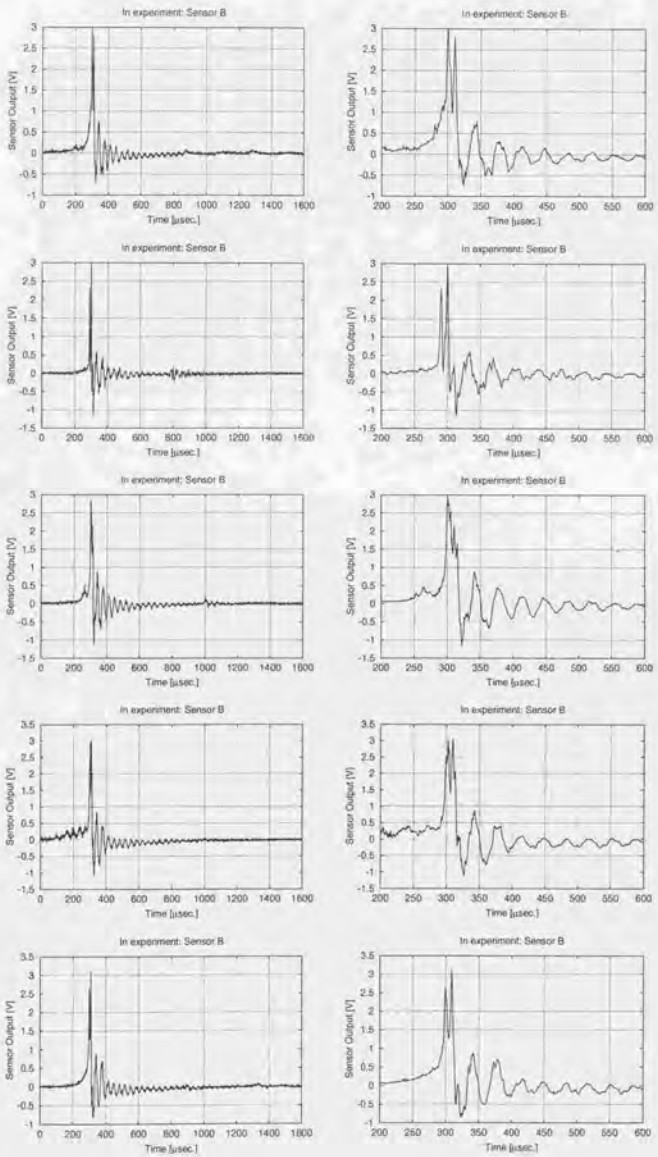

Fig. B.2: (continued)

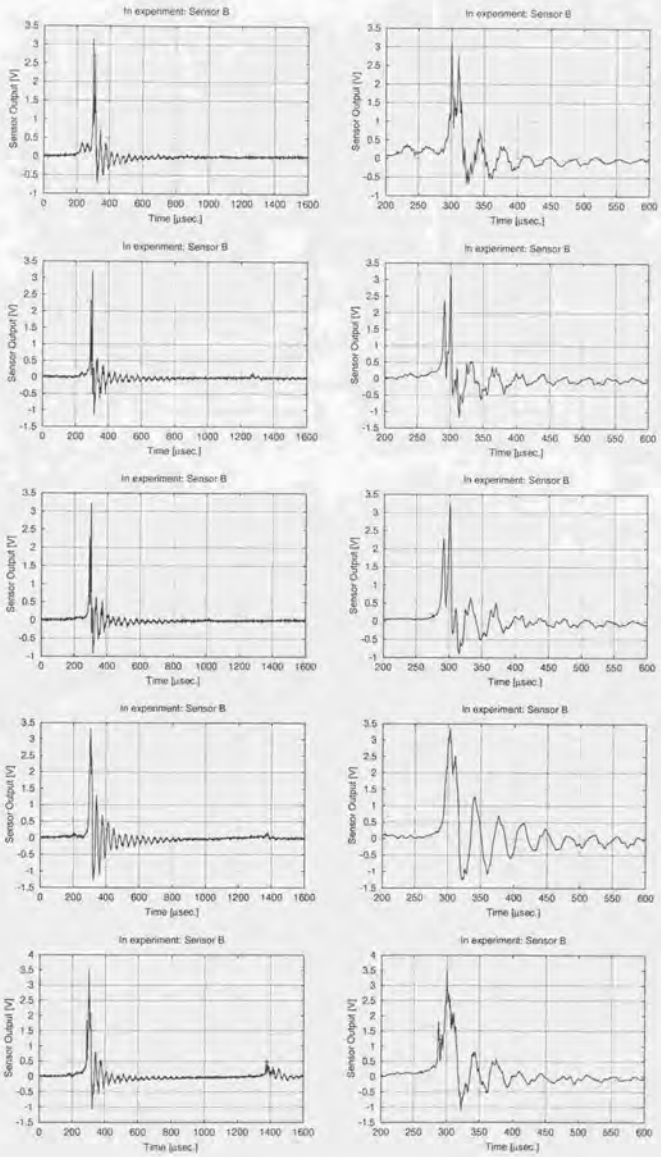

Fig. B.2: (continued)

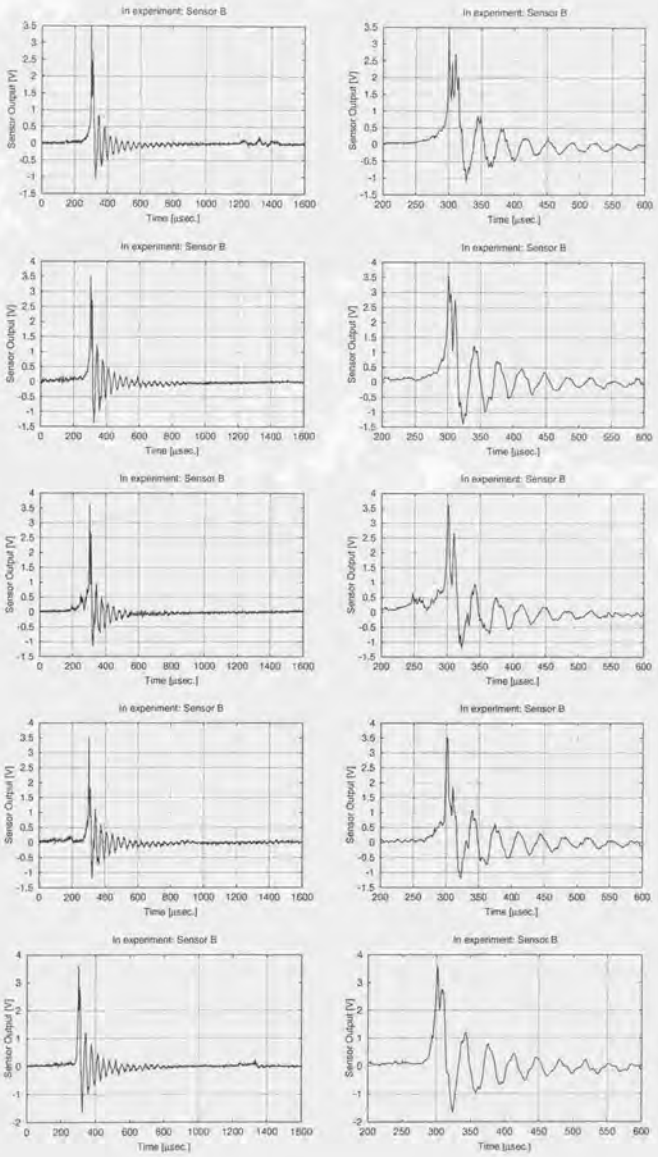

Fig. B.2: (continued)

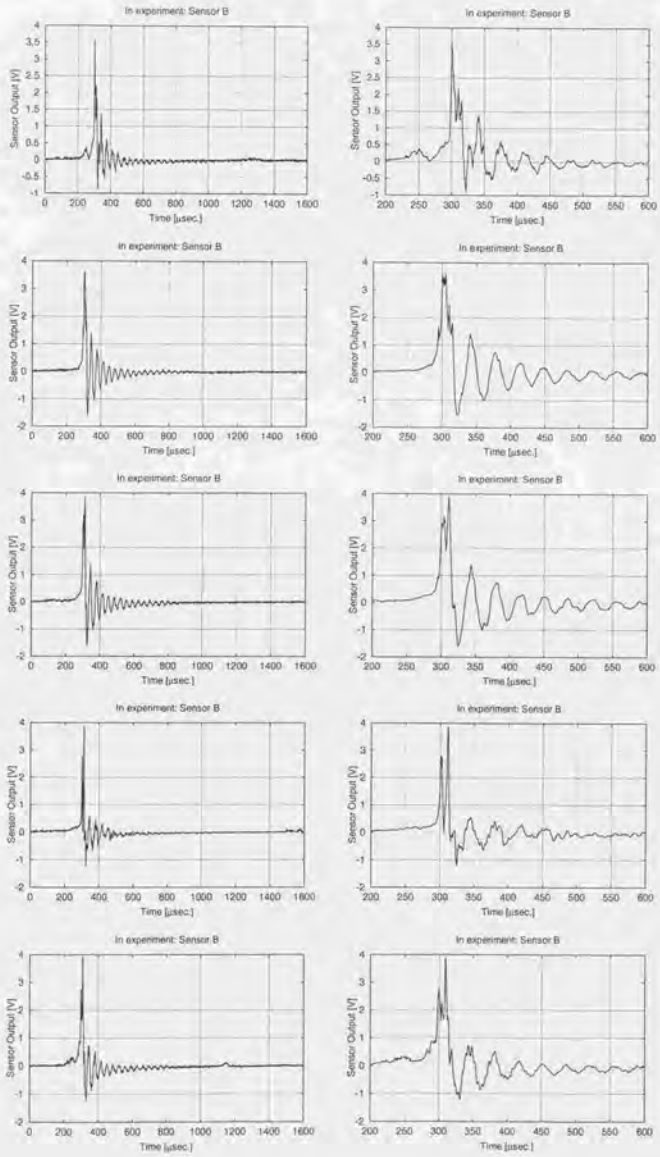

Fig. B.2: (continued)

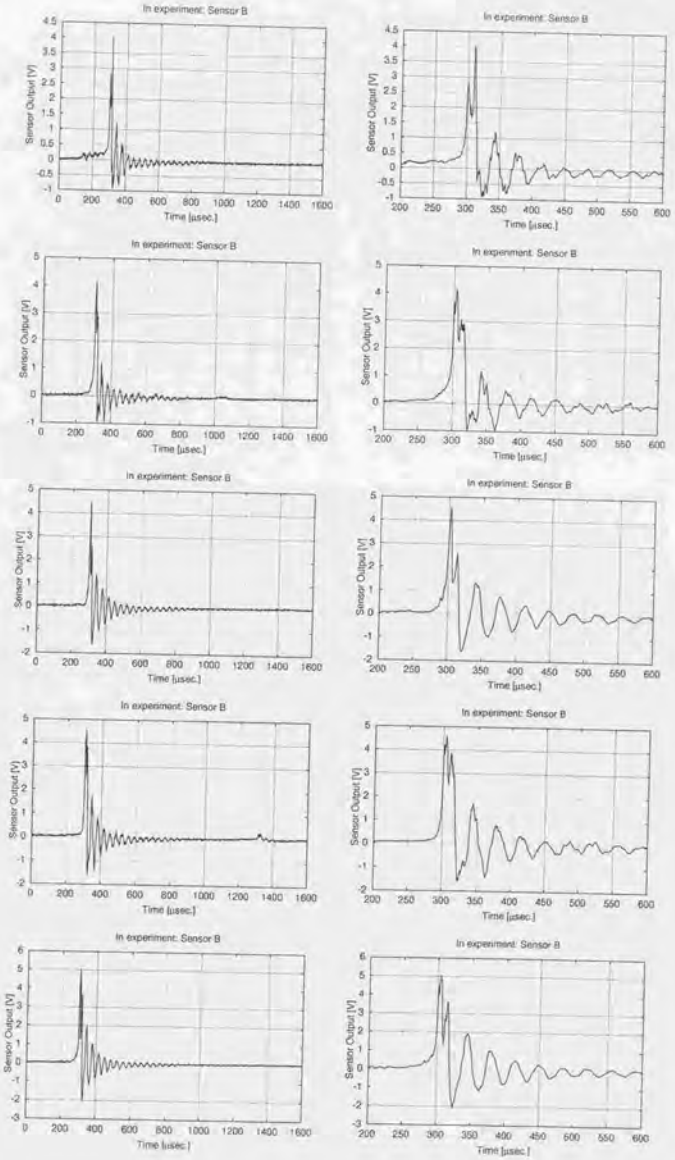

Fig. B.2: (continued)

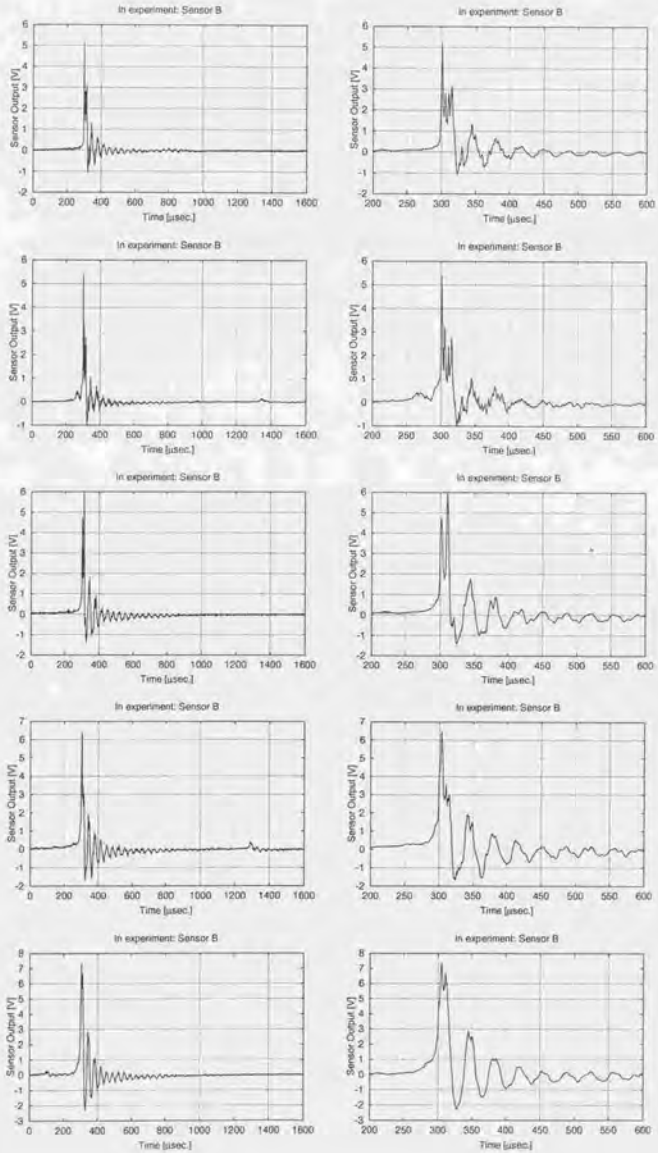

Fig. B.2: (continued)

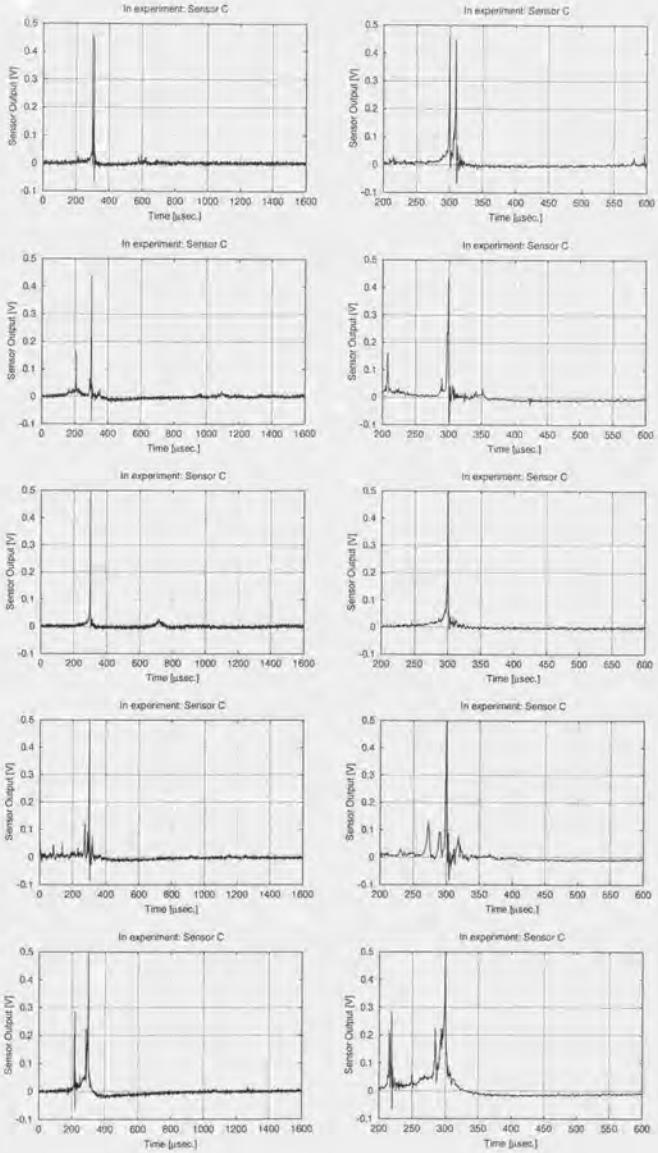

Fig. B.3: Produced signal of sensor C in experiment

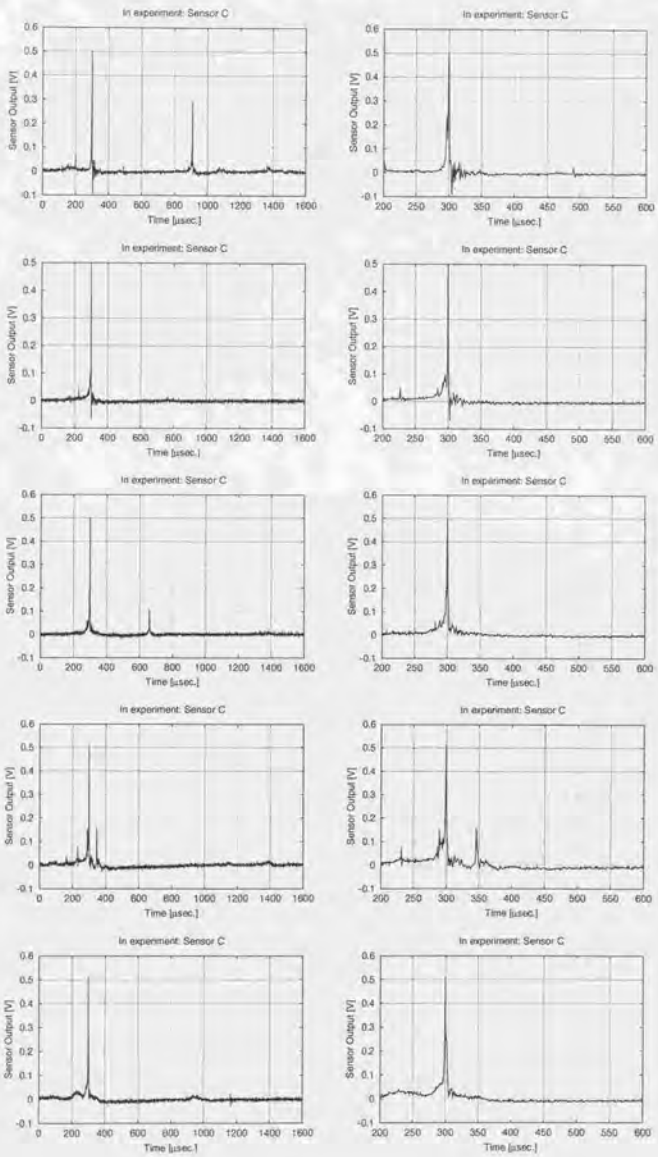

Fig. B.3: (continued)

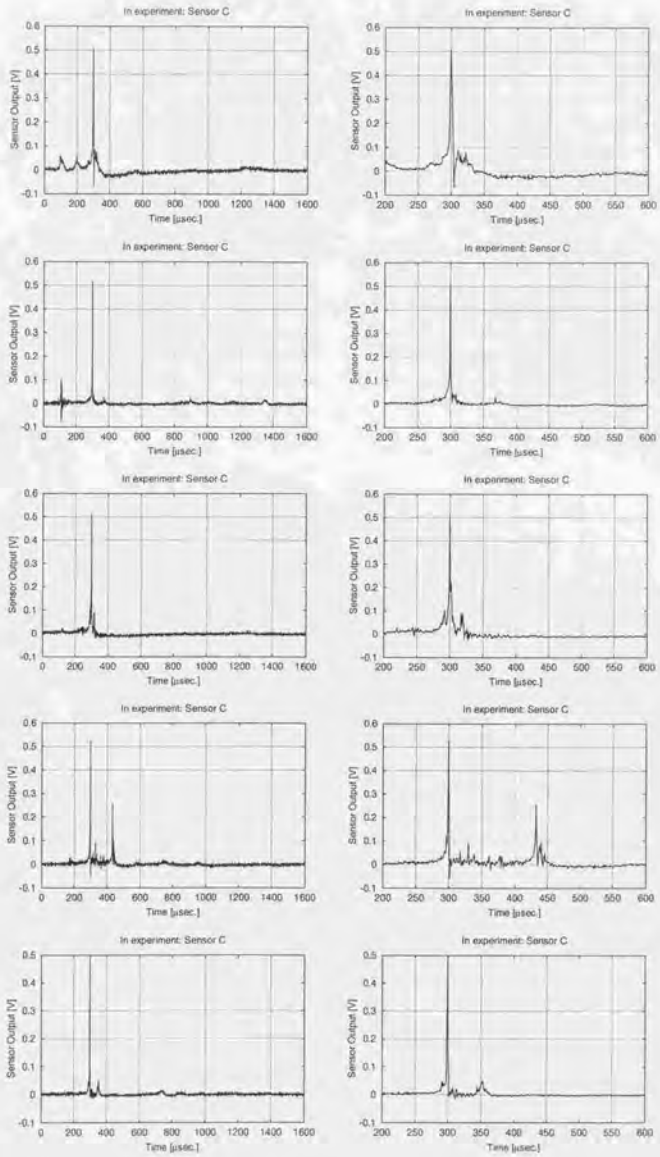

Fig. B.3: (continued)

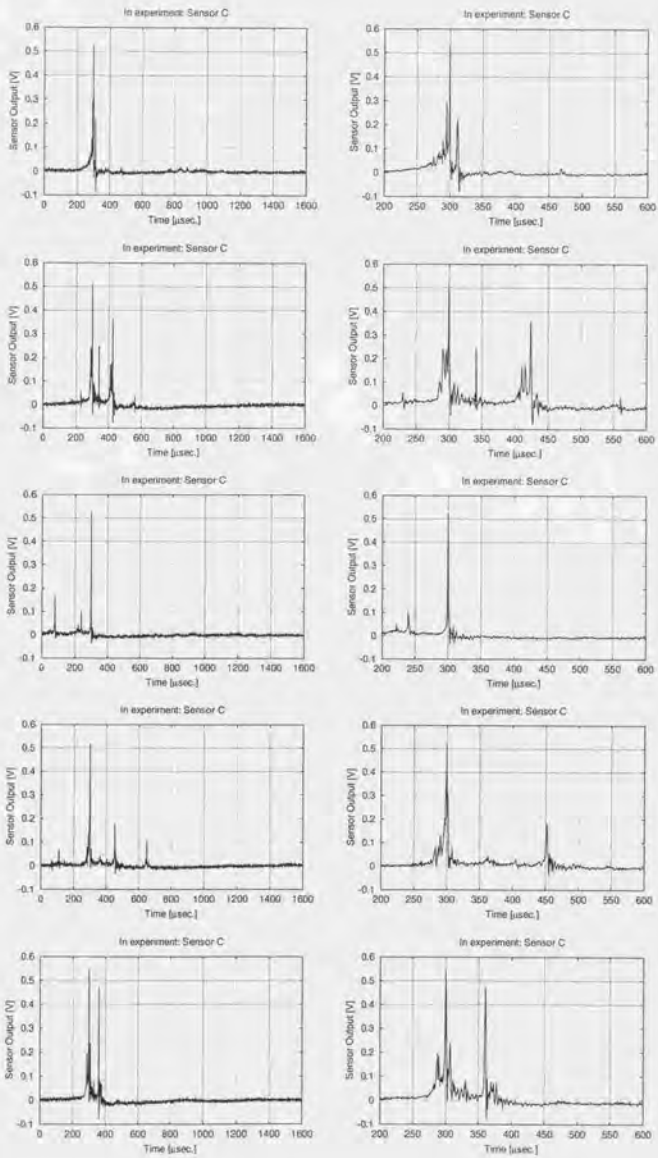

Fig. B.3: (continued)

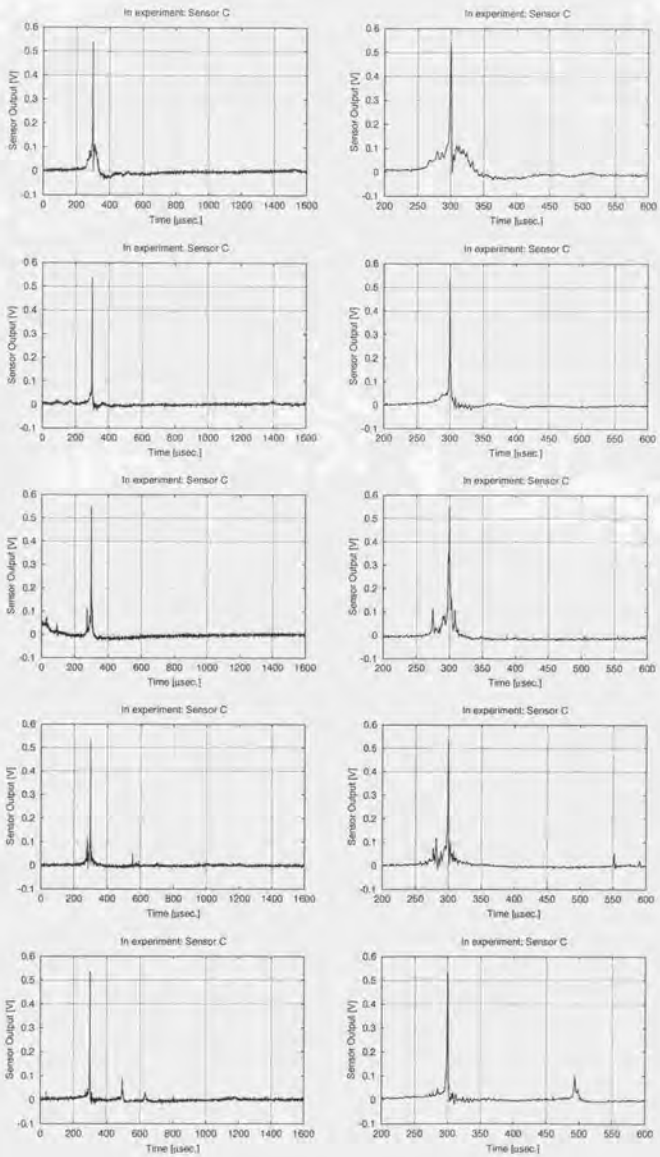

Fig. B.3: (continued)

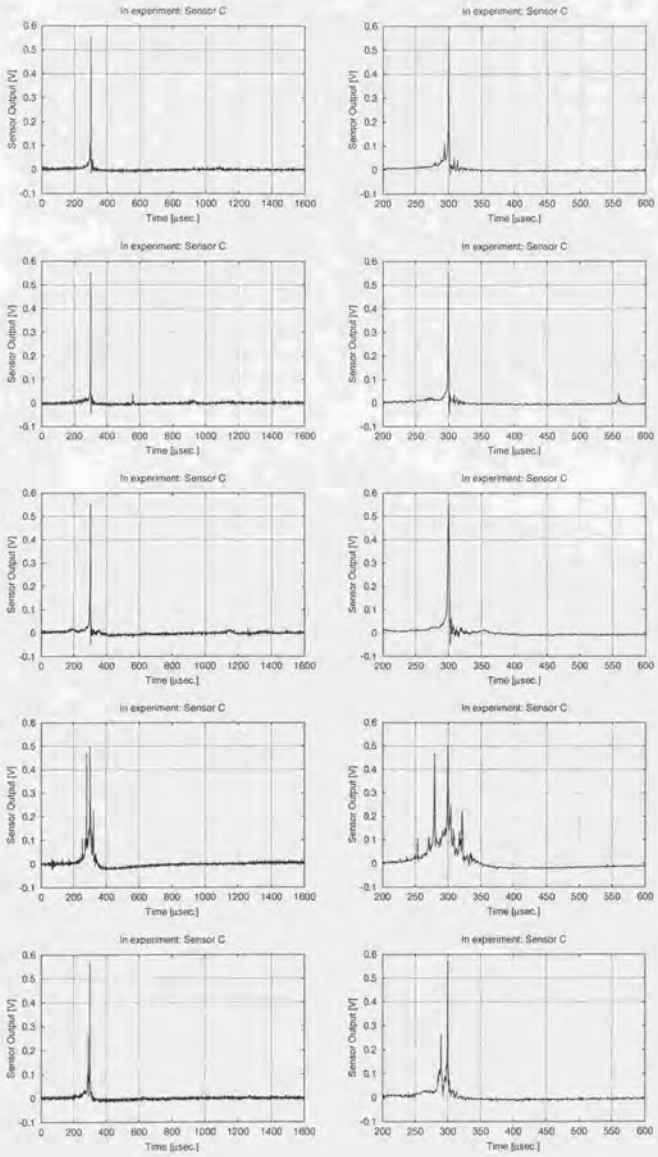

Fig. B.3: (continued)

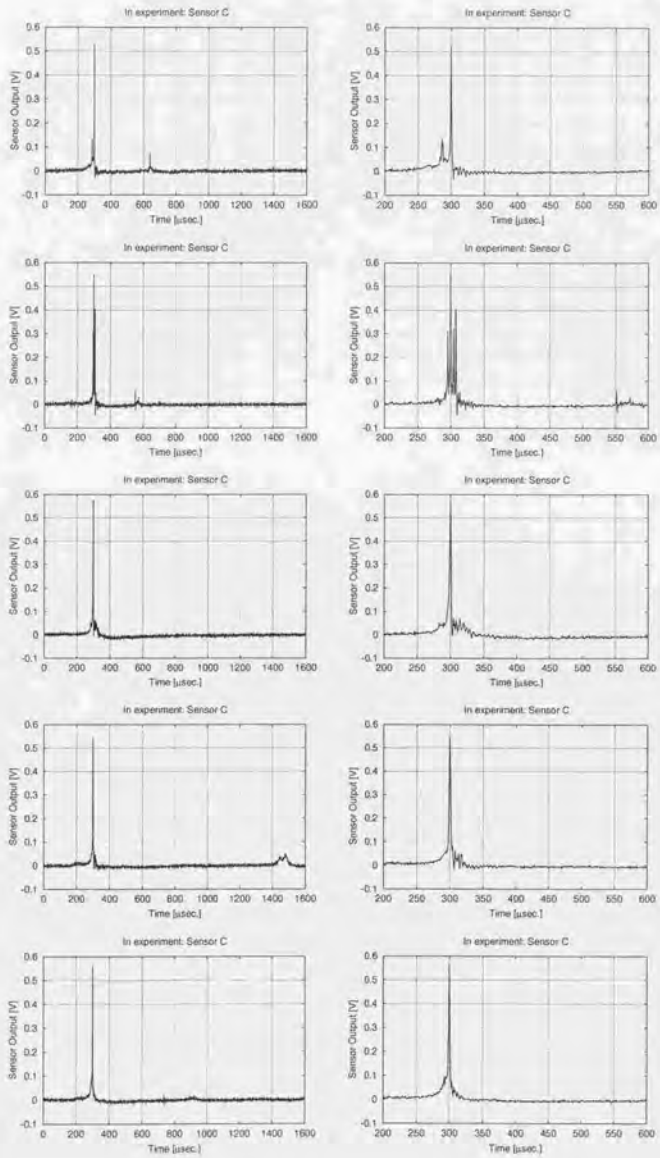

Fig. B.3: (continued)

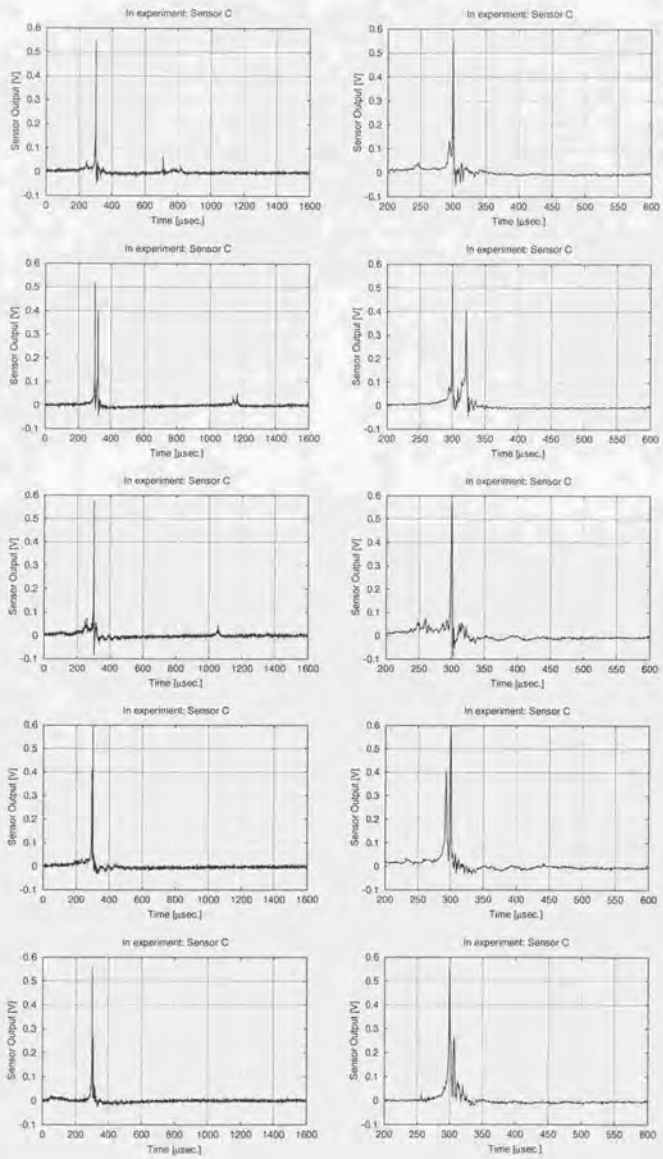

Fig. B.3: (continued)

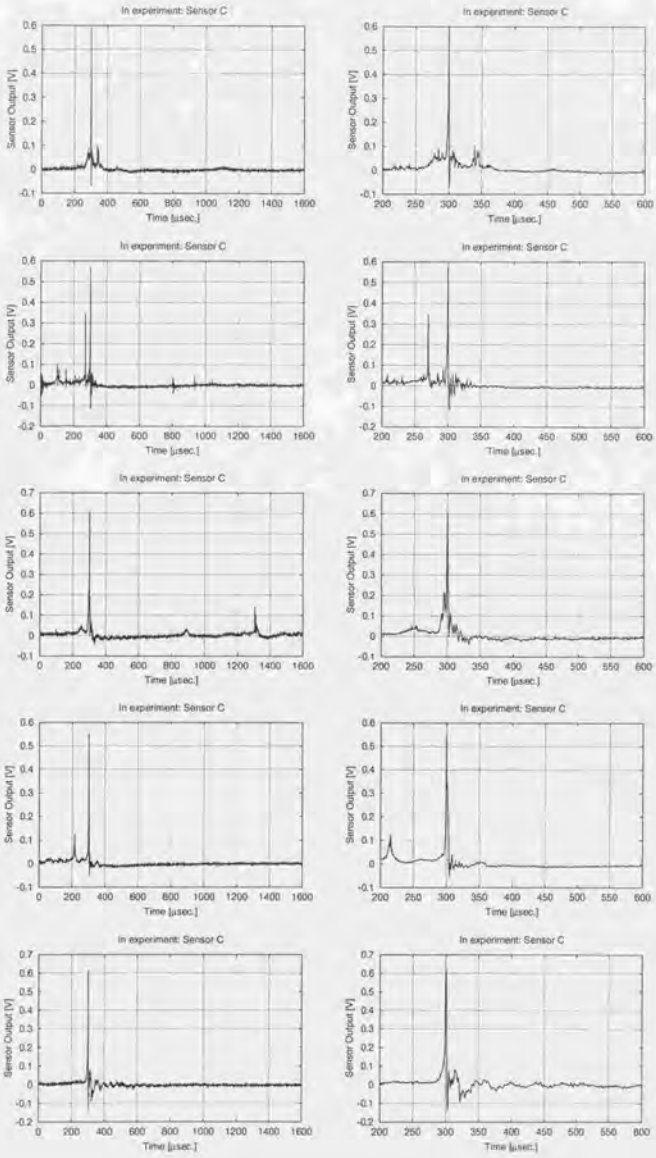

Fig. B.3: (continued)

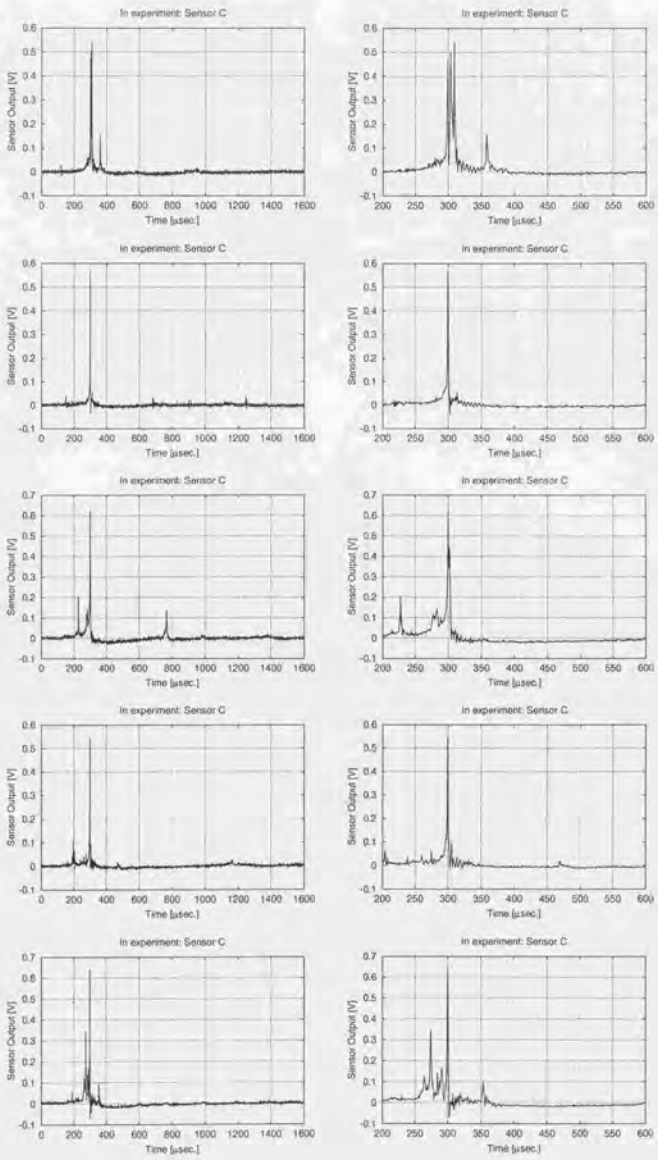

Fig. B.3: (continued)

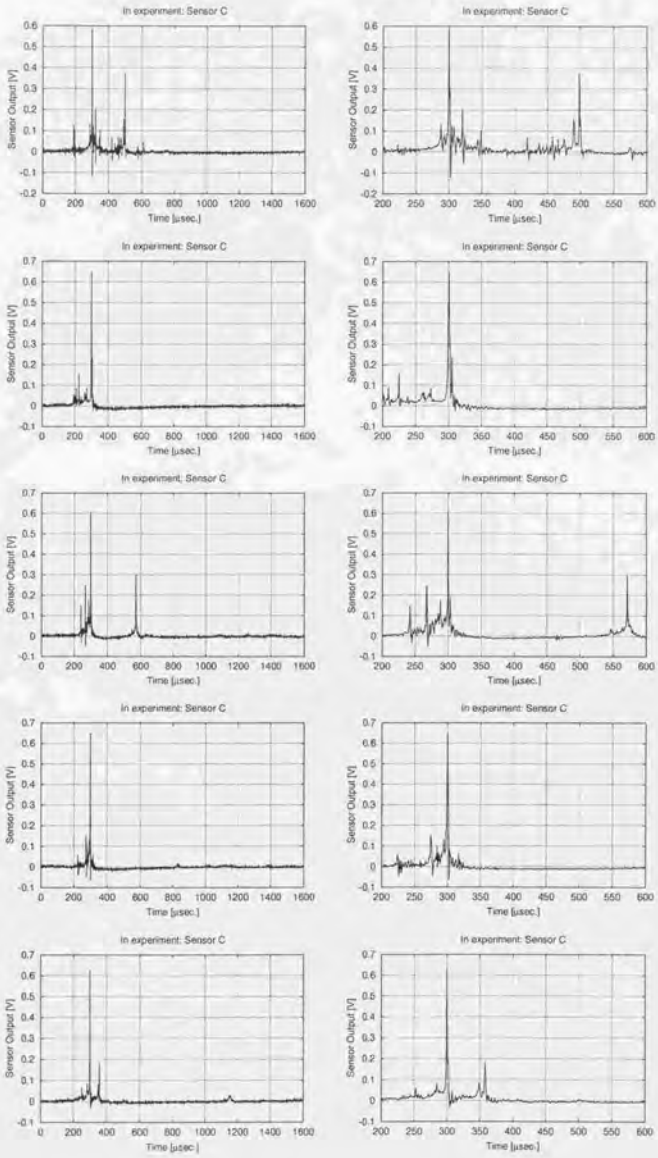

Fig. B.3: (continued)

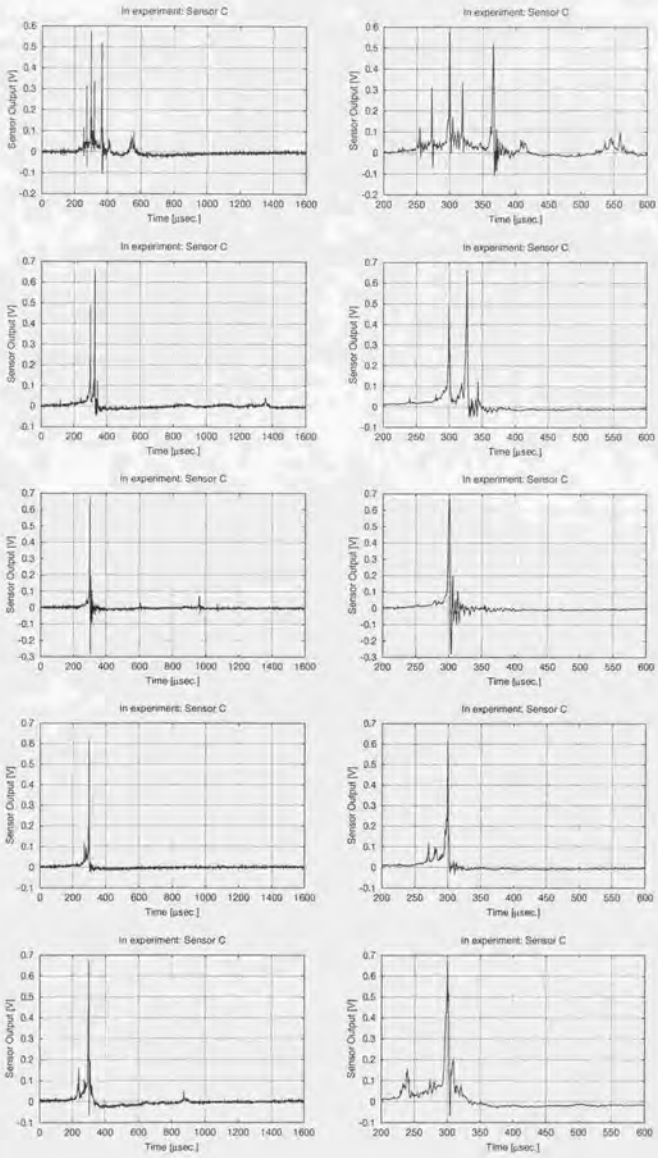

Fig. B.3: (continued)

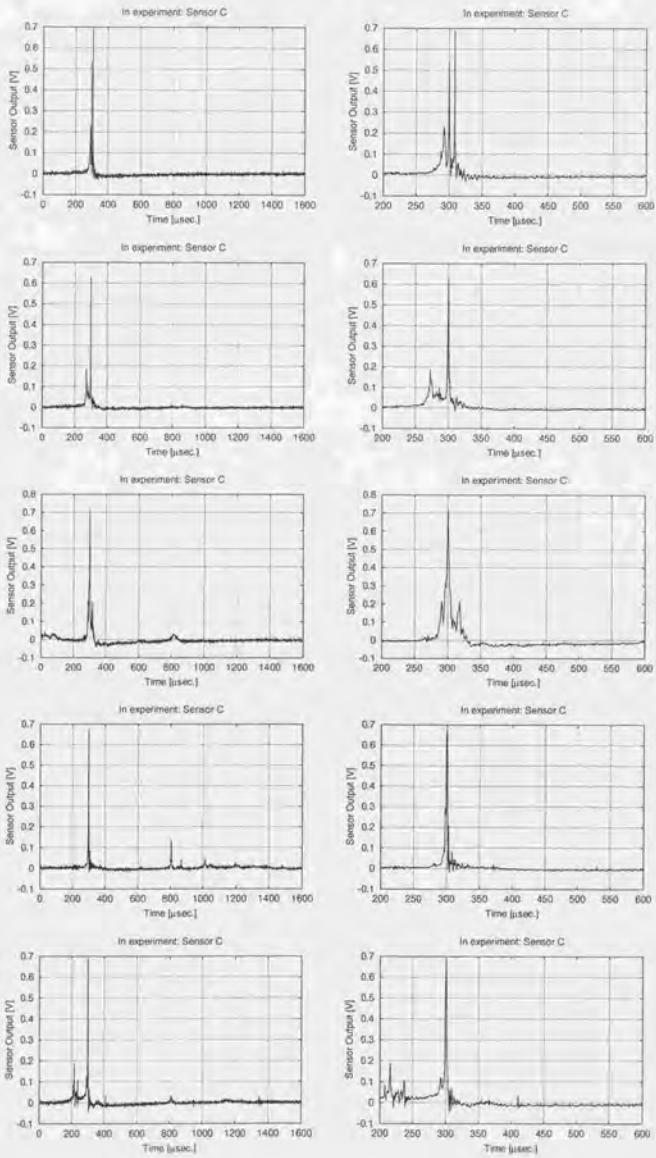

Fig. B.3: (continued)

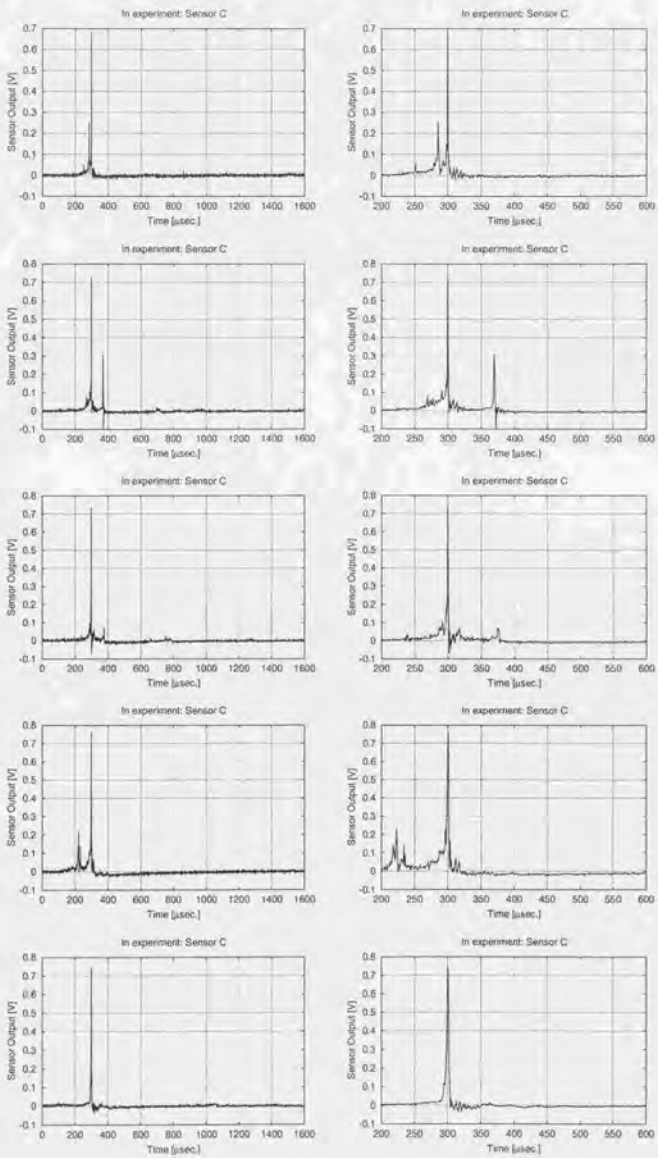

Fig. B.3: (continued)

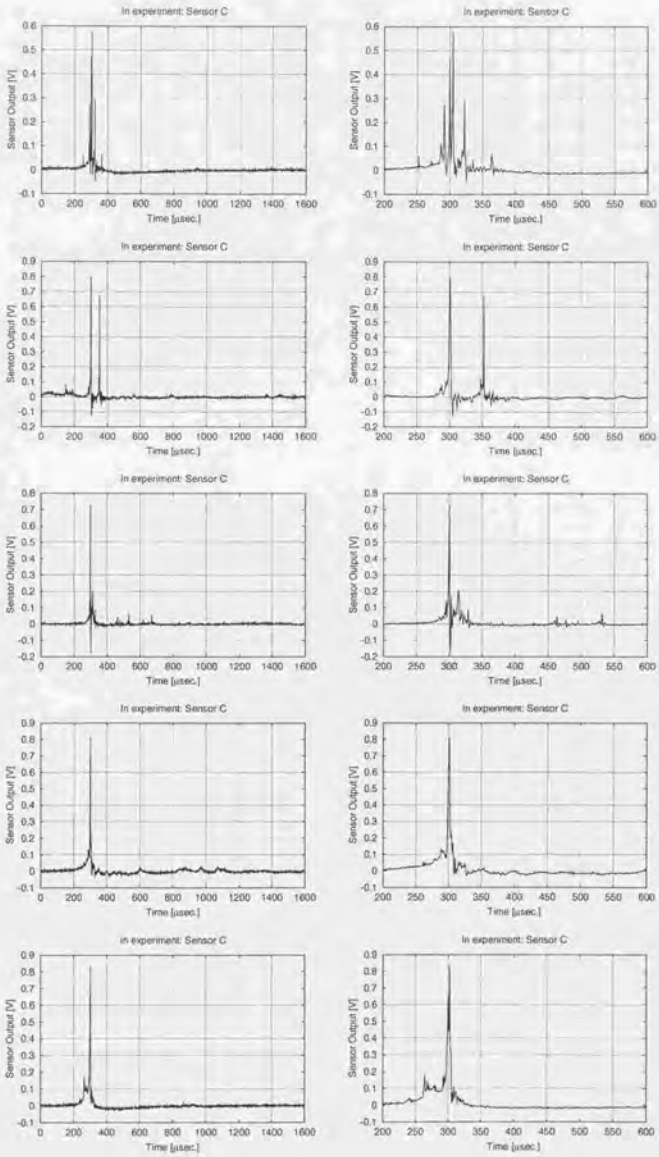

Fig. B.3: (continued)

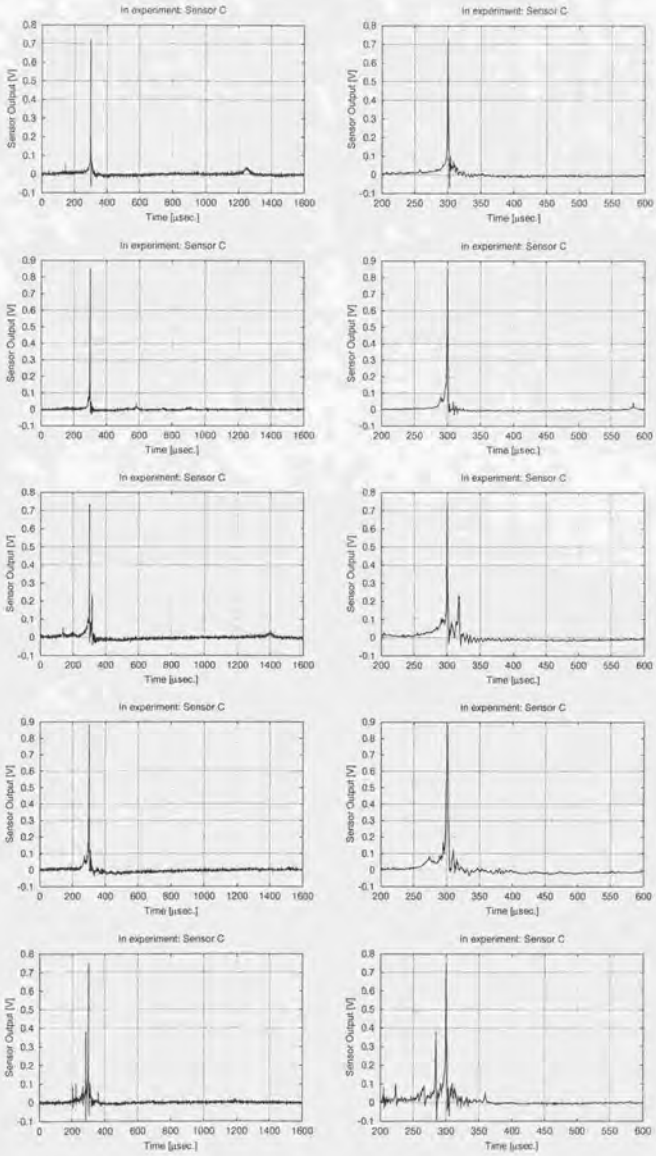

Fig. B.3: (continued)

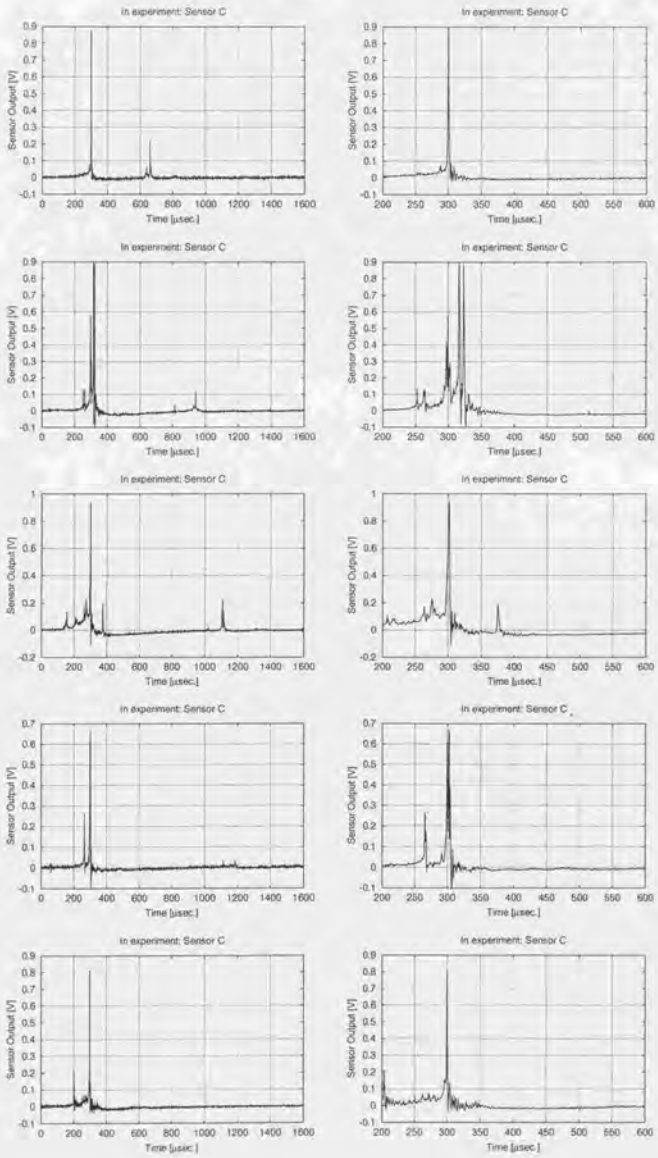

Fig. B.3: (continued)

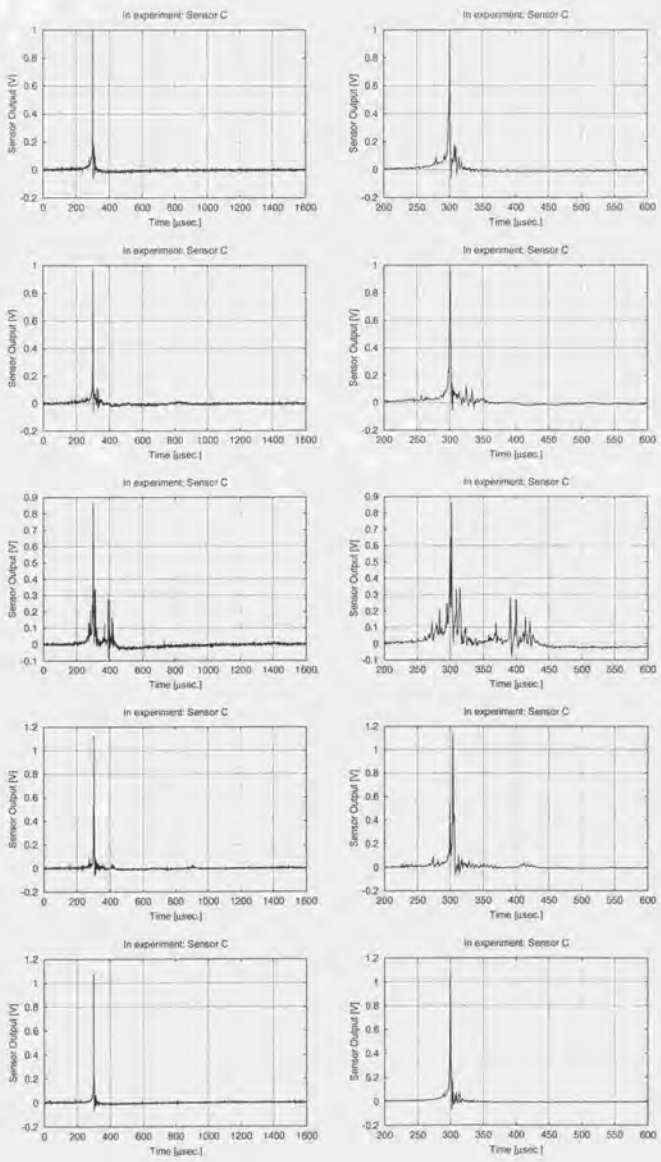

Fig. B.3: (continued)

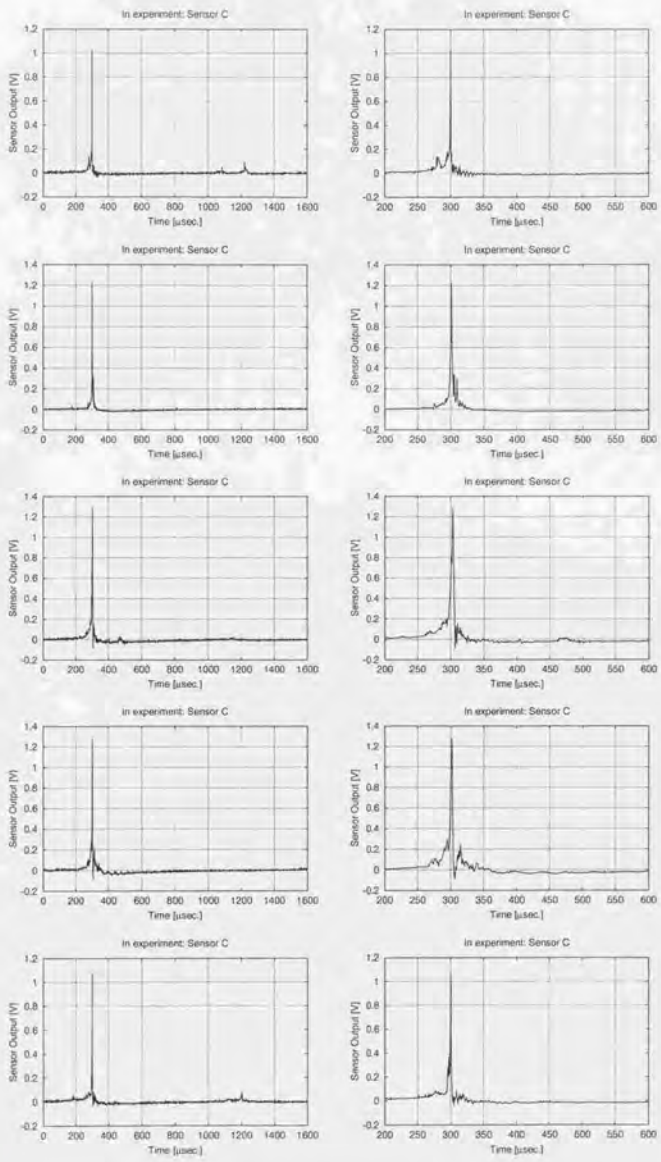

Fig. B.3: (continued)

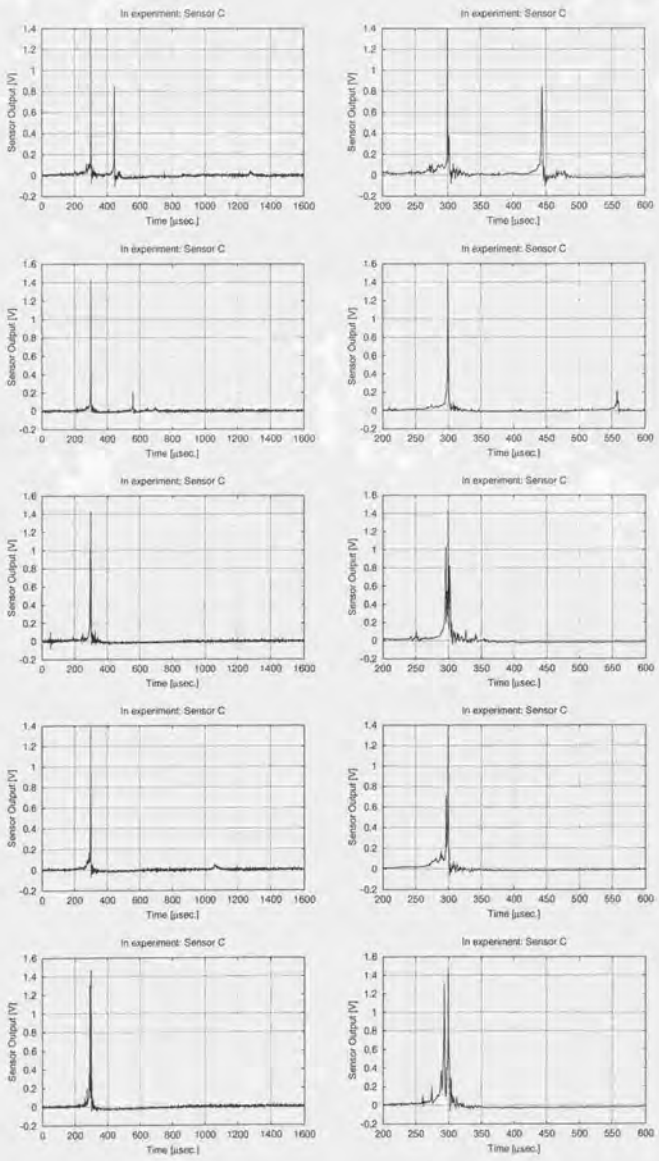

Fig. B.3: (continued)

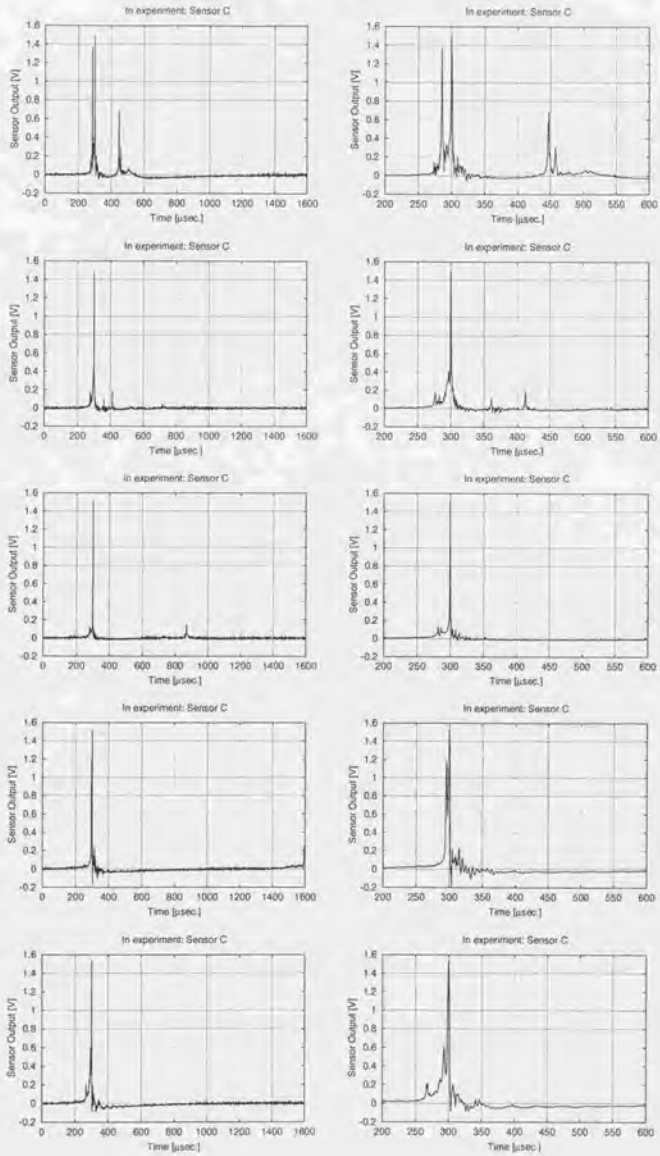

Fig. B.3: (continued)

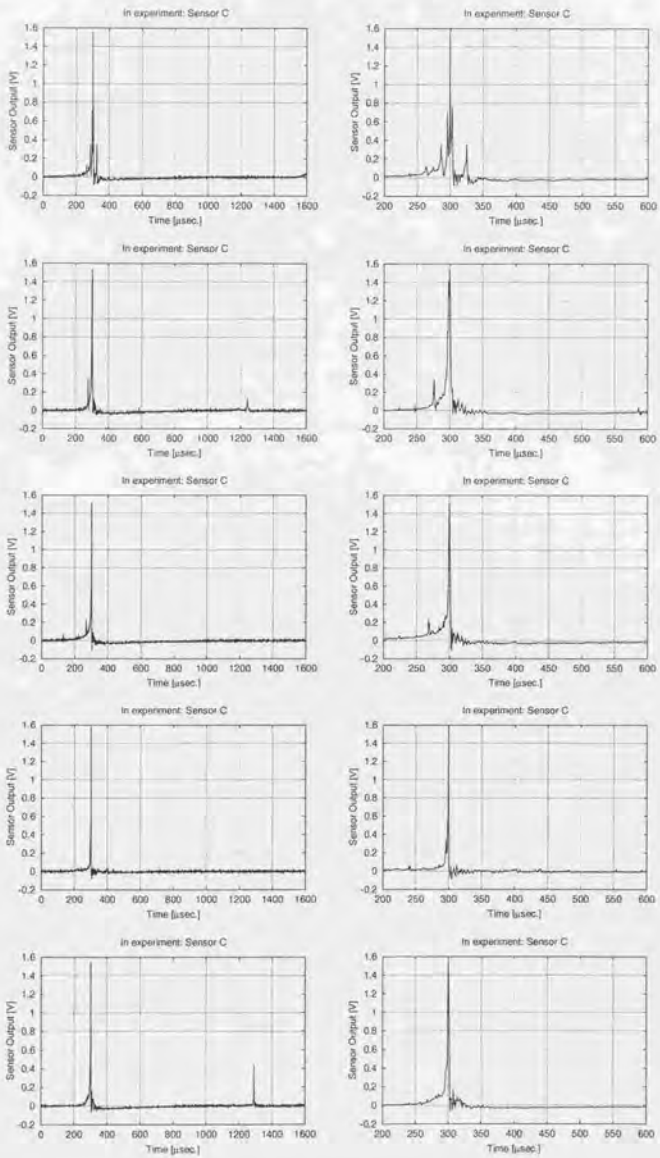

Fig. B.3: (continued)

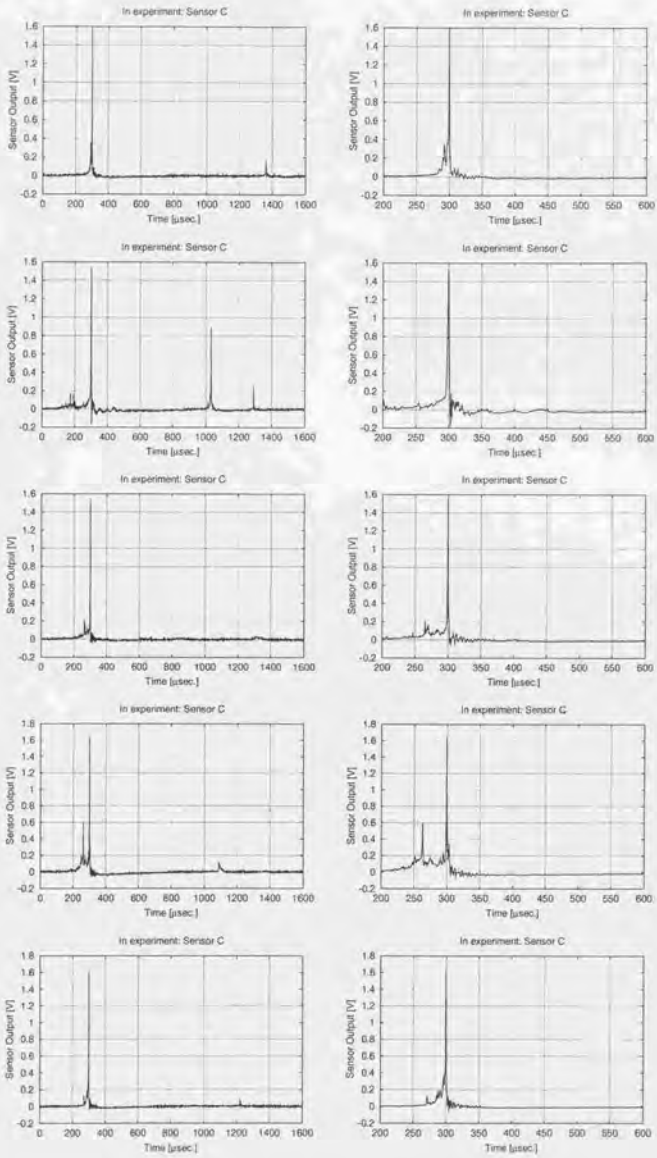

Fig. B.3: (continued)

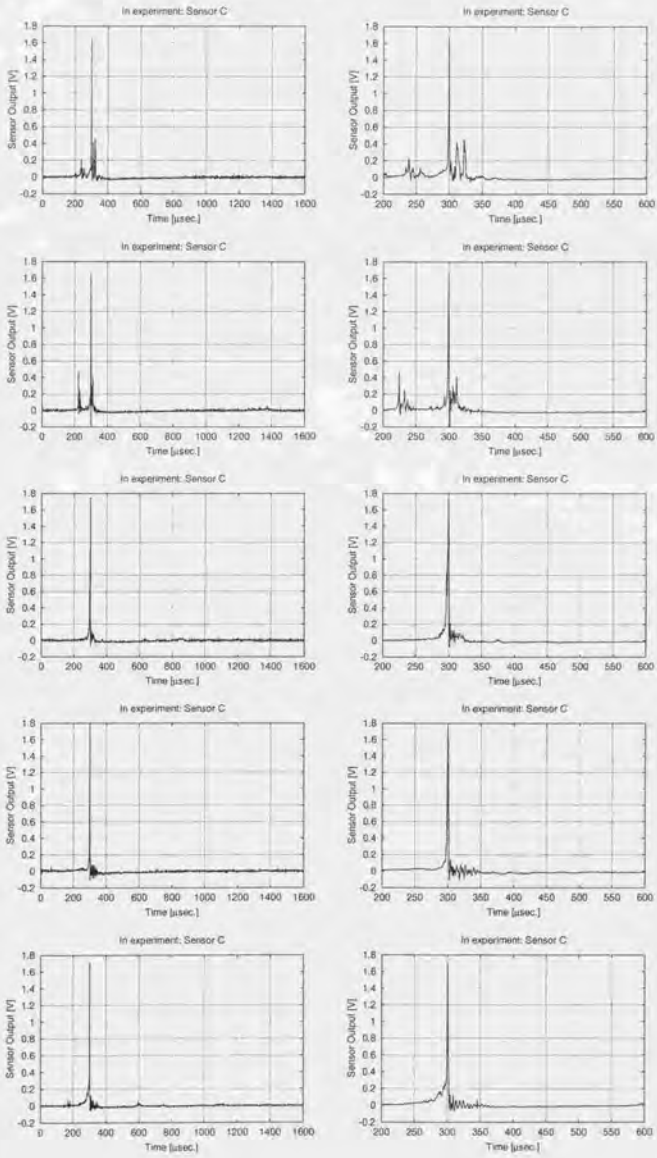

Fig. B.3: (continued)

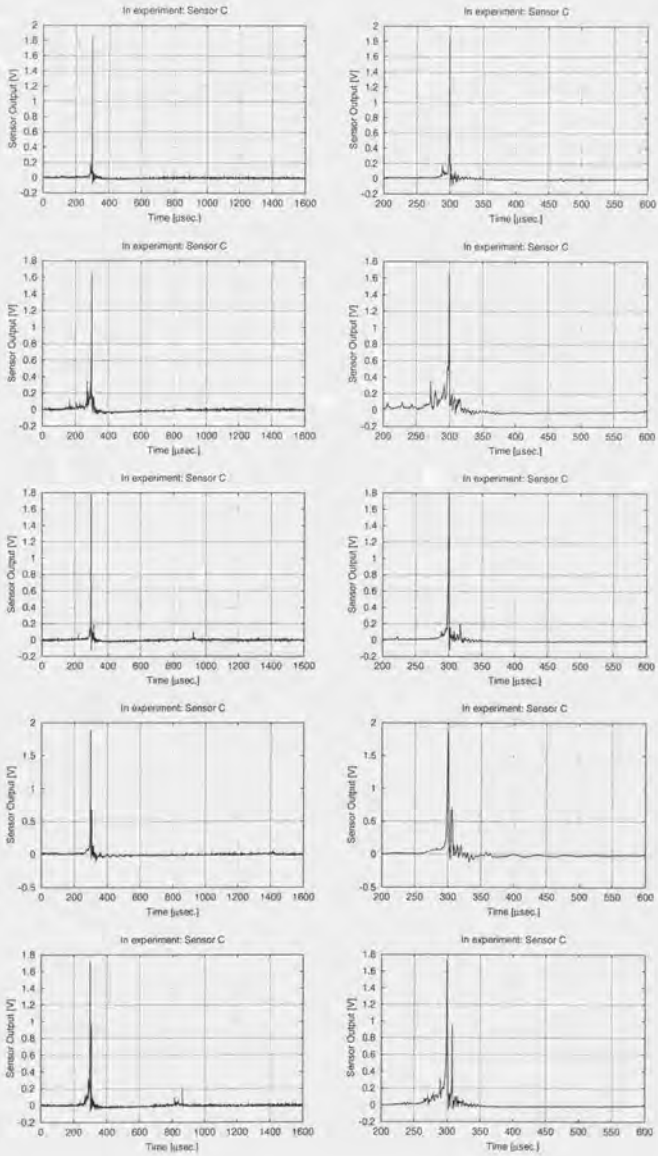

Fig. B.3: (continued)

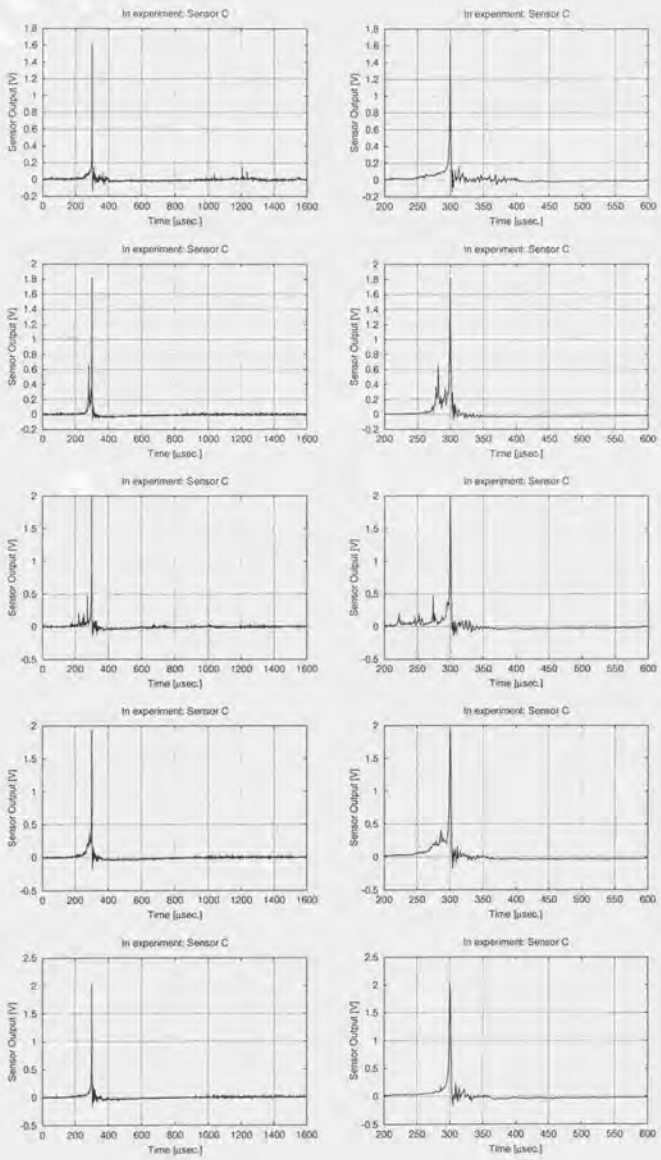

Fig. B.3: (continued)

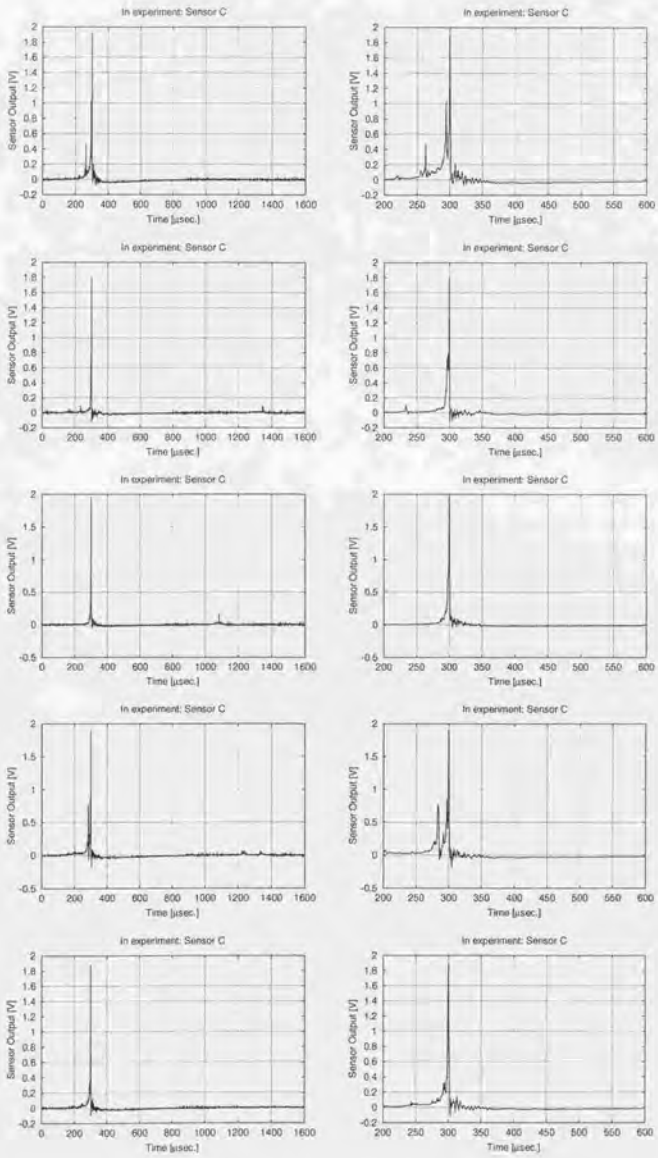

Fig. B.3: (continued)

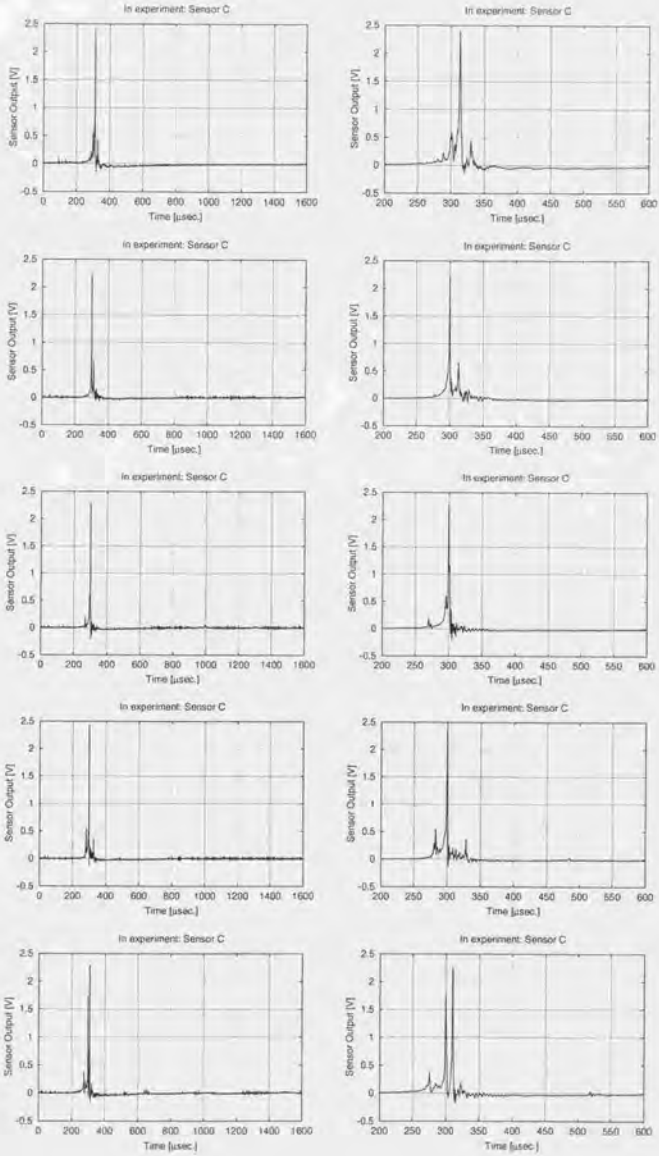

Fig. B.3: (continued)

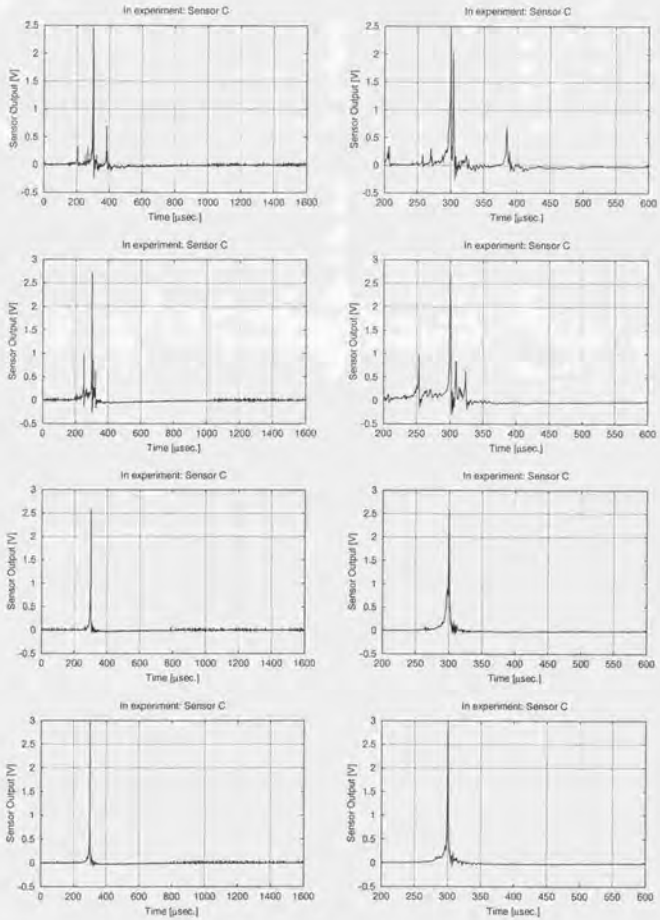

Fig. B.3: (continued)

付 録C　高速度ビデオカメラによる衝撃力発生の瞬間の映像と、発生する衝撃力

第II部にて説明したように、高速度ビデオカメラと衝撃力センサにより、キャビティ気泡群の崩壊時の挙動と、崩壊時に発生する衝撃力とを同時に計測した。高速度ビデオカメラによる映像を次ページ以降のFig. C.1に示す。映像に対応する衝撃力、およびこれらの映像を解析した結果については、付録D (155ページ以降)に載せる。

実験の詳細は、第II部の第11章で説明しているので、ここでは実験条件のみを示す。実験にはNACA 0015翼模型を用い、、迎角8°、流速8m/sec.、キャビテーション数$\sigma_B = 1.5$の条件下で行った。この条件では周期的なクラウドキャビテーションが発生する。キャビテーション全体のようすは第11章で説明している。

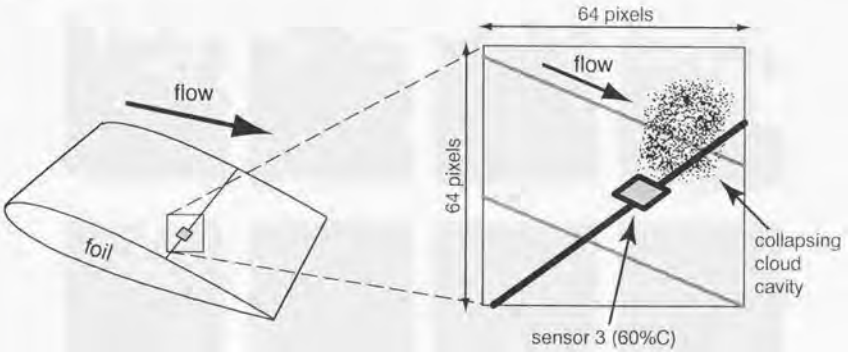

(Same figure of Fig. 11.5)

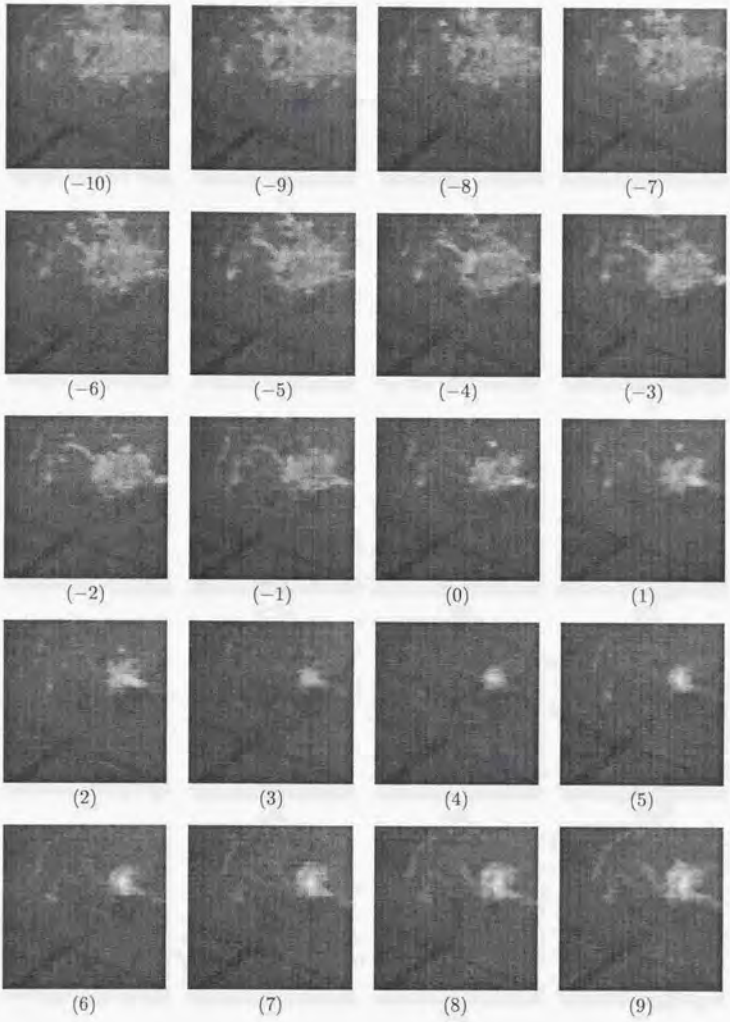

Fig. C.1: Sequences of bird's-eye pictures by high-speed video camera at the time when impulsive forces were measured (No.1)

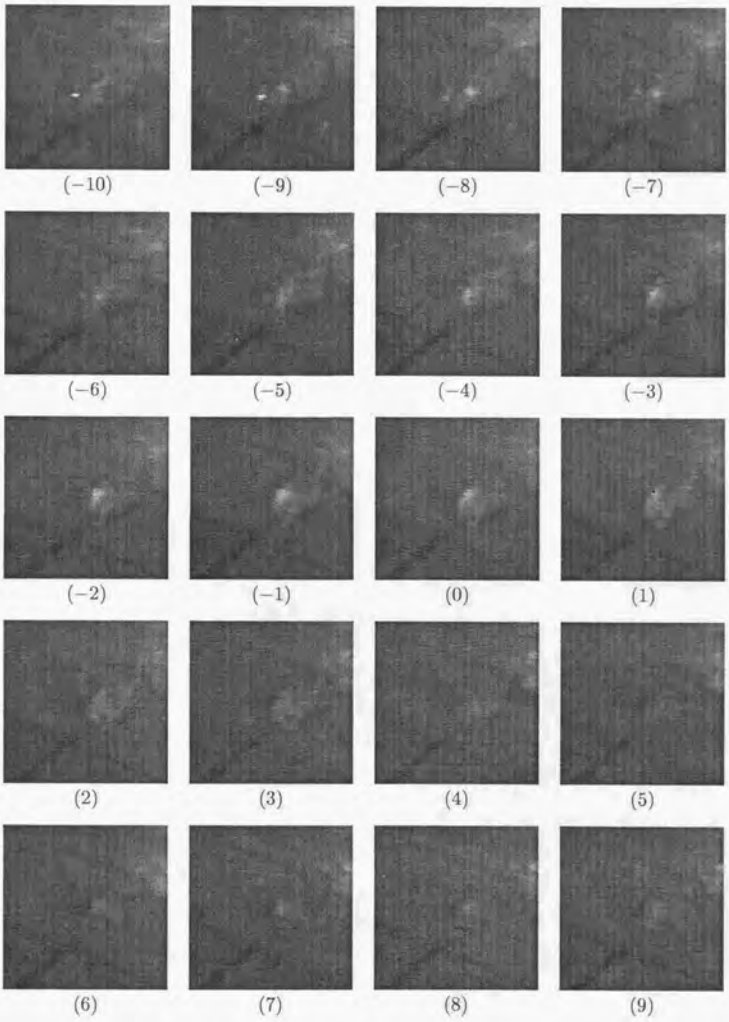

Fig. C.1: (No.2)

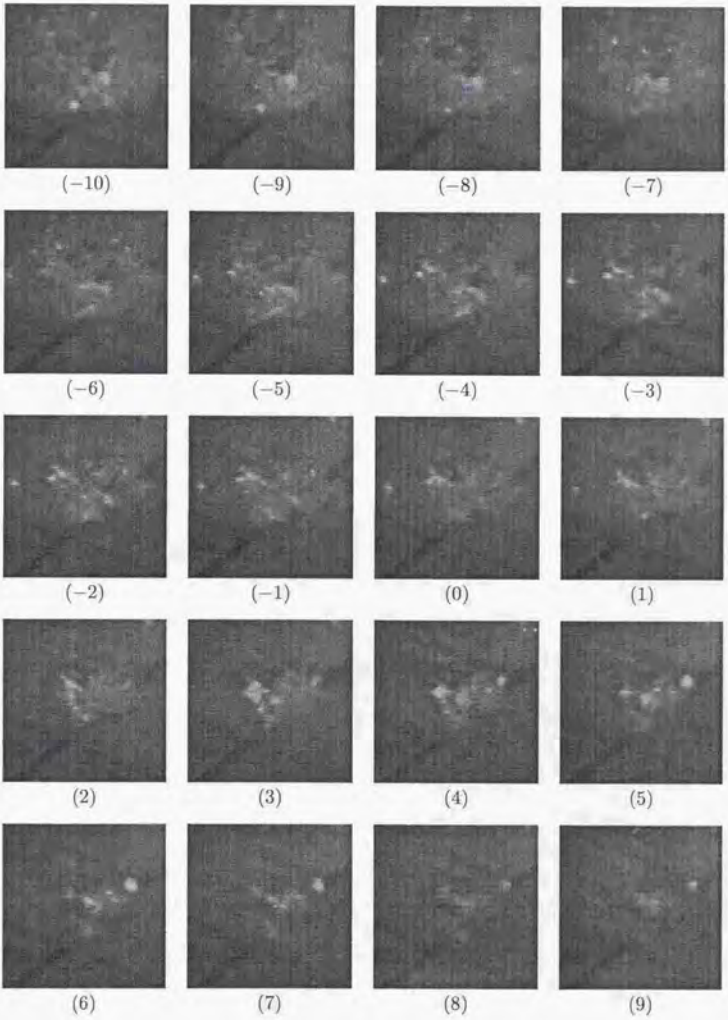

Fig. C.1: (No.3)

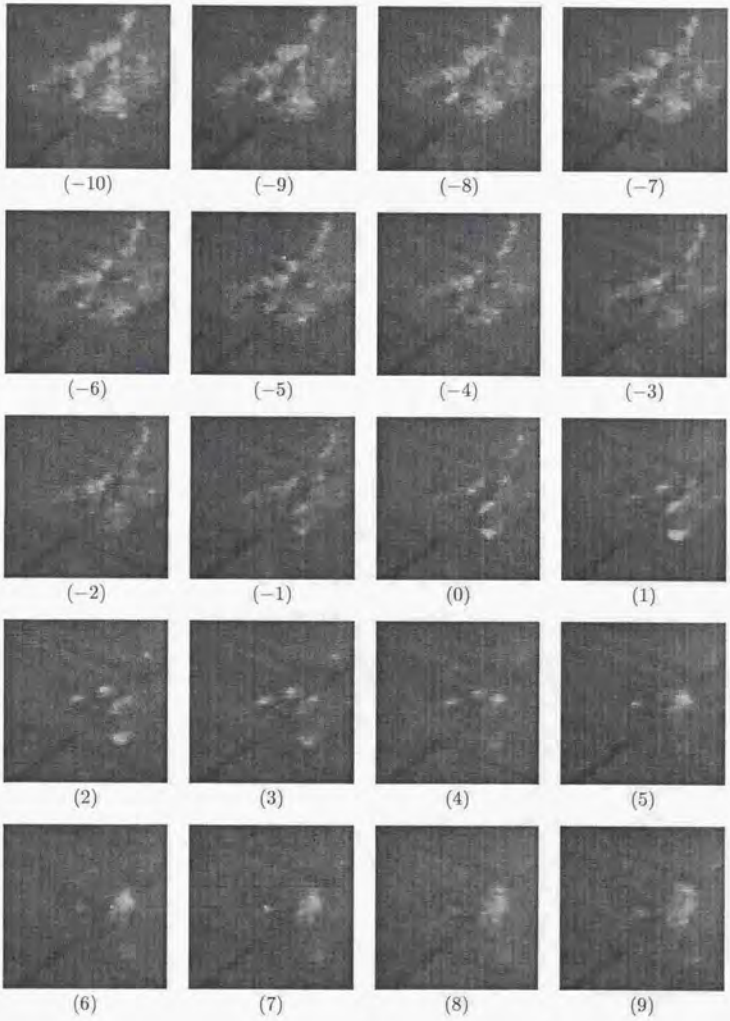

Fig. C.1: (No.4)

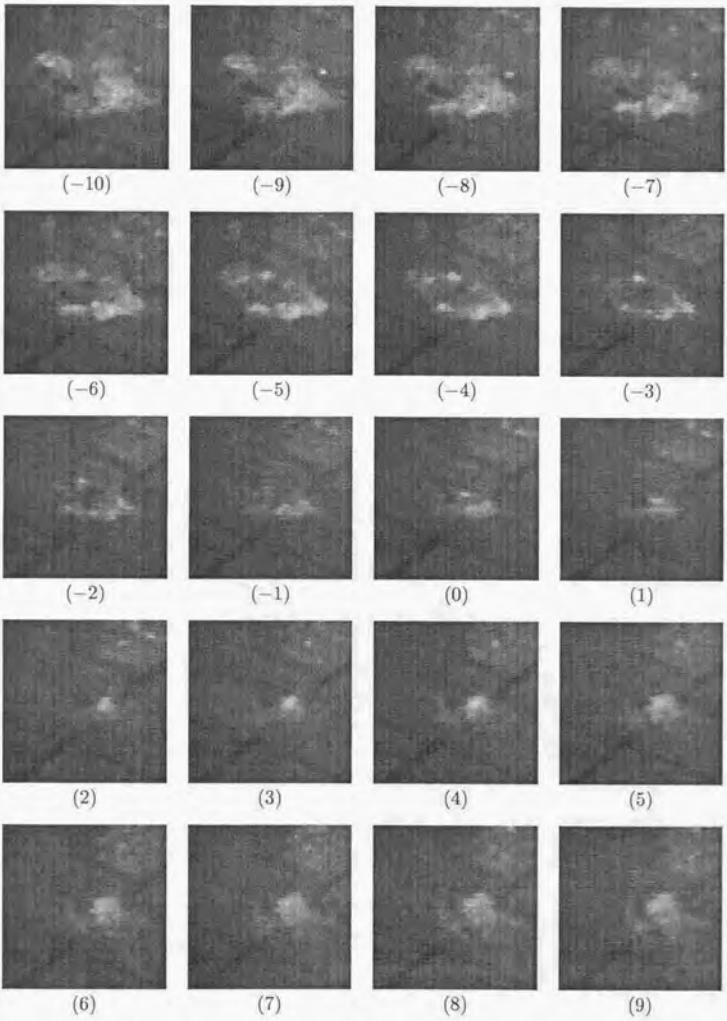

Fig. C.1: (No.5)

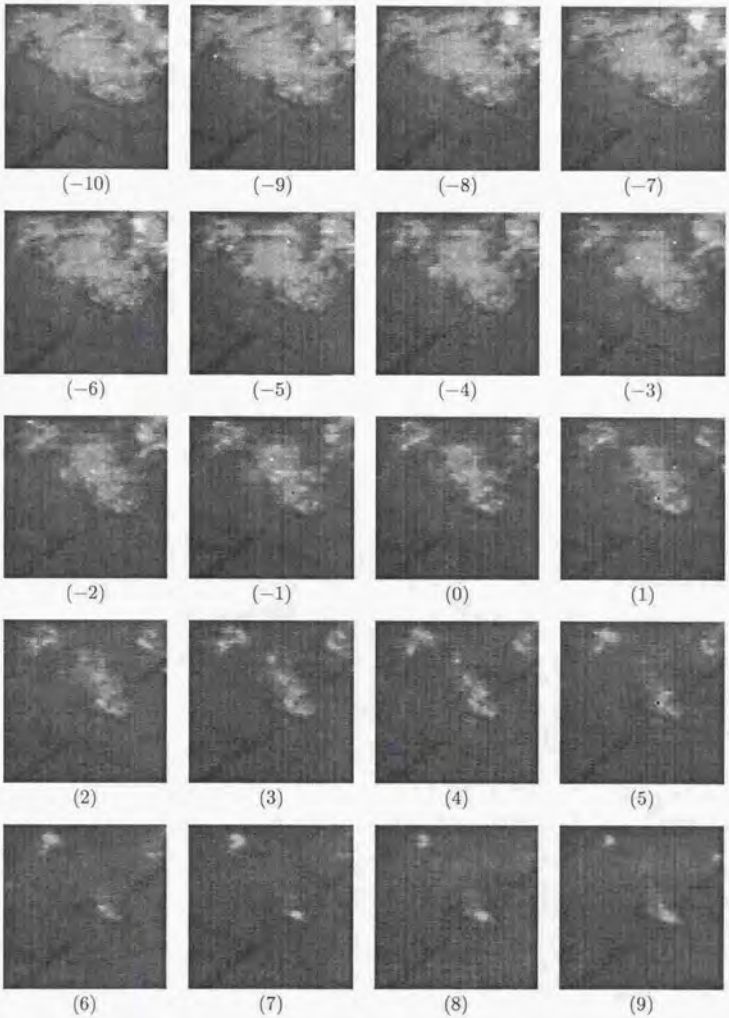

Fig. C.1: (No.6)

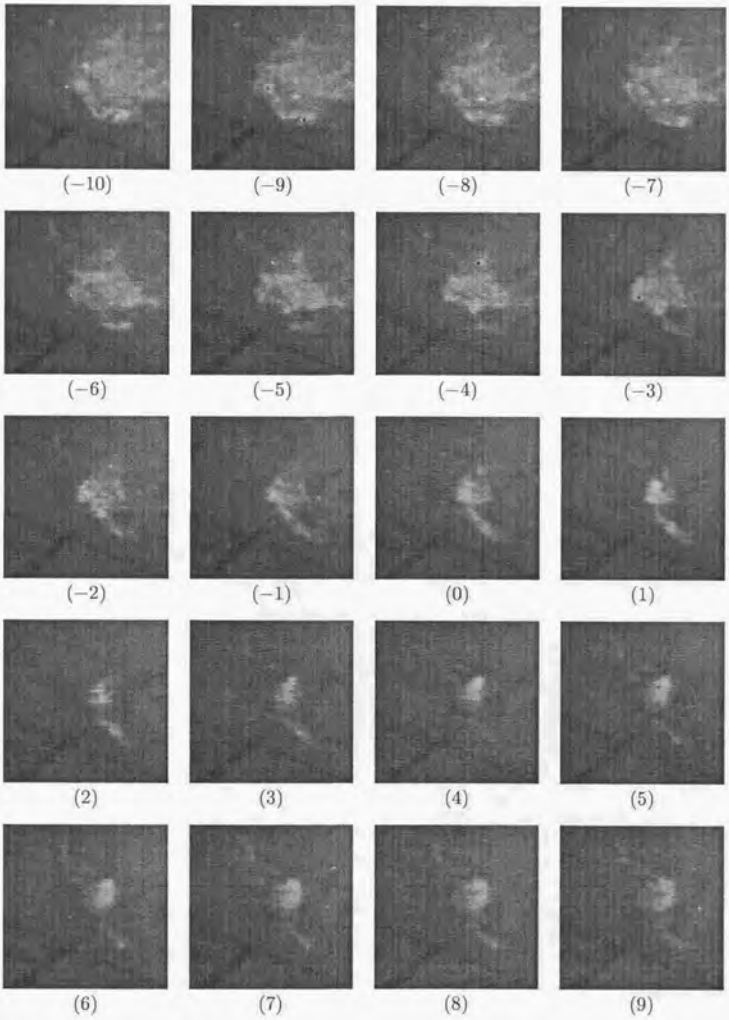

Fig. C.1: (No.7)

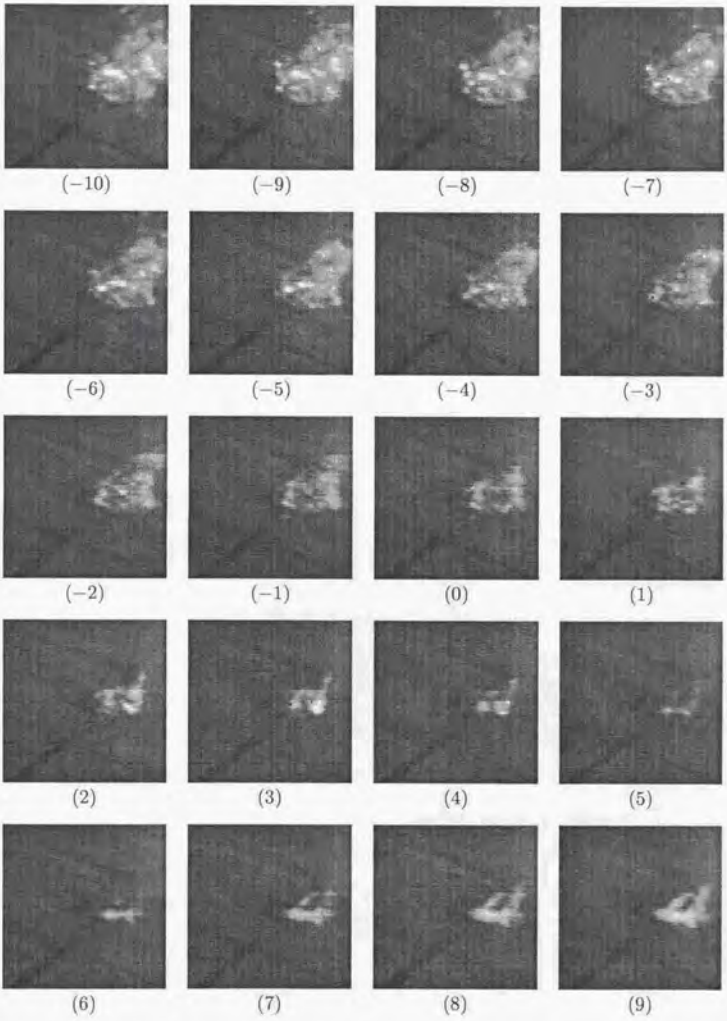

Fig. C.1: (No.8)

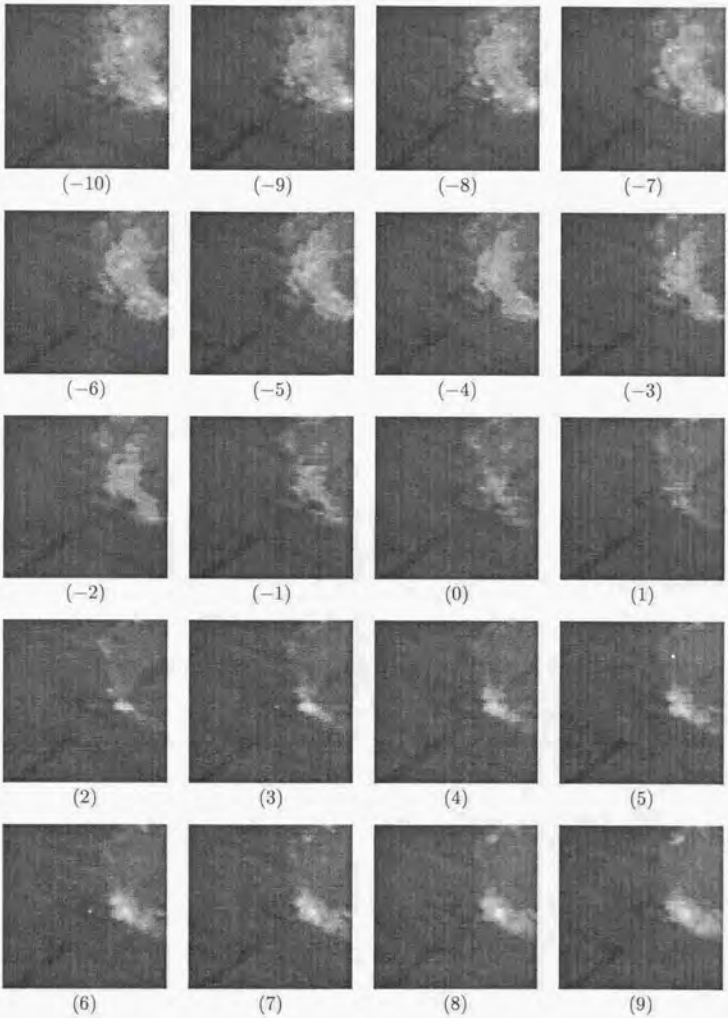

Fig. C.1: (No.9)

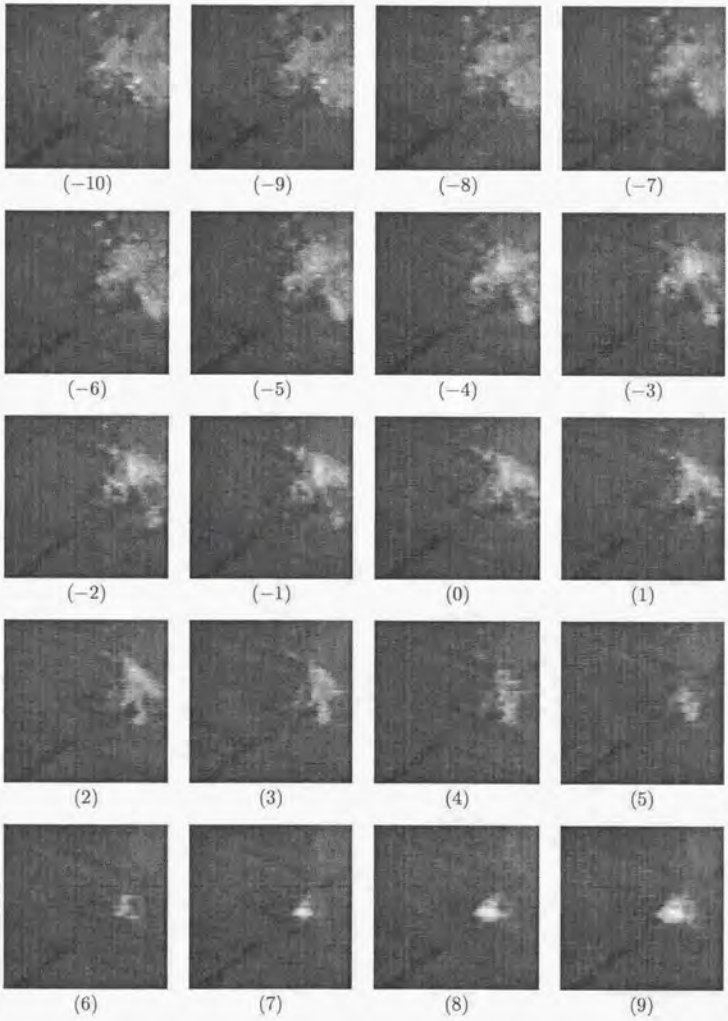

Fig. C.1: (No.10)

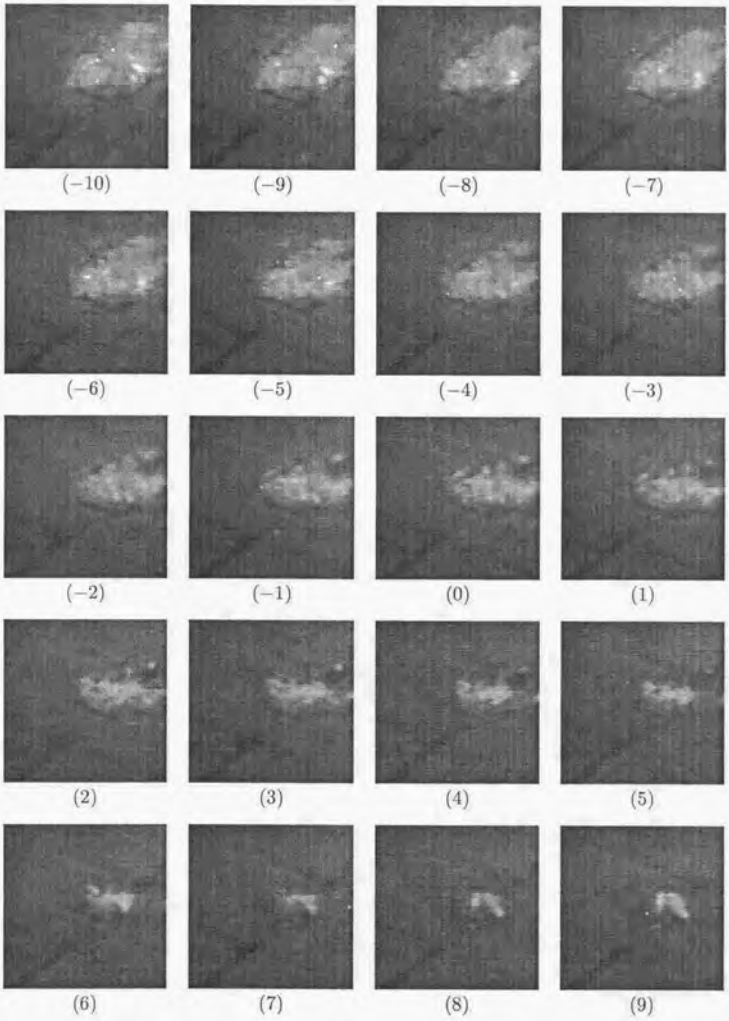

Fig. C.1: (No.11)

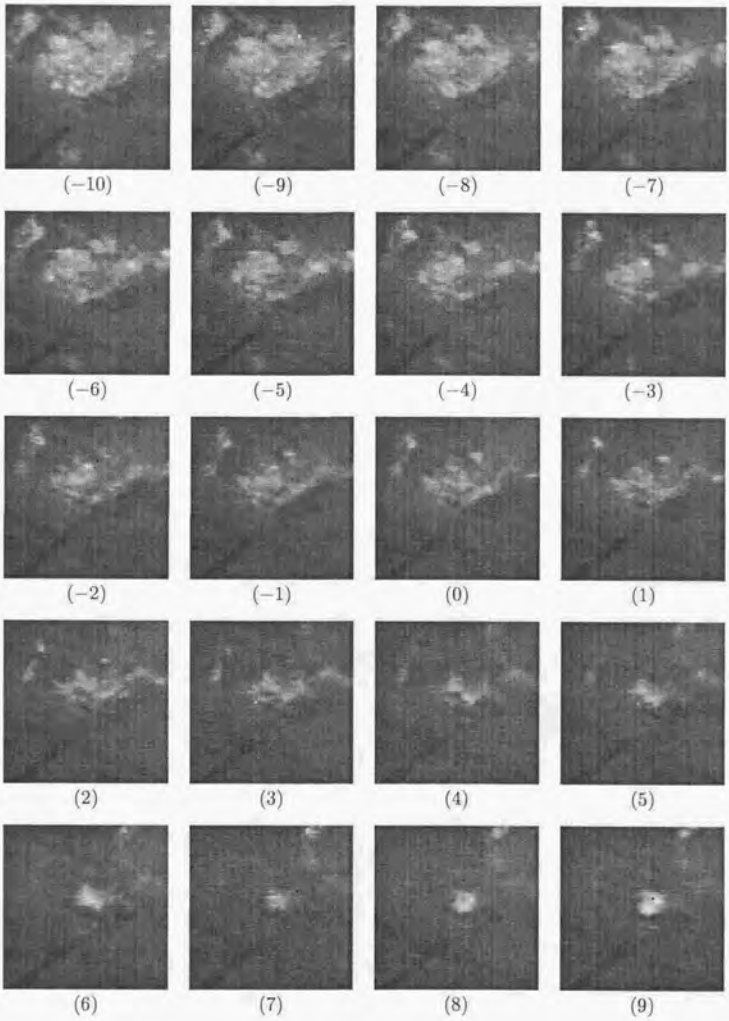

Fig. C.1: (No.12)

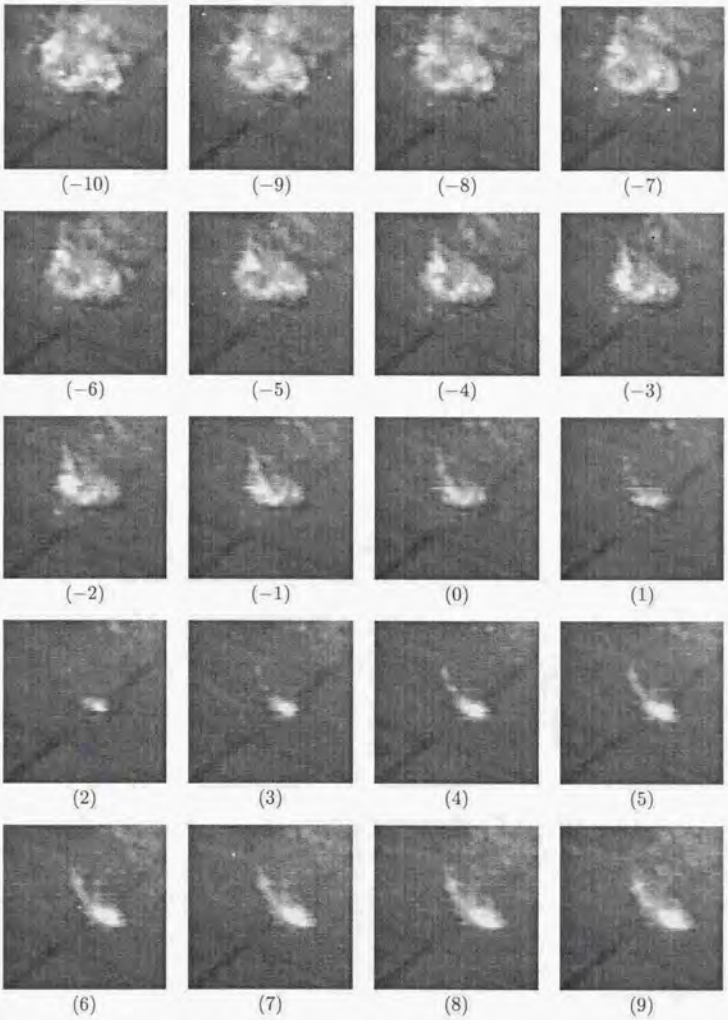

Fig. C.1: (No.13)

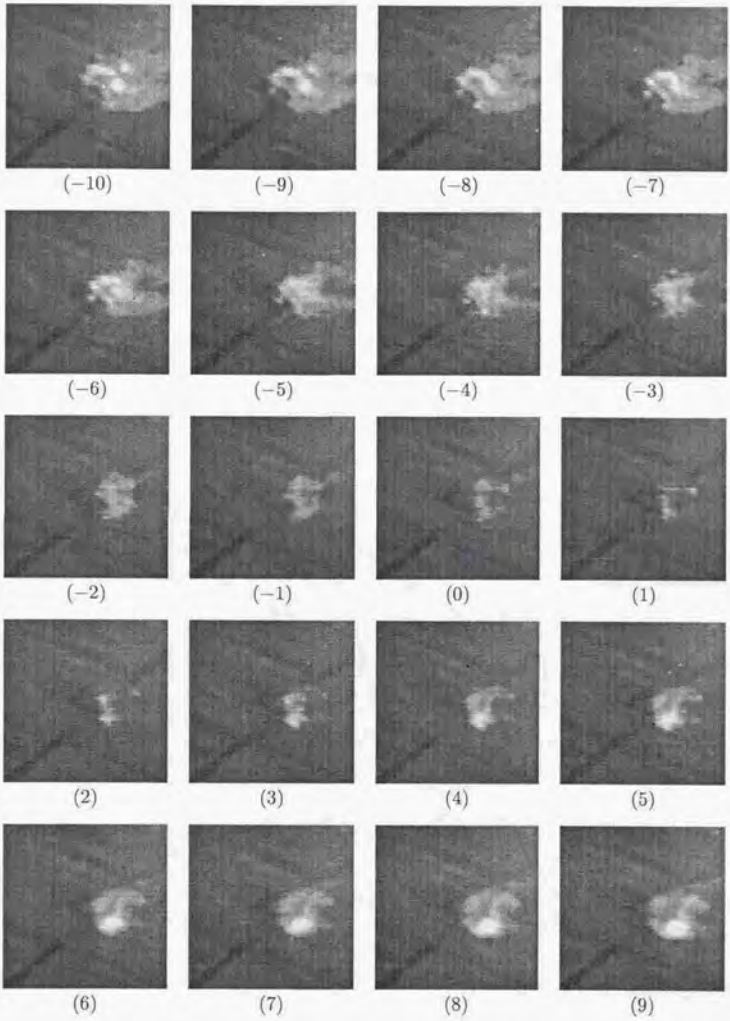

Fig. C.1: (No.14)

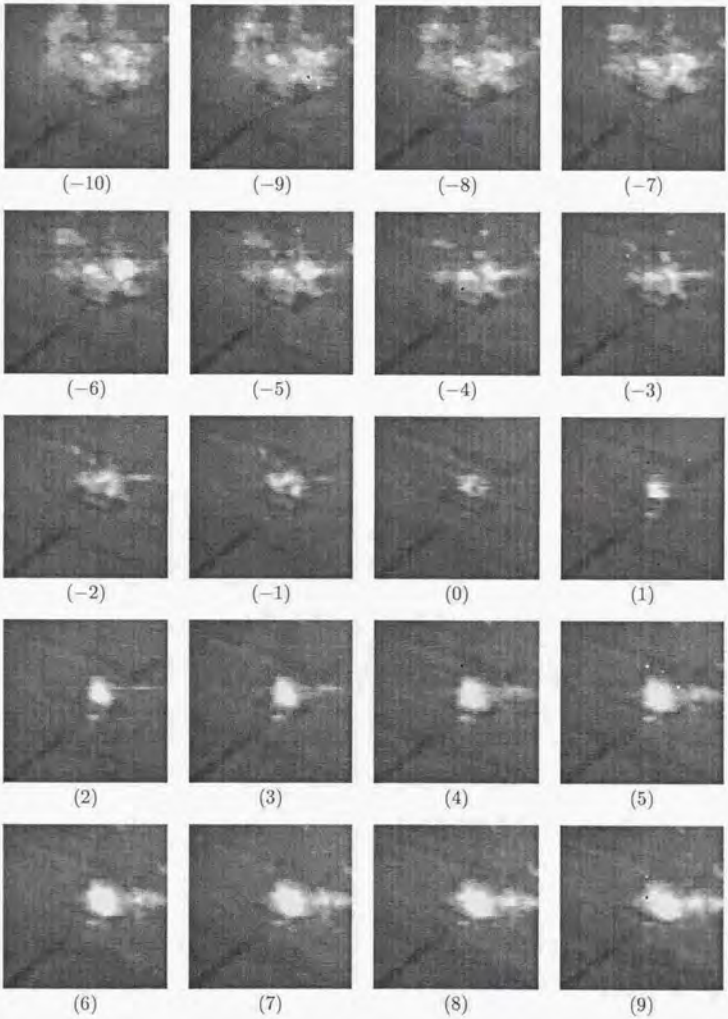

Fig. C.1: (No.15)

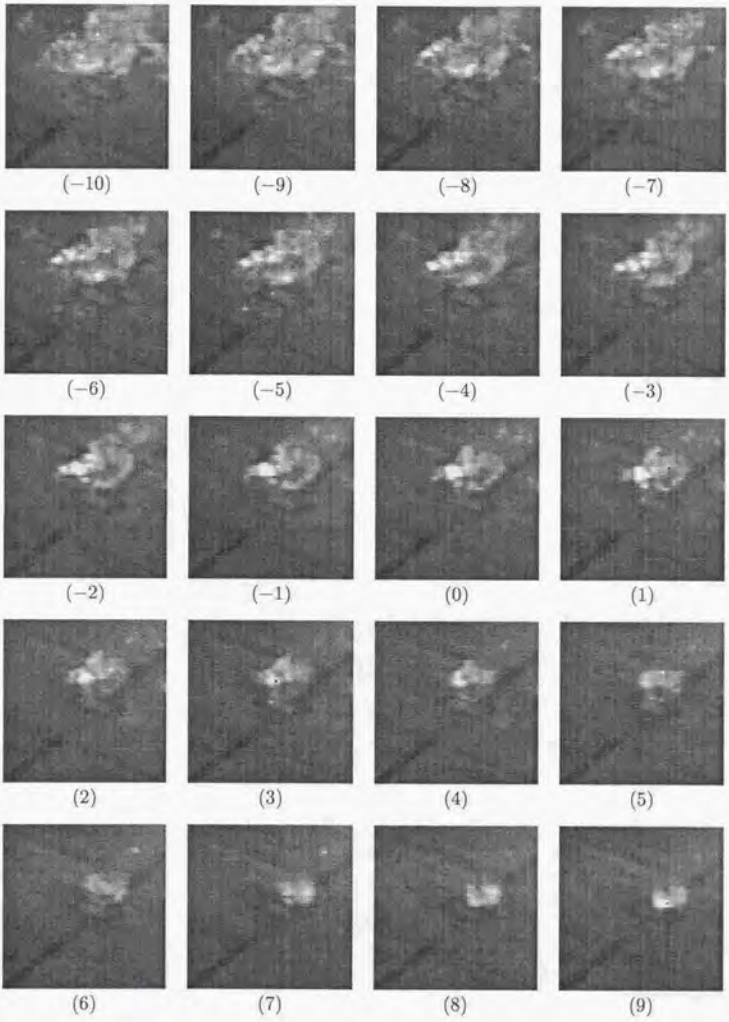

Fig. C.1: (No.16)

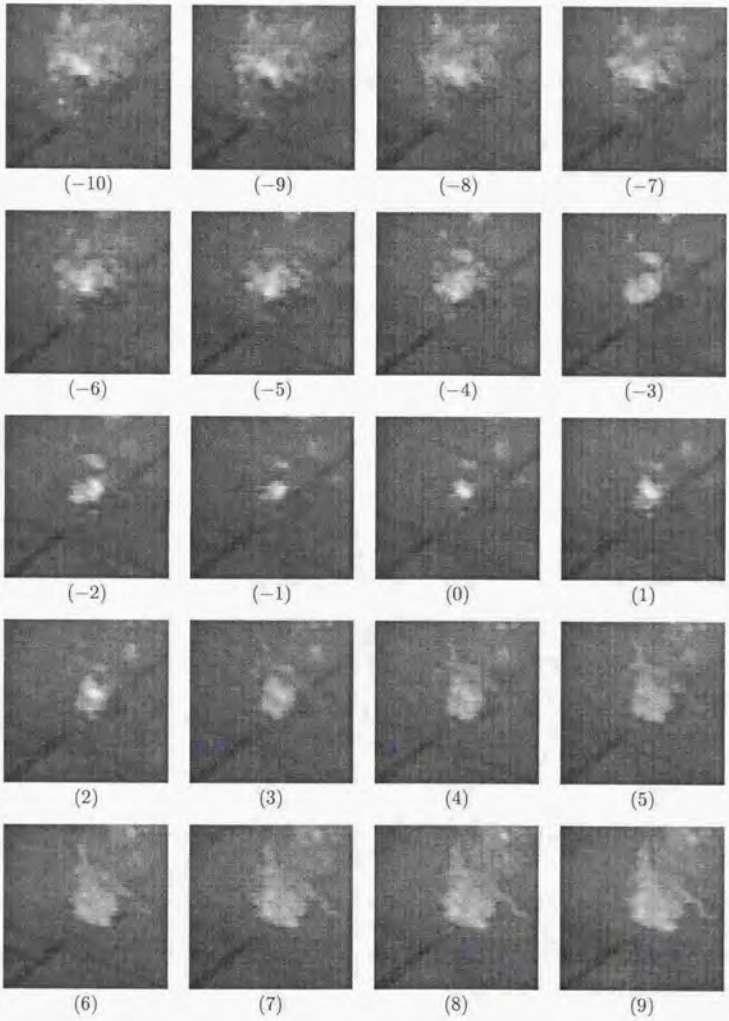

Fig. C.1: (No.17)

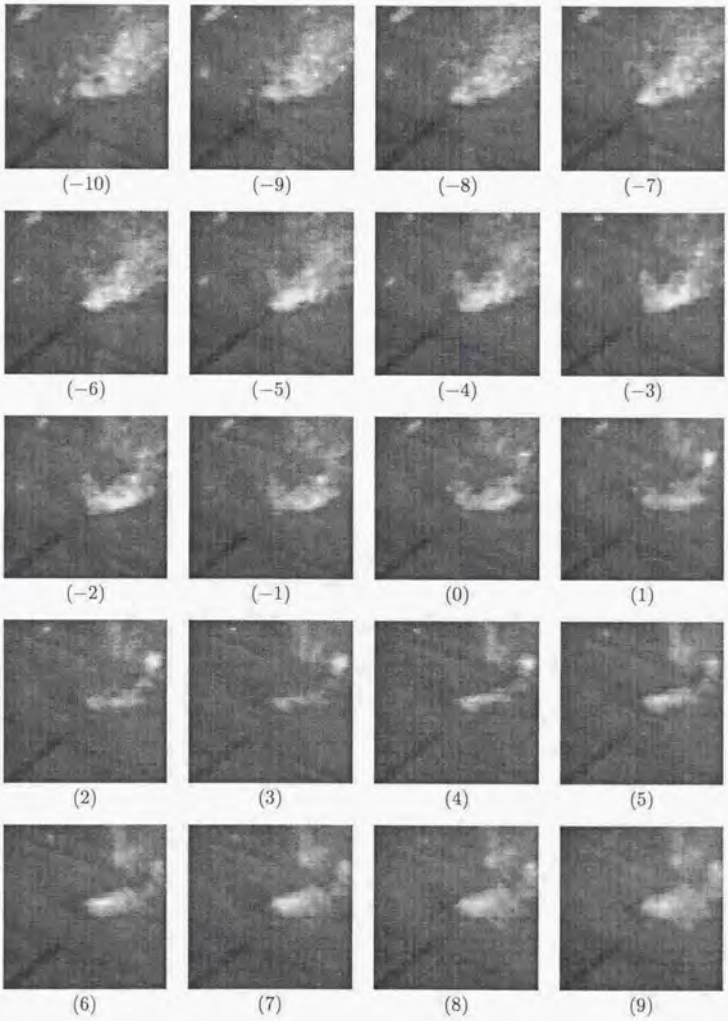

Fig. C.1: (No.18)

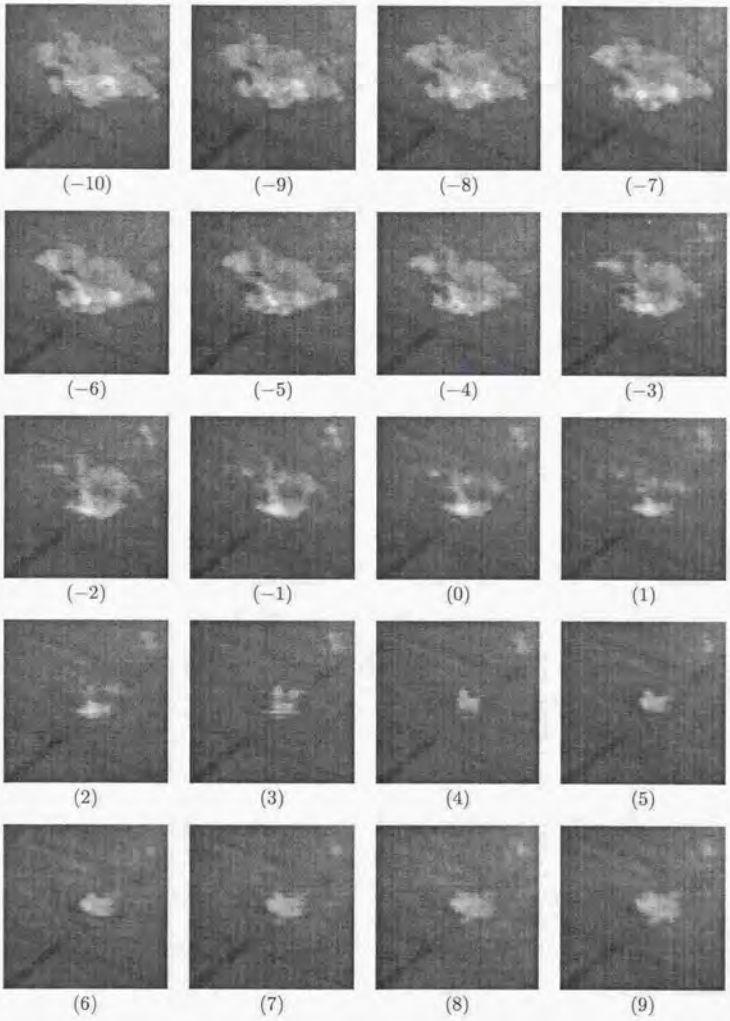

Fig. C.1: (No.19)

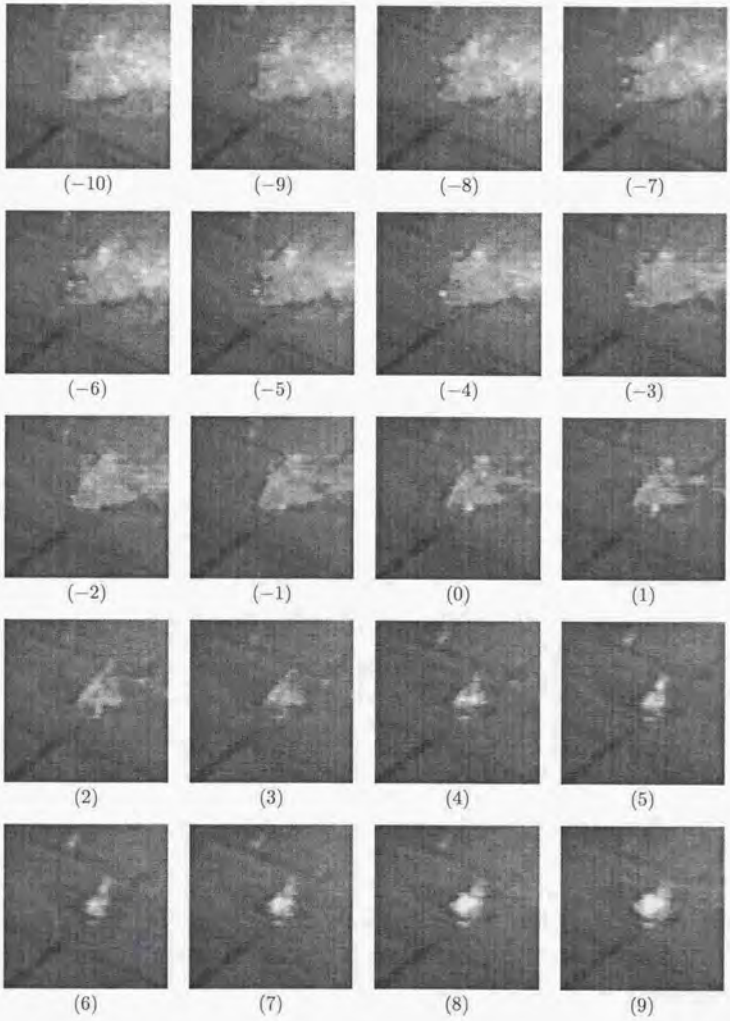

Fig. C.1: (No.20)

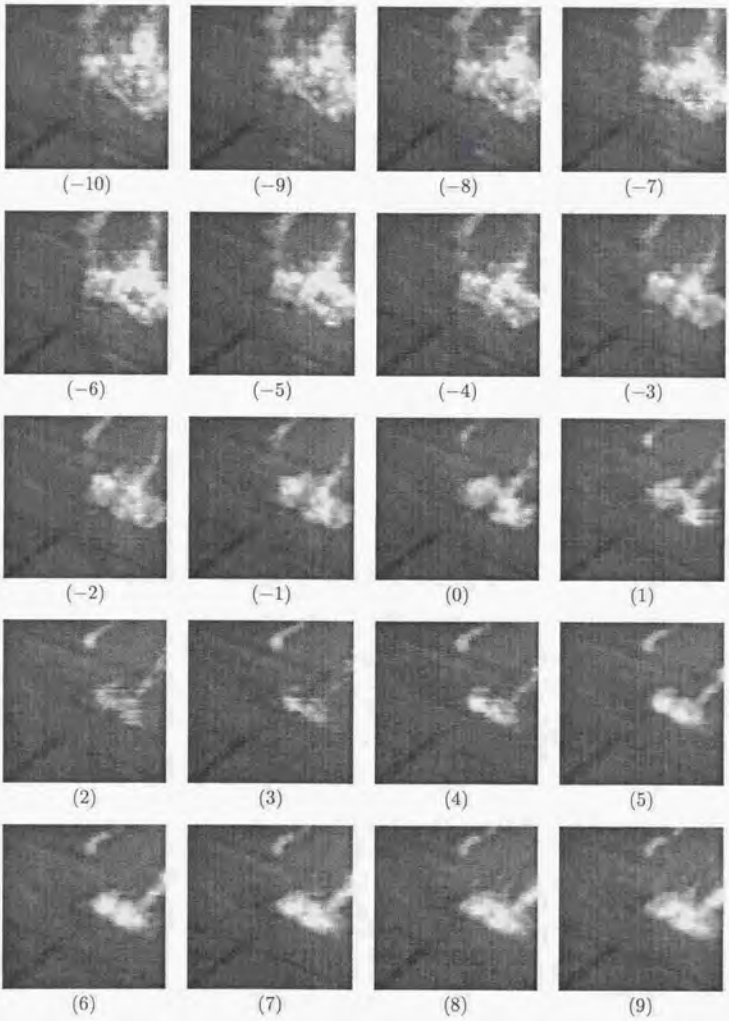

Fig. C.1: (No.21)

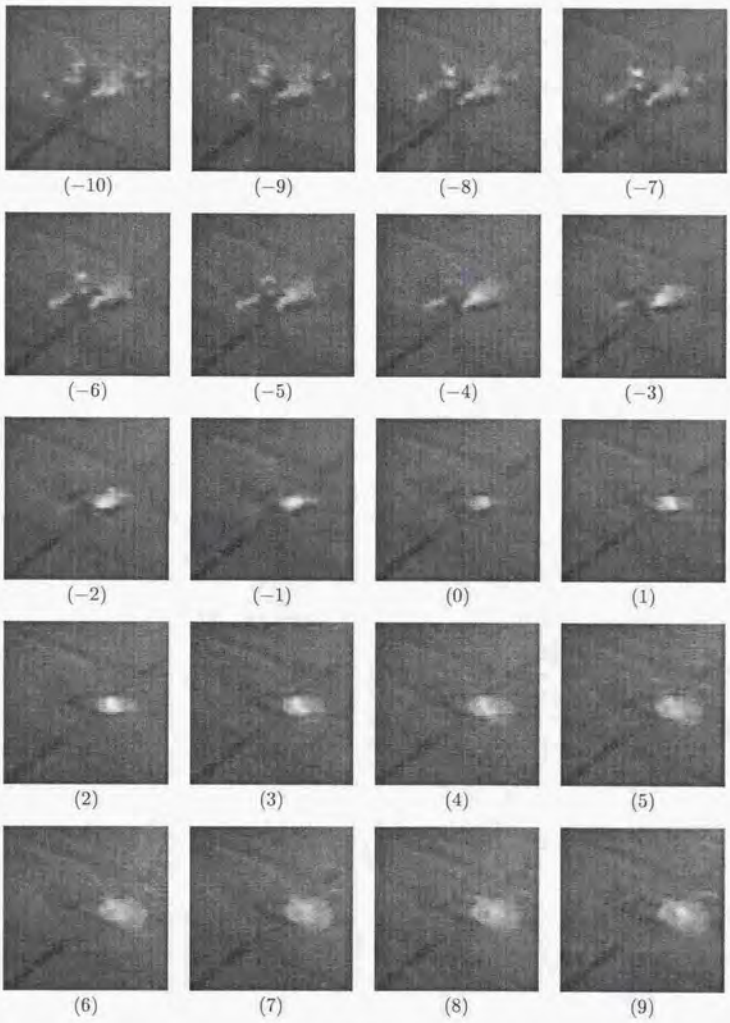

Fig. C.1: (No.22)

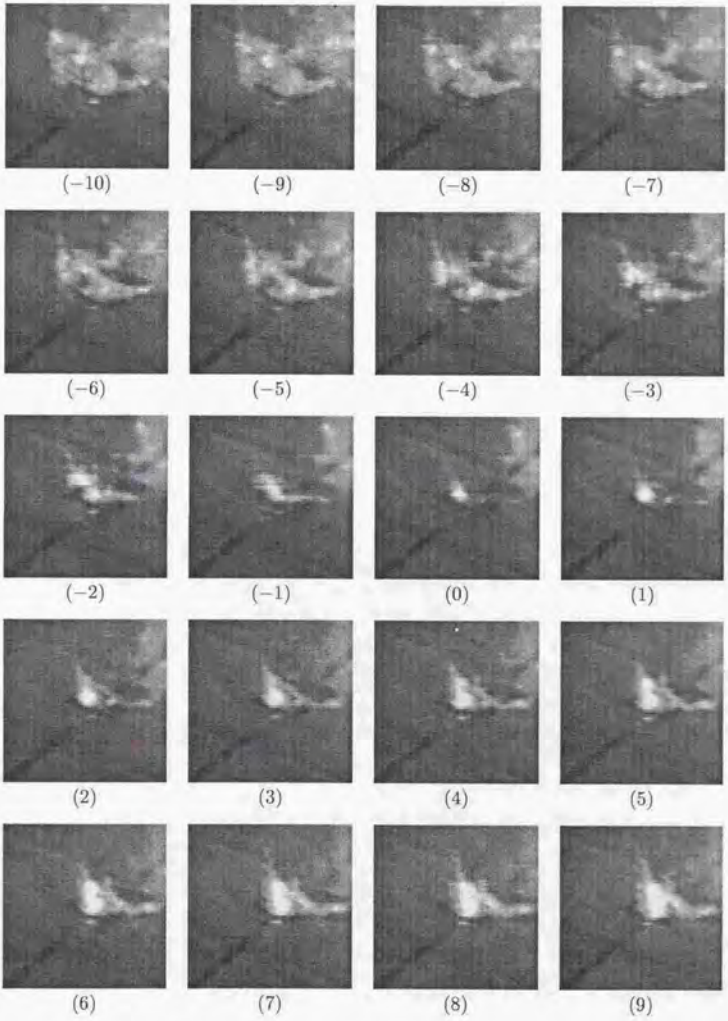

Fig. C.1: (No.23)

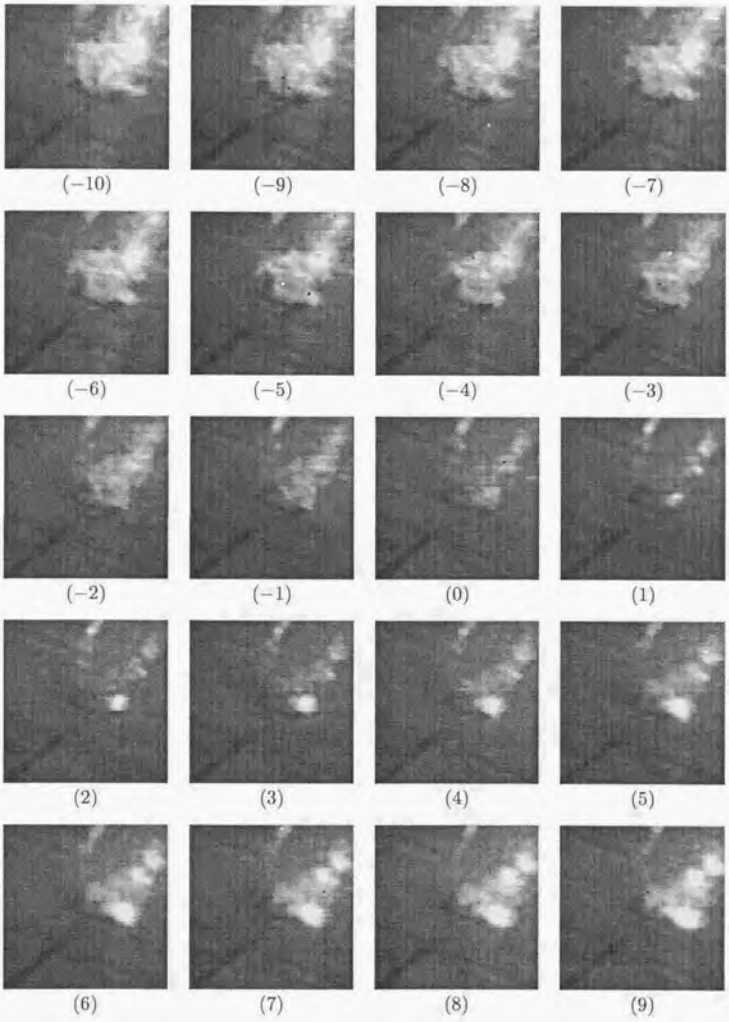

Fig. C.1: (No.24)

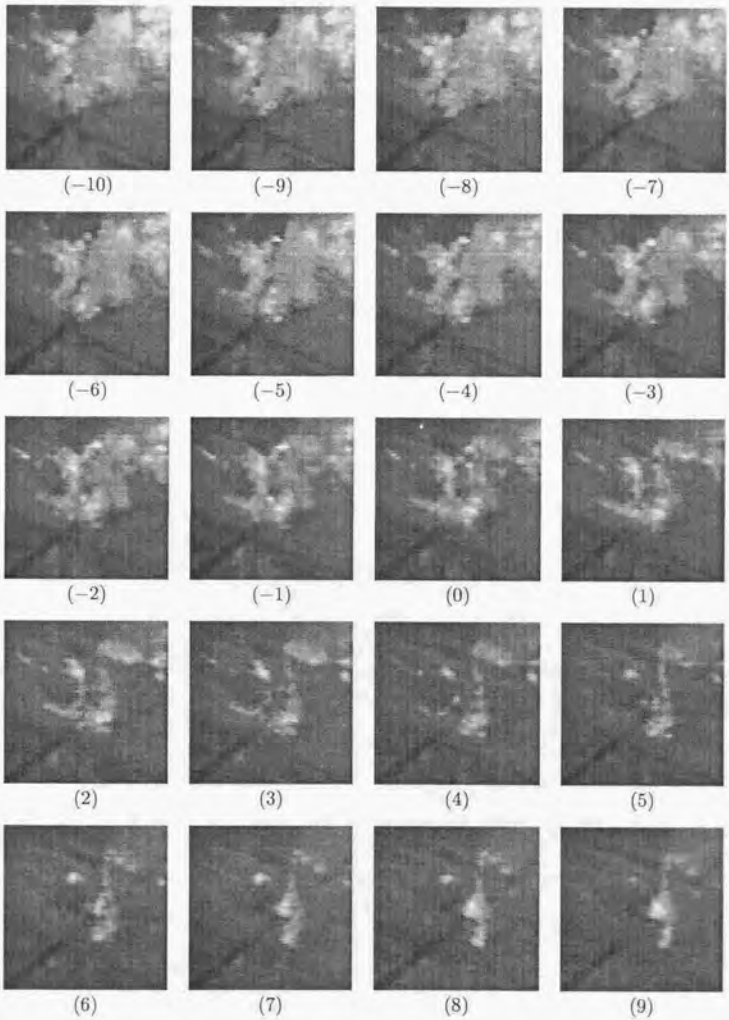

Fig. C.1: (No.25)

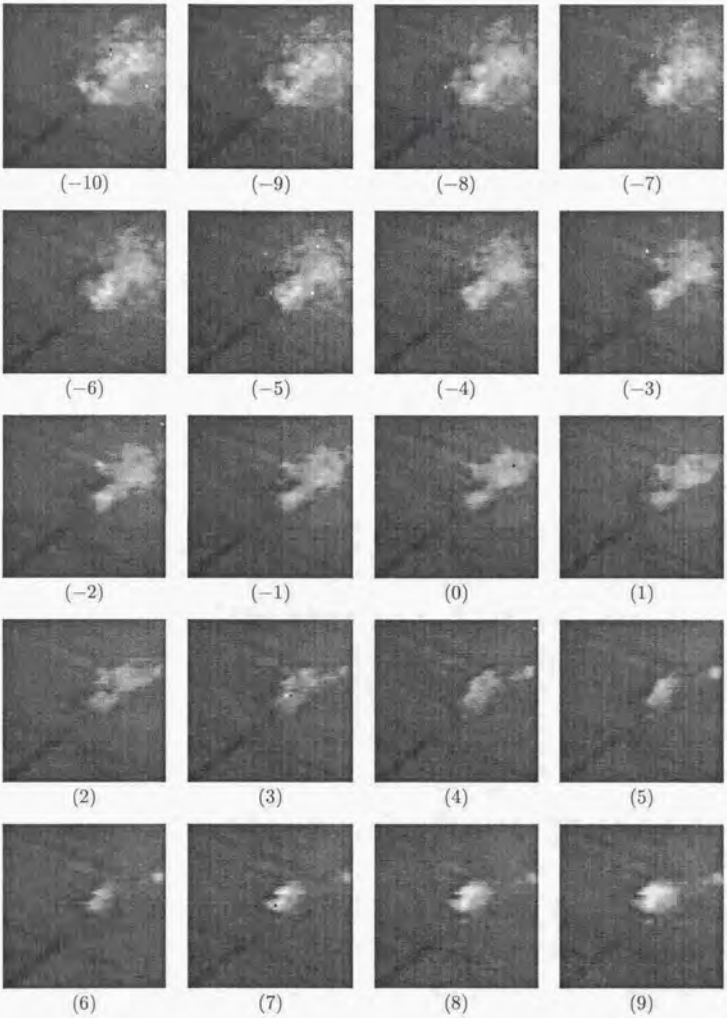

Fig. C.1: (No.26)

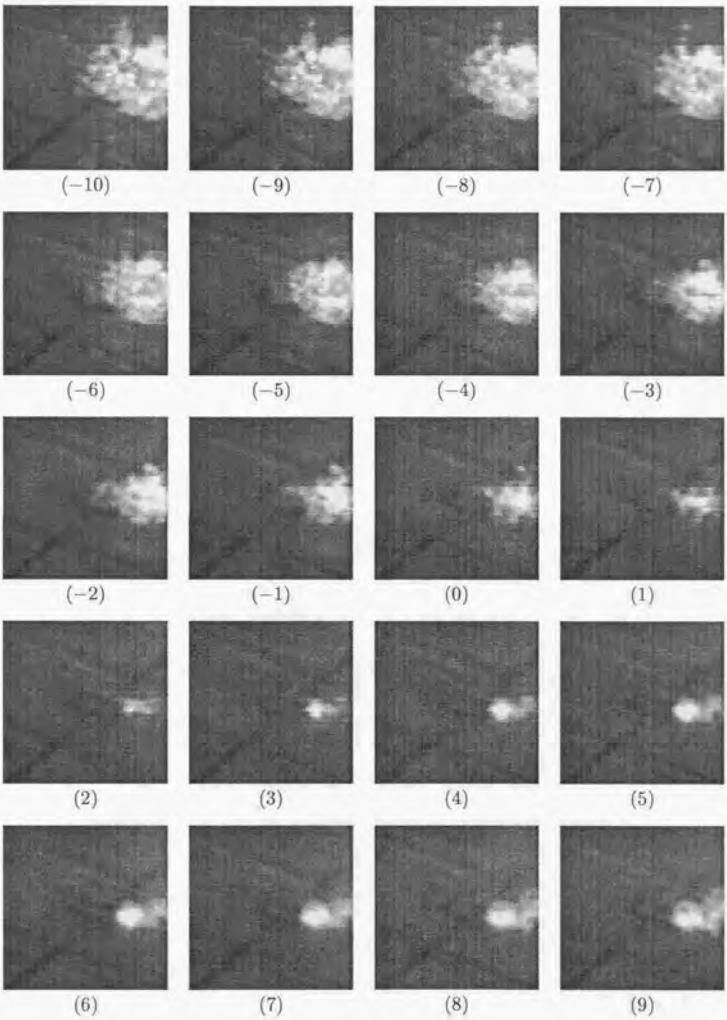

Fig. C.1: (No.27)

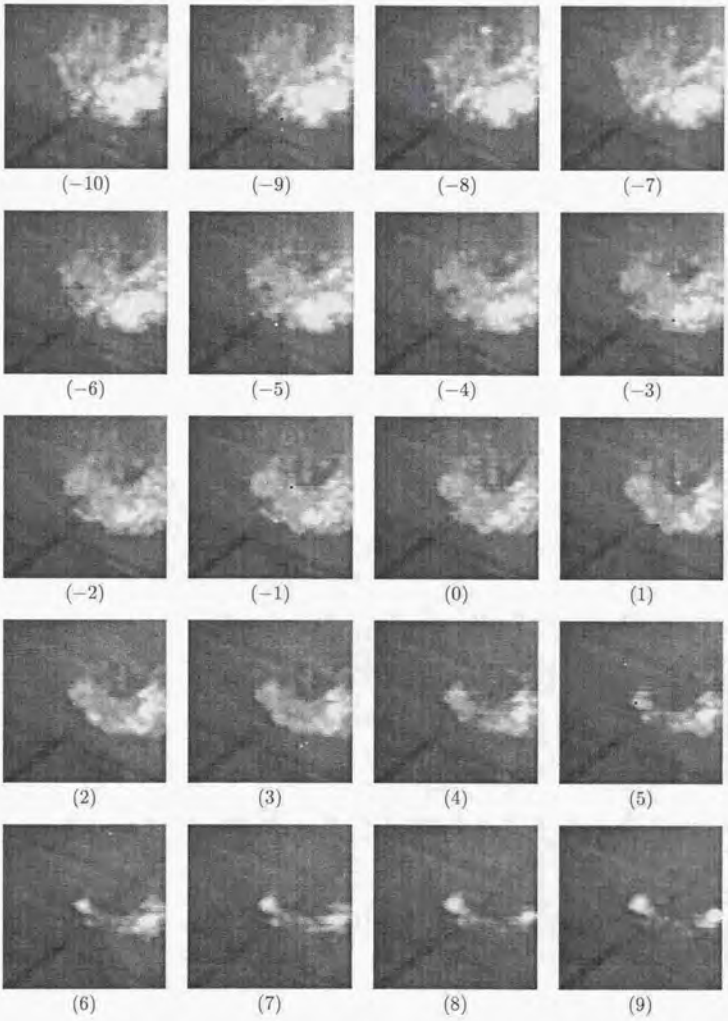

Fig. C.1: (No.28)

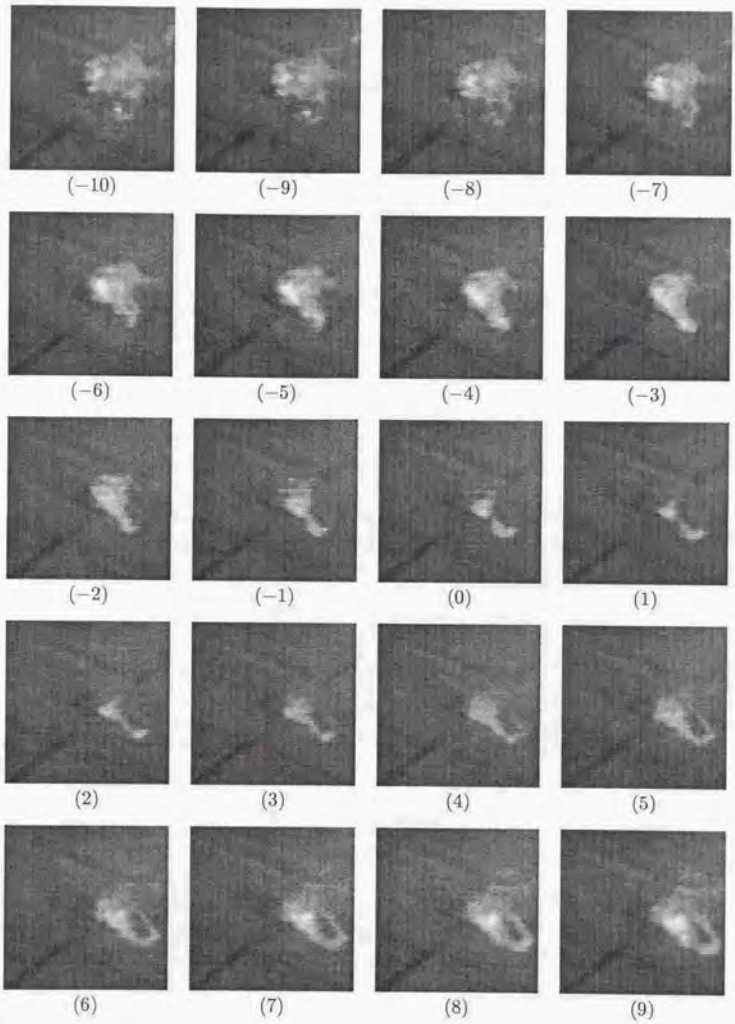

Fig. C.1: (No.29)

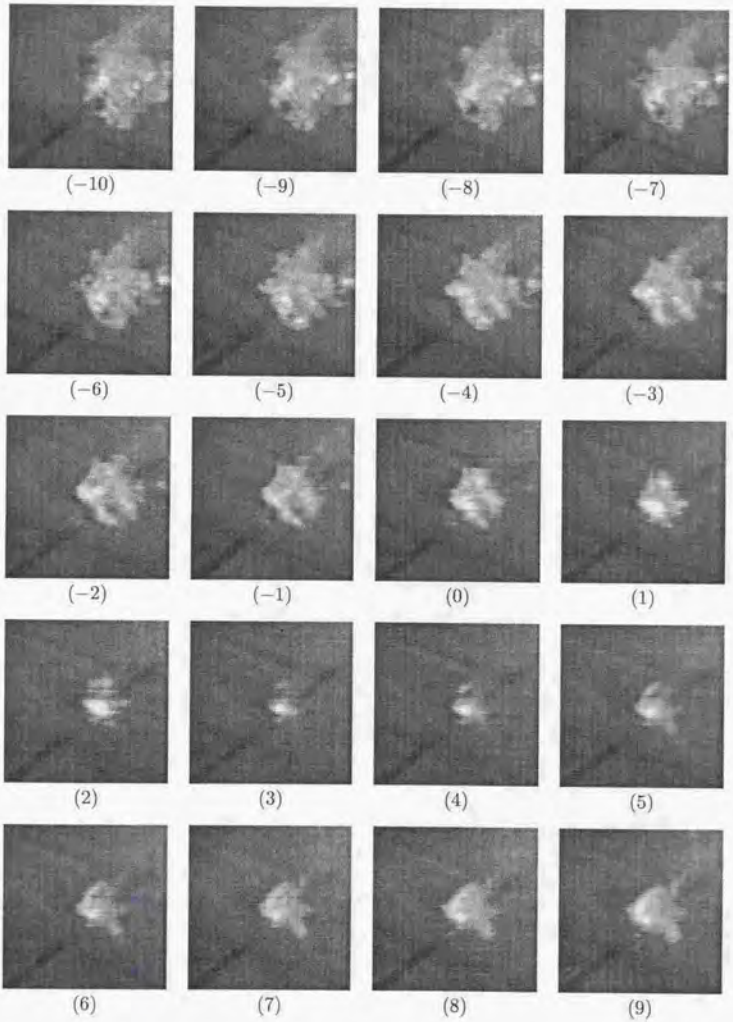

Fig. C.1: (No.30)

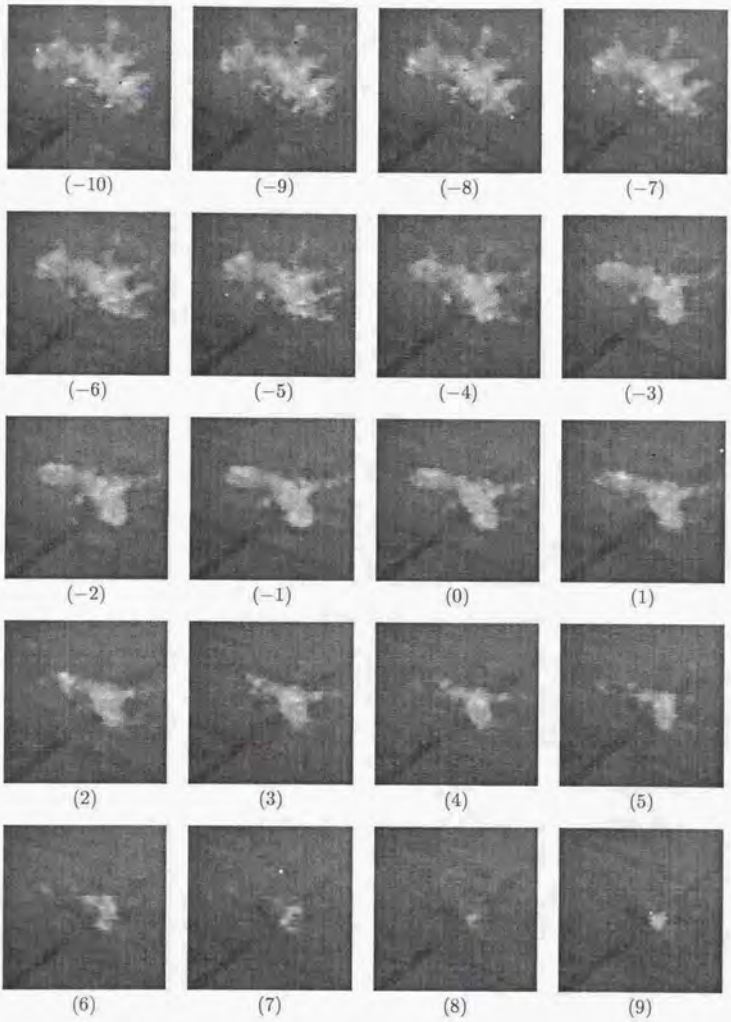

Fig. C.1: (No.31)

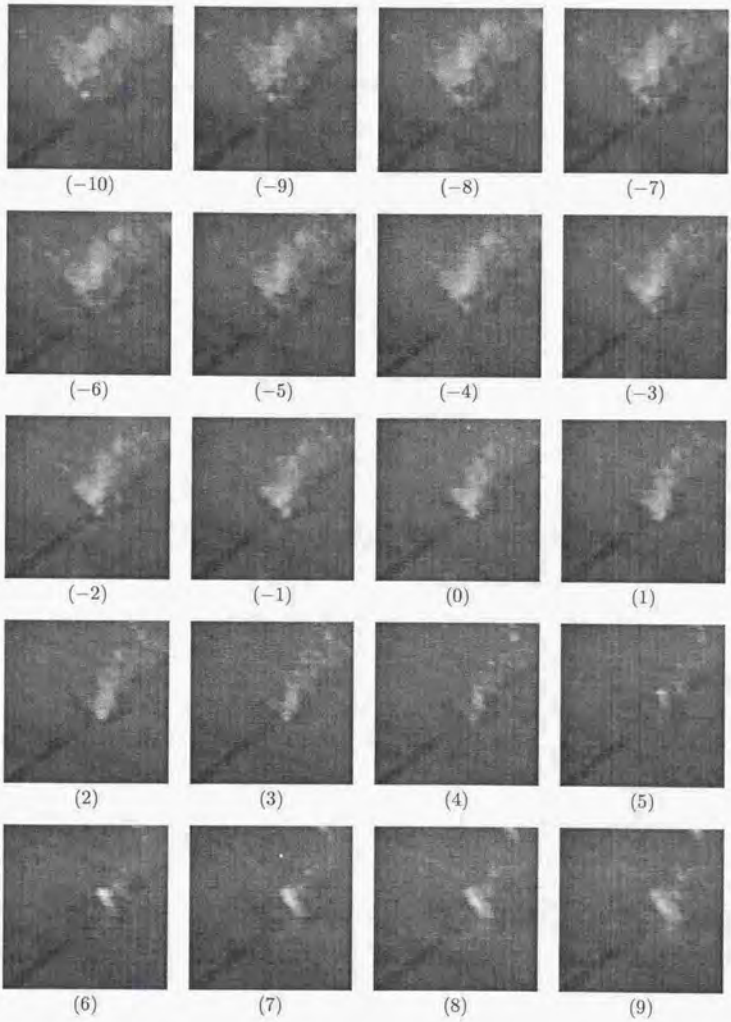

Fig. C.1: (No.32)

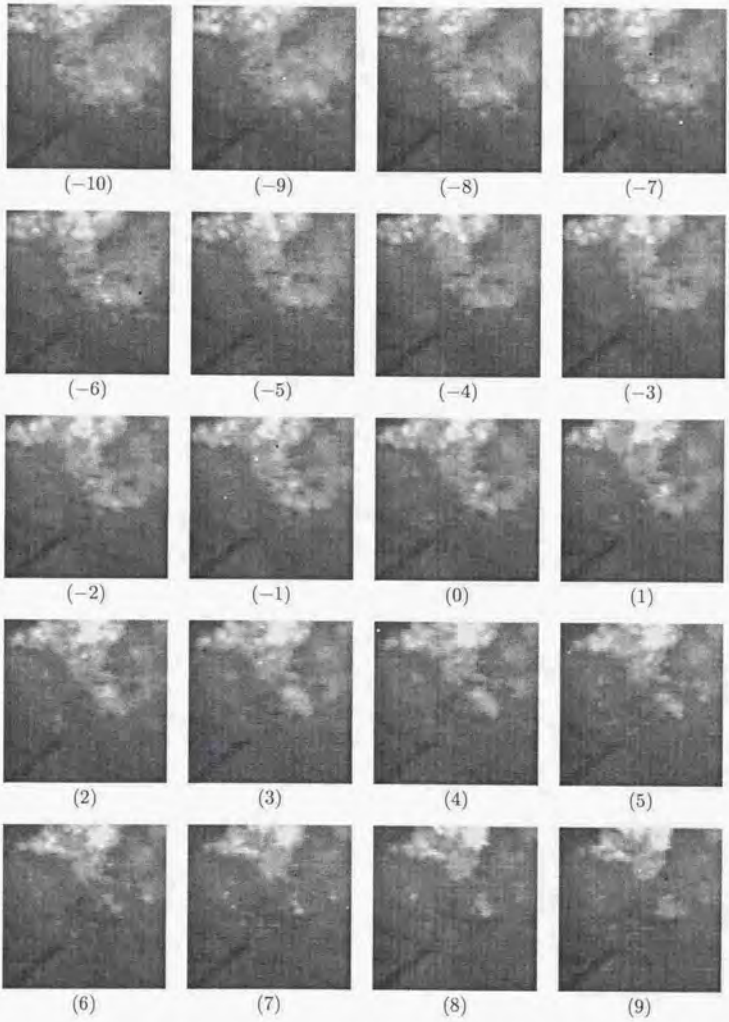

Fig. C.1: (No.33)

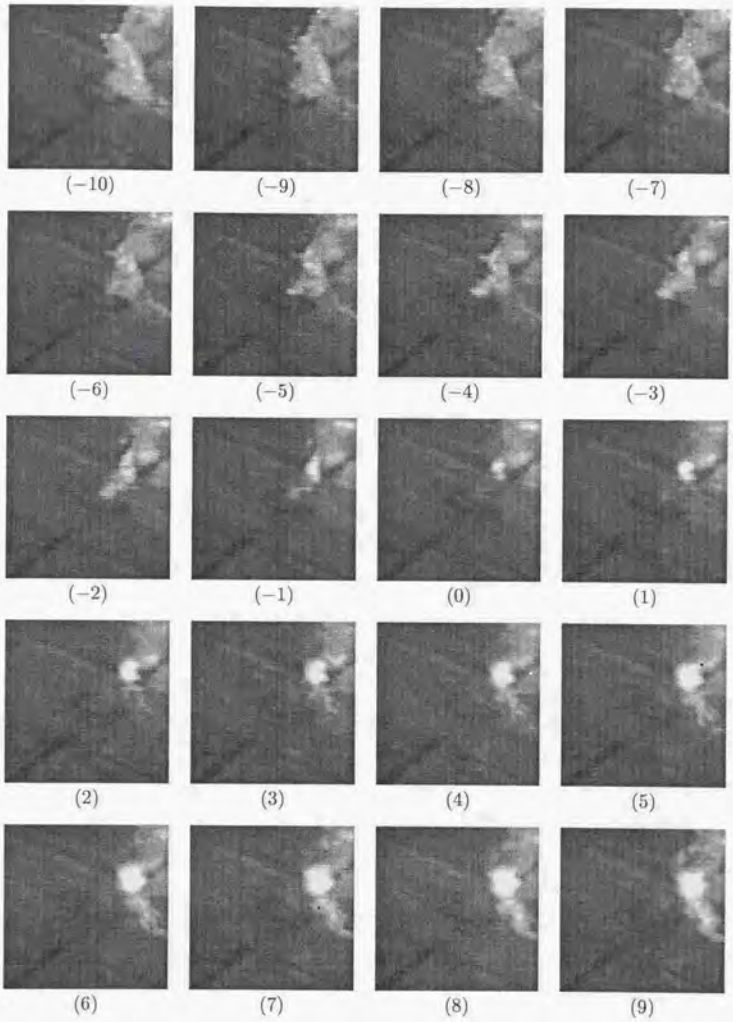

Fig. C.1: (No.34)

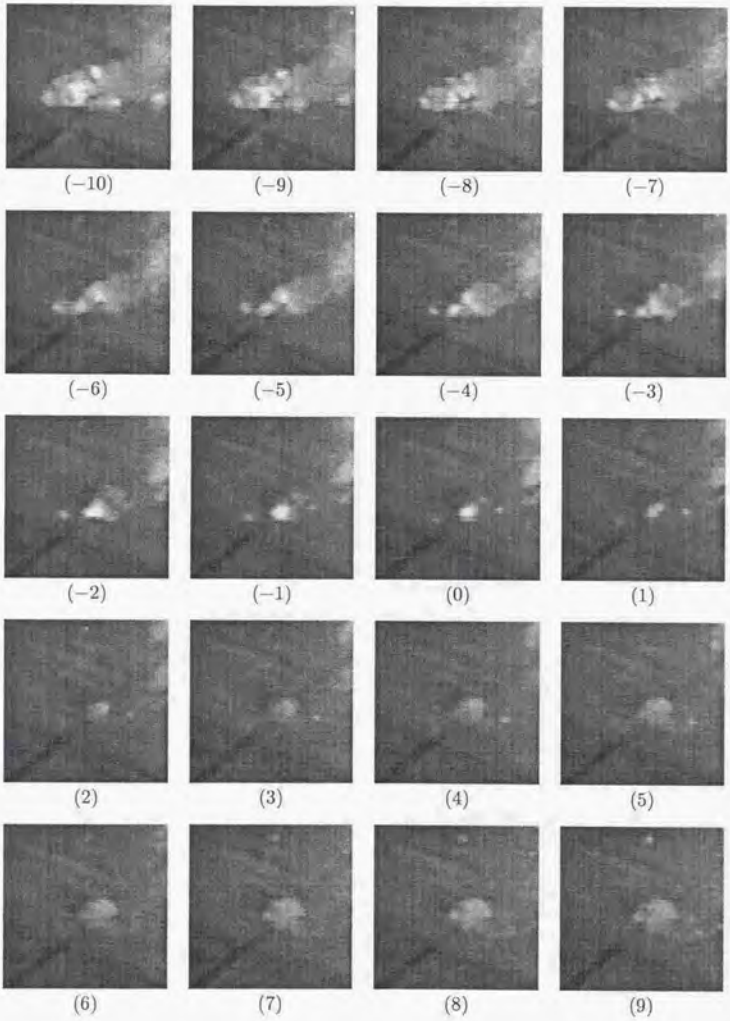

Fig. C.1: (No.35)

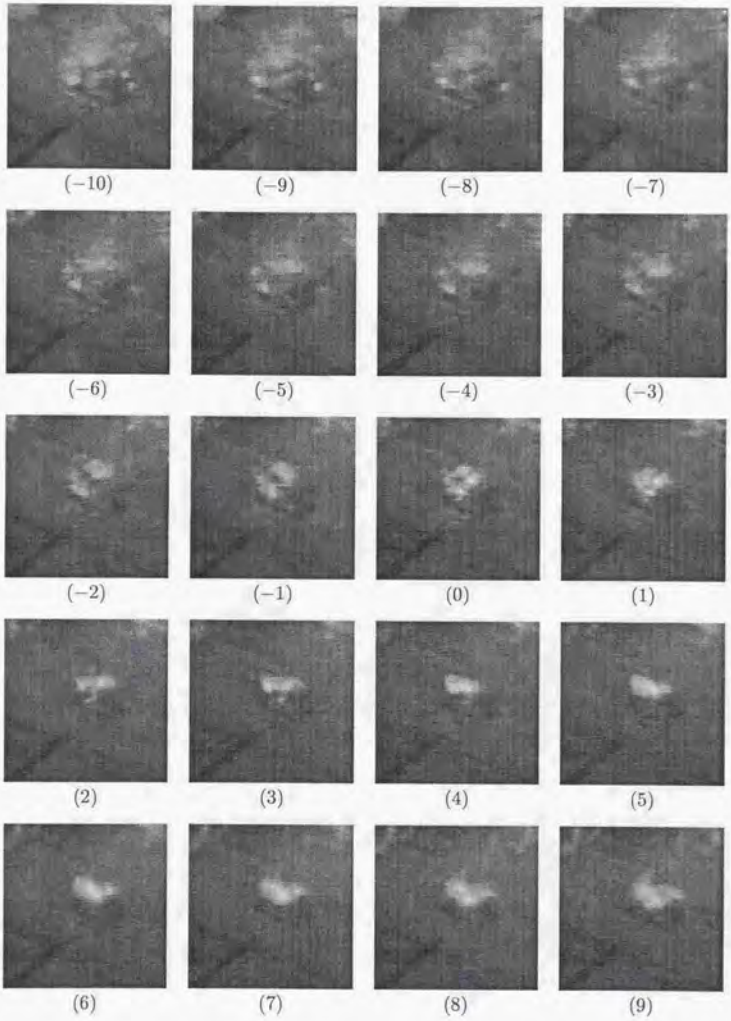

Fig. C.1: (No.36)

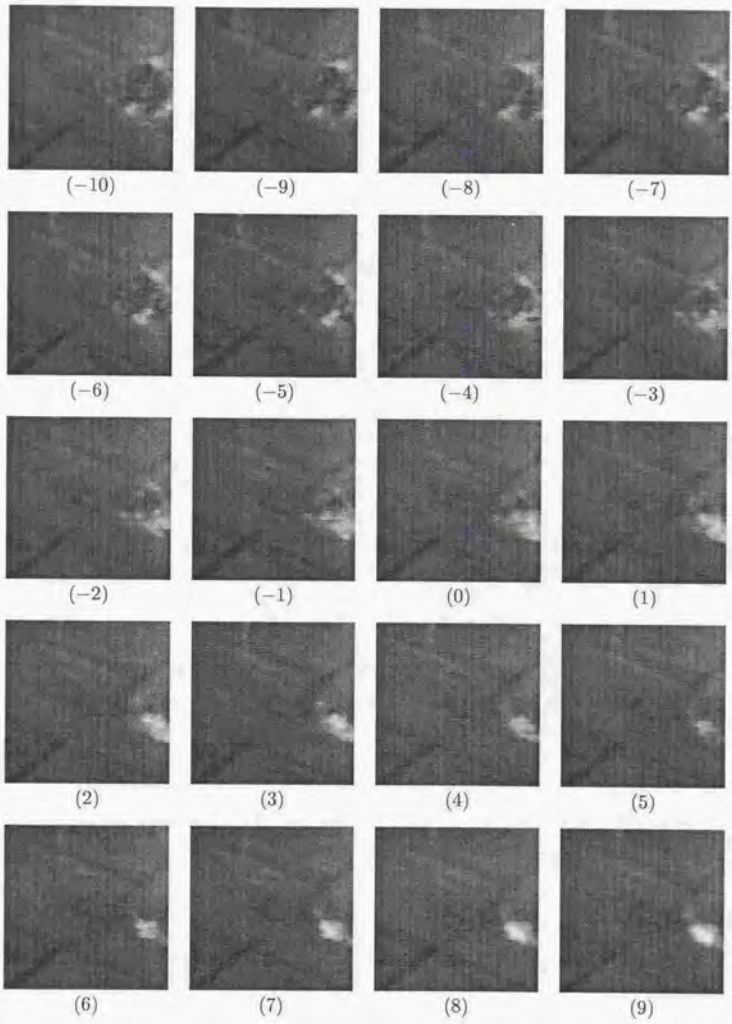

Fig. C.1: (No.37)

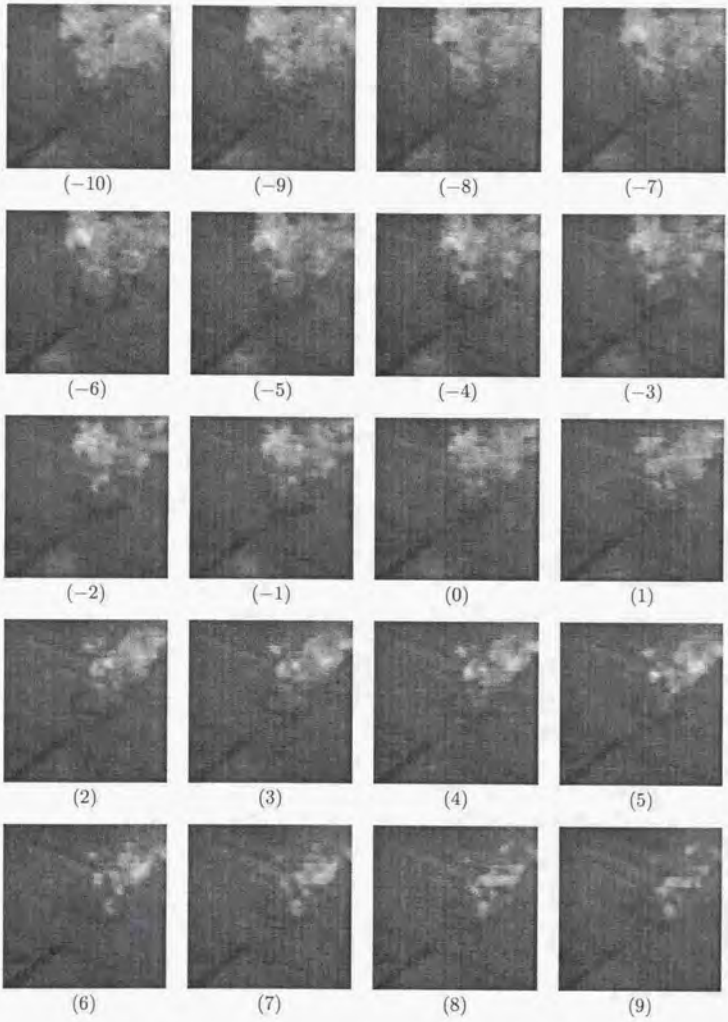

Fig. C.1: (No.38)

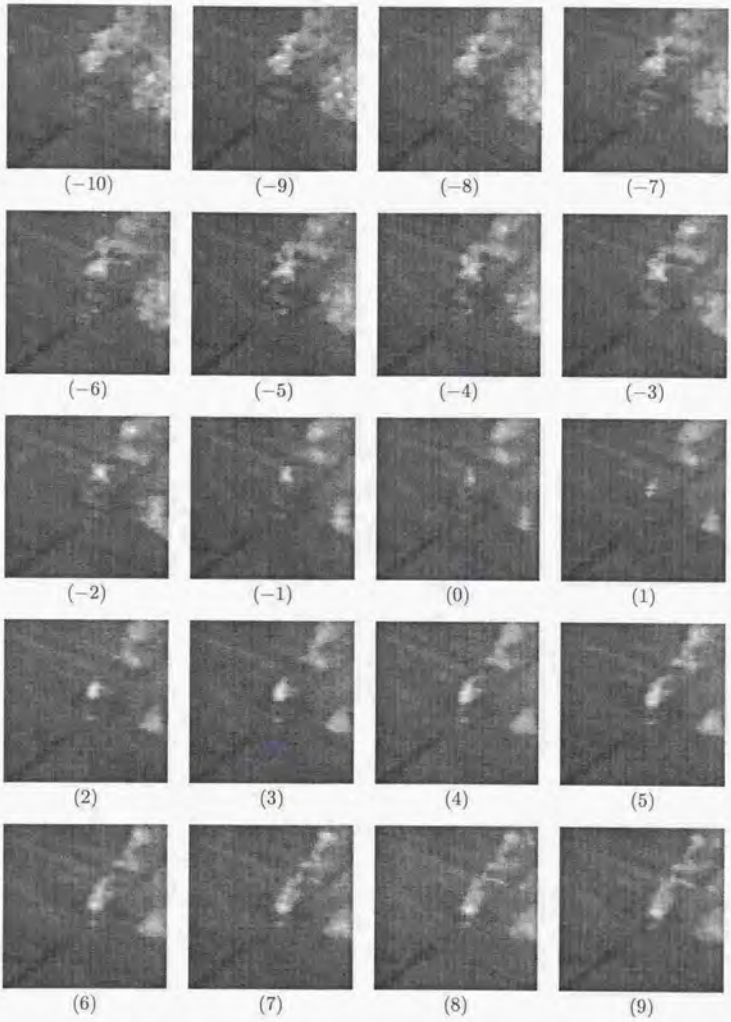

Fig. C.1: (No.39)

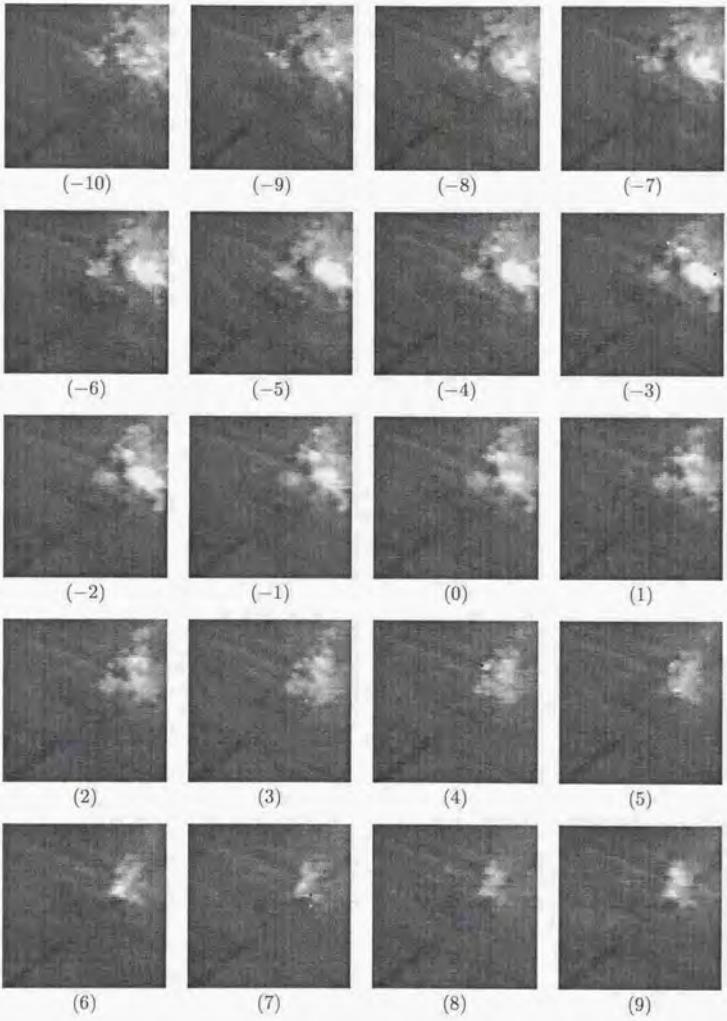

Fig. C.1: (No.40)

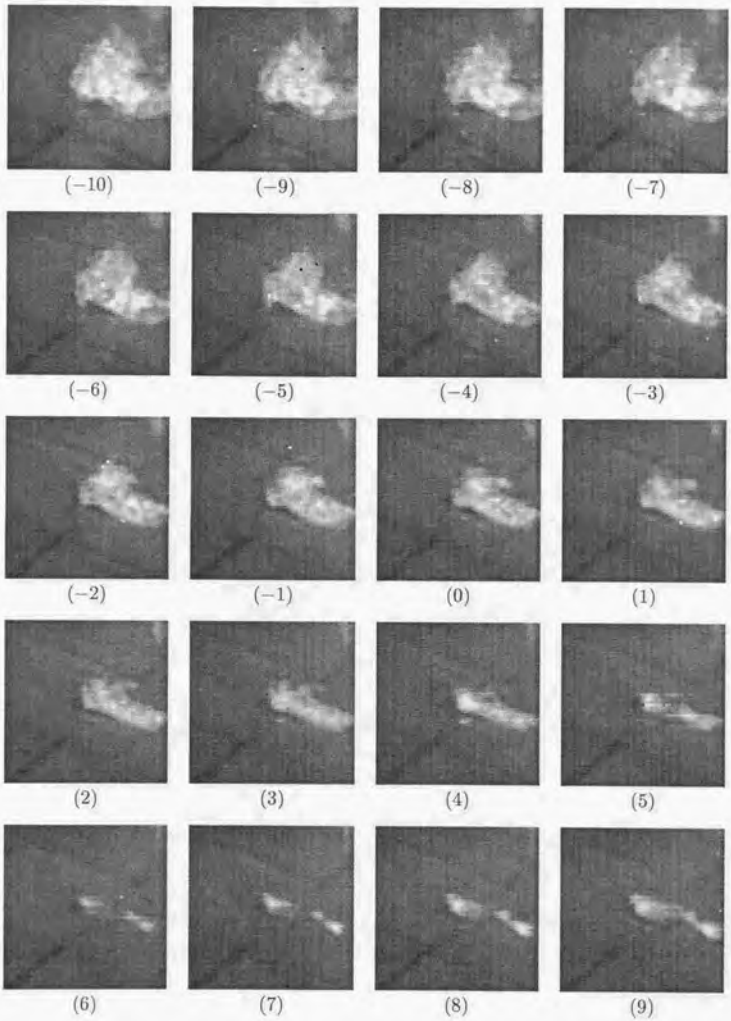

Fig. C.1: (No.41)

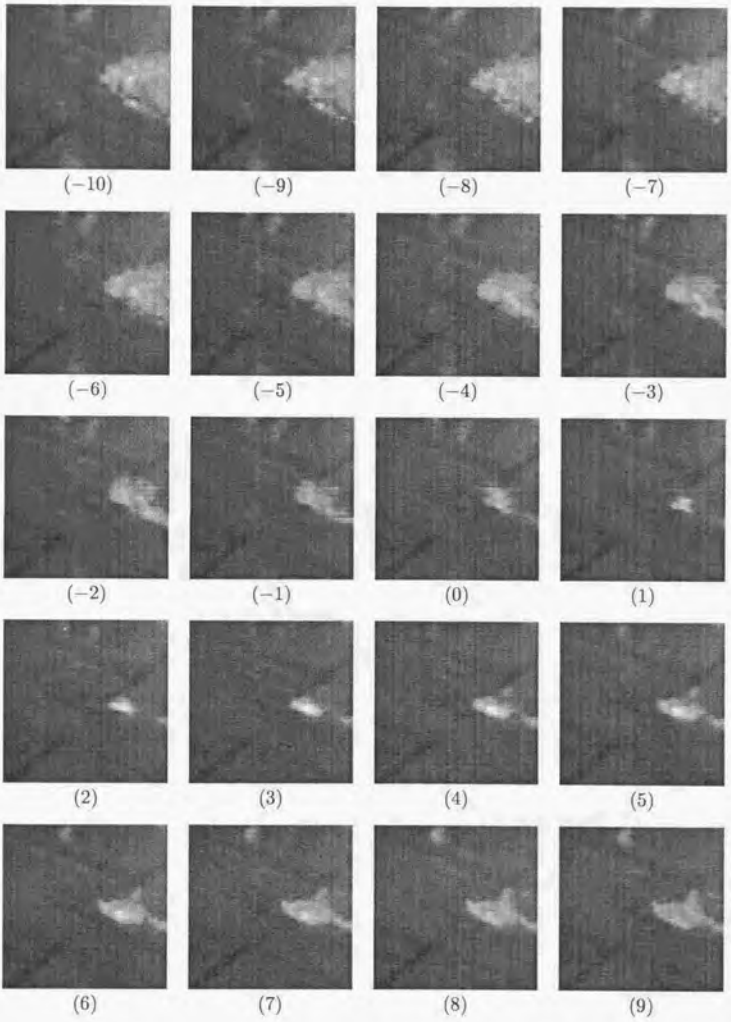

Fig. C.1: (No.42)

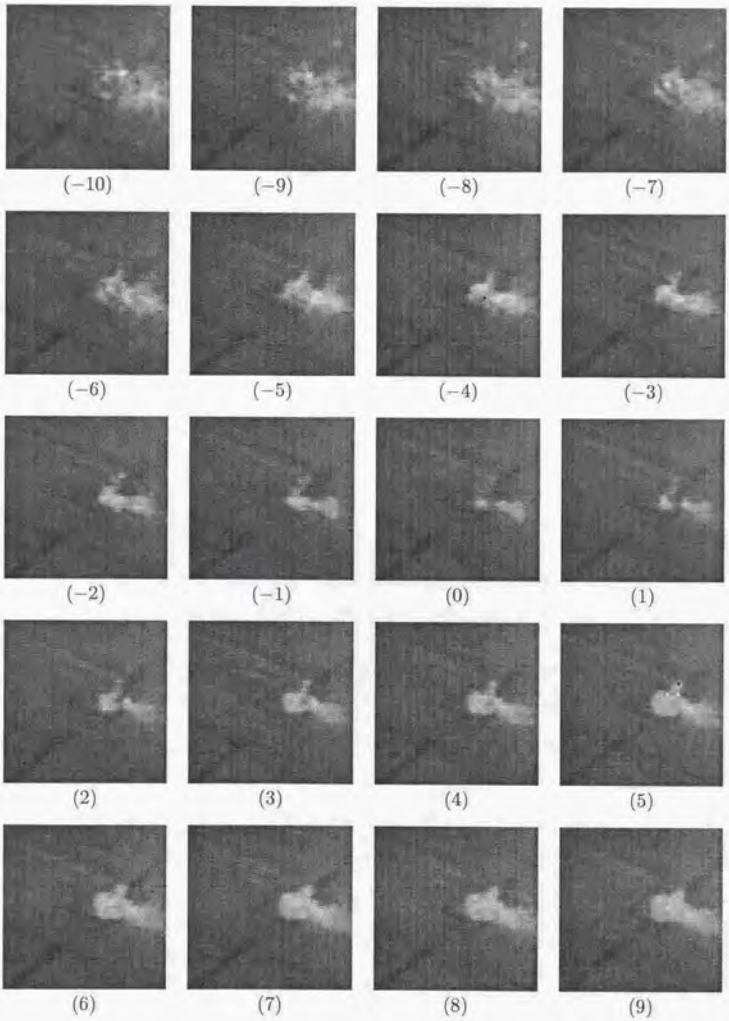

Fig. C.1: (No.43)

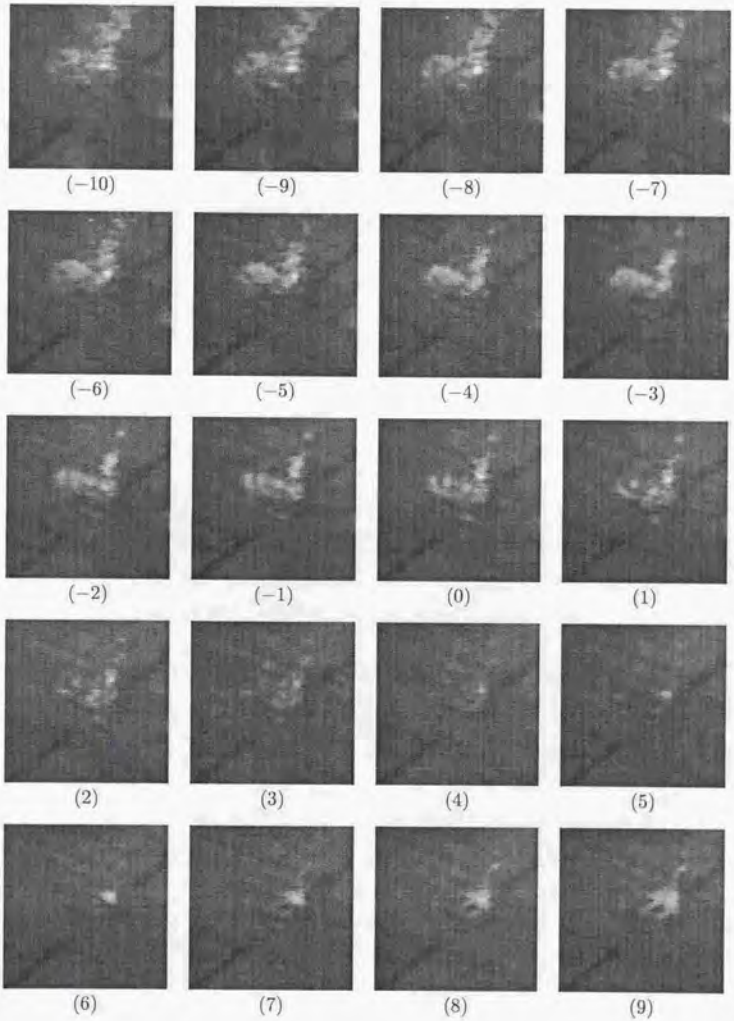

Fig. C.1: (No.44)

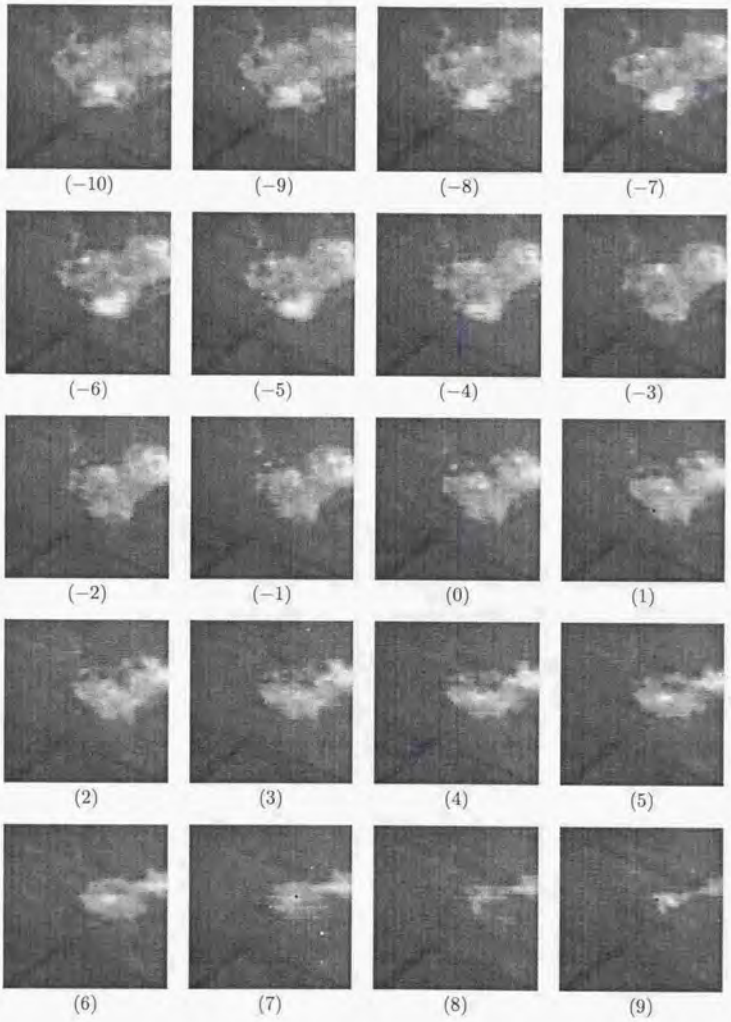

Fig. C.1: (No.45)

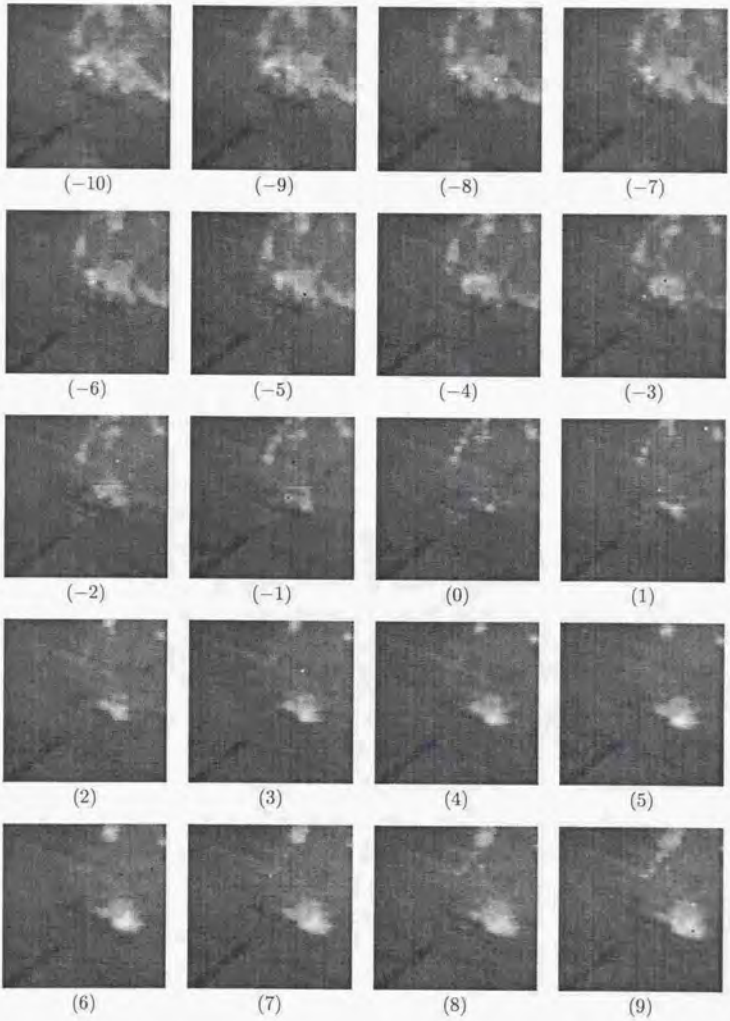

Fig. C.1: (No.46)

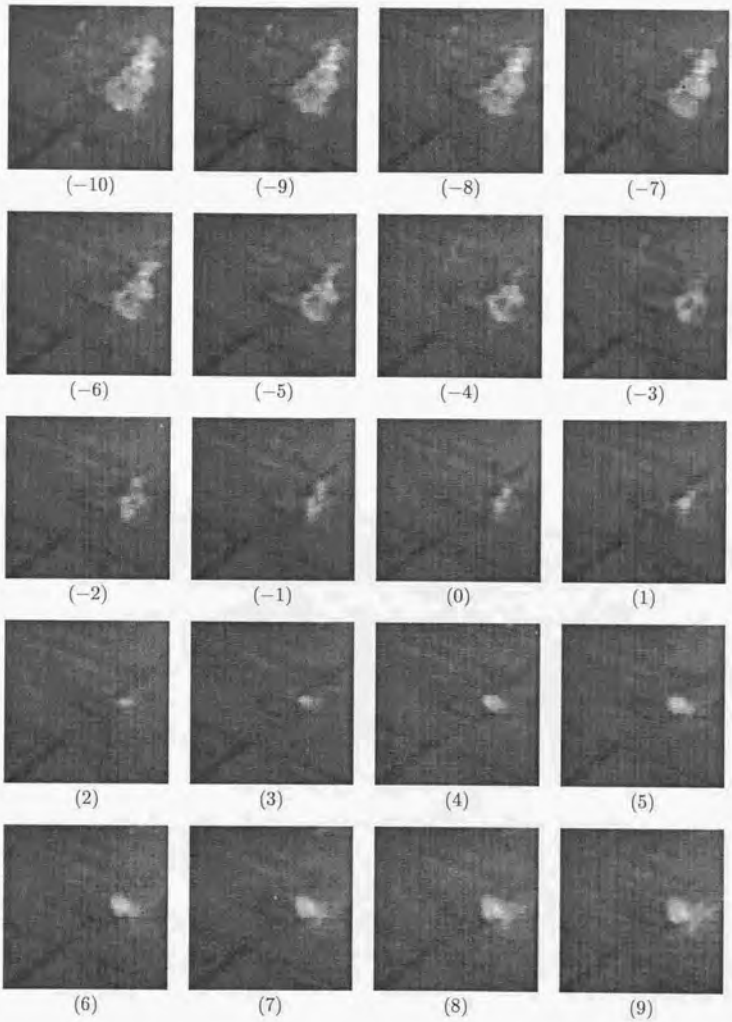

Fig. C.1: (No.47)

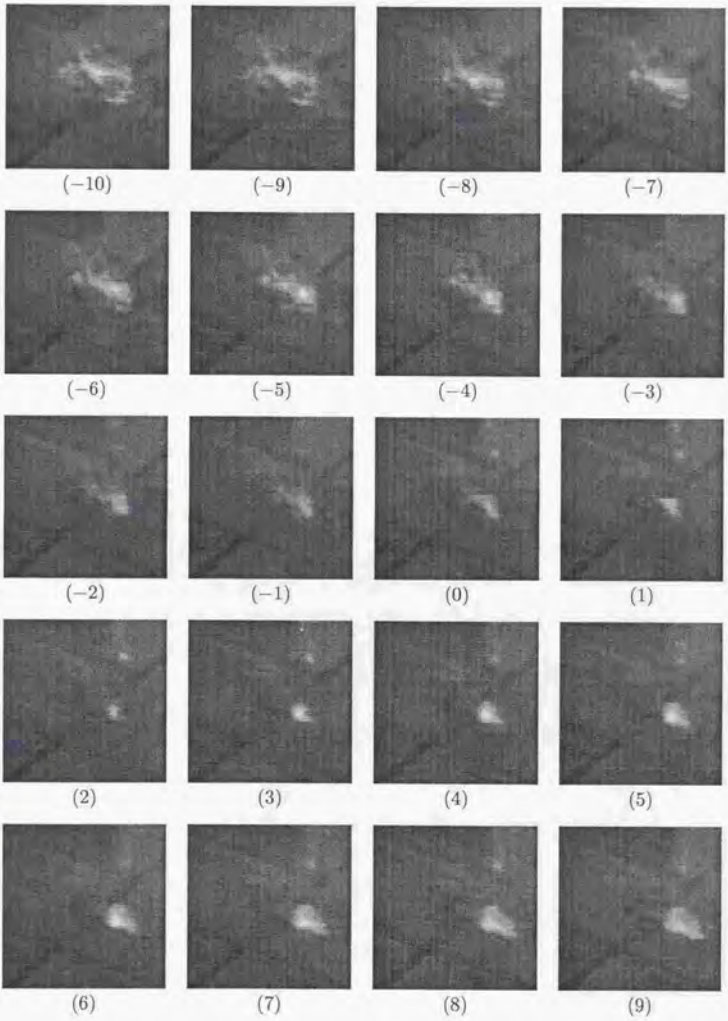

Fig. C.1: (No.48)

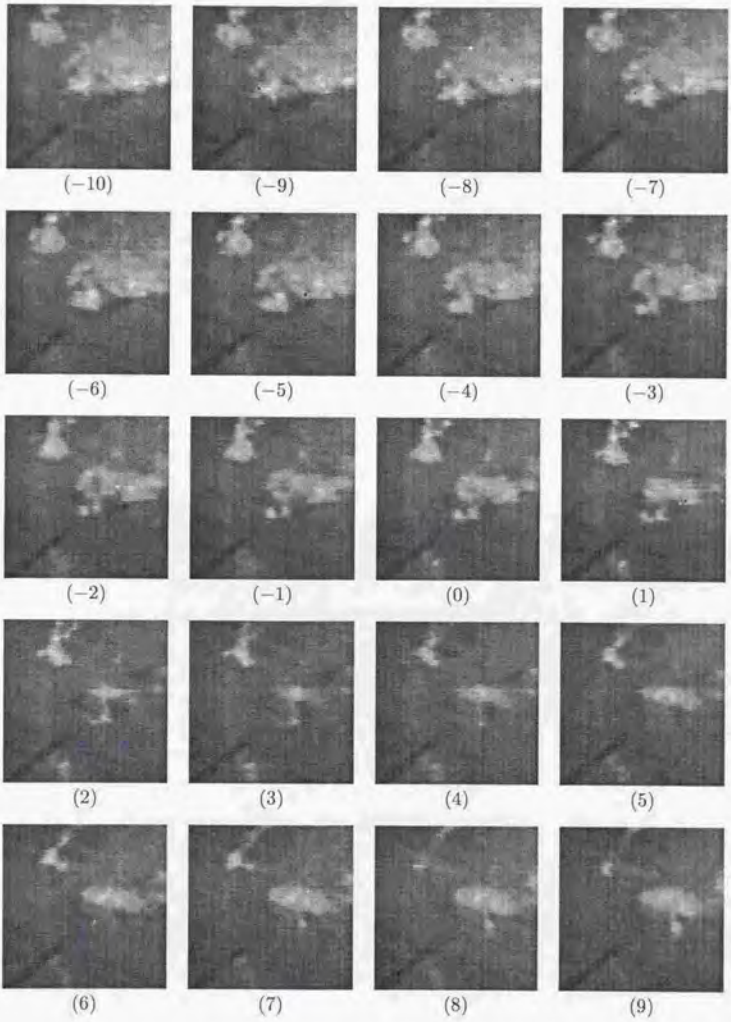

Fig. C.1: (No.49)

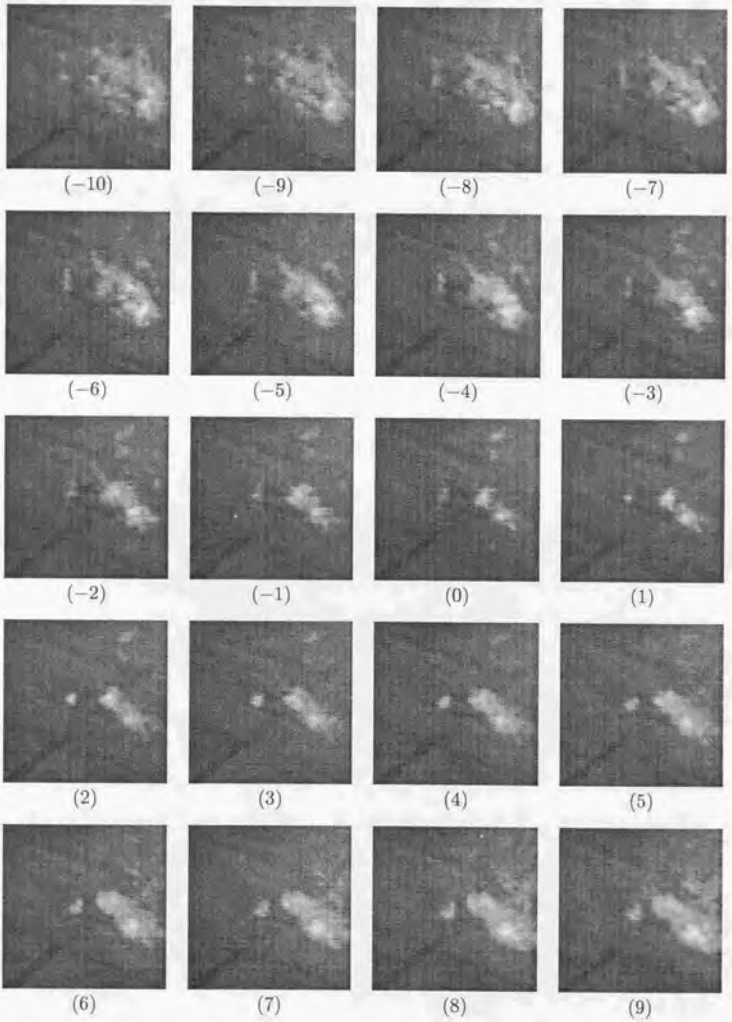

Fig. C.1: (No.50)

付 録D　発生する衝撃力と、キャビティ崩壊の様子の要約

付録Cに載せた高速度ビデオカメラによる映像に対応する衝撃力波形、キャビティ投影面積および明るさの尺度の時間変化をFig. D.1に示す。

実験の詳細は、第II部の第11章で説明している。No.20のキャビティ投影面積と明るさの尺度のグラフがないのは、No.20の映像ではキャビティの明るさと翼面の明るさが近く、キャビティ周縁の判断が難しいからである。

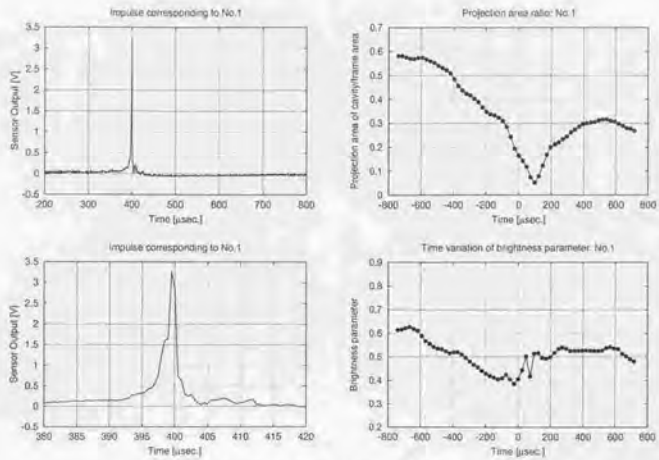

No.1　Impulsive force: 63.8 N
Collapsing type: Spherical

Fig. D.1: Output voltage of impulsive force sensors and summarized parameters corresponding to Fig. C.1

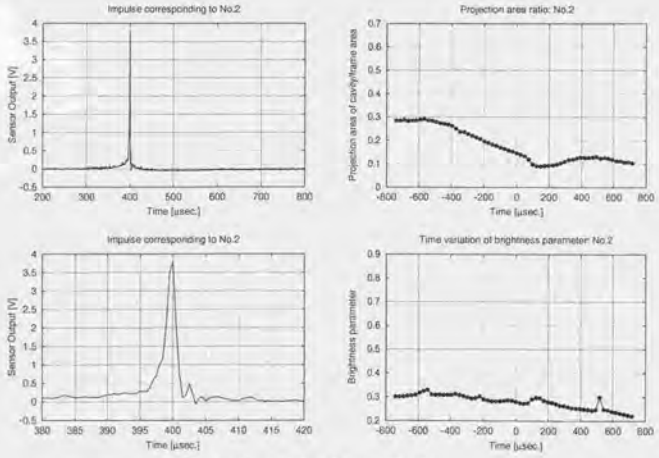

No.2　Impulsive force: 67.2 N
Collapsing type: Cylindrical

Fig. D.1: (continued)

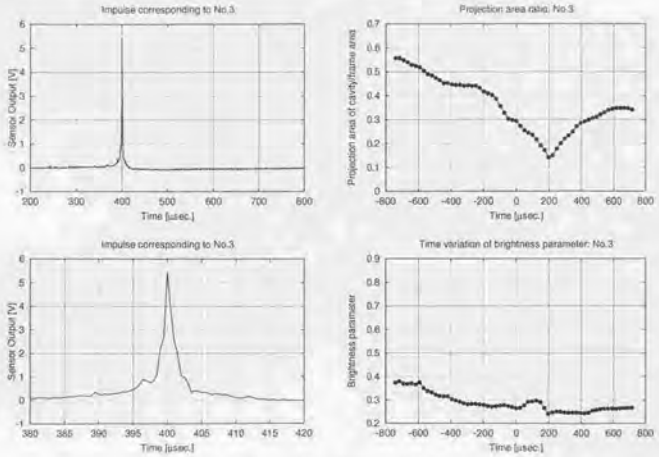

No.3　Impulsive force: 89.7 N
Collapsing type: Spherical

Fig. D.1: (continued)

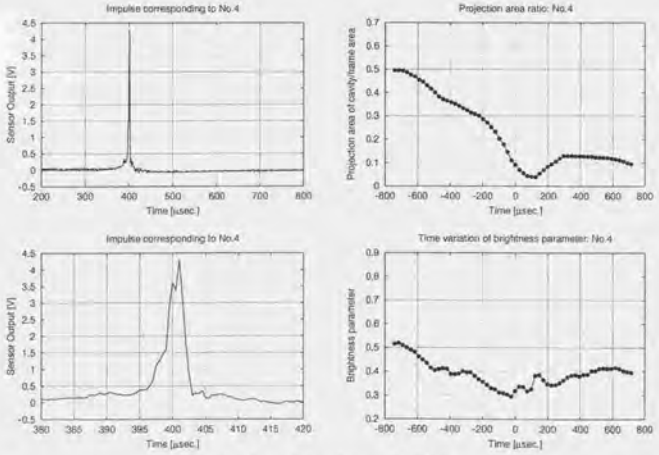

No.4　Impulsive force: 70.1 N
Collapsing type: Spherical

Fig. D.1: (continued)

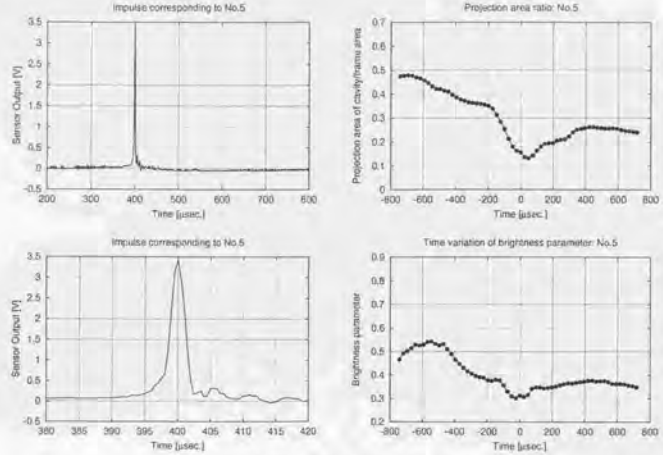

No.5　Impulsive force: 56.5 N
Collapsing type: Spherical

Fig. D.1: (continued)

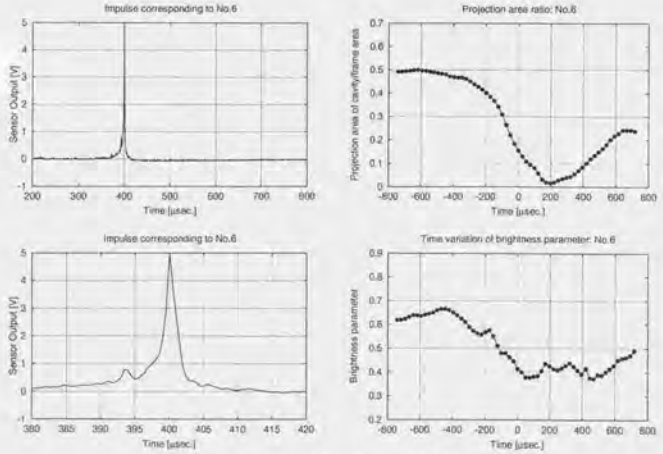

No.6　Impulsive force: 81.4 N
Collapsing type: Axial

Fig. D.1: (continued)

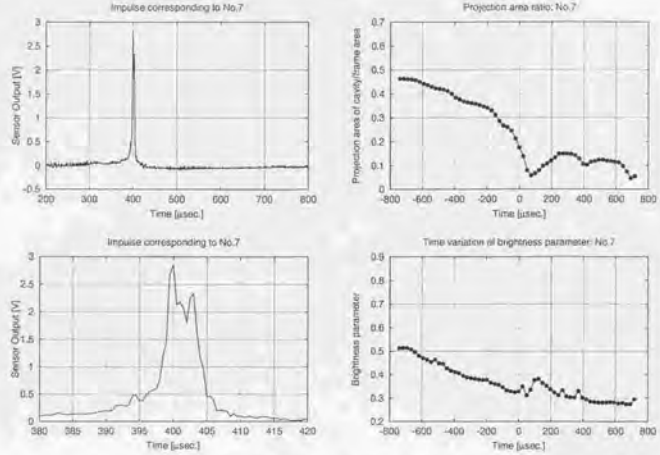

No.7　Impulsive force: 53.6 N
Collapsing type: Spherical

Fig. D.1: (continued)

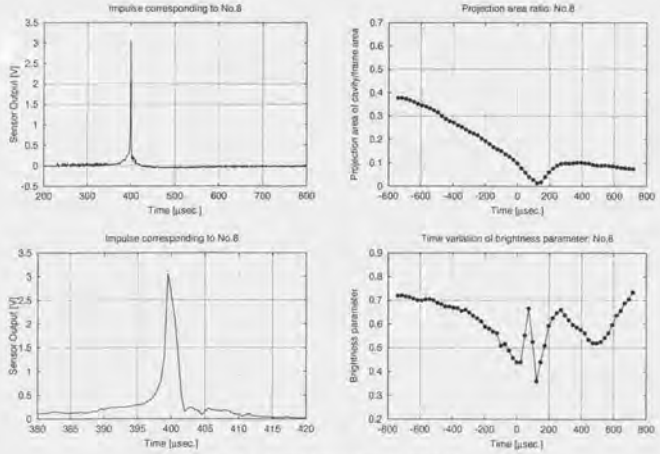

No.8　Impulsive force: 50.5 N
Collapsing type: Axial

Fig. D.1: (continued)

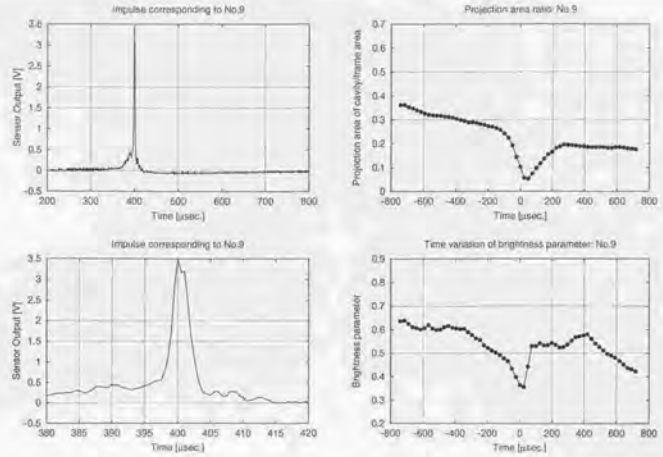

No.9　Impulsive force: 59.1 N
Collapsing type: Spherical

Fig. D.1: (continued)

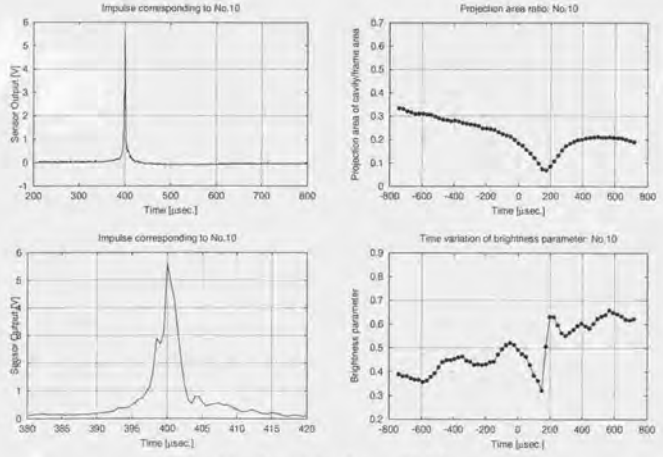

No.10　Impulsive force: 92.2 N
Collapsing type: Spherical

Fig. D.1: (continued)

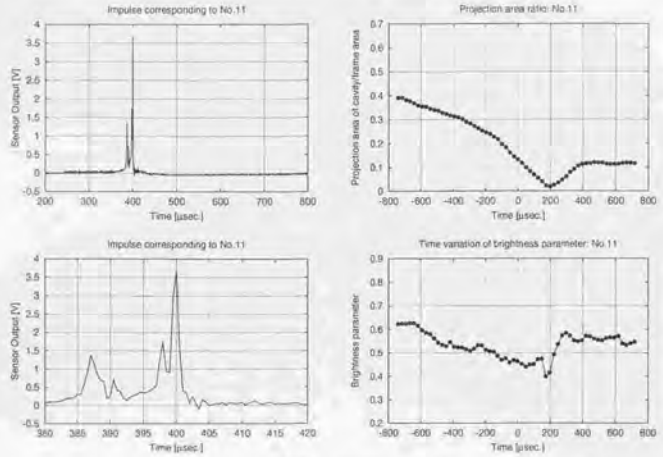

No.11　Impulsive force: 70.6 N
Collapsing type: Spherical

Fig. D.1: (continued)

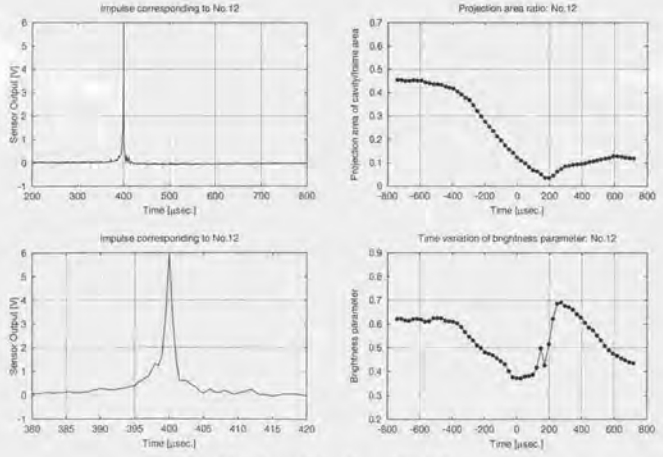

No.12　Impulsive force: 98.6 N
Collapsing type: Spherical

Fig. D.1: (continued)

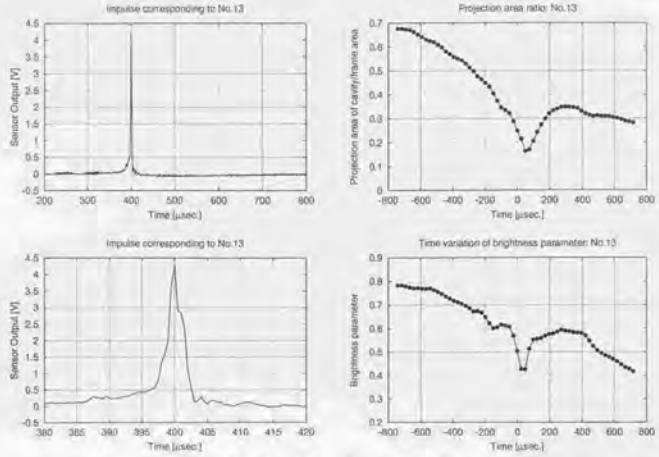

No.13　Impulsive force: 75.1 N
Collapsing type: Spherical

Fig. D.1: (continued)

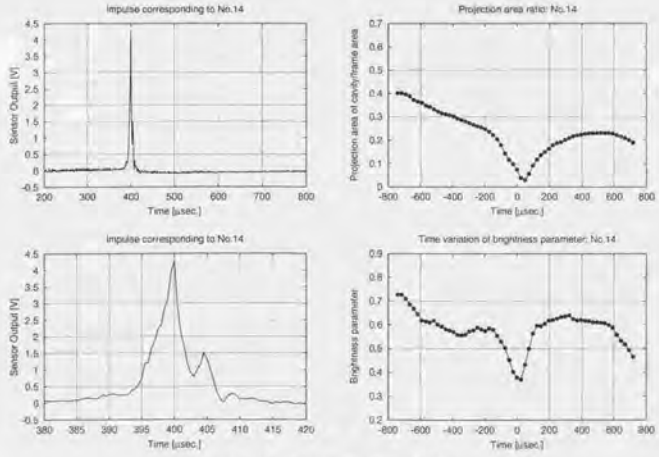

No.14　Impulsive force: 74.0 N
Collapsing type: Spherical

Fig. D.1: (continued)

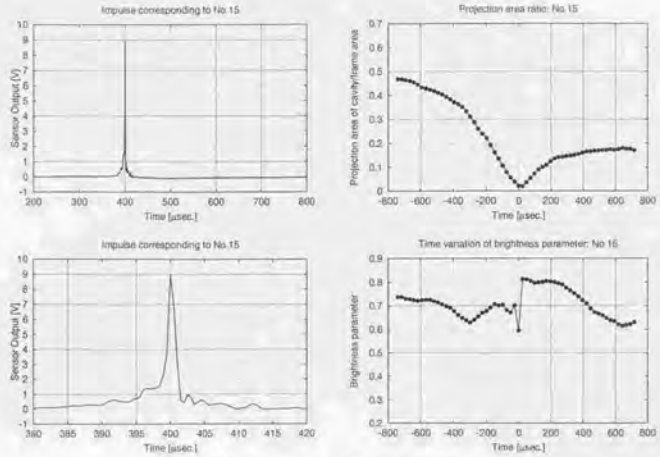

No.15　Impulsive force: 148.7 N
Collapsing type: Spherical

Fig. D.1: (continued)

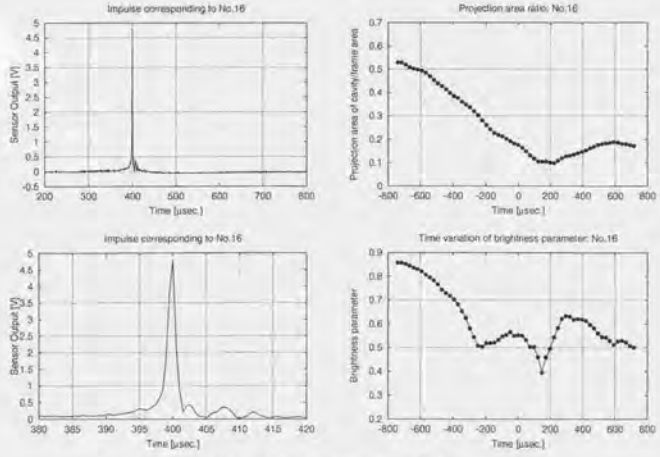

No.16　Impulsive force: 79.4 N
Collapsing type: Spherical

Fig. D.1: (continued)

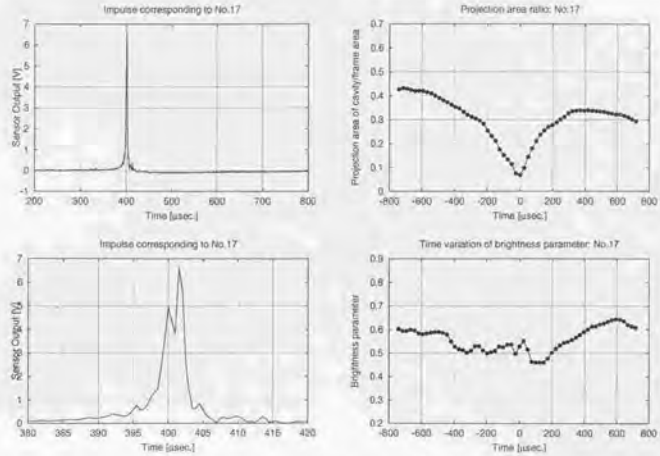

No.17　Impulsive force: 117.9 N
Collapsing type: Spherical

Fig. D.1: (continued)

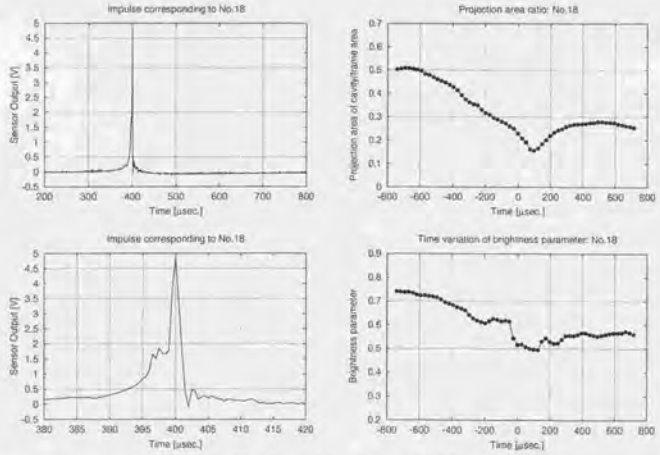

No.18　Impulsive force: 83.9 N
Collapsing type: Axial

Fig. D.1: (continued)

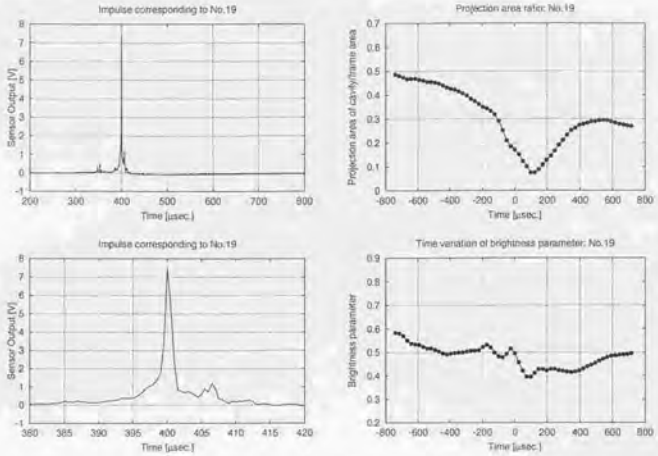

No.19　Impulsive force: 124.3 N
Collapsing type: Spherical

Fig. D.1: (continued)

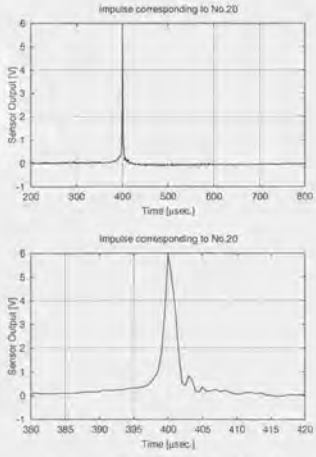

Projection area
not available

Brightness parameter
not available

No.20　Impulsive force: 97.3 N
Collapsing type: Spherical

Fig. D.1: (continued)

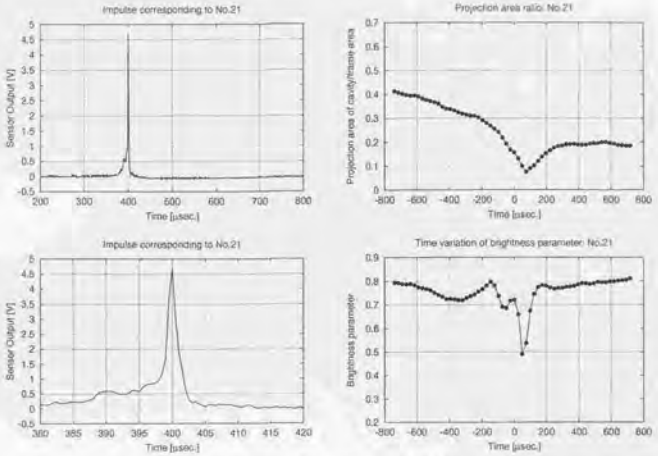

No.21　Impulsive force: 79.7 N
Collapsing type: Spherical

Fig. D.1: (continued)

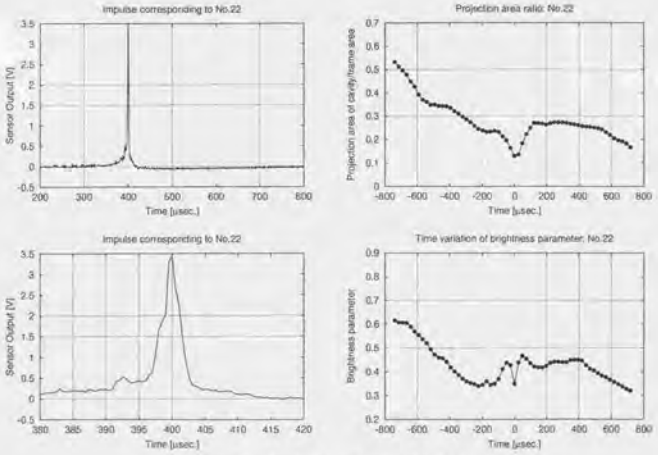

No.22　Impulsive force: 61.7 N
Collapsing type: Axial

Fig. D.1: (continued)

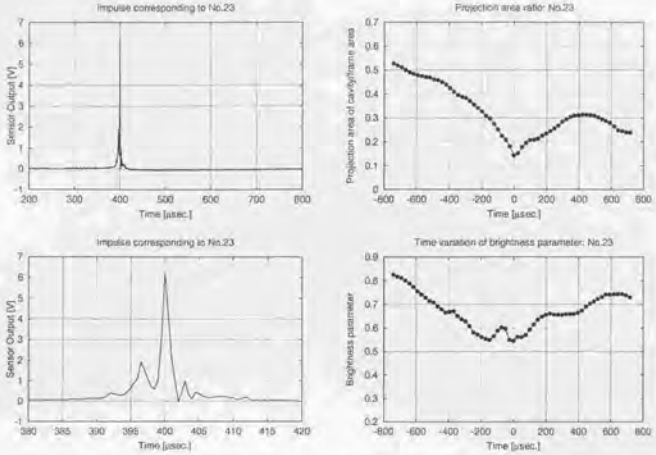

No.23　Impulsive force: 101.9 N
Collapsing type: Spherical

Fig. D.1: (continued)

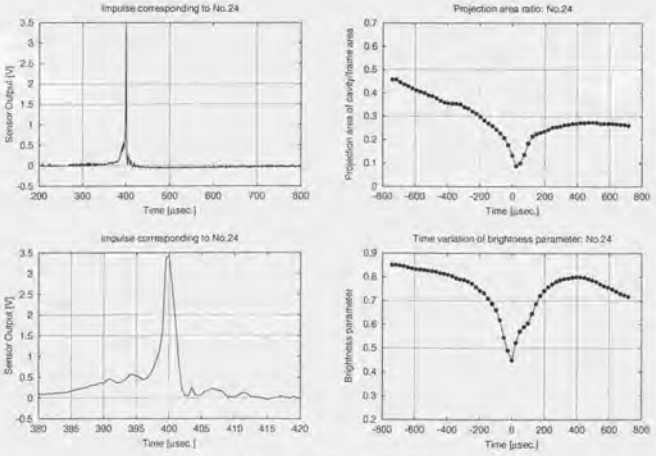

No.24　Impulsive force: 61.9 N
Collapsing type: Cylindrical

Fig. D.1: (continued)

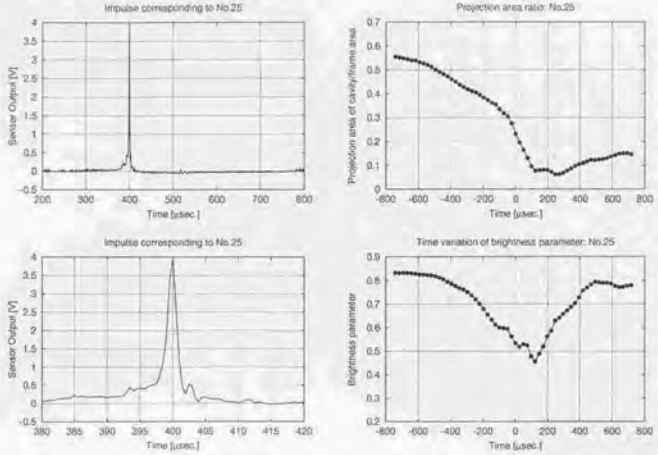

No.25　Impulsive force: 68.5 N
Collapsing type: Spherical

Fig. D.1: (continued)

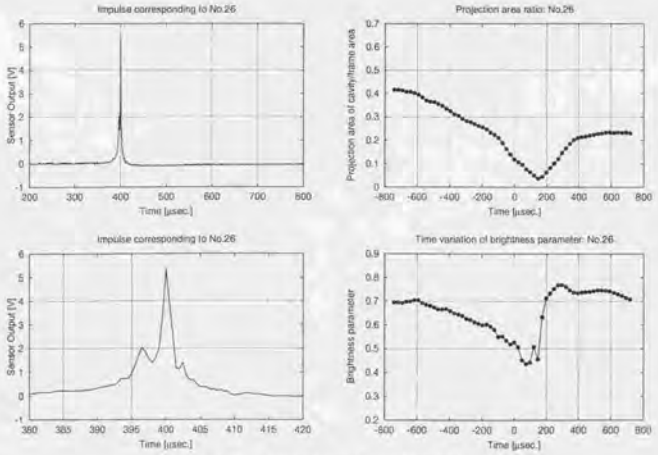

No.26　Impulsive force: 87.9 N
Collapsing type: Axial

Fig. D.1: (continued)

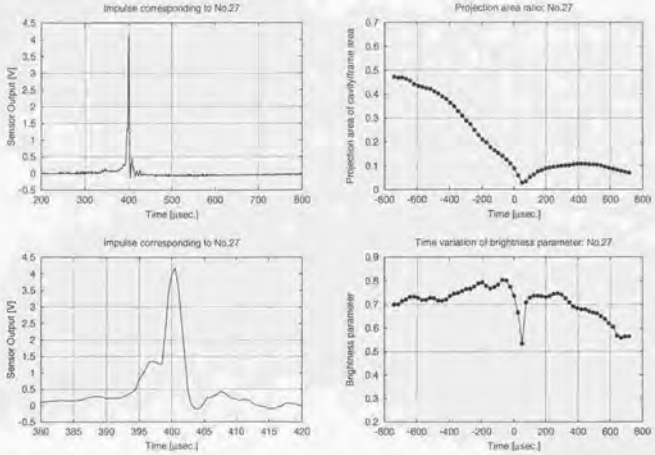

No.27　Impulsive force: 69.1 N
Collapsing type: Spherical

Fig. D.1: (continued)

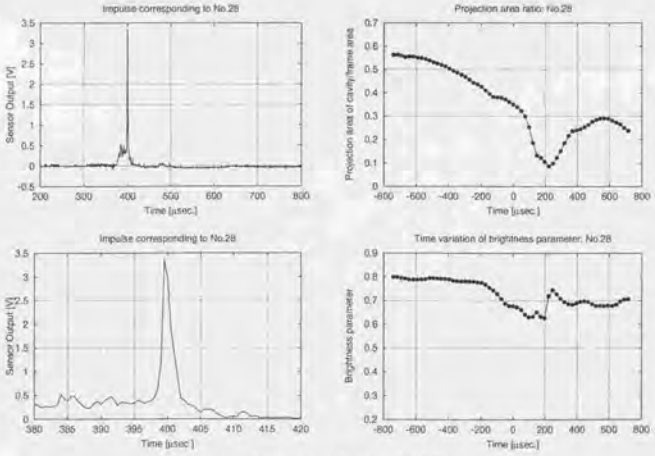

No.28　Impulsive force: 59.3 N
Collapsing type: Spherical

Fig. D.1: (continued)

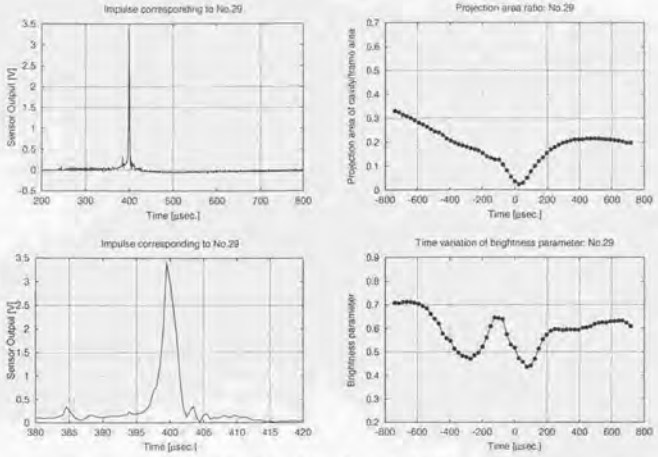

No.29　Impulsive force: 56.8 N
Collapsing type: Spherical

Fig. D.1: (continued)

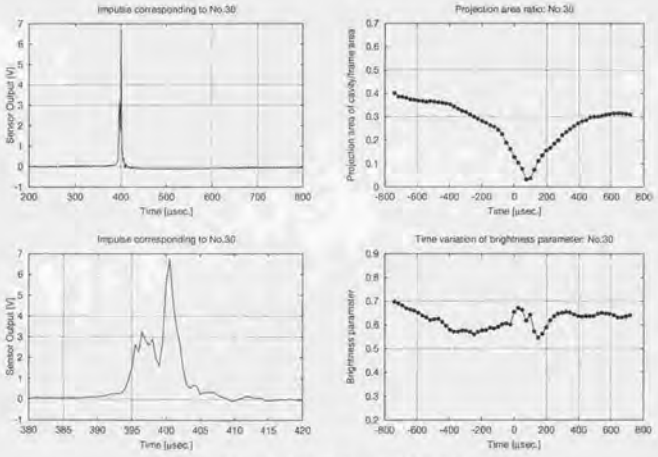

No.30　Impulsive force: 113.0 N
Collapsing type: Spherical

Fig. D.1: (continued)

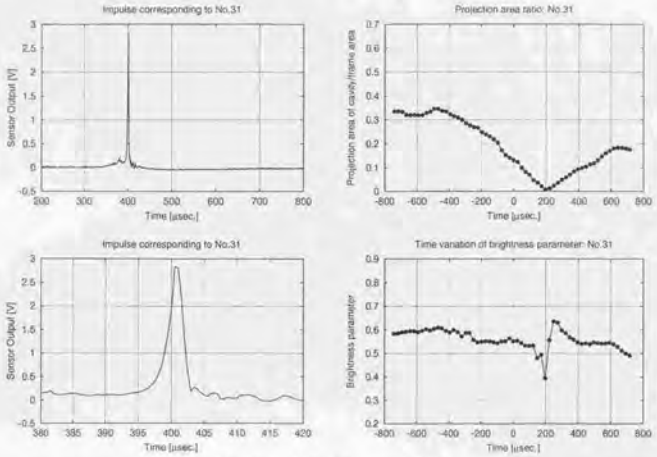

No.31　Impulsive force: 47.9 N
Collapsing type: Spherical

Fig. D.1: (continued)

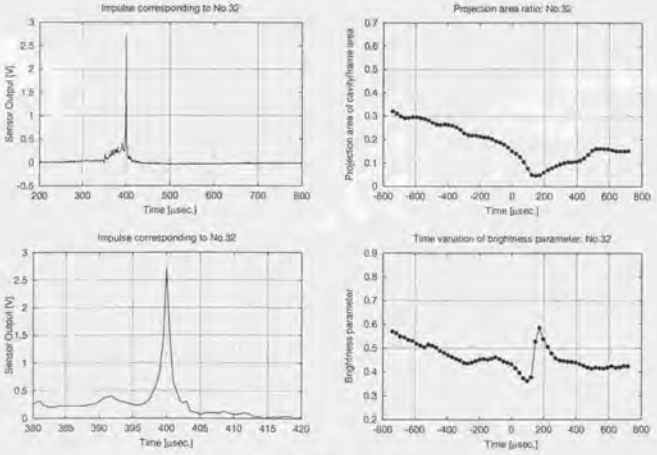

No.32　Impulsive force: 44.1 N
Collapsing type: Cylindrical

Fig. D.1: (continued)

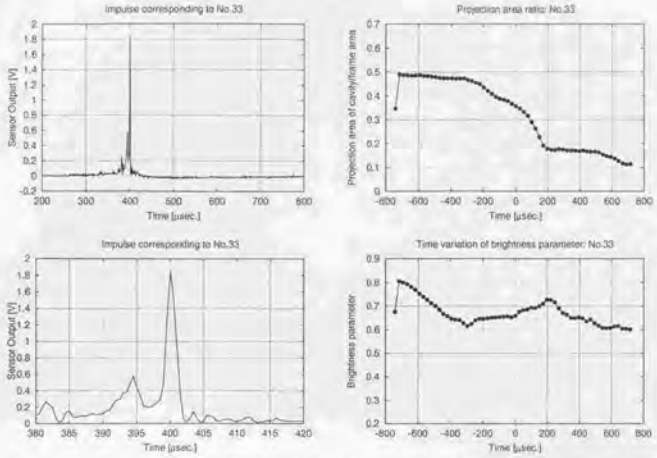

No.33　Impulsive force: 29.9 N
Collapsing type: Spherical

Fig. D.1: (continued)

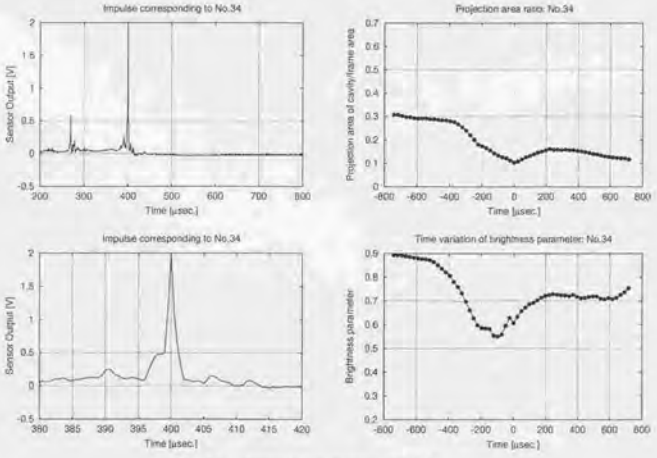

No.34　Impulsive force: 32.7 N
Collapsing type: Cylindrical

Fig. D.1: (continued)

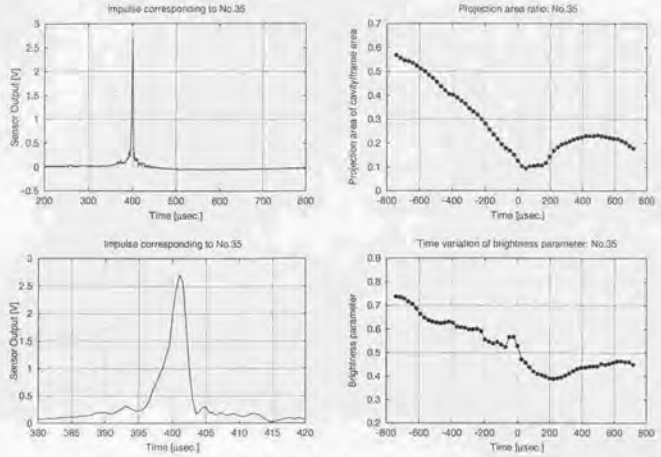

No.35　Impulsive force: 44.4 N
Collapsing type: Spherical

Fig. D.1: (continued)

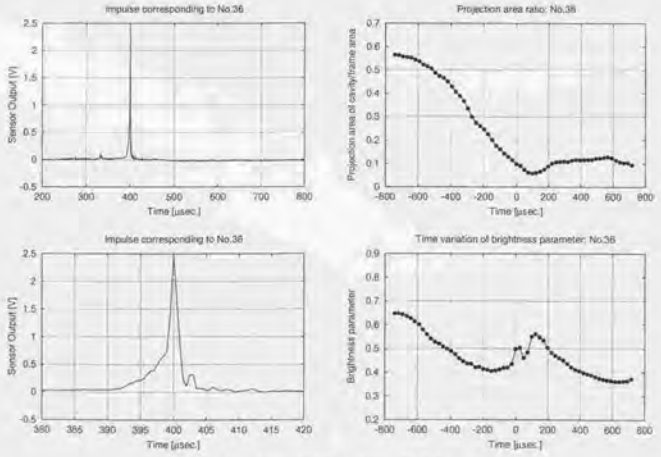

No.36　Impulsive force: 41.0 N
Collapsing type: Spherical

Fig. D.1: (continued)

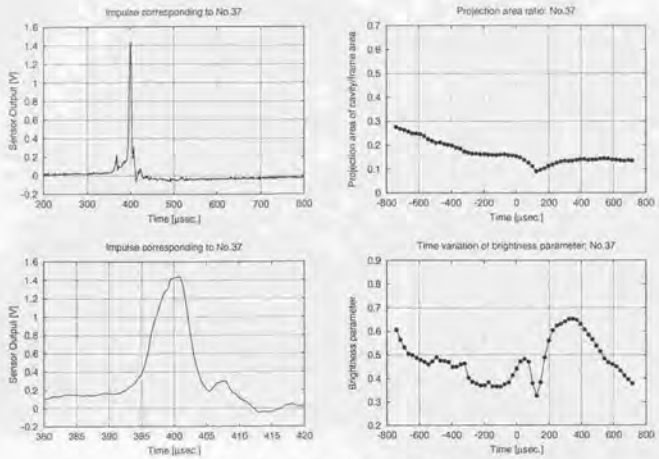

No.37　Impulsive force: 23.5 N
Collapsing type: Spherical

Fig. D.1: (continued)

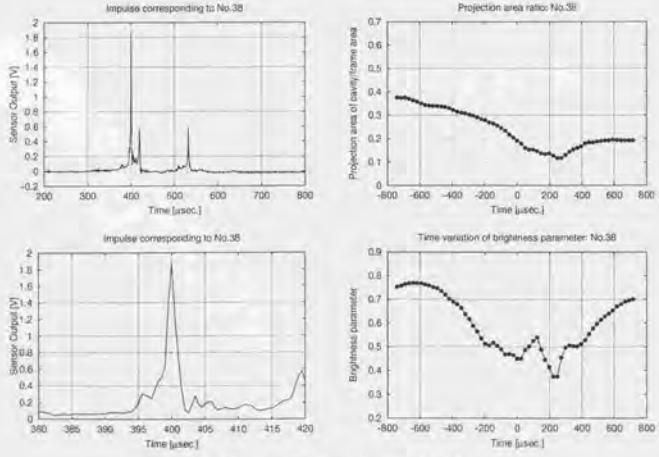

No.38　Impulsive force: 30.8 N
Collapsing type: Axial

Fig. D.1: (continued)

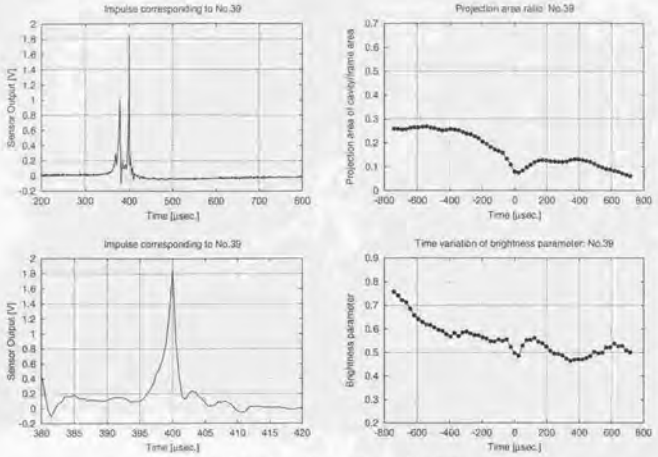

No.39　Impulsive force: 30.9 N
Collapsing type: Axial

Fig. D.1: (continued)

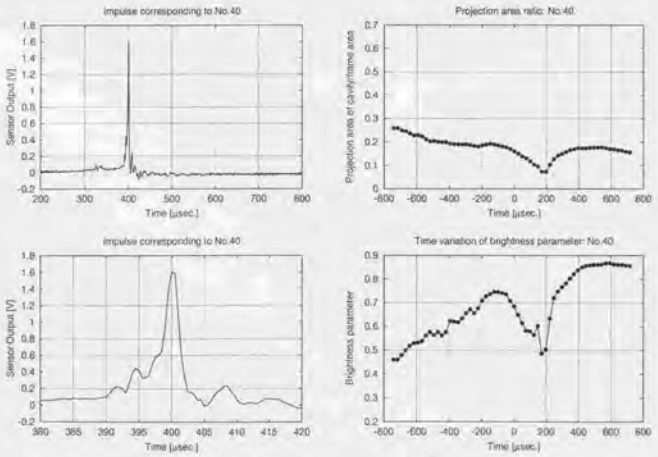

No.40　Impulsive force: 26.6 N
Collapsing type: Spherical

Fig. D.1: (continued)

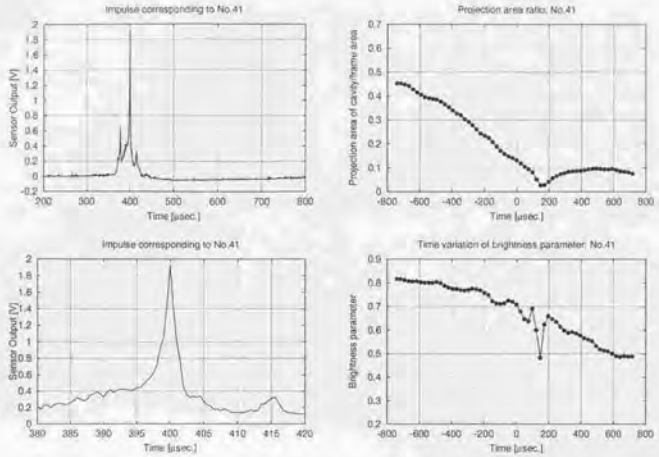

No.41　Impulsive force: 31.8 N
Collapsing type: Spherical

Fig. D.1: (continued)

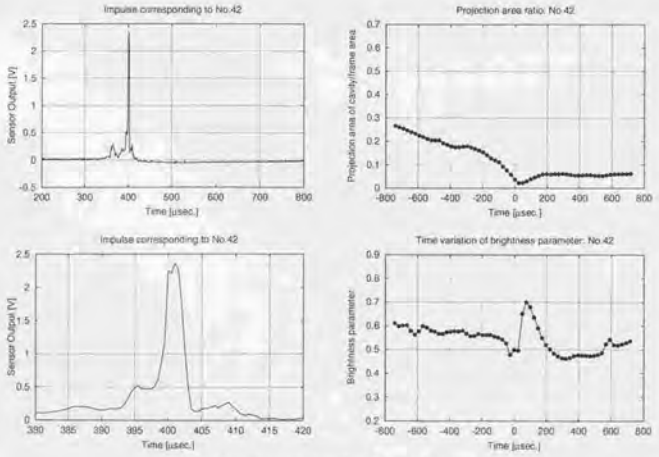

No.42　Impulsive force: 38.8 N
Collapsing type: Spherical

Fig. D.1: (continued)

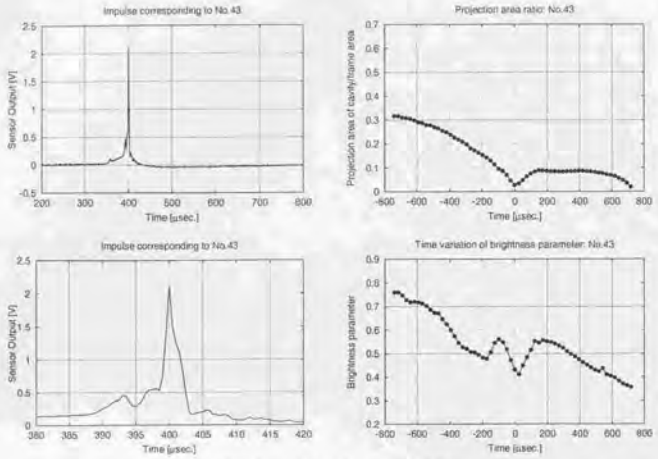

No.43　Impulsive force: 34.6 N
Collapsing type: Spherical

Fig. D.1: (continued)

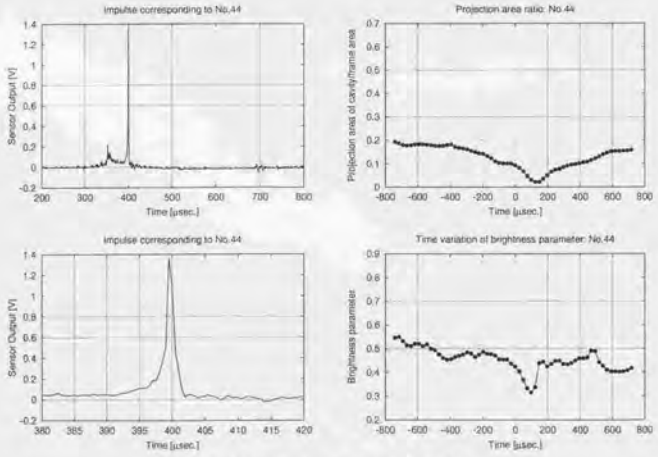

No.44　Impulsive force: 24.7 N
Collapsing type: Axial

Fig. D.1: (continued)

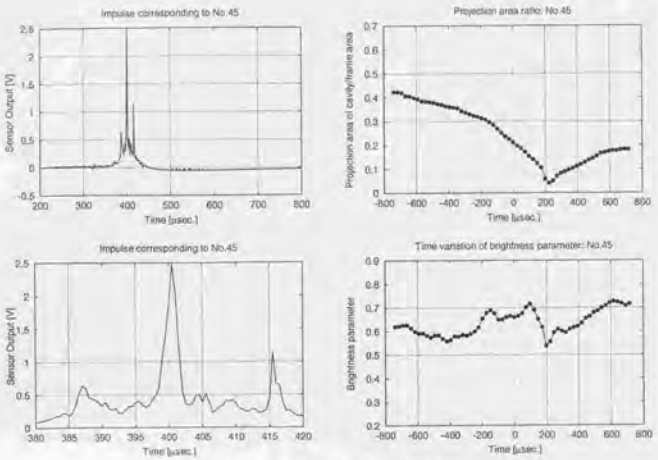

No.45　Impulsive force: 40.3 N
Collapsing type: Spherical

Fig. D.1: (continued)

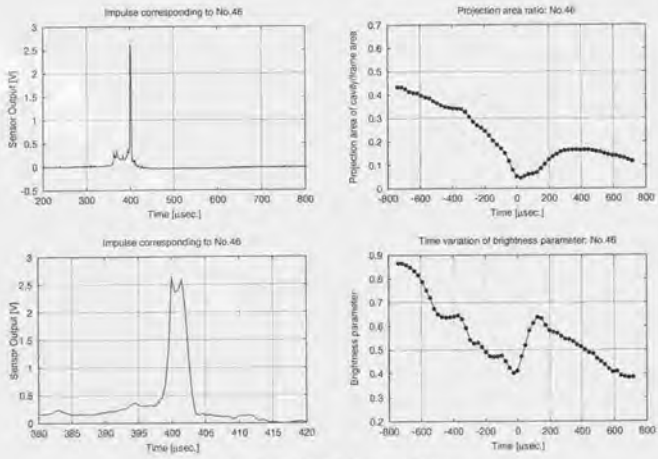

No.46　Impulsive force: 42.7 N
Collapsing type: Spherical

Fig. D.1: (continued)

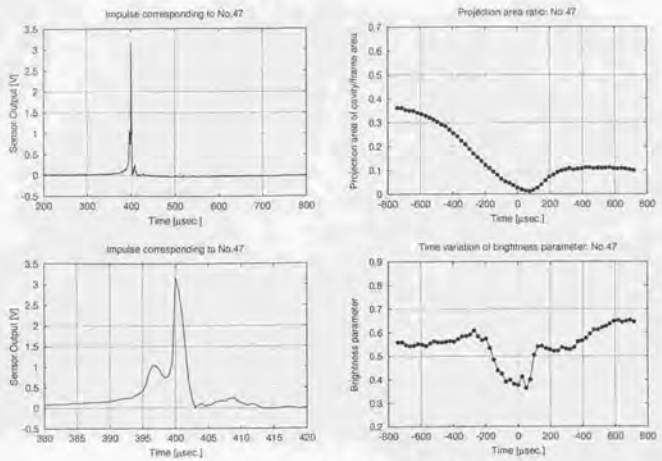

No.47　Impulsive force: 53.2 N
Collapsing type: Axial

Fig. D.1: (continued)

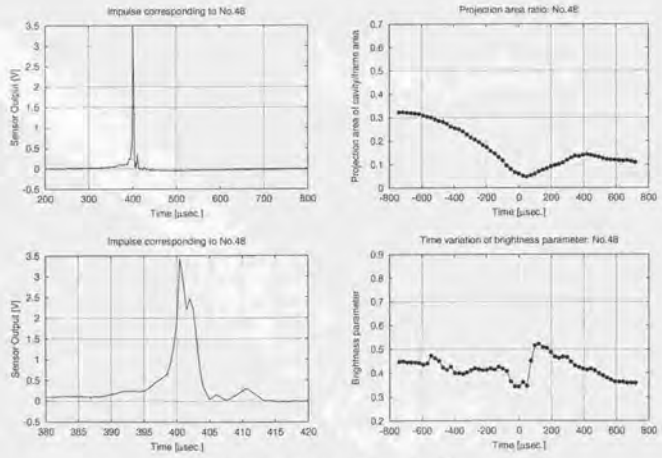

No.48　Impulsive force: 58.1 N
Collapsing type: Spherical

Fig. D.1: (continued)

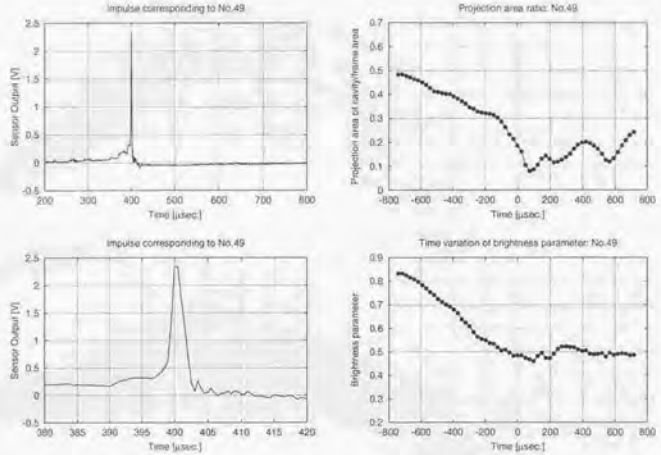

No.49　Impulsive force: 39.9 N
Collapsing type: Spherical

Fig. D.1: (continued)

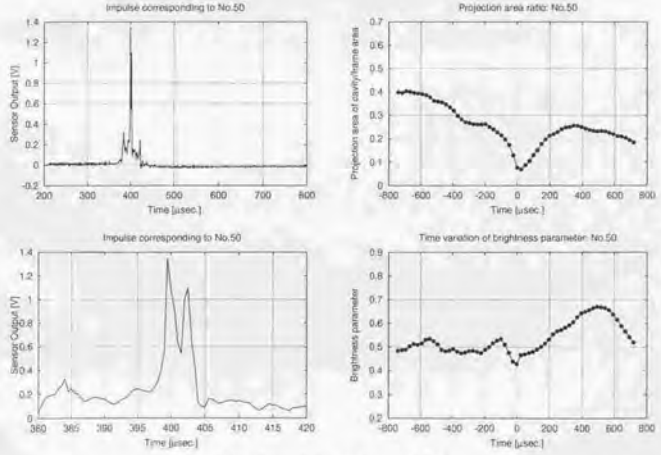

No.50　Impulsive force: 22.9 N
Collapsing type: Spherical

Fig. D.1: (continued)

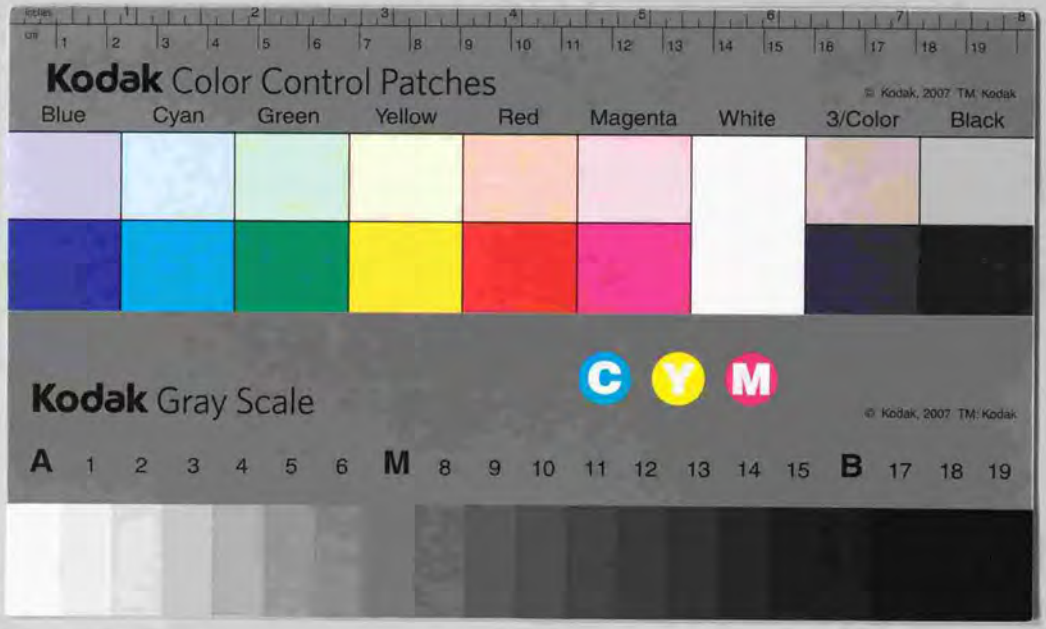
Kodak Color Control Patches
© Kodak, 2007 TM Kodak
Blue
Cyan
Green
Yellow
Red
Magenta
White
3/Color
Black
Kodak Gray Scale
C
Y
M
© Kodak, 2007 TM Kodak
A 1 2 3 4 5 6 M 8 9 10 11 12 13 14 15 B 17 18 19